FNTG Research Society

第 50 回
フラーレン・ナノチューブ・グラフェン
総合シンポジウム

The 50th Fullerenes-Nanotubes-Graphene General Symposium

講演要旨集
Abstracts

2016 年 2 月 19 日（金） ～ 22 日（月）
東京大学　伊藤国際学術研究センター
The University of Tokyo, ITO INTERNATIONAL RESEARCH CENTER

主催　フラーレン・ナノチューブ・グラフェン学会
The Fullerenes, Nanotubes and Graphene Research Society

共催
東京大学工学系研究科　School of Engineering, The University of Tokyo
東京大学 CIAiS　Consortium for Innovation of Advanced Integrated Science (UTokyo)
東京大学 GMSI　Graduate Program for Mechanical Systems Innovation (UTokyo)
日本化学会　The Chemical Society of Japan
JST 戦略的国際共同研究プロジェクト IRENA
IRENA Project by JST-EC DG RTD, SICORP

協賛
日本物理学会　The Physical Society of Japan
応用物理学会　The Japan Society of Applied Physics
高分子学会　The Society of Polymer Science, Japan
電気化学会　The Electrochemical Society of Japan

シミュレーションを高速化

インテル® Parallel Studio XE 2016

最新のインテル® プロセッサー向けに最適化された実行コードを生成するコンパイラーと、パフォーマンス分析ツールなどにより、C/C++ および Fortran アプリケーションの信頼性とパフォーマンスの向上を支援します。

インテル® Parallel Studio XE 2016 の主な新機能

- パフォーマンスが更に向上した日本語版コンパイラー
- ビッグデータ解析のためのライブラリーを新たにバンドル
- 並列化のアドバイスに加え、ベクトル化に関するアドバイスを提供し、高速化を支援 (Professional/Cluster Edition のみ)
- 次世代のインテル® Xeon Phi™ プロセッサー / コプロセッサー (開発コード名 : Knights Landing) をサポート

インテル® Fortran コンパイラーによる優れた Fortran アプリケーション・パフォーマンス — Windows*/Linux*
(数値が大きいほど高性能)

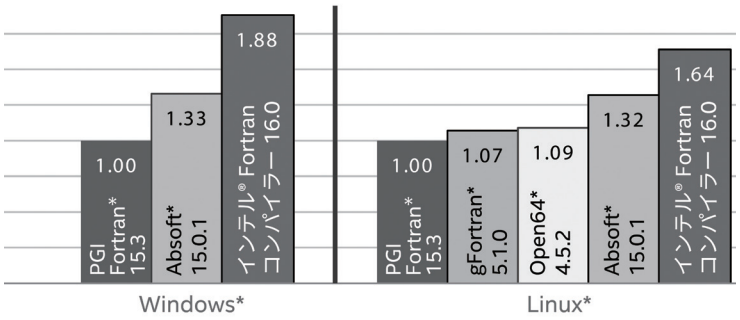

相対 (相乗平均) パフォーマンス Polyhedron* ベンチマーク

システム構成 : ハードウェア : インテル® Core™ i7-4770K プロセッサー @ 3.50GHz、ハイパースレッディング無効、16GB RAM。ソフトウェア : インテル® Fortran コンパイラー 16.0、Absoft* 15.0.1、PGI Fortran* 15.3、Open64* 4.5.2、gFortran* 5.1.0。 Linux*: Red Hat* Enterprise Linux* Server release 7.0 (Maipo)、カーネル 3.10.0-123.el7.x86_64、Windows*: Windows* 7 SP1。Windows* コンパイラー・オプション : Absoft*: -m64 -O5 -speed_math=10 -fast_math -march=core -xINTEGER -stack:0x80000000。インテル® Fortran コンパイラー : /fast /Qparallel /link /stack:64000000。PGI* Fortran: -fastsse -Munroll=n:4 -Mipa=fast,inline -Mconcur=numa。Linux* コンパイラー・オプション : Absoft*: -m64 -mavx -O5 -speed_math=10 -march=core -xINTEGER。gFortran*: -Ofast -mfpmath=sse -flto -march=native -funroll-loops -ftree-parallelize-loops=4。インテル* Fortran コンパイラー : -fast -parallel。PGI* Fortran: -fast -Mipa=fast,inline -Msmartalloc -Mfprelaxed -Mstack_arrays -Mconcur=bind。Open64*: -march=bdver1 -mavx -mno-fma4 -Ofast -mso -apo。Polyhedron* Fortran ベンチマーク (www.polyhedron.com)。

性能に関するテストに使用されるソフトウェアとワークロードは、性能がインテル® マイクロプロセッサー用に最適化されていることがあります。SYSmark* や MobileMark* などの性能テストは、特定のコンピューター・システム、コンポーネント、ソフトウェア、操作、機能に基づいて行ったものです。結果はこれらの要因によって異なります。製品の購入を検討される場合は、他の製品と組み合わせた場合の本製品の性能など、ほかの情報や性能テストも参考にして、パフォーマンスを総合的に評価することをお勧めします。ベンチマークの出典 : インテル コーポレーション

最適化に関する注意事項 : インテル® コンパイラーでは、インテル® マイクロプロセッサーに限定されない最適化に関して、他社製マイクロプロセッサー用に同等の最適化を行えないことがあります。これには、インテル® ストリーミング SIMD 拡張命令 2、インテル® ストリーミング SIMD 拡張命令 3、インテル® ストリーミング SIMD 拡張命令 3 補足命令などの最適化が該当します。インテルは、他社製マイクロプロセッサーに関して、いかなる最適化の利用、機能、または効果も保証いたしません。本製品のマイクロプロセッサー依存の最適化は、インテル® マイクロプロセッサーでの使用を前提としています。インテル® マイクロアーキテクチャーに限定されない最適化のなかにも、インテル® マイクロプロセッサー用のものがあります。この注意事項で言及した命令セットの詳細については、該当する製品のユーザー・リファレンス・ガイドを参照してください。

注意事項の改訂 #20110804

製品詳細、無料評価版はこちらから
http://www.xlsoft.com/intel/pharm2

XLSOFT エクセルソフト株式会社

intel Software

Abstract of
The 50th Fullerenes-Nanotubes-Graphene General Symposium

Sponsored by : The Fullerenes, Nanotubes and Graphene Research Society

Co-Sponsored by : School of Engineering, The University of Tokyo
Consortium for Innovation of Advanced Integrated Science(UTokyo)
Graduate Program for Mechanical Systems Innovation(UTokyo)
The Chemical Society of Japan
IRENA Project by JST-EC DG RTD, SICORP

Supported by : The Physical Society of Japan
The Japan Society of Applied Physics
The Society of Polymer Science, Japan
The Electrochemical Society of Japan

Date : February 19th (Fri.) – 22nd (Mon.), 2016

Place : The University of Tokyo, ITO INTERNATIONAL RESEARCH CENTER
7-3-1 Hongo, Bunkyo-ku, Tokyo 113-8656

Presentation Time : Special Lecture (25 min presentation + 5min discussion)
General Lecture (10 min presentation + 5min discussion)
Poster Preview (1 min presentation without discussion)

第 50 回フラーレン･ナノチューブ･グラフェン総合シンポジウム
講演要旨集

主催 ： フラーレン･ナノチューブ･グラフェン学会

共催 ： 東京大学大学院工学系研究科
東京大学 CIAiS
東京大学 GMSI
日本化学会
JST 戦略的国際共同研究プロジェクト IRENA

協賛 ： 日本物理学会、応用物理学会、高分子学会、電気化学会

日時 ： 平成 28 年 2 月 19 日（金） ～ 22 日（月）

場所 ： 東京大学　伊藤国際学術研究センター　伊藤謝恩ホール
〒113-8656　東京都文京区本郷 7-3-1

発表時間 ： 特別講演　（発表 25 分 ＋ 質疑応答 5 分）
一般講演　（発表 10 分 ＋ 質疑応答 5 分）
ポスタープレビュー　（発表 1 分・質疑応答 なし）

展示団体御芳名 （五十音順、 敬称略）

アイクストロン（株）
IOP英国物理学会出版局
QuantumWise Japan（株）
サイバネットシステム(株)
シグマ　アルドリッチ　ジャパン（同）
（株）島津製作所
（株）セントラル科学貿易
東京ダイレック(株)
ナカライテスク（株）
ナノフォトン（株）
（株）ニューメタルスエンドケミカルスコーポレーション
日立工機（株）
フリッチュ・ジャパン（株）
（株）堀場製作所
（株）三ツワフロンテック
（株）名城ナノカーボン

広告掲載団体御芳名 （五十音順、 敬称略）

アイクストロン(株)
エクセルソフト（株）
（株）コロナ社
（株）セントラル科学貿易
ナカライテスク（株）
日本電子（株）
フロンティアカーボン（株）
（株）三ツワフロンテック

Contents

目次

プログラム早見表

2月20日 （土）

	受付開始 8:30～ 講演開始 9:30～
9:30	特別講演（Esko I. Kauppinen） 9:30-10:00
10:00	特別講演（古月文志） 10:00-10:30
10:30	休憩 10:30-10:45
10:45	一般講演 4件 （フラーレン ・ グラフェンの物性） 10:45-11:45
11:45	昼食 （幹事会） 11:45-13:00
13:00	特別講演（黒部 篤） 13:00-13:30
13:30	一般講演 3件 （原子層） 13:30-14:15
14:15	ポスタープレビュー （ 1P-1 ～ 1P-49 ） 14:15-15:15
15:15	ポスターセッション （多目的スペース） 15:15-17:00
17:00	特別講演（橋本 剛） 17:00-17:30
17:30	一般講演 3件 （ナノチューブの応用） 17:30-18:15
18:15	休憩 18:15-18:30
18:30	チュートリアル 講師： 吾郷 浩樹 九州大学 （伊藤謝恩ホール） 18:30-20:00
20:00	

2月19日 （金）

16:30	特別講演 （Mildred S. Dresselhaus） 16:30-17:30
17:30	

2月21日 （日）

	受付開始 8:30～ 講演開始 9:00～
9:00	特別講演（Yan Li） 9:00-9:30
9:30	一般講演 3件 （ナノチューブの生成と精製 ・ ナノチューブの物性）9:30-10:15
10:15	休憩 10:15-10:30
10:30	特別講演（福島 孝典） 10:30-11:00
11:00	一般講演 3件 （グラフェン生成・フラーレン・金属内包フラーレン）11:00-11:45
11:45	昼食 11:45-13:00
13:00	授賞式 13:00-13:30
13:30	特別講演 （牧 英之） 13:30-14:00
14:00	ポスタープレビュー （ 2P-1 ～ 2P-49 ） 14:00-15:00
15:00	ポスターセッション （ 多目的スペース ） 15:00-16:45
16:45	第50回記念 温故知新 パネルディスカッション 阿知波洋次，飯島澄男，今堀博，岩佐義宏，遠藤守信，大澤映二，小松紘一，斎藤晋，齋藤弥八，田中一義，谷垣勝己，日野照純 16:45-18:45
18:45	懇親会 （多目的スペース） 18:45-20:45
20:45	

2月22日 （月）

	受付開始 8:30～ 講演開始 9:00～
9:00	特別講演（仁科 勇太） 9:00-9:30
9:30	一般講演 4件 （グラフェンの物性 ・ 原子層） 9:30-10:30
10:30	休憩 10:30-10:45
10:45	特別講演（湯本 潤司） 10:45-11:15
11:15	一般講演 3件 （ナノチューブの物性） 11:15-12:00
12:00	昼食 12:00-13:15
13:15	ポスタープレビュー （ 3P-1 ～ 3P-48 ） 13:15-14:15
14:15	ポスターセッション （多目的スペース） 14:15-16:00
16:00	特別講演 （宮内 雄平） 16:00-16:30
16:30	一般講演 4件 （フラーレンの応用・ナノ炭素粒子・ナノチューブの応用・その他） 16:30-17:30
17:30	

講演会場 伊藤謝恩ホール
特別講演 発表25分・質疑5分
一般講演 発表10分・質疑5分
ﾎﾟｽﾀｰﾌﾟﾚﾋﾞｭｰ 発表1分・質疑なし

Time table

February 20 (Sat.)	
	Registration begins at 8:30 Lectures begin at 9:30
9:30	Special Lecture (Esko I. Kauppinen) 9:30–10:00
10:00	Special Lecture (Bunshi Fugetsu) 10:00–10:30
10:30	Coffee Break 10:30–10:45
10:45	General Lectures [4] (Fullerenes・ Properties of graphene) 10:45–11:45
11:45	Lunch (Administrative meeting) 11:45–13:00
13:00	Special Lecture (Atsushi Kurobe) 13:00–13:30
13:30	General Lectures [3] (Atomic Layers) 13:30–14:15
14:15	Poster Preview (1P–1 through 1P–49) 14:15–15:15
15:15	Poster Session (Event Space) 15:15–17:00
17:00	Special Lecture (Takeshi Hashimoto) 17:00–17:30
17:30	General Lectures [3] (Applications of nanotubes) 17:30–18:15
18:15	Coffee Break 18:15–18:30
18:30	Tutorial Lecturer : Hiroki Ago Kyushu University (Ito Hall) 18:30–20:00
20:00	

February 19 (Fri.)	
16:30	Special Lecture (Mildred S. Dresselhaus) 16:30–17:30
17:30	

February 21 (Sun.)	
	Registration begins at 8:30 Lectures begin at 9:00
9:00	Special Lecture (Yan Li) 9:00–9:30
9:30	General Lectures [3] (Formation and purification of nanotubes・Properties of nanotubes) 9:30–10:15
10:15	Coffee Break 10:15–10:30
10:30	Special Lecture (Takanori Fukushima) 10:30–11:00
11:00	General Lectures [3] (Graphene synthesis・Fullerenes・Endohedral metallofullerenes)11:00–11:45
11:45	Lunch 11:45–13:00
13:00	Award Ceremony 13:00–13:30
13:30	Special Lecture (Hideyuki Maki) 13:30–14:00
14:00	Poster Preview (2P–1 through 2P–49) 14:00–15:00
15:00	Poster Session (Event Space) 15:00–16:45
16:45	50th Memorial Panel Discussion (Yohji Achiba, Sumio Iijima, Hiroshi Imahori, Yoshihiro Iwasa, Morinobu Endo, Eiji Osawa, Koichi Komatsu, Susumu Saito, Yahachi Saito, Kazuyoshi Tanaka, Katsumi Tanigaki, Shojun Hino) 16:45–18:45
18:45	Banquet (Event Space) 18:45–20:45
20:45	

February 22 (Mon.)	
	Registration begins at 8:30 Lectures begin at 9:00
9:00	Special Lecture (Yuta Nishina) 9:00–9:30
9:30	General Lectures [4] (Properties of graphene・Atomic Layers) 9:30–10:30
10:30	Coffee Break 10:30–10:45
10:45	Special Lecture (Junji Yumoto) 10:45–11:15
11:15	General Lectures [3] (Properties of nanotubes) 11:15–12:00
12:00	Lunch 12:00–13:15
13:15	Poster Preview (3P–1 through 3P–48) 13:15–14:15
14:15	Poster Session (Event Space) 14:15–16:00
16:00	Special Lecture (Yuhei Miyauchi) 16:00–16:30
16:30	General Lectures [4] (Applications of fullerenes・Other topics・Applications of nanotubes・Carbon nanoparticles)16:30–17:30
17:30	

Place : Ito Holl
Special Lecture : 25 min (Presentation) + 5 min (Discussion)
General Lecture : 10 min (Presentation) + 5 min (Discussion)
Poster Preview : 1 min (Presentation)

座長一覧 (Chairpersons)

2月19日(金)

（敬称略）

セッション	時　　間	座　　長
特別講演(Mildred S. Dresselhaus)	16:30 ～17:30	齋藤 理一郎

2月20日(土)

セッション	時　　間	座　　長
特別講演(Esko I. Kauppinen)	9:30 ～10:00	北浦 良
特別講演(古月 文志)	10:00 ～10:30	丸山 茂夫
一般講演	10:45 ～ 11:45	岡田 晋
特別講演(黒部 篤)	13:00～ 13:30	山本 貴博
一般講演	13:30 ～ 14:15	山本 貴博
ポスタープレビュー	14:15 ～ 15:15	長谷川 馨 小川 友以
特別講演(橋本 剛)	17:00 ～17:30	野田 優
一般講演	17:30 ～ 18:15	野田 優
チュートリアル(吾郷 浩樹)	18:30 ～ 20:00	松尾 豊

2月21日(日)

セッション	時　　間	座　　長
特別講演(Yan Li)	9:00 ～ 9:30	大野 雄高
一般講演	9:30 ～10:15	大野 雄高
特別講演(福島 孝典)	10:30 ～11:00	竹延 大志
一般講演	11:00 ～ 11:45	松尾 豊
特別講演(牧 英之)	13:30 ～ 14:00	長汐 晃輔
ポスタープレビュー	14:00 ～ 15:00	桜井 俊介 項 榮
温故知新 パネルディスカッション	16:45 ～ 18:45	湯田坂 雅子 丸山 茂夫

2月22日(月)

セッション	時　　間	座　　長
特別講演(仁科 勇太)	9:00 ～ 9:30	長汐 晃輔
一般講演	9:30 ～ 10:30	長汐 晃輔
特別講演(湯本 潤司)	10:45 ～ 11:15	丸山 茂夫
一般講演	11:15 ～ 12:00	千足 昇平
ポスタープレビュー	13:15 ～ 14:15	白木 智丈 井ノ上 泰輝
特別講演(宮内 雄平)	16:00 ～ 16:30	小鍋 哲
一般講演	16:30 ～ 17:30	高井 和之

2月19日（金）

特別講演　　発表 40分 ・ 質疑応答 20分

特別講演（ 16:30−17:30 ）

2月20日（土）

特別講演　　発表 25分 ・ 質疑応答 5分
一般講演　　発表 10分 ・ 質疑応答 5分
ポスタープレビュー　　発表 1分 ・ 質疑応答 なし

特別講演（ 9:30−10:00 ）

特別講演（ 10:00−10:30 ）

＞＞＞＞＞＞＞ 休憩（ 10:30−10:45 ）＜＜＜＜＜＜＜

一般講演（ 10:45−11:45 ）
フラーレン ・ グラフェンの物性

＞＞＞＞＞＞＞ 昼食（ 11:45−13:00 ）＜＜＜＜＜＜＜

特別講演（ 13:00−13:30 ）

2月20日（土）

一般講演（ 13:30−14:15 ）
原子層

ポスタープレビュー（ 14:15−15:15 ）
ポスターセッション（ 15:15−17:00 ）　（☆） 若手奨励賞候補
フラーレンの化学

金属内包フラーレン

フラーレン

ナノチューブの物性

2月20日（土）

ナノチューブの応用

ナノチューブの生成と精製

2月20日（土）

グラフェン生成

グラフェンの応用

グラフェンの物性

原子層

2月20日（土）

ナノホーン

ナノ炭素粒子

その他

2月20日（土）

特別講演（ 17:00−17:30 ）

一般講演（ 17:30−18:15 ）

ナノチューブの応用

＞＞＞＞＞＞＞ 休憩（ 18:15−18:30 ）＜＜＜＜＜＜＜

チュートリアル（ 18:30−20:00 ）

2月21日（日）

特別講演　　発表 25分 ・ 質疑応答 5分
一般講演　　発表 10分 ・ 質疑応答 5分
ポスタープレビュー　　発表 1分 ・ 質疑応答 なし

特別講演（ 9:00-9:30 ）

一般講演（ 9:30-10:15 ）
ナノチューブの生成と精製 ・ ナノチューブの物性

＞＞＞＞＞＞ 休憩（ 10:15-10:30 ）＜＜＜＜＜＜

特別講演（ 10:30-11:00 ）

一般講演（ 11:00-11:45 ）
グラフェン生成 ・ 金属内包フラーレン ・ フラーレン

＞＞＞＞＞＞ 昼食（ 11:45-13:00 ）＜＜＜＜＜＜

大澤賞・飯島賞・若手奨励賞の授賞式（ 13:00-13:30 ）

2月21日（日）

2月21日（日）

2月21日（日）

グラフェン生成

グラフェンの応用

グラフェンの物性

2月21日（日）

原子層

ナノ炭素粒子

その他

第50回記念 温故知新パネルディスカッション（ 16:45-18:45 ）

阿知波 洋次，飯島 澄男，今堀 博，岩佐 義宏，遠藤 守信，大澤 映二，小松 紘一，斎藤 晋，齋藤 弥八，田中 一義，谷垣 勝己，日野 照純

懇親会（ 18:45-20:45 ）

2月22日（月）

特別講演　　発表 25分 ・ 質疑応答 5分
一般講演　　発表 10分 ・ 質疑応答 5分
ポスタープレビュー　　発表 1分 ・ 質疑応答 なし

＞＞＞＞＞＞＞ 休憩（ 10:30−10:45 ）＜＜＜＜＜＜＜

＞＞＞＞＞＞＞ 昼食（ 12:00−13:15 ）＜＜＜＜＜＜＜

2月22日（月）

ポスタープレビュー（ 13:15−14:15 ）
ポスターセッション（ 14:15−16:00 ）　　（☆） 若手奨励賞候補
フラーレンの応用

金属内包フラーレン

フラーレン

ナノチューブの物性

2月22日（月）

ナノチューブの応用

ナノチューブの生成と精製

内包ナノチューブ

2月22日（月）

2月22日（月）

2月22日（月）

特別講演（ 16:00-16:30 ）

一般講演（ 16:30-17:30 ）

フラーレンの応用 ・ その他 ・ ナノチューブの応用 ・ ナノ炭素粒子

February 19th, Fri.

Special Lecture: 40min (Presentation) + 20min (Discussion)

February 20th, Sat.

Special Lecture: 25min (Presentation) + 5min (Discussion)
General Lecture: 10min (Presentation) + 5min (Discussion)
Poster Preview: 1min (Presentation)

>>>>>>> Coffee Break（10:30–10:45）<<<<<<<

>>>>>>> Lunch Time（11:45–13:00）<<<<<<<

February 20th, Sat.

February 20th, Sat.

February 20th, Sat.

>>>>>>> Coffee Break（18:15-18:30）<<<<<<<

Tutorial（18:30-20:00）

Graphene –CVD growth, characterization, and application–
** Hiroki Ago*

February 21st, Sun.

Special Lecture: 25min (Presentation) + 5min (Discussion)
General Lecture: 10min (Presentation) + 5min (Discussion)
Poster Preview: 1min (Presentation)

Special Lecture（9:00–9:30）

General Lecture（9:30–10:15）
Formation and purification of nanotubes ・ Properties of nanotubes

>>>>>>> Coffee Break（10:15–10:30）<<<<<<<

Special Lecture（10:30–11:00）

General Lecture（11:00–11:45）
Graphene synthesis ・ Endohedral metallofullerenes ・ Fullerenes

>>>>>>> Lunch Time（11:45–13:00）<<<<<<<

Awards Ceremony（13:00–13:30）

February 21st, Sun.

50th Memorial Panel Discussion （16:45-18:45）

Yohji Achiba, Sumio Iijima, Hiroshi Imahori, Yoshihiro Iwasa, Morinobu Endo, Eiji Osawa, Koichi Komatsu, Susumu Saito, Yahachi Saito, Kazuyoshi Tanaka, Katsumi Tanigaki, Shojun Hino

Banquet（18:45-20:45）

February 22nd, Mon.

Special Lecture: 25min (Presentation) + 5min (Discussion)
General Lecture: 10min (Presentation) + 5min (Discussion)
Poster Preview: 1min (Presentation)

February 22nd, Mon.

Poster Preview （ 13:15–14:15 ）
Poster Session （ 14:15–16:00 ） （☆）Candidates for the Young Scientist Poster Award

February 22nd, Mon.

February 22nd, Mon.

特別講演
Special Lecture

S – 1

1S – 1 ～ 1S – 4

2S – 5 ～ 2S – 7

3S – 8 ～ 3S – 10

The 50th Fullerene-Nanotube-Graphene Society Meeting (Tokyo) 2016.2.19, Univ. Tokyo

What can we learn about low-symmetry materials from spectroscopy?

Mildred S. Dresselhaus

Departments of Physics and Electrical Engineering,

Massachusetts Institute of Technology, Cambridge, MA 02139, USA

In this talk, we overview the spectroscopy of lower-symmetry materials. In optical spectroscopy, because of the van Hove singularity for electronic density of states, optical spectra show sharp peaks in resonant optical process such as resonance Raman scattering and resonance Rayleigh scattering, which are useful for characterizing the structure of single-wall carbon nanotubes. However, lower-symmetry layered materials nevertheless yield some specific selection rules for optical transitions in which group theory still works well, such as for analyzing the spectra of transition metal dichalcogenides, using graphene as reference material. By showing examples that we have investigated so far, we will discuss what we can learn about lower-symmetry materials from spectroscopy.

Mildred Dresselhaus e-mail: millie@mgm.mit.edu

Direct dry printing of SWNT thin films for flexible electronics applications

Esko I. Kauppinen

Department of Applied Physics, Aalto University School of Science
PO Box 15100, FI-00076 Aalto, FINLAND
e-mail: esko.kauppinen@aalto.fi

We present the industrial scale, ISO 9001:2008 certified direct dry printing (DPP) manufacturing of single walled carbon nanotube (SWNT) transparent conducting films (TCF) for touch sensors with electrical properties on par with those of ITO-on-PET, and with optical properties and flexibility better than those of ITO, metal nanowire and metal mesh [1,2]. We demonstrate SWNT thin film TCF applications as the capacitive touch sensors for mobile phones, laptop computers, gaming controls etc. All carbon transparent, flexible and stretchable thin film field effect transistors (TFT-FET) with properties comparable to those of polycrystalline siliconTFT-FETs as well as integrated circuits have been made using percolating SWNT network as the semiconductor and SWNT TCF as the source, drain, gate and interconnect material [3,4]. We discuss the SWNT bundling mechanisms during FC-CVD synthesis and how the bundling affects both the tube growth rate and the TCF performance [5]. We present the estimate for the ultimate performance of SWNT thin film TCFs to be lower than 30 ohms/sq sheet resistance at 90 % transmission [6].

[1] A. Kaskela et al. *NanoLetters* 10, 4349 (2010).
[2] A.G. Nasibulin et al. *ACS Nano*. 5, 3214 (2011).
[3] D.-M. Sun et al. *Nature Nanotechnology*. 6, 156 (2011).
[4] D.-M. Sun et al. *Nature Communications* **4,** 2302. (2012).
[5] K. Mustonen et al. (2015) Appl. Phys. Lett. **107**, 013106.
[6] K. Mustonen et al. (2015) *Appl. Phys. Lett*. **107**, 143113.

Graphene oxide: massive production and practical application

(酸化グラフェン：量産技術と応用実例)

○ Bunshi Fugetsu[1], Yanqing Wang[1, 2], Ichiro Sakata[1, 2]

[1] *Policy Alternative Research Institute, The University of Tokyo, Tokyo 113-0033, Japan*
[2] *School of Engineering, The University of Tokyo, Tokyo 113-0032, Japan*

Graphene oxide was first introduced in 1859 [1] in Britain but has been recalled worldwide in recent years for a number of reasons. First, GO is a truly sheet-shaped giant-sized molecule. A single GO molecule can have a length or breadth that is typically larger than micrometers while its thickness is only one or a few atoms thick. It is possible to cover or overlap a single and/or a few numbers of certain substances with the atom-thick molecular sheet. Second, GO bears many oxygenated functional groups on the basal plane and at the edge; hybrids at molecular level of combinations which can be further converted into nanoparticles can be generated simply by linking a suitable chemical species on to GO via the potential interactions with the oxygenated moieties of GO. Third, GO is highly dispersible and/or soluble in both aqueous and organic solvents; also, compared with carbon nanotubes (CNTs), it is much easier to mix GO with other polymers via the solution/solution mixing method with the polymers and GO being ideally dispersed. Furthermore, GO can be converted to graphene through a chemical reduction or with a heating treatment. Graphene has many unusual properties (high in-plane thermal and electrical conductivity and excellent mechanical stiffness); this enables us to generate a broad new class of high-performance materials by using GO as the starting element. Moreover, GO is commonly produced by exfoliating graphite, an abundant material, through simple chemical/physical reactions; thus, GO has the advantages of low cost and plentiful supply of the starting material. Hummers method [2] has long been the cornerstone for producing GO; the development of a safer method with higher yields for producing GO in large quantities still remains a big challenge. We have introduced a novel approach with expanded graphite as the starting material to massive production of GO. A foam-like intermediate was firstly produced by intercalating H_2SO_4 into the expanded graphite; this has further expanded the graphite. The foam-like graphite was subsequently oxidized by using $KMnO_4$ as the oxidant; followed by a sonication or a milling treatment, the fully exfoliated GO was obtained. Graphene-dye-printed yarns/fabrics [3], graphene-enhanced photocatalysts [4], graphene-based high-performance capacitors [5] and graphene/PVA-based three-dimensional monolith [6] have been stablished by using GO as the key element. The applications of GO and/or the reduced GO (namely, graphene) is close to unlimited.

[1] B. Brodie, On the atomic weight of graphite, Phil. Trans., 149, 249 (1859).
[2] W. S. Hummers, R. E. Offeman, Preparation of graphite oxide, J. Am. Chem., Soc., 80, 1339 (1958).
[3] B. Fugetsu, E. Sano, H. Yu, K. Mori, T. Tanaka, Graphene oxide as dyestuffs for the creation of electrically conductive fabrics, Carbon, 48, 3340 (2010).
[4] Y. Wang, L. Sun, B. Fugetsu, Morphology-controlled synthesis of sunlight-driven plasmonic photocatalysts Ag@AgX(X=Cl, Br) with graphene oxide template, J. Mater. Chem. A, 1, 1256 (2013).
[5] H. Yu, J. He, L. Sun, S. Tanaka, B. Fugetsu, Influence of the electrochemical reduction process on the performance of graphene-based capacitors, Carbon, 51, 94 (2013).
[6] Y. Wang, B. Fugetsu, I. Sakata, M. Terrones, M. Endo, M. Dresselhaus, Morphology-controlled fabrication of a three-dimensional mesoporous poly(vinyl alcohol) monolith through the incorporation of graphene oxide, Carbon, 98, 334 (2016).

Corresponding Author: B. Fugetsu, Tel: +81-3-5841-5815, Fax: +81-3-5841-5815, E-mail: bunshifugetsu@pari.u-tokyo.ac.jp

JST/CREST on "2D Materials"
- Research Supervisor's Policy and the Invitation for Applications -

○Atsushi Kurobe[1, 2]

[1] *Research Supervisor, JST/CREST, Tokyo 102-0076, Japan*
[2] *Corporate R&D Center, Toshiba Corporation, Kawasaki 212-8582, Japan*

Recently, there has been a growing interest in 2D materials, such as graphene and transition metal dichalcogenides (TMDs), as they offer intriguing new phenomena which might be useful in future applications[1]. In 2014, Japan Science and Technology Agency (JST) launched a new CREST research-area "Development of Atomic or Molecular Two-Dimensional Functional Films and Creation of Fundamental Technologies for Their Applications"[2], where the target area is "2D materials" in short.

CREST is a funding program for team-oriented research with the aim of achieving the strategic goals set forth by the government ("2D materials" in the present case), by promoting and encouraging the development of break-through technologies. We started to select proposals from 2014, and this year will be the last (third) year to call for proposals.

We would like this research area to cover an extensive range of disciplines. Fig.1 shows the overview of the received proposals in 2014 and 2015. Total number of applications was 141 (86 in 2015, 55 in 2016); 75 from Physics, 30 from Chemistry, 27 from Engineering, and 9 from Biology. The diversity in the research expertise is evident. Because of financial difficulties, we could accept only 7 best proposals after intensive discussions with 10 research-area advisors. We welcome additional first-class applications this year as well.

While it is very important to have envisioned outcomes of the research proposal including potential applications, clinging too stubbornly to any forced expectations might suppress fresh ideas and discoveries that could arise during the course of research. We wish to conduct basic task-oriented research firmly rooted in science and aimed at investigating principles and establishing device guidelines, while being cognizant of what needs the proposed technology is targeting.

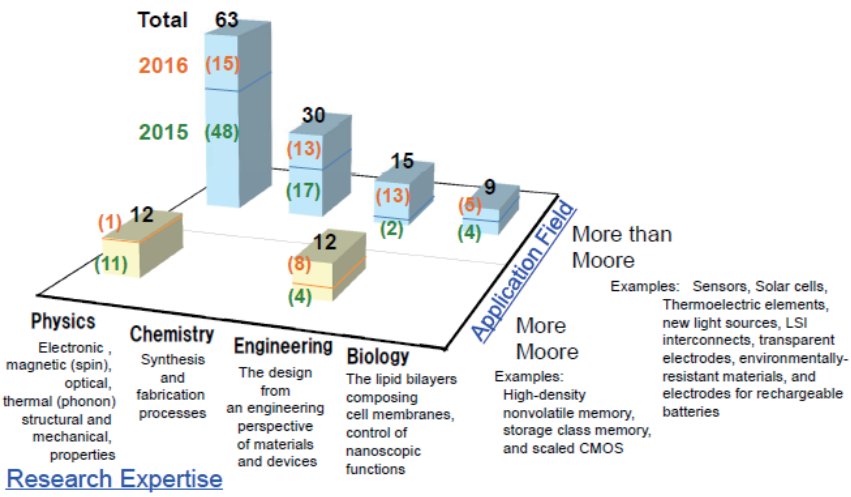

Fig.1 Portfolio of the received proposals in 2015 and 2016

[1] For example: A. C. Ferrari *et al*., Nanoscale **7**, 4587 (2015); F. Bonaccorso *et al*., Science **347** 1246501 (2015); G. Fiori *et al*., Nature Nanotechnology **9**, 768 (2014); M. Xu *et al*., Chem. Rev. **113**, 3766 (2013).
[2] http://www.jst.go.jp/kisoken/crest/research_area/ongoing/bunyah26-4.html

Corresponding Author: A. Kurobe Tel:+81-44-549-2050 E-mail:atsushi.kurobe@toshiba.co.jp

For industrial applications of the future of carbon nanotubes

Takeshi Hashimoto

MEIJO NANO CARBON CO.,LTD.
2271-129 Anagahora, Shimoshidami Moriyama, Nagoya, Aichi 463-0003, Japan

We have already passed more than 20 years from the discovery of carbon nanotubes. And MEIJO NANO CARBON was passed more than 10 years as a carbon nanotubes venture . Since foundation, we have been operated as the position of development and manufacturer company which is specialized to carbon nanotubes.

Now, markets of carbon nanotubes are LIB additive and resin additive. Other ones are a market for development. LIB and resin are using conductivity of carbon nanotubes. Those are the use by which conductivity is required for the addition amount less than carbon black. For a market of carbon nanotubes to become big, we have to find difficult application by carbon black. We would like to think about industrial applications of the future of carbon nanotubes while considering such thing.

Corresponding Author: T. Hashimoto
Tel: +81-52-736-2322, Fax: +81-52-736-5222,
E-mail: hashimo@meijo-nano.com

Structure-controlled growth of single-walled carbon nanotubes: from catalyst design to growth conditions

○Yan Li

College of Chemistry and Molecular Engineering, Peking University, Beijing 100871, China

Single-walled carbon nanotubes (SWNTs) have shown great potentials in various applications attribute to their unique structure-dependent properties. Therefore the controlled preparation of chemically and structurally pristine SWNTs is a crucial issue for their advanced applications (e.g. nanoelectronics) and has been a great challenge for two decades.The composition and morphology of the catalyst nanoparticles were widely reported to affect the chirality distribution of SWNTs. Yet chirality-specific SWNT growth had not been realized by alternating catalysts. Inspired by the specificity of enzyme-catalyzed reactions, we realized that only catalysts with unique crystal structure and desired atomic arrangements can act as the structural templates for chirality specific growth of SWNTs, relying on the high selectivity in geometry match between catalysts and SWNTs. We developed a new family of catalysts, tungsten-based intermetallic compounds, which have high melting point and very special crystal structure, to synthesize SWNTs with designed chirality. Using W_6Co_7 catalysts, (12, 6) SWNTs was directly grown with the purity higher than 92%. The selective growth of (12, 6) tubes is due to a good structural match between the carbon atom arrangement around the nanotube circumference and the metal atom arrangement of (0 0 12) planes in the catalyst. Similarly, (16, 0) SWNT exhibits good structural match to (1 1 6) plane of Co_7W_6 catalyst. By manipulating the chemical vapor deposition (CVD) conditions, zigzag (16, 0) SWNTs, which are generally known as a kinetically unfavorable species in CVD growth, were obtained at the purity of ~80%. The chirality-specific growth of SWNTs is realized by the cooperation of two factors: the structural match between SWNTs and the catalysts makes the growth of SWNTs with specific chirality thermodynamically favorable; and further manipulation of CVD conditions obtains optimized growth kinetics for SWNTs with this designed chirality. This idea has also been proved to be valid for SWNTs with other chiralities and intermetallic catalysts. We expect that this advanced epitaxial growth strategy will pave a way for the ultimate goal of chirality control growth of SWNTs.

[1] F. Yang *et al*. Nature **510**, 522-524 (2014).
[2] F. Yang *et al*. J. Am. Chem. Soc. **137**, 8688-8691 (2015).
[3] Y. Li *et al*., Adv. Mater **22**, ,1508-1515 (2010).

Corresponding Author: Y. Li
Tel & Fax: +86-10-6275-6773
E-mail: yanli@pku.edu.cn

Precision Assembly of C_{60} Functionality Using Supramolecular Scaffolds

○Takanori Fukushima[1]

[1] *Chemical Resources Laboratory, Tokyo Institute of Technology, 4259 Nagatsuta, Midori-ku, Yokohama 226-8503, Japan*

Molecular self-assembly has been considered to be a useful approach to creating functional organic materials with high structural precision. If molecular arrangements and orientations in self-assembled materials could be perfectly controlled, one may exploit full potential of the intrinsic properties of constituent molecules for developing high-performance materials that exhibit, for example, anisotropic charge- and energy-transports, dipolar properties, and even mechanical responses. However, in reality, it is difficult to predict the structures of molecular assemblies from those of their building blocks. To address this issue, we have designed supramolecular scaffolds, which direct controlled assembly of a wide variety of functional molecular units. This presentation will focus on the precision assembly of C_{60} functionalities into particular structures using these supramolecular scaffolds. For example, when C_{60} is attached to a Gemini-shaped hexa-*peri*-hexabenzocoronene (HBC) capable of forming a nanotubular assembly, a coaxial nanotube results, where the wall consists of hole-transporting HBC arrays, while the inner and outer surfaces are covered by an electron-transporting monolayer of C_{60} [1]. We have also shown that an amphiphilic design of an oligothiophene-C_{60} dyad provides a rational strategy for tailoring well-defined electron donor and acceptor arrays [2]. We recently found that a paraffinic tripodal triptycene self-assembles into a 2D hexagonal structure by nested packing [3]. The interpenetration of the triptycene part may suppress structural fluctuation, thus enabling the formation of organic films with a remarkably long-range structural order. Using this tripodal triptycene as a supramolecular scaffold, a C_{60} functionality can be assembled into a two-dimensional sheet-like structure. The synthesis and properties of these self-assembled materials containing C_{60} will be described.

[1] Y. Yamamoto, T. Fukushima, T. Aida *et al.*, *Proc. Natl. Acad. Sci. U.S.A.* **2009**, 106, 21051–21056.
[2] W.-S. Li, T. Fukushima, T. Aida *et al.*, *J. Am. Chem. Soc.* **2008**, *130*, 8886–8887.
[3] N. Seiki, Y. Shoji, T. Fukushima *et al.*, *Science* **2015**, *348*, 1122–1126.

Corresponding Author: T. Fukushima
Tel: +81-45-924-5220, Fax: +81-45-924-5976
E-mail: fukushima@res.titech.ac.jp

2S-7

Nanocarbon-based light sources for integrated optoelectronics and optical communications

○Hideyuki Maki[1,2]

[1] *Department of Applied Physics and Physico-Informatics, Keio University, Yokohama 223-8522, Japan*
[2] *JST, PRESTO, 4-1-8 Honcho, Kawaguchi, Saitama, 332-0012, Japan*

NIR light emitters are widely used in the areas of optical communication with optical fibers and silicon photonics. However, because of their large footprints, the low crystallinity of the compound semiconductors grown directly on Si wafers, these emitters face significant challenges with respect to their integration with silicon-based platforms. Here we talk about two topics: (i) single photon generation from an carbon nanotubes (CNTs) [1] and (ii) electrically driven, high-speed light emitters based on nanocarbon materials [2-4].

Photon antibunching from low dimensional materials, such as semiconductor quantum dots, have been attracted much attention for use as single-photon sources in quantum cryptography. However, single photon sources at both room temperature and telecommunication wavelength have not been reported so far. In this study, we demonstrated the photon antibunching in a SWNT at telecommunication wavelength and room temperature [1].

We also report the electrically driven, high-speed light emitter based on CNTs and graphene [1-3]. Nanocarbon light emitters, which are based on electron-hole recombination or blackbody radiation, have advantages for their integration with silicon-based platforms: (i) a small footprint and simple fabrication processes, (ii) direct integration on a Si wafer.

This work was partially supported by PRESTO and A-STEP from JST, KAKENHI from MEXT, SCOPE from MIC, Japan.

[1] T. Endo, J. I-Hayase, H. Maki, Appl. Phys. Lett., **106**, 113106 (2015).
[2] T. Mori, Y. Yamauchi, S. Honda, H. Maki, Nano Lett. **14**, 3277 (2014)..
[3] M. Fujiwara, D. Tsuya, H. Maki, Appl. Phys. Lett., **103**, 143122 (2013).
[4] N. Hibino, S. Suzuki, H. Wakahara, Y. Kobayashi, T. Sato, H. Maki, ACS Nano, **5**, 1215 (2011).

Corresponding Author: H. Maki
Tel: +81-45-566-1643, Fax: +81-45-566-1587
E-mail: maki@appi.keio.ac.jp

Process study of graphite oxidation toward tailor-made graphene oxide

○Yuta Nishina[1, 2], Naoki Morimoto[3], Hideyuki Suzuki[1]

[1] *Research Core for Interdisciplinary Sciences, Okayama University, Okayama 700-8530, Japan*
[2] *Precursory Research for Embryonic Science and Technology, Japan Science and Technology Agency, Saitama 332-0012, Japan*
[3] *Graduate School of Medicine, Dentistry, and Pharmaceutical Sciences, Division of Pharmaceutical Sciences, Okayama University, Okayama 700-8530, Japan.*

Oxidation of graphite was reported 175 years ago [1], which was recently improved to the preparation of graphene oxide [2, 3]. Although there have been reported a lot of modification, the optimization of the oxidation conditions has depended on try-and-error. The reason would be because the *in situ* analysis of the oxidation process is tough to investigate since the reaction is performed in concentrated sulfuric acid or nitric acid with strong oxidant.

Here, we focused on *in situ* analysis of the oxidation of graphite with potassium permanganate in concentrated sulfuric acid using synchrotron X-ray absorption fine structure (XAFS) and X-ray diffraction (XRD) analyses, both of which are suitable for the strongly acidic and oxidative conditions due to the non-contact and non-destructive measurement.

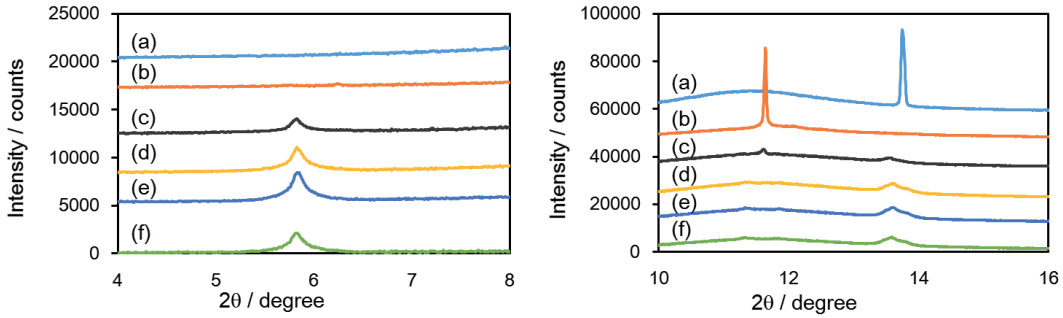

Fig. 1 Time course analysis of graphite oxidation using $KMnO_4$ in H_2SO_4 by XRD. (a) Graphite dispersion in H_2SO_4. (b) 1 min, (c) 30 min, (d) 60 min, (e) 90 min, and (f) 120 min after $KMnO_4$ addition. $\lambda = 0.8$ Å.

Fig. 1 shows the XRD analysis during the oxidation of graphite. A peak at 13.8° is graphite (002), which is instantly shifted to 11.6° after $KMnO_4$ addition. As the peak at 11.6° decreased, new peak appeared at 5.8°. XAFS analysis showed that most of active Mn species (Mn^{7+}) disappeared after 120 min. These results suggest that oxidation of graphite can almost complete within 120 min.

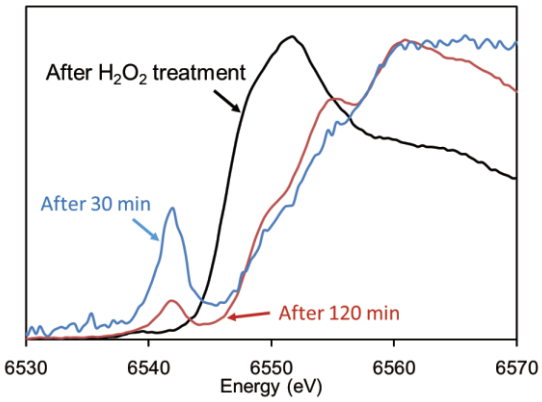

Fig. 2 Time course analysis of graphite oxidation using $KMnO_4$ in H_2SO_4 by XAFS.

[1] C. Schafhaeutl, J. Prakt. Chem. 21, 129-157 (1840).
[2] N. I. Kovtyukhova, *et al.* Chem. Mater. 11, 771-778 (1999).
[3] D. C. Marcano, *et al.*, ACS Nano, 4, 4806-4814 (2010).

Corresponding Author: Y. Nishina
Tel: +81-86-251-8718, Fax: +81-86-251-8718,
E-mail: nisina-y@cc.okayama-u.ac.jp

Exploring Ultimate Coherent Photon Technology and its Applications

Junji Yumoto
Institute for Photon Science and Technology, Graduate School of Science
The University of Tokyo, Tokyo 113-0033, Japan

More than 55 years have passed since the first laser demonstration in 1960. Over these several decades, laser physics and laser technology have been developed at a rapid pace, and high power & ultra-short pulses with a high peak power of several 100 GW, and a pulse duration in the range of femtoseconds have been achieved. This advanced laser technology has been creating new fields not only in science but also in industry.

A 10 femtosecond optical pulse at a wavelength of 800nm has a bandwidth of 500nm-1100nm (300 THz) according to the time-bandwidth product limited by uncertain relations. However, it is very difficult to obtain a Fourier Transform limited pulse because the wide bandwidth of 300 THz deforms the temporal pulse shape due to optical dispersion.

Every media like atom, condensed matter, even biomaterial interacting with strong light fields demonstrates a lot of phenomena which are beyond our imagination. Interaction between ultra-short optical pulses and atoms generates higher harmonic optical fields called High-Harmonic Generation (HHG). Harmonic generation higher than the 100th order, pumped by 800-nm short laser pulse have been observed and it reached to EUV [1].

A “Coherent Photon Ring (CPR)” is now under development with Laser Technology Laboratory, RIKEN. CPR is a short pulse ring laser and covers the range from EUV, visible, IR and THz. It has a feature of simultaneous multi-wavelength operation, which is achieved by placing wavelength conversion elements in the cavity. To achieve multi-wavelength operation, high peak power & short pulse generation is essential. It is an obstacle, however, to generate a high peak power of more than 1GW while avoiding optical damage to the optical components that make up the cavity. To work around this issue, a 100m ring cavity is employed to reduce the average power in the cavity. That is, a low repetition rate due to the long cavity length enables high peak power pulses to be generated but with a relatively low average power. A CPR consisting of a 100m ring cavity has been already demonstrated at a repetition rate of 2.55MHz. It operates at a wavelength of 1030nm with a pulse-width of 710fsec, and the peak power reaches 1.4×10^{14}W/cm^2. Argon gas is placed in the cavity and laser light focused onto the gas is converted to coherent UV light [2].

On the other hand, the development of laser technology also creates a lot of applications, for example, laser material processing. With this type of processing, light-matter interaction is one of the fundamental mechanisms. We are now working to understand the physics behind the laser cutting of composite materials (Carbon Fiber Reinforced Plastic) and wide-bandgap materials (glass and sapphire). Recent laser processing results are also included in the talk.

[1] M. Protopapas, et al., "Atomic physics with super-high intensity lasers", Rep. Prog. Phys. 60, 389 (1997), K. Ohmori ed., “Attosecond Science”, Kagakudojin (2015) (Japanese)

[2] N. Kanda, et al., “Yb:YAG thin disk mode-locked oscillator with high pulse energy for intra-cavity high harmonic generation”, IEEE Photonics Conference 2014, WG1.3 (Invited).

Corresponding Author: J. Yumoto
Tel: +81-3-5841-4082
E-mail: yumoto@ipst.s.u-tokyo.ac.jp

Physics and engineering of excitons in carbon nanotubes

○Yuhei Miyauchi [1,2]

[1] *Institute of Advanced Energy, Kyoto University, Kyoto 611-0011, Japan*
[2] *Graduate School of Science, Nagoya University, Chikusa, Nagoya 464-8602, Japan*

Since the first report of near infrared photoluminescence from individually dispersed semiconducting single-walled carbon nanotubes (SWNTs) in 2002 [1], their optical properties, dominated by correlated electron–hole bound states known as excitons [2,3], have been intensively studied for exploring photophysics in nearly ideal quasi-one-dimensional systems and their applications in the fields of optoelectronics and bioimaging. Here we discuss some of the interesting photophysics related to excitons in SWNTs clarified over the past decade [4]. These include impacts of the photoluminescence spectroscopy in the researches of SWNT growth [5,6], effects of exciton–phonon interactions [7], anisotropy in optical absorption and emission [8,9], effects of surrounding materials on the exciton energies [10], radiative lifetimes of the excitons [11], exciton migration along SWNTs [12], and tunable electronic correlation effects by carrier doping [13]. On the basis of these knowledge, we will discuss how the excitonic optical properties in SWNTs can be engineered for their future applications as near infrared light emitting materials. Especially, we will focus on the impact of localized states intentionally embedded in SWNTs on their luminescence properties, such as brightening of exciton photoluminescence due to dimensionality modification [14,15], and emergence of anomalously efficient upconversion photoluminescence in SWNTs [16]. Potential applications of SWNTs with the engineered localized states and remaining problems will also be discussed.

[1] M. J. O'Connell *et al*., *Science* **297**, 593 (2002).
[2] T. Ando, *J. Phys. Soc. Jpn*. **66**, 1066 (1997).
[3] F. Wang, G. Dukovic, L. E. Brus, and T. F. Heinz, *Science* **308**, 838 (2005).
[4] Y. Miyauchi, *J. Mater. Chem. C* **1**, 6499 (2013).
[5] S. Maruyama, R. Kojima, Y. Miyauchi, S. Chiashi, and M. Kohno, *Chem. Phys. Lett.* **360**, 229 (2002).
[6] Y. Miyauchi, S. Chiashi, Y. Murakami, Y. Hayashida, and S. Maruyama, *Chem. Phys. Lett.* **387**, 198 (2004).
[7] Y. Miyauchi, and S. Maruyama, *Phys. Rev. B* **74**, 035415 (2006).
[8] Y. Miyauchi, M. Oba, and S. Maruyama, *Phys. Rev. B* **74**, 205440 (2006).
[9] Y. Miyauchi, H. Ajiki, and S. Maruyama, *Phys. Rev. B* **81**, 121415(R) (2010).
[10] Y. Miyauchi *et al*., *Chem. Phys. Lett.* **442**, 394 (2007).
[11] Y. Miyauchi, H. Hirori, K. Matsuda, and Y. Kanemitsu, *Phys. Rev. B* **80**, 081410(R) (2009).
[12] Y. Miyauchi *et al*., *J. Phys. Chem. C* **114**, 12905 (2010).
[13] Y. Miyauchi, *et al*., *Phys. Rev. B* **92**, 205407 (2015).
[14] Y. Miyauchi, M. Iwamura, S. Mouri, T. Kawazoe, M. Ohtsu, and K. Matsuda, *Nat. Photonics* **7**, 715 (2013).
[15] M. Iwamura, N. Akizuki, Y. Miyauchi *et al*., *ACS Nano* **8**, 11254 (2014).
[16] N. Akizuki, S. Aota, S. Mouri, K. Matsuda, and Y. Miyauchi, *Nat. Commun.* 6:8920 (2015).

Corresponding Author: Y. Miyauchi
Tel: +81-774-38-3463, Fax: +81-774-38-3467,
E-mail: miyauchi@iae.kyoto-u.ac.jp

一般講演
General Lecture

1 – 1 ～ 1 – 10
2 – 1 ～ 2 – 6
3 – 1 ～ 3 – 11

Microscopic Growth Process of Fullerenes and Extreme Abundance of C_{60}

Yusuke Ueno[1], Joseph Chan[1], Masayuki Toyoda[1], and ○Susumu Saito[1-3]

[1]*Department of Physics, Tokyo Institute of Technology, Tokyo 152-8551, Japan*
[2]*International Research Center for Nanoscience and Quantum Physics, Tokyo Institute of Technology, Tokyo 152-8551, Japan*
[3]*Materials Research Center for Element Strategy, Tokyo Institute of Technology, Yokohama, Kanagawa 226-8503, Japan*

The C_{60} cluster with truncated-icosahedron geometry was first proposed theoretically by Osawa in 1970 [1], and the first experimental indication of the abundant production of C_{60} and other even-number carbon clusters was reported in 1984 although not cage geometries but linear-chain geometries were considered [2]. One year later, the *extreme abundance* of C_{60} in the carbon cluster beam under specific production condition was observed and the icosahedral C_{60} cage geometry was proposed [3]. However, it took five more years for the *macroscopic amount* of fullerene-cage C_{60} clusters to be produced from graphite [4]. Although the icosahedral geometry of the C_{60} cluster is *beautiful*, its binding energy per atom is pointed out to be less than that of the D_{5h} C_{70} cluster which is usually much less abundant than the C_{60} cluster [5]. The origin of the extreme abundance of the C_{60} cluster is, therefore, to be explained *not from the energetics but from the kinetics*. However, a quarter century already passed away but the full understanding of the miscroscopic growth process of C_{60} and other fullerenes has not been obtained yet. We previously studied the microscopic growth process of carbon clusters and fullerenes using the transferable tight-binding model combined with the constant-temperature molecular-dynamics method, and clarified the importance of the weak but long-range attractive interaction in the fullerene growth process [6]. The closed fullerene cage geometry was observed for relatively small clusters, and also the shrinkage of larger fullerene cages via C_2 loss process was observed.

In the present work, we report the statistical analysis of the carbon-cluster growth/shrinkage process. At certain conditions, the extreme abundance of C_{60} is found to emerge (Fig. 1). In our presentation, we discuss the details of this finding.

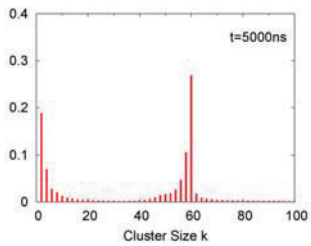

Fig. 1 Population densities of carbon clusters

[1] E. Osawa, Kagaku (Kyoto) **25**, 854 (1970).
[2] E. A. Rohlfing, D. M. Cox, and A. Kaldor, J. Chm. Phys. **81**, 3322 (1984).
[3] H.W. Kroto, J. R. Heath, S. C. O'Brien, R. F. Curl, and R. E. Smalley, Nature **318**, 162 (1985).
[4] W. Krätschmer, Lowell D. Lamb, K. Fostiropoulos, and D. R. Huffman, Nature **347**, 354 (1990).
[5] S. Saito and A. Oshiyama, Phys. Rev. B **44**, 11532 (1991).
[6] Y. Ueno and S. Saito, Phys. Rev. B 77, 085403 (2008).

Corresponding Author: Susumu Saito
E-mail: saito@stat.phys.ttiech.ac.jp

Molecular dynamics simulation of the growth of fullerenes from carbon atoms

Joseph Chan and Susumu Saito

Department of Physics, Tokyo Institute of Technology, Tokyo 152-8550, Japan

In a study by Ueno and Saito [1], the geometries and energetics of small carbon clusters and the reaction between carbon clusters are studied using the long-range transferable tight-binding model parametrized by Omata *et al.* (Omata TB) [2], the local-density approximation (LDA) in the framework of the density-functional theory, and the constant-temperature molecular dynamics combined with Omata-TB (Omata TBMD). The study has clarified the microscopic formation process of C_{60} and other fullerenes.

In this study we use the same Omata TBMD to revisit in more details the formation of carbon clusters and reactions among these clusters in the formation process of fullerenes. We first fill the Molecular Dynamic cell (MD cell) with 300 C atoms with randomized initial positions. Using constant-temperature molecular dynamics, we carefully monitor and examine the evolution of the system.

In Fig. 1, during an early state of the simulation with 300 C atoms, we observe that short chains emerge and then larger clusters start to form from these short chains. Rings start to form too. In Fig. 2, larger clusters emerged. Based on the MD results, we discuss the formation of cage clusters and fullerenes.

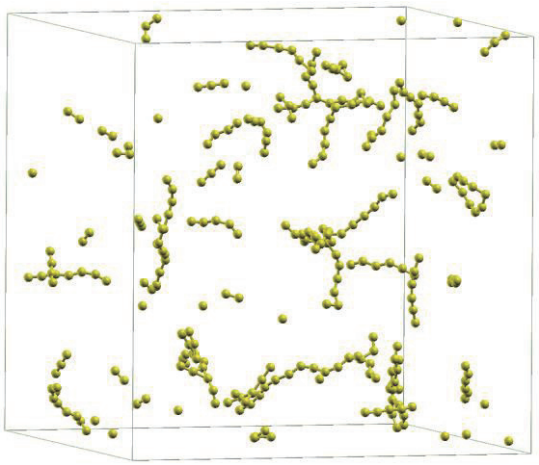

Fig.1 Snapshot of an early state of the MD cell.
Small chains and clusters are formed.
Elapsed time = 1.2 ps
Average energy per atom = -1.65 eV

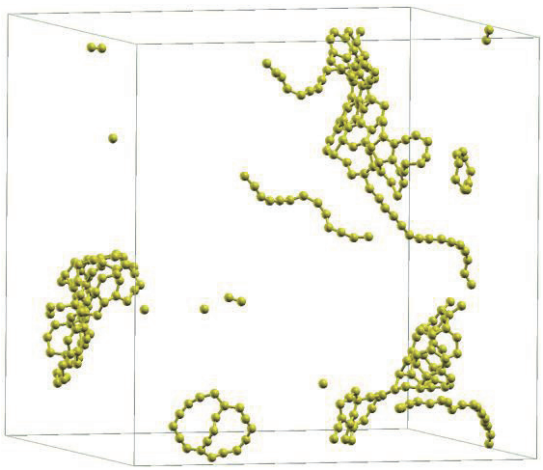

Fig.2 Snapshot of an evolving state of the MD cell.
Larger chains and clusters are formed.
Elapsed time = 12 ps
Average energy per atom = -8.05 eV

[1] Y. Ueno and S. Saito, Phys. Rev. B **77,** 085403 (2008).

[2] Y. Omata, Y. Yamagami, K. Tadano, T. Miyake, and S. Saito, Physica E **29,** 454–468 (2005).

Corresponding Author: J. Chan

E-mail: joechan@stat.phys.titech.ac.jp

Electrochemical Evaluation of Proton Permeability of Monolayer Graphene Grown on Au(111) Electrode

Koji Nakashima, Ryota Kumagai, ○Satoshi Yasuda, Kei Murakoshi

Department of Chemistry, Hokkaido University, Sapporo 060-0810, Japan

Graphene has been attracted attention as novel two-dimensional separation membrane because of high throughput arising from its one-atomic thickness. Current experimental studies demonstrated that molecules as small as He is impermeable for monolayer graphene while proton is permeable. The proton permeability is fundamentally important as well as industrially useful for hydrogen-based technologies. However, despite of the significant importance, there have been few experimental studies on understanding of the intrinsic proton permeability of the monolayer graphene. In this study, proton permeability of monolayer graphene grown on Au(111) electrode was evaluated using electrochemical technique. Monolayer graphene with high crystalline structure was synthesized on Au(111) single crystal by atmospheric CVD.[1] Cyclic voltammetry measurement of the graphene on Au(111) electrode in 0.1M H_2SO_4 aqueous solution showed inhibition of the oxidation-reduction reactions of the Au, indicating that the graphene efficiently blocks water molecule to access the underlying Au surface. On the other hand, cathodic current arising from hydrogen evolution reaction (HER) could be observed in spite of the graphene covering. AFM measurement of the graphene on the Au electrode after the HER showed that several nanometer-size balloon structures were clearly observed at grain boundaries in the graphene (Fig. 1(b)). These results strongly suggest that defect structures at the grain boundaries behave as proton channel, and that the protons selectively penetrates underlying Au surface through the defects, resulting in the balloon structure formation.

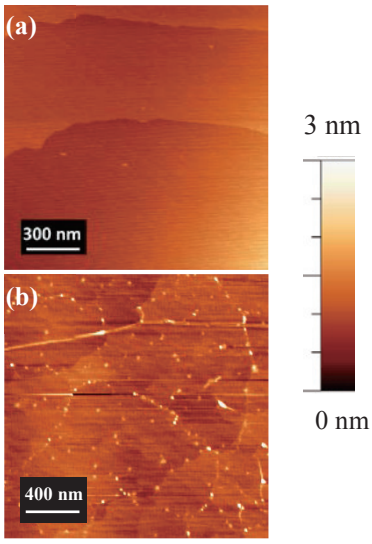

Fig.1 AFM images of graphene/Au(111) (a) before and (b) after HER.

[1] S. Yasuda et al., *J. Phys. Chem. Lett.*, **6**, 3403 (2015).

Corresponding Author: S. Yasuda and K. Murakoshi
TEL & FAX: +81-(0)11-706-4811
E-mail: satoshi-yasuda@sci.hokudai.ac.jp

Magnetic property of two-dimensional networks of high-spin hydrocarbon molecules

○Mina Maruyama, Susumu Okada

Graduate School of Pure and Applied Sciences, University of Tsukuba, Tsukuba 305-8571, Japan

Hydrocarbon molecules occasionally possess high spin states due to the unpaired π electrons corresponding to the number difference between two sublattices of their hexagonal networks. A phenalenyl radical ($C_{13}H_9$ molecule with a triangular shape) is one of representative example of such high-spin molecules. In the case, due to the sublattice imbalance, the molecule possesses an unpaired electron leading to the S=1/2 ground state. By connecting the high-spin molecules via sp^2 network, we can easily design the one- or two-dimensional (2D) sp^2 C networks possessing the various magnetic orderings. In this work, we theoretically design novel 2D magnetic hydrocarbon network consisting of phenalenyl radicals and benzene molecules which are alternately arranged with the C_3 symmetry by using density functional theory with generalized gradient approximation.

We find that the 2D phenalenyl network possesses planar atomic network with various conformations of benzene units connecting the phenalenyl units. Furthermore, we find that the networks possess two spin states as their stable states (Fig. 1): The polarized radical spin on the phenalenyl unit has the antiparallel and parallel coupling spin states and the antiparallel spin coupling states is more stable than parallel spin coupling state by 13.9 meV per unit cell. Furthermore, the relative stability of the spin polarized states depends on the relative arrangements of the benzene rings connecting the phenalenyl units. By rotating the benzene ring between phenalenyl units from the flat to perpendicular conformations, the spin interaction between phenalenyl units monotonically decrease, indicating that the spin states of the sheet is tunable by controlling the orientation of benzene rings (Fig. 2).

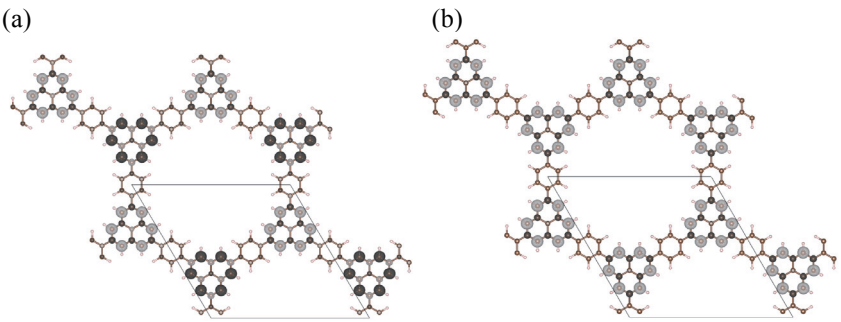

Fig.1 Isosurfaces of spin density of phenalenyl sheet with (a) antiprallel and (b) parallel spin coupling states.

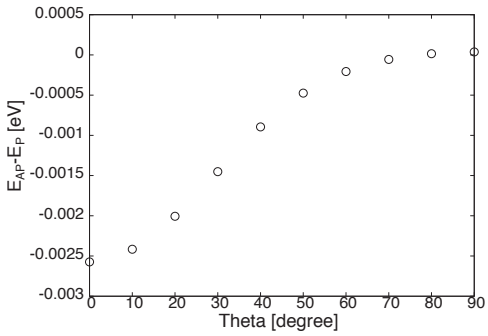

Fig. 2 The spin interaction between phenalenyl units as a function of the rotational angle of benzene ring.

Corresponding Author: M. Maruyama
Tel: +81-29-853-5600 (ext. 8233), Fax: +81-29-853-5924,
E-mail: mmaruyama@comas.frsc.tsukuba.ac.jp

Edge effect on electrode contacts to transition metal dichalcogenides

○Ryo Nouchi[1]

[1] *Nanoscience and Nanotechnology Research Center, Osaka Prefecture University, Sakai, Osaka 599-8570, Japan*

The operation of semiconductor electronic devices such as field-effect transistors (FETs) is largely governed by metal/semiconductor interfaces where charge carriers (electrons or holes) are injected from the metallic electrode into the semiconductor channel. A total electric resistance of a semiconductor device is expressed by a summation of the semiconductor channel resistance and the parasitic electrode contact resistances. In a short channel device, the channel resistance is very small, and the contact resistance becomes a dominant contribution instead. The magnitude of the contact resistance is determined by the height of a charge injection (Schottky) barrier formed at the electrode contact. In the ideal case, the barrier height can be controlled fully by changing the work function of the electrode. However, interfacial electronic states formed at the metal contacts generally deteriorate the controllability, which is known as the Fermi-level pinning.

This study focuses on metallic electrode contacts to emergent ultrathin two-dimensional (2D) sheets obtained from exfoliation of semiconducting transition metal dichalcogenides (TMDCs). In the case of three-dimensional (3D) semiconductors, dangling bonds should appear at the crystal surface, leading to significant Fermi-level pinning. On the other hand, in the case of 2D semiconductors obtained from layered crystals, small amount of dangling bonds are expected because of the weak inter-layer coupling based on van der Waals interactions, which results in the higher controllability of the electrode contacts than 3D counterparts [1,2].

However, the previous considerations on electrode contacts to TMDC sheets have not taken into account their edges. Miniaturization of semiconductor devices requires the narrowing of the channel in addition to the well-known shortening. In the narrow channel devices, the effect of the edges should be significantly large. In this presentation, the edge-induced effect on the electrode contacts to exfoliated flakes of molybdenum disulfide (MoS_2), an archetypal TMDC, will be discussed. The Schottky barrier height has been found to increase as the channel becomes narrower, which can be understood by the Fermi-level pinning to the edge states that locate around the mid gap (Fig. 1).

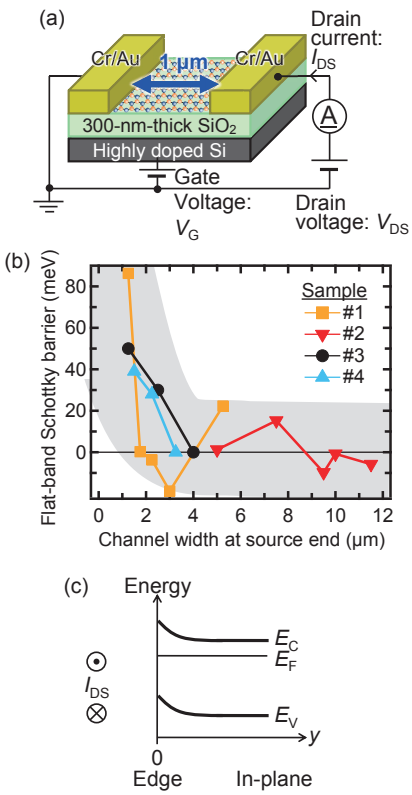

Fig. 1 (a) Structure of the MoS_2 FET. (b) Channel-width dependent Schottky barrier. (c) Edge-induced band bending.

[1] H. Fang *et al.*, Nano. Lett. **12**, 3788 (2012).
[2] W. Liu *et al.*, Nano. Lett. **13**, 1983 (2013).

Corresponding Author: R. Nouchi
Tel: +81-72-254-8394, Fax: +81-72-254-8394,
E-mail: r-nouchi@21c.osakafu-u.ac.jp

Bandgap modulation in one-dimensional interface of MoS_2/WS_2-based semiconductor heterojunction

○Yu Kobayashi[1], Shoji Yoshida[2], Ryuji Sakurada[2], Tetsuki Saitoh[1], Kenji Watanabe[3], Takashi Taniguchi[3], Yutaka Maniwa[1], Hidemi Shigekawa[2], Yasumitsu Miyata[1,4,*]

[1]*Department of Physics, Tokyo Metropolitan University, Hachioji 192-0397, Japan*
[2]*Faculty of Pure and Applied Sciences, University of Tsukuba, Tsukuba 305-8573, Japan*
[3]*National Institute for Materials Science, 1-1 Namiki, Tsukuba 305-0044, Japan*
[4]*JST-PRESTO, Kawaguchi 332-0012, Japan*

Interface of semiconductor heterojunctions has been one of the central topics in modern solid state physics and applications in electronics and optoelectronics. Recently, atomic layers of semiconducting transition metal dichalcogenides (TMDCs) are expected to realize novel one-dimensional state at their heterojunction interface [1-5]. However, the realization of conducting interface state still remains as an unsolved issue. Here, we report the observation of conductivity enhancement and unique bandgap modulation of the one-dimensional heterojunction interface based on bilayer TMDCs. The heterojunction is composed of bilayer WS_2 and vertically-stacked MoS_2/WS_2 heterostructure (Fig.1a), which can be grown on graphite by chemical vapor deposition as reported in our previous work [6]. This conductivity enhancement has never seen for the heterojunctions of monolayer MoS_2-WS_2, and monolayer-bilayer WS_2. Furthermore, STM/STS measurements reveal the upshift of both valence and conduction band edges and band-gap narrowing around the heterointerface (Fig.1b). This bandgap modulation could be explained by stacking mismatch due to lattice strain around the heterointerface. The present findings indicate that highly tunable electronic properties of TMDC systems provide an ideal system to realize 1D confined electronic system in the heterointerface.

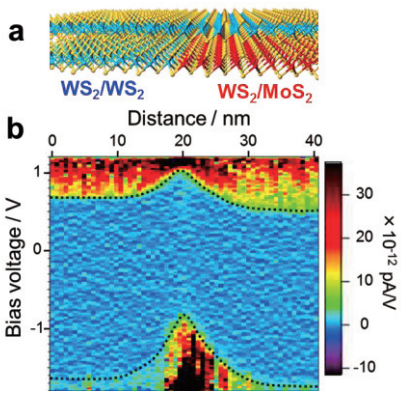

Fig.1 (a) Structure model of the present bilayer heterojunction. (b) Map of color scale dI/dV curves calculated from the spatially-resolved STS spectra.

[1] Y. Gong, *et al.* ***Nat. Mater.,*** 13, 1135 (2014)., [2] X. Duan, *et al.* ***Nat. Nanotechnol.***, 9, 1024 (2014).,
[3] C. Huang, *et al*. ***Nat. Mater.,*** 13, 1096 (2014)., [4] Y. Kobayashi *et al*., ***Nano Res.***, 8, 3261 (2015).,
[5] S. Yoshida, *et al*. ***Sci. Rep.***, 5, 14808 (2015)., [6] Y. Kobayashi *et al.,* ***ACS Nano***, 9, 4056 (2015).
Corresponding Author: Yasumitsu Miyata, Tel: 042-677-2508, E-mail: ymiyata@tmu.ac.jp

Geometric and electronic properties of thin-layer GeSe and GeSe/MoS_2 heterostructures

○Mari Ohfuchi

Fujitsu Laboratories Ltd., Atsugi 243-0197, Japan

Since graphene was discovered, there has been no sign of abandoning the exploration of novel two-dimensional materials. Continuous requirements for diversity have been extending their reach into group IV monochalcogenides, such as GeSe; nevertheless, only a few theoretical studies have investigated monolayer GeSe [1]. In this study, we perform first-principles calculations to examine the geometric and electronic properties of thin-layer GeSe and GeSe/MoS_2 heterostructures.

We employed the density functional theory (DFT) code, OpenMX [2]. The lattice constants of GeSe drastically change as the thickness decreases. Accordingly, the internal atomic positions also undergo a significant transformation. The Ge atoms lie outside the layer for the bulk material (Fig. 1(c)), whereas Se atoms lie outside the layer for monolayer (Fig. 1(a)). We found that the direct band gap of bilayer GeSe (Fig.1 (b)) becomes identical to the indirect band gap as does monolayer GeSe [1] because of the quantum confinement of the state at Γ that spreads over the layers. We also studied the properties of GeSe/MoS2 heterostructures (Fig.2). We found that the lattices of GeSe(4×4) and MoS_2(3×5) match to within 1%. Although the atomic positions in the GeSe layer approach those of bilayer GeSe to some extent, the Se atoms still lie outside the layer. The distance between the Se layer and the S layer in MoS_2 was obtained to be 0.36 nm, which is slightly greater than the value of 0.31 nm for bilayer GeSe and MoS_2. We also found that the discontinuities of the conduction band minimum (E_C) and the valence band maximum (E_V) are 0.71 and 1.46 eV respectively. Taking into consideration that the experimental band gap of the monolayer MoS_2 is 1.89 eV [3], the band gap of monolayer GeSe is expected to be 1.14 eV.

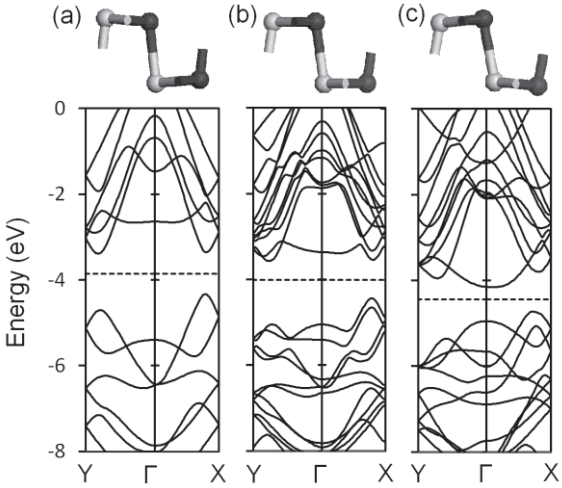

Fig.1: Side views of atomic geometry and band structures of (a) monolayer, (b) bilayer, and (c) bulk GeSe. The dark and light gray spheres represent Ge and Se atoms respectively.

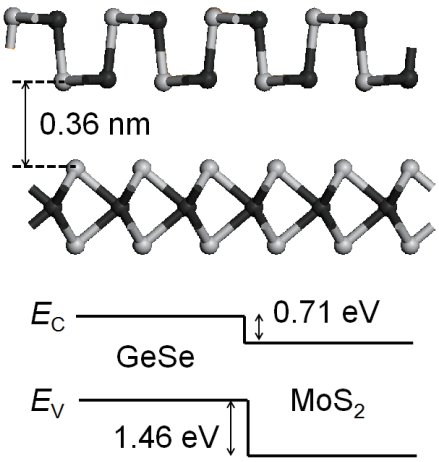

Fig.2: Side view of GeSe/MoS_2 heterostructure and schematic band diagram. The dark and light gray spheres also represent Mo and S atoms respectively.

[1] Y. Hu et al., Appl. Phys. Lett. 107, 122107 (2015). [2] http://www.openmx-square.org/.
[3] K. F. Mak et al., Phys. Rev. Lett. 105, 136805 (2010).

Corresponding Author: M. Ohfuchi
Tel: +81-46-250-8194, Fax: +81-46-250-8274, E-mail: mari.ohfuti@jp.fujitsu.com

1 wt% carbon nanotubes realized lithium ion batteries without binder nor metal foil

Kei Hasegawa and Suguru Noda

Department of Applied Chemistry, Waseda University, Tokyo 169-8555, Japan

Carbon nanotubes (CNTs) have been extensively studied as a promising material for next-generation energy storage devices. Freestanding films of few wall CNTs (FWCNTs) can capture any material in the conductive matrix without polymer binders and work as current corrector replacing heavy foils of metal. We have developed scalable synthesis of FWCNTs with fluidized bed chemical vapor deposition (CVD) [1] and demonstrated the binder-free CNT/activated carbon freestanding composites for electrochemical capacitor electrodes [2]. To examine the practicality of CNTs for energy storage, we fabricated a graphite/$LiCoO_2$ lithium ion battery with the electrodes only by 1 wt% FWCNTs and 99 wt% active materials and demonstrated full cells without binder nor metal foil.

Freestanding electrodes of 1-10 wt% FWCNTs with graphite and $LiCoO_2$ were prepared by co-dispersion in 2-propanol and filtration. Graphite electrodes of 4.5 mg/cm^2 (corresponding to 20 μm-thick bulk graphite) and $LiCoO_2$ electrode of 11.3 mg/cm^2 (22 μm) were prepared. 2-electrode coin cells were prepared with Hipore^{TM} (12 μm-thick) separator and electrolyte of 1 M $LiClO_4$ in ethylene carbonate/ diethyl carbonate and galvanostatic charge/discharge tests were carried out.

Both graphite and $LiCoO_2$ flexible freestanding films were fabricated with FWCNTs of 1 wt% or more. The films showed higher mechanical stability and electric conductivity with larger amount of CNTs. On the other hand, those with fewer CNTs had higher packing density. 1 wt% CNT networks roughly covered and captured all the 99 wt% active material particles (Fig. 1). Fair cycle durability were shown not only at the half cells but also the Graphite/$LiCoO_2$ full cell (Fig. 2 (left)). The discharge capacity was 267 mAh/$g_{graphite}$ even at a charge/discharge rate as high as 1C (full charge/discharge in 1 hour). The performance of the full cell with line-patterned metal current collectors will also be demonstrated by the 5 cm × 5 cm laminate cells.

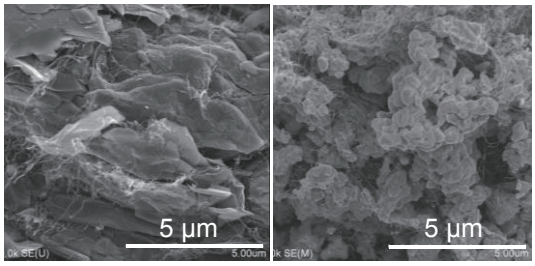

Fig. 1 SEM images of 1 wt% FWCNT electrodes with graphite (left) and $LiCoO_2$ (right).

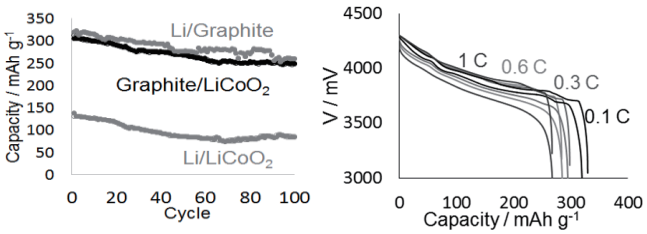

Fig. 2 Cycle performances of 1 wt% FWCNT cells at 1C charge/discharge (372 mAh/$g_{graphite}$ or 160 mA/g_{LiCoO2}) (left). Rate performance of the full cell (right).

Acknowledgements: The authors thank Prof. Osaka, Prof. Momma and Mr. Mikuriya in their support in making cells. This work is supported in part by Grant-in-Aid for Scientific Research (A) #25249111 from MEXT, Japan.

[1] D.Y. Kim, et al., *Carbon* **49** (2011) 1972. [2] R. Quintero, et al., *RSC Adv.* **4** (2014) 8230.

Corresponding Author: Suguru Noda, TEL/FAX: +81-3-5286-2769, E-mail: noda@waseda.jp

Metal-free Transparent Organic Solar Cell with a P-dopant Enhanced Carbon Nanotube Electrode

○ Il Jeon[1], Clement Delacou[2], Antti Kaskela[3], Esko I. Kauppinen[3], Shigeo Maruyama[2], Yutaka Matsuo[1]

[1] *Department of Chemistry, School of Science, The University of Tokyo, 7-3-1 Hongo, Bunkyo-ku, Tokyo 113-0033, Japan*
[2] *Department of Mechanical Engineering, School of Engineering, The University of Tokyo, 7-3-1 Hongo, Bunkyo-ku, Tokyo 113-8656, Japan*
[3] *Department of Applied Physics, Aalto University School of Science, 15100, FI-00076 Aalto, Finland*

Future organic solar cells are greener technology that possesses multi-functionality such as wearable devices and surface conforming photovoltaic textiles, and window solar cells. Prerequisites of these include metal-free, mechanical resilience, and translucency while retaining high power conversion efficiency. For this to be realized, replacing metal electrode with flexible and transparent material is the first step towards this achievement. Previously, many attempts have been made in demonstrating visibly transparent and mechanically resilient solar cells. However, transparent conductors often result in low visible light transparency and device efficiency with no flexibility because no suitable material as a transparent conductor was deployed in device design and fabrication.

Here we report a carbon nanotube based metal-free OSC and its doping that are most effectively structured to date. High-quality dry-deposited carbon nanotube film doped with nitric acid was used as an anode in a transparent organic photovoltaic device. Such concept is unprecedented in the field of organic solar cells and application of CNT doping in this structure is the first-time attempt in a transparent photovoltaic device. Our doped and non-doped SWCNTs employed transparent OSCs showed PCEs of 4.1% and 2.2%, while the leading ITO-based OSC showed a PCE of 7.8%.

Corresponding Author: Y. Matsuo
Tel: +81 3 5841 1476, Fax: +81 3 5841 1476,
E-mail: matsuo@chem.s.u-tokyo.ac.jp

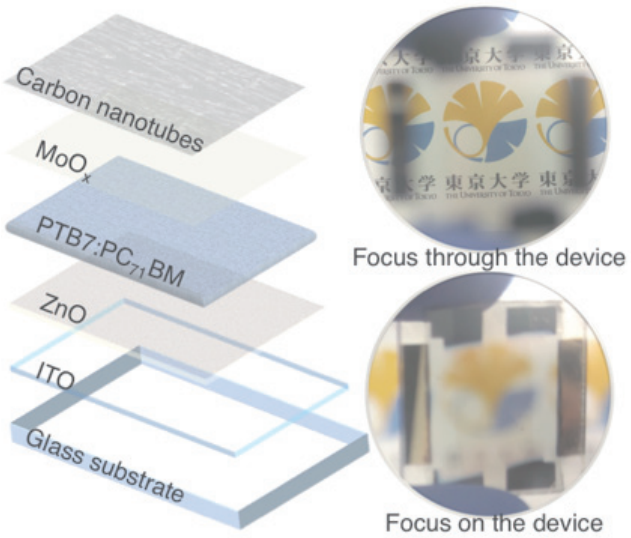

Fig.1 An anatomical illustration of the SWNT-laminated transparent solar cell (left) and its real images with different foci (right).

Oxygen-doped carbon nanotubes as near-infrared imaging probes and fluorescent labels

○Yoko Iizumi[1], Masako Yudasaka[2], Tsukasa Takeuchi[1,3] and Toshiya Okazaki[1]

[1] *National Institute of Advanced Industrial Science and Technology (AIST), CNT-Application Research Center, 1-1-1 Higashi Tsukuba 305-8565, Japan*
[2] *National Institute of Advanced Industrial Science and Technology (AIST), Nanomaterials Research Institute, 1-1-1 Higashi Tsukuba 305-8565, Japan*
[3] *Shimadzu Corporation, 1-3 Kanda Nishiki-cho Chiyoda Tokyo 101-8448, Japan*

Optical imaging using near-infrared (NIR) fluorescence is a new imaging modality that has recently emerged in the fields of biology and medicine. Especially, the wavelength range of above 1300 nm is ideal for biological imaging because of the low tissue autofluorescence and the low absorption coefficient of water. Single-walled carbon nanotubes (SWCNTs) show photoluminescence (PL) in the wavelength region of 1000-1400 nm.

Recently, it was found that the PL efficiency of SWCNTs can be enhanced by substituting oxygen atoms to the carbon network of the tube wall [1]. The oxygen-doped SWCNTs (o-SWCNTs) have been mostly prepared by the exposure of ozone to the SWCNTs solution under the UV light. This method can provide only a small amount of o-SWCNTs, which prevents further applications of the material.

In this conference, we report a very simple method for obtaining o-SWCNTs in bulk quantities. The produced oxygen-doped (6, 5) SWCNTs show NIR fluorescence at a much longer wavelength than that of the o-SWCNTs reported previously, which is just advantageous for NIR imaging (~1280 nm). Immunoassay and fluorescent angiography of mouse using the o-SWCNTs as the NIR fluorescent labels and imaging agents, respectively, are demonstrated.

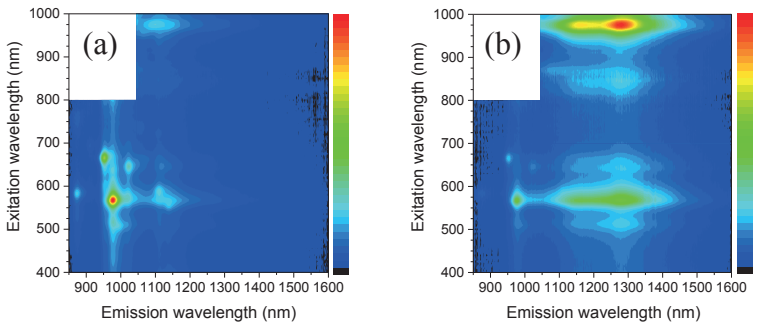

Fig. 1 Photoluminescence contour maps of (a) pristine SWCNTs and (b) oxygen-doped SWCNTs

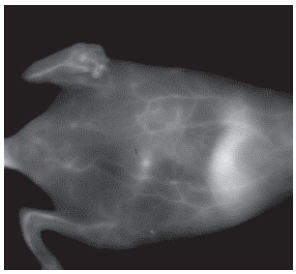

Fig. 2 Photoluminescence image of mouse with o-SWCNT solution injected from tail vein

[1] S. Ghosh, S. M. Bachilo, R. A. Simonette, K. M. Beckingham, R. B. Weisman, *Science*, 330, 1656 (2010).

Corresponding Author: Toshiya Okazaki
Tel: +81-29-861-4173, Fax: +81-29-861-6241
E-mail: toshi.okazaki@aist.go.jp

Highly Efficient Synthesis of Vertically-Aligned Carbon Nanotube Array at Temperature Exceeding 900 ºC Enhanced by Carbon Monoxide

○Shunsuke Sakurai, Maho Yamada, Don N. Futaba, Kenji Hata

CNT-Application Center, National Institute of Advanced Industrial Science and Technology (AIST), Tsukuba 305-8565, Japan

Temperature is one of the most critical factors governing the several fundamental aspects of carbon nanotube (CNT) synthesis, such as efficiency, purity, and the quality of CNTs including the distributions of diameter, chirality, and crystallinity. However, the effect of temperature is highly dependent on the growth technique (e.g. arc-discharge method, and chemical vapor deposition (CVD) from catalyst array on a substrate) and is not yet fully understood, because temperature simultaneously affects multiple aspects of CNT synthesis process. Specifically, in addition to driving the chemical reaction on catalyst surface, temperature also governs gas phase decomposition of carbon feedstock and the evolution of metal catalyst particle. The CVD technique using catalyst array on a substrate has been well established to synthesize a vertically aligned CNTs (forests) in a high yield; however, the standard temperature window typically falls within 700−850 ºC, especially for high yield single-walled CNT (SWNT) synthesis. Although extending to a higher temperature window is an attractive target to study CNT growth termination, for example, a steep decrease in yield has been reported above 850 ºC when using H_2O as a growth enhancer [1].

In this study, we used the growth enhancers, such as CO and CO_2, in place of H_2O, with a C_2H_2 carbon feedstock and sequentially sputtered catalyst substrate film of Fe (1.8 nm)/AlO_x (40 nm) for CNT synthesis at higher temperature. Unsurprisingly, a very poor yield (< 0.1 mg/cm^{-2}) was obtained at a high temperature of 900 ºC when using a H_2O; however, in contrast, the use of CO results in a significant increase in yield of SWNT forests (>2 mg/cm^{-2}) at identical process temperatures, i.e., 900 ºC (Figure 1). The above result, combined with further studies including the observation of catalyst evolution at high temperature and the forest growth rate analysis based on *in-situ* height measurement, indicate that a growth termination mechanism for CO at > 900 ºC stems from a rapid Ostwald ripening of Fe catalyst. The mechanism for the growth termination at lower temperature invoked by using H_2O, and the temperature effect on the structure of synthesized CNT are also discussed in the presentation.

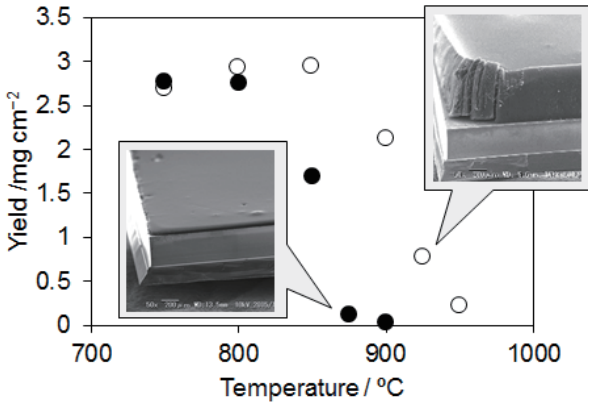

Fig. 1. CNT yield vs temperature for different growth enhancers (white: CO, black: H_2O). Inset: SEM images of SWNT forests grown on Si substrates.

[1] H. Kimura, Don N. Futaba, M. Yumura, K. Hata. *J. Am. Chem. Soc.* **134**, 9219 (2012).

Corresponding Author: S. Sakurai
Tel: +81-29-861-6205, Fax: +81-29-861-4851,
E-mail: shunsuke-sakurai@aist.go.jp

2-2

Extended alcohol catalytic chemical vapor deposition for efficient growth of small-diameter single-walled carbon nanotubes beyond (6,5)

○Bo Hou[1], Rong Xiang[2], Taiki Inoue[2], Shohei Chiashi[2], Shigeo Maruyama[1,2]

[1] *Energy NanoEngineering Lab., Department of Energy and Environment, AIST, Tsukuba 305-8564, Japan*
[2] *Department of Mechanical Engineering, The University of Tokyo, Tokyo 113-8656, Japan*

SWNTs with diameters smaller than (6,5) (~0.8 nm) are known to be very inefficient to grow unless inside of special zeolite pore or inside of an outer nanotube. Hence, super-small diameter SWNTs were rarely directly grown in reported works. Here we extended the work window of alcohol catalytic chemical vapor deposition (ACCVD) for efficient growth of super-small diameter SWNTs. The temperature range of growing high-quality SWNTs was extended lower than 500 ^{o}C combining with very low partial pressure of ethanol down to 0.02 Pa. Growth mechanism is clarified through kinetic discussion on the experimental map. The relationship of temperature and pressure was identified: SWNTs can grow in lower CVD temperature accompanied with proper lower pressure, and it was found that pressure is proportional to temperature for growing SWNTs with stable quality.

In particular, the small diameter limit was extended and the ratio of smaller diameter tubes was significantly increased in the expanded ACCVD. During the decreasing CVD temperature, super-small diameter SWNTs (0.8 nm > d_t > 0.52 nm) were obtained around 500 ^{o}C, 5 Pa. Resonant Raman with 5 excitation laser lines, absorption and photoluminescence (PL) are used to characterize the abundance of small diameter nanotubes, and chirality of super-small diameter SWNTs were assigned as (6,4), (5,4), (5,3), (6,1) etc..

Corresponding Author: Shigeo Maruyama
Tel: +81-29-861-2073, Fax: +81-29-851-7523,
E-mail: maruyama.nano@aist.go.jp

High resolution EELS on individual carbon nanotubes

○Ryosuke Senga[1], Thomas Pichler[2] and Kazu Suenaga[1]

[1] *Nanomaterial research institute, AIST, Tsukuba 305-8565, Japan*
[2]*Faculty of Physics, University of Vienna, Strudlhofgasse 4, A-1090 Vienna, Austria*

Carbon nanotube has been known as an ideal quantum object that can widely alter physical properties upon its atomic arrangement. However the direct identification of physical properties for individual carbon nanotubes is still difficult. For instance, photoemission and X-ray absorption spectroscopies which are widely used to measure the optical and electronic properties do not have the spatial resolution to identify the local changes of the band structure on an isolated carbon nanotubes. Scanning tunneling spectroscopy is one of the ways to measure the local density of states (DOS) of individual carbon nanotubes, though the modification of the DOS by substrates is hardly excluded. Thus, it is necessary to realize both high-energy resolution spectroscopy and high-spatial resolution imaging simultaneously on individual freestanding carbon nanotubes.

Herein, we successfully demonstrate highly-localized electronic properties of individual carbon nanotubes with precise atomic structures by means of transmission electron microscopy (TEM) consisting of a monochromator (JEOL TripleC#2). The electron energy loss spectroscopy (EELS) with the monochromated electron source provides well-separated sharp peaks at the carbon K (1s) absorption edge and in the valence-loss spectra from isolated single-wall carbon nanotubes (Fig. 1). These peaks unambiguously correspond to the van Hove singularities and indicate the unique properties of carbon nanotubes with different characters. Furthermore, we have experimentally investigated the effect on the electronic structures induced by the nonperiodic structure, such as topological defects or serial junctions. Such localized measurement of electronic properties for individual carbon nanotubes has never been realized by any other methods.

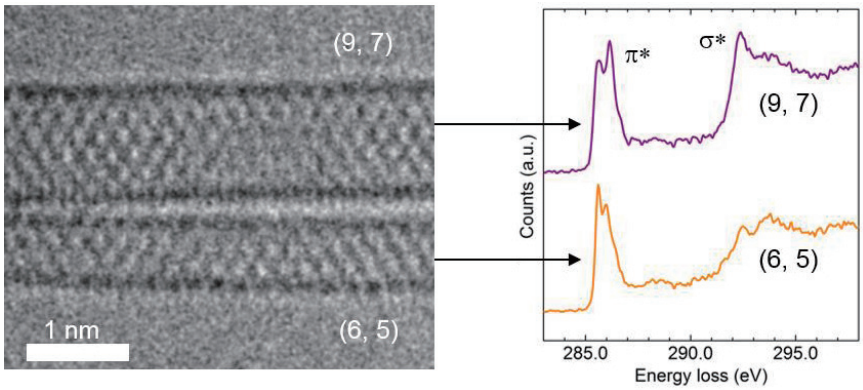

Fig. 1 TEM image (left) and EEL spectra of carbon *K-edge* (right) for two closely aligned single-wall nanotubes.

Corresponding Author: R. Senga
Tel: +81-29-862-6518
E-mail: ryosuke-senga@aist.go.jp

2-4

Surface Synthesis of Acene-type Graphene Nanoribbon

○Takahiro Nakae, Shaotang Song, Takahiro Kojima, Hiroshi Sakaguchi

Institute of Advanced Energy, Kyoto University, Uji, Kyoto 611-0011, Japan

Graphene nanoribbon (GNR), which is a one-dimensional carbon structure, exhibits semiconductor properties, whereas graphene is a two-dimensional carbon sheet with pseudo-metal, zero band gap characteristics. Bottom-up techniques can produce GNRs with a defined edge-structure and narrow widths, less than 1 nm. The bottom-up approaches reported to date provide GNRs with a defined edge structure, however suffer from the systematic synthesis of GNR having different width because of the low solubility of GNRs and the need for special environments and instruments. Therefore, a simple bottom-up synthetic method for large-scale production of GNR is eagerly sought not only for complete characterization of the material but also for device applications. Recently, we developed synthetic method of GNR, 2-zone temperature controlled radical-polymerized chemical vapor deposition (2Z RP-CVD).[1] 2Z RP-CVD method is highly efficient, therefore we can fabricate all 3 families of armchair-edged GNRs (3p, 3p+1, and 3p+2; p is defined as the number of carbon atoms along the width) on Au(111) even in extremely low-vacuum conditions.

Here, we synthesized acene-type GNR by using newly designed "Z-bar linkage precursor".[2] Using 2Z RP-CVD technique, Z-bar linkage precursor was supplied to Au(111) substrate at 250 °C to achieve surface polymerization. Surprisingly, homochiral polymerization of monomer, which has surface induced chirality, proceeded and afforded high density self-assembled array of polymers. The substrate was subsequently annealed to produce partially fused polymer, defective GNR, and acene-type GNR at 375, 450 and 500 °C, respectively, observed by STM. Stepwise dehydrogenation to acene-type GNR required ordered conformation of polymer and high density of self-assembled structure. Therefore, we concluded that stepwise dehydrogenation proceeded newly found "conformation-controlled mechanism."

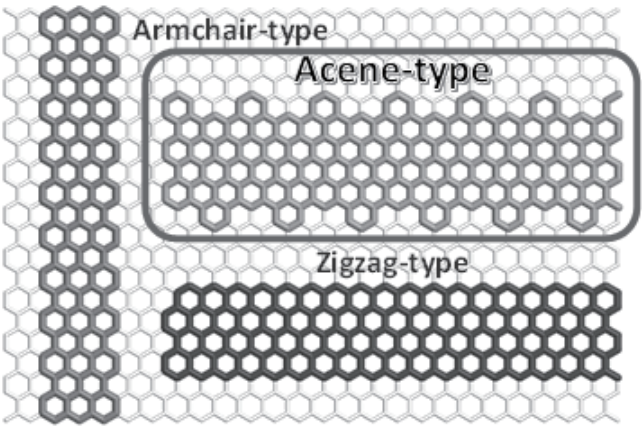

Figure 1. Category of Graphene nanoribbon cut out from graphene sheet. Acene-type GNR will report in this presentation.

[1] H. Sakaguchi, Y. Kawagoe, Y. Hirano, T. Iruka, M. Yano, T. Nakae, Adv. Mater., **26**, 4134 (2014).
[2] Submitted.

Corresponding Author: H. Sakaguchi
Tel: +81-774-38-3505, Fax: +81-774-38-3508,
E-mail: sakaguchi.hiroshi.7z@kyoto-u.ac.jp

Multiple photosynthetic reaction centers of porphyrinic polypeptide/$Li^+@C_{60}$ supramolecular complexes

○Kei Ohkubo[1,2], Tetsuya Hasegawa[1], Régis Rein[3], Nathalie Solladié[3], Shunichi Fukuzumi[1,2]

[1] *Department of Material and Life Science, Graduate School of Engineering, Osaka University, ALCA and SENTAN, Japan Science and Technology Agency (JST), Suita, Osaka 565-0871, Japan.*
[2] *Faculty of Science and Technology, Meijo University, ALCA and SENTAN, Japan Science and Technology Agency (JST), Nagoya, Aichi 468-8502, Japan*
[3] *CNRS, LCC (Laboratoire de Chimie de Coordination), 205 route de Narbonne, BP 44099, F-31077 Toulouse Cedex 4, France; Université de Toulouse, UPS, INPT, F-31077 Toulouse Cedex 4, France*

Extensive efforts have so far been devoted to mimic light harvesting and charge separation processes in natural photosynthesis. Light-harvesting and charge-separation units have been combined by coordination bonds between metalloporphyrins and electron acceptor moieties bearing Lewis base ligands. Thus, metal centres have been required for construction of supramolecular complexes between porphyrins acting as light harvesting units and electron acceptors containing Lewis base ligands for coordination to the metal centers. We report herein construction of supramolecular complexes of free base porphyrin polypeptides ($P(H_2P)_n$: n = 4, 8) with lithium ion-encapsulated C_{60} ($Li^+@C_{60}$)[1].

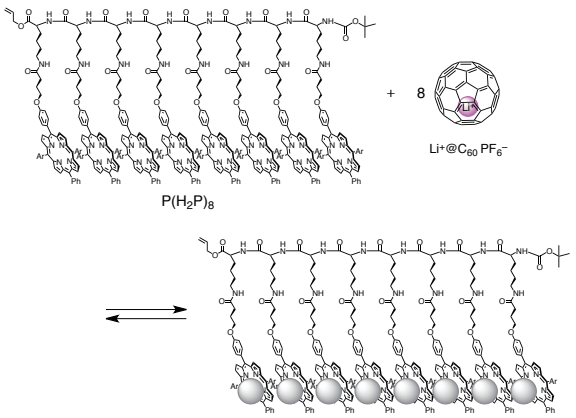

Nanosecond laser-induced transient absorption spectra of $P(H_2P)_8$ with $Li^+@C_{60}$ at the excitation wavelength of 532 nm showed the transient absorption band at 730 nm due to the triplet excited state of $Li^+@C_{60}$ ($^3Li^+@C_{60}^*$) observed together with the absorption band at 1035 nm due to $Li^+@C_{60}^{\bullet-}$. The decay of the absorption at 730 nm coincides with the appearance of $Li^+@C_{60}^{\bullet-}$. Thus, electron transfer from $P(H_2P)_8$ to $^3Li^+@C_{60}^*$ occurs to produce the triplet charge-separate (CS) state of $P(H_2P)_8^{\bullet+}$ and $Li^+@C_{60}^{\bullet-}$. The decay of the absorbance at 1035 nm due to $Li^+@C_{60}^{\bullet-}$ obeyed first-order kinetics with the lifetime of 210 μs. Thus, back electron transfer from $Li^+@C_{60}^{\bullet-}$ to $P(H_2P)_8^{\bullet+}$ occurs in the supramolecular complex. The lifetime is long because of the spin-forbidden back electron transfer in the triplet CS state.[1]

[1] K. Ohkubo *et al*. Chem. Commun. **51**, 17517 (2015).
Corresponding Author: K. Ohkubo
Tel: +81-6-6879-4734, Fax: +81-6-6879-7370,
E-mail: ookubo@chem.eng.osaka-u.ac.jp

Physical control of insulator-to-metal transition in overexpanded A_3C_{60}

○Yasuhiro Takabayashi [1], Ruth H. Zadik [2], Takeshi Nakagawa [1], Kosmas Prassides [1, 3]

[1] *WPI - Advanced Institute for Materials Research (WPI-AIMR), Tohoku University, Sendai 980-8577, Japan*

[2] *Department of Chemistry, Durham University, Durham DH1 3LE, UK*

[3] *Japan Science and Technology Agency, ERATO Isobe Degenerate π-Integration Project, Tohoku University, Sendai 980-8577, Japan*

Recently, we found that superconductivity and magnetism in A_3C_{60} (A = alkali metal) can be sensitively controlled both physically by applying external pressure and chemically through partial substitution of the intercalated alkali ions [1]. We also reported the occurrence of a temperature-induced isosymmetric phase transformation accompanying the onset of the Mott insulator-to-metal transition (MIT) in overexpanded A_3C_{60} under isobaric conditions [1]. This transition is also characterized by a large volume collapse. In this study, the pressure-dependent structural and magnetic properties of the normal state of the $Rb_{0.5}Cs_{2.5}C_{60}$ superconductor were investigated using synchrotron X-ray powder diffraction (SXRPD) and SQUID magnetometry.

SXRPD of $Rb_{0.5}Cs_{2.5}C_{60}$ under high pressure at ambient temperature showed the occurrence of a pressure-induced isosymmetric phase transition at $P \approx 0.5$ GPa ($V \approx 765$ Å^3/C_{60}). At ambient pressure, the temperature dependence of paramagnetic susceptibility, χ, of $Rb_{0.5}Cs_{2.5}C_{60}$ showed a well-defined cusp on cooling. The cusp provides the signature of the MIT. It broadens and shifts to higher T by increasing P. These results allow us to construct an updated global electronic phase diagram of fullerides encompassing the competing electronic states - the antiferromagnetic insulator, the superconductor and the normal metal – as a function of interfullerene separation both under isothermal and isobaric conditions.

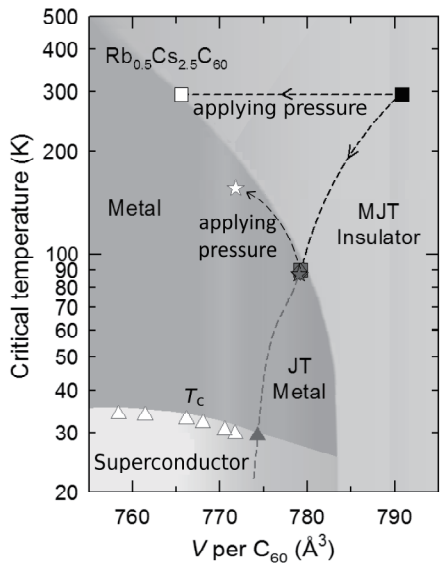

Fig.1 Electronic phase diagram for the A_3C_{60} systems using only data for the $Rb_{0.5}Cs_{2.5}C_{60}$ composition. Insulator-to-metal and superconducting transition temperatures and volumes obtained from SXRPD, magnetic susceptibility and IR measurement are included.

[1] R. H. Zadik et al., Science Advances 1, e1500059 (2015).

Corresponding Author: Yasuhiro Takabayashi
Tel: +81-22-217-5953, Fax: +81-22-217-5995
E-mail: yasuhiro.takabayashi.e4@tohoku.ac.jp

Direct probing of the electron-phonon scattering in the single-layered epitaxial graphene

○Shin-ichiro Tanaka[1], Takahiro Maruyama [2], Kiyoshisa Tanaka[3], Shin-ichiro Ideta[3], Hiroyuki Yamane [3]

[1] *Institute of Scientific and Industrial Research, Osaka University, Ibaraki 567-0047, Japan*
[2] *Department of Applied Chemistry, Meijo University, Nagoya 468-8502, Japan*
3 UVSOR Facility, Institute for Molecular Science, Okazaki 444-8585, Japan

The electron-phonon coupling (EPC) is one of the key issues in the solid/surface state physics. Recently, we proposed a new experimental method which enables us to probe the elemental process of the EPC (electron-phonon scattering) in HOPG graphite with resolving the momentum and energy of both the electron and the phonon by using the angle-resolved photoelectron spectroscopy (ARPES)[1]. Here, we demonstrate the validity of this method for the EPC in the graphene by applying to the electron-phonon scattering in the Dirac cone of the epitaxial single layer graphene on SiC.

Experiments were carried out at the beamline 7U of the UVSOR facility of the Institute for Molecular Science, Japan. Figure 1(a) shows the surface normal photoelectron spectra taken at several photon energies. In Fig. 1(a), there are steps near 160meV of the binding energy which are converted into peak shapes as shown in Fig. 1(b) by differentiating them with respect to the binding energy. The intensities of the steps are plotted as a function of the photon energy in Fig. 1(c). According to the reference [1], the steps in the ARPES spectra can be ascribed to the Fermi edge which is shifted in energy as much as the phonons; the electron in the Dirac cone near the K-point of the graphene is scattered by the TO- phonon with conserving the total energy and momentum. Fig 1(c) clearly shows the particular final states of the photoexcitation is necessary to detect this process. Fig. 2 shows the angle-resolved spectra displayed in the differentiated form, and the dispersion of the interacting TO-phonon is clearly observed. The detail of the scattering process will be discussed in the presentation.

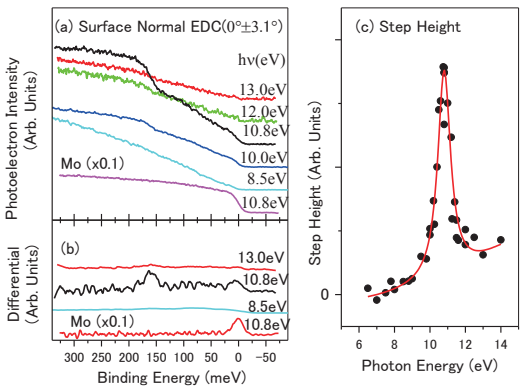

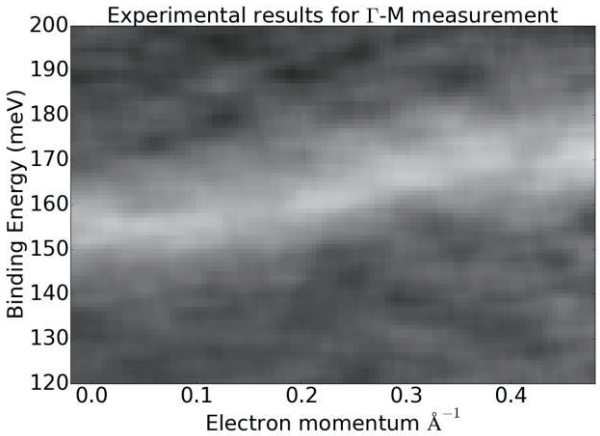

[1] S. Tanaka *et al*. Sci. Rep. 3(2013)3031.

Corresponding Author: S. Tanaka
Tel: +81-6-6879-8491, Fax: +81-6-6879-8494, E-mail: stanaka@sanken.osaka-u.ac.jp

Anisotropic optical properties of layered monochalcogenide GeSe nanosheets

○Dezhi Tan, Yuhei Miyauchi, Shinichiro Mouri, Koirala Sandhaya and Kazunari Matsuda

Institute of Advanced Energy, Kyoto University, Uji, Kyoto 611-0011, Japan

Two-dimensional (2D) layered materials including graphene and transition metal dichalcogenides (TMDs) have attracted much interest owing to their unique physical properties and potential applications [1,2]. The 2D layered materials offer the fascinating possibility of novel semiconductors with a single atomic layer thickness, which also be utilized for the optical and electronic device application using charge, spin and valley degree of freedom. Among them, the 2D layered materials with anisotropic structure such as black phosphorus, which are different from other 2D materials with hexagonal in-plane lattice such as graphene and TMD, have been intensively studied. The DFT calculation predicts that 2D monochalcogenide, germanium selenide (GeSe) has anisotropic layered structure with a narrow band gap (1.08 eV) p-type semiconducting properties [3]. However, the detail experimental studies of optical properties and their anisotropy have not been reported in GeSe.

Here, we studied a new 2D monochalcogenide, germanium selenide (GeSe) with anisotropic layered structure. Figure 1(a) shows the schematic of crystal structure of GeSe, which exhibits high intrinsic anisotropy with zigzag and armchair directions. We measured polarized Raman scattering spectra of GeSe nanosheets (thickness of 70 nm) with changing the direction of incident linear polarized light (2.33 eV). In the Raman spectra (Fig. 1(b)), the three Raman peaks are clearly observed at 81.4 cm^{-1} (A_g^1 mode), 150.7 cm^{-1} (B_{3g}), and 189.0 cm^{-1} (A_g^2). The intensities of Raman peak (A_g^1 mode) clearly show strong polarization dependence in Fig. 1(c), which obviously suggests that the atomic vibrational properties and electronic structures in GeSe have strong anisotropic characteristics. We also conducted polarization dependence of differential reflectivity measurements in GeSe nanosheets. Our work on the anisotropic properties of GeSe nanosheets will extend the research field of 2D layered materials, as well as helping GeSe to find novel applications.

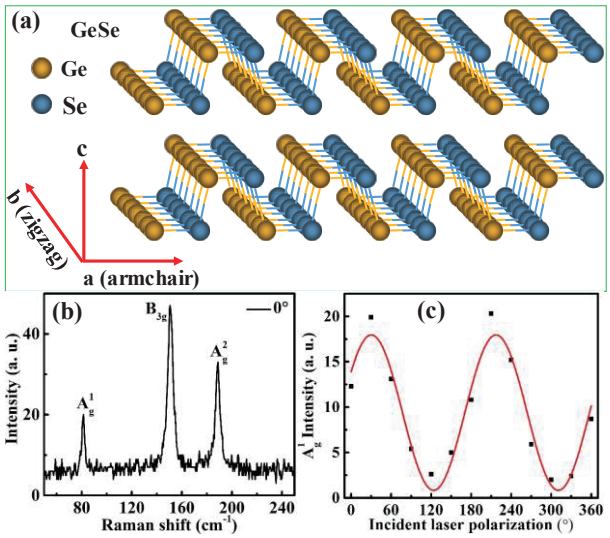

Fig. 1 (a) Structure of GeSe, (b) Raman spectrum of GeSe nanosheets (Incident laser polarization: 0°. (c) Polarization dependent Raman scattering intensity of A_g^1 mode.

[1] X. Duan *et al. Chem. Soc. Rev.* **44**, 8859 (2015).
[2] X. Xia *et al. Nat. Photonics* **8**, 899 (2014).
[3] G. Shi *et al. Nano Lett.* **15**, 6926 (2015).

Corresponding Author: Dezhi Tan
Tel: 0774-38-3465, Fax: 0774-38-3460
E-mail: wcdennytun@gmail.com

Photovoltaic features of few-layer WSe_2 schottky solar cells

○Toshiki Akama, Toshiaki Kato, Toshiro Kaneko

Department of Electronic Engineering, Tohoku University, Sendai, 980-8579, Japan

Atomic scale 2D sheets attract intense attention due to their superior electrical, mechanical, and optical features. Layered transition metal dichalcogenide (TMD) is known as a true 2D material with excellent semiconducting properties [1]. TMD is one of the most attractive materials for future high performance transparent and flexible solar cells due to their atomically thin structure, band gap in visible light range, and high optical transparency.

Although the solar cell of TMD has been widely investigated by many groups, those are based on the pn junction type solar cell. Since complicated structures are required to form pn junction structures in TMD such as dual gate electrodes or position selective doping, the device size of pn junction solar cell with TMD is limited within very small region (few μm). The schottky type solar cell is known as another type of solar cell, and it is possible to scale up the device up to the practical size because of the simple device structures. However, the detailed study of schottky type solar cell with TMD has not been reported.

Because the schottky barrier is formed at the contact region between electrode and TMD, it is important to select appropriate electrode pairs for left and right electrodes. In this study, we have investigated the combination of left and right electrodes and the distance of each electrode to obtain the better performance. Through the adjustment of these factors we have succeeded in the fabrication of the high performance schottky type solar cells with few-layer WSe_2.

The systematic investigations reveal that energy conversion efficiency increases with work function difference between left and right electrodes. The highest power conversion efficiency can be obtained with the combination of Ni and Pd electrodes, which can be explained by the high schottky barrier and nearly ohmic contact at Ni-WSe_2 and Pd-WSe_2 contact region, respectively. The electrode distance was varied between 0.5 to 14 μm, and the highest efficiency can be given with 2.2 μm distance. The photocurrent mapping measurements revealed that the suitable distance should be decided by the balance of exciton diffusion length and momentum transfer distance of separated carriers. Based on these optimizations of electrodes and distance, the power conversion efficiency can be reached up to 0.01 %, which is 40 times higher than that before the optimization (symmetric electrodes with long distance). This power conversion efficiency is comparative or slightly higher than that of pn junction type solar cell with similar TMD thickness. Since our established schottky type solar cell with asymmetric electrodes can be easily scale up, our findings can contribute to the practical application of TMD-based flexible and transparent solar cells.

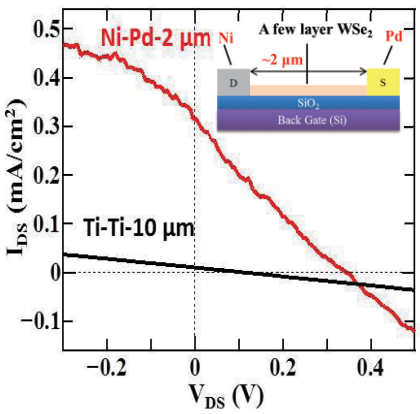

Fig.1: I_{DS}-V_{DS} characteristics of few-layer WSe_2 schottky solar cells with light illumination.

[1] T. Kato and T. Kaneko, ACS Nano **8**, 12777 (2014).

Corresponding Author: T. Akama
Tel: +81-22-795-7046, Fax: +81-22-263-9225,
E-mail: akama13@ecei.tohoku.ac.jp

Tuning of polarization of h-BN nanoribbons by the edge hydrogenation

○Ayaka Yamanaka, Susumu Okada

Graduate School of Pure and Applied Sciences, University of Tsukuba, Tennodai, Tsukuba 305-8577, Japan

Hexagonal boron nitride (h-BN) is attracting much attention as an insulating version of graphene, due to its unique physical properties, such as mechanically strong hexagonal covalent network, high thermal conductivity, and an insulating electronic structure with wide band gap. Because of these properties, h-BN is regarded as a potential material for the wide areas in the current and future nanotechnologies. For practical applications of h-BN, it is mandatory to understand their fundamental properties. In this work, we study the electronic structure of h-BN with various edge structures to give a theoretical insight into the physical properties of h-BN with nanostructures. All calculations are performed by using the density functional theory (DFT) with the generalized gradient approximation. The effective screening medium (ESM) method is applied to avoid the unintentional dipole interactions with the periodic images.

In this study, we investigate the electrostatic potential of h-BN nanoribbons with hydrogenated and clean edges of which edge angles are ranging from θ = 0° (armchair) to 30° (zigzag). Figure 1 shows the electrostatic potential of h-BN nanoribbons with hydrogenated and clean edges. The potential difference between the right and left edges of hydrogenated nanoribbons is opposite to that of nanoribbons with clean edges. We found that potential difference also depends on the edge shapes of h-BN nanoribbons. Nanoribbons do not have potential difference in both hydrogenated and clean edges for the θ = 0°. With increasing θ, the potential difference monotonically increases for then hydrogenated nanoribbons. On the other hand, potential difference exhibits an unusual property with respect to the θ for the clean edges. The facts indicate that the edge shapes and termination can control the polarization of h-BN nanoribbon.

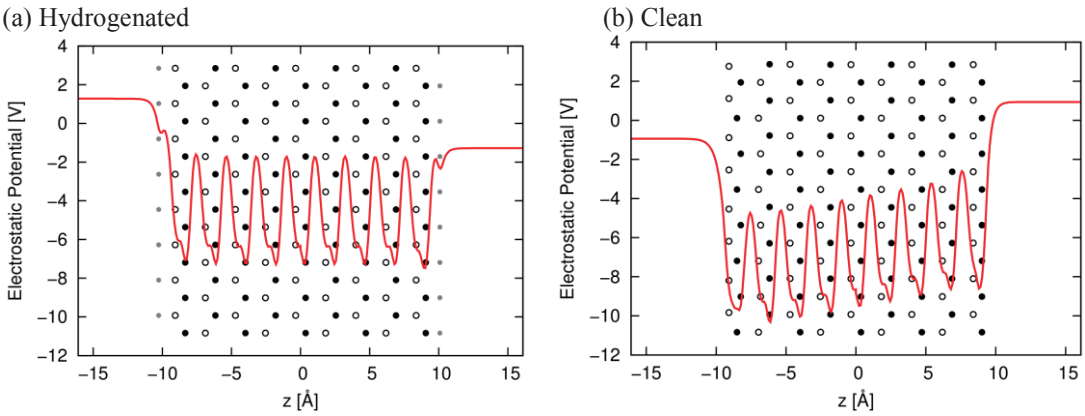

Fig.1: Electrostatic potential of zigzag h-BN nanoribbons with (a) hydrogenated and (b) clean edges. Small gray, large white, and black circles denote H, B, and N atoms, respectively.

Corresponding Author: A. Yamanaka
Tel: +81-29-853-5600 (ext. 8233), Fax: +81-29-853-5924,
E-mail: ayamanaka@comas.frsc.tsukuba.ac.jp

3-5

Gate-voltage induced trions in suspended carbon nanotubes

○M. Yoshida, A. Popert, Y. K. Kato*

Institute of Engineering Innovation, The University of Tokyo, Tokyo 113-8656, Japan

We observe trion emission from suspended carbon nanotubes where carriers are introduced electrostatically using field-effect transistor structures [1]. The trion peak emerges below the E_{11} emission energy at gate voltages that coincide with the onset of bright exciton quenching. By investigating nanotubes with various chiralities, we verify that the energy separation between the bright exciton peak and the trion peak becomes smaller for larger diameter tubes. Trion binding energies that are significantly larger compared to surfactant-wrapped carbon nanotubes are obtained, and the difference is attributed to the reduced dielectric screening in suspended tubes.

Work supported by JSPS (KAKENHI 24340066), the Canon Foundation, the Sasakawa Scientific Research Grant, and MEXT (Photon Frontier Network Program, Nanotechnology Platform). M.Y. is supported by ALPS.

[1] M. Yoshida, A. Popert, and Y. K. Kato, Phys. Rev. B **93,** 041402(R) (2016).

*Corresponding Author: Y. K. Kato
Tel: +81-3-5841-7702, Fax: +81-3-5841-7772
E-mail: ykato@sogo.t.u-tokyo.ac.jp

3-6

Evaluation of DNA-SWNT interaction depending on base type by photoluminescence

○Masahiro Ito, Eri Sando, Kazuo Umemura, Yoshikazu Homma

Department of Physics, Tokyo University of Science, Tokyo 152-8601, Japan

Photoluminescence (PL) can be observed from DNA-SWNT ensembles under the dry condition [1]. PL can be distinguished sensitively the difference of dielectric constant around SWNT. However, it is difficult to evaluate purely the effect of DNA adsorption from DNA-SWNTs in solution or their ensembles on a substrate. In this study, we prepared low density DNA-SWNTs on the silica substrate to detect an isolated DNA-SWNT in the laser spot. We used homo-sequenced ssDNA to evaluate the effect of base type (i.e., U, T, A, C, and G).

PL from isolated DNA-SWNT exhibited different peaks depended on the base type of DNA, as shown in Fig. 1 for (9,4) SWNT [2]. Clear tendency of the PL peak energy dependence on the base type, T > A > C > G, can be seen. This tendency was almost the same for different charilities. We compared the PL peak shift with the adsorption energy of DNA base. Some theoretical groups [3] and one experimental group [4] have reported adsorption energies in the same trend as the PL peak shift. Although adsorption energies calculated by many groups [5] are C < A < T < G in fact, the interaction of U with SWNT is the smallest in any theoretical case. Calculated binding energies are listed in Table 1. The polarizability of a DNA base plays a key role in governing the strength of interaction with the SWNT. It is thus reasonable to assume that the PL emission peak energy shift represents the actual adsorption energies of the DNA bases on the SWNT surface.

In conclusion, we revealed that the PL peak from DNA-SWNT shifted in the order of $(dT)_{30}$, $(dA)_{30}$, $(dC)_{30}$ and $(dG)_{30}$, which might reflect the adsorption energy of DNA on SWNT. Based on the result, we will discuss the PL of isolated $(dU)_{30}$-SWNT.

[1] M. Ito et al. Appl. Phys. Lett. **104**, 043102 (2014), [2] M. Ito et al. J. Phys. Chem. C. **119**, 21141 (2015)
[3] M. K. Shukla et al. Chem. Phys. Lett. **480**, 269, (2009), [4] F. Albertorio et al. Nanotechnology **20**, 395101, (2009), [5] S. Gowtham et al. Nanotechnology **19**, 125701, (2008)

Corresponding Author: M. Ito
Tel: +81-3-3260-4271 ex. 2298, Fax: +81-3-5228-7388,
E-mail: m-ito@rs.tus.ac.jp

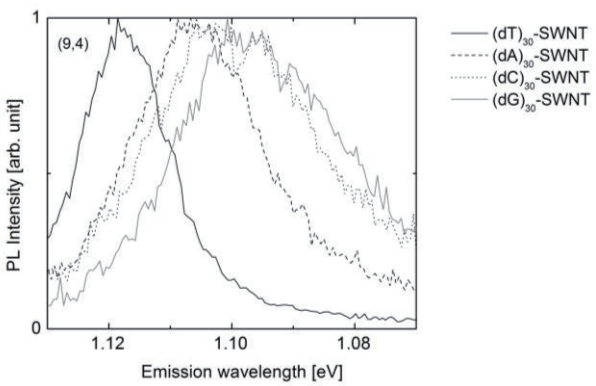

Fig 1. PL peaks from various isolated DNA-SWNTs.

Table 1. Calculated binding energy of DNA with SWNT.

	Binding energy	
	Shukla et al. [3]	Gowtham et al. [5]
	[kJ/mol]	[eV]
G	32.9	0.49
C	25.1	0.29
A	24.0	0.39
T	23.7	0.34
U	23.0	0.28

3-7

Circular Dichroism of Single Wall Carbon Nanotubes

Riichiro Saito○, Naomichi Sato, Yuki Tatsumi
Department of Physics, Tohoku University, Sendai

Recently, single wall carbon nanotubes (SWNTs) can be separated by various techniques and we can get physical properties of not only each chirality (n,m) but also handness of SWNT. Depeneding on the handness of SWNTs, Kataura et al. showed that circular dichroism (CD, The effect of CD is defined by the different optical absorption of a material for incident left and right circular light. CD can be observed by chiral (or spiral) molecules) for left and right handed purified SWNT in which the sign of CD values changes at each Eii energy and give the opposite values for left and right handed SWNTs.

In this presentation, we theoretically investigated the symmetry of the wavefunction and discuss the possible mechanism of CD. Although the complete analysis is not finished as a function of (n,m), we can basically explain the formula for obtaining CD values by using so-called dipole vector approximations that are discussed in linear polarization of the light in the past. Most mechanism can be expluded by time-reversal symmetry of the system. It would be nice if we can discuss in this opportunity for possible mechanism.

This work is partially supported by MEXT grant (Nos. 25286006, 25107005)

Corresponding author: Riichiro Saito
e-mail: rsaito@flex.phys.tohoku.ac.jp
web: http://flex.phys.tohoku.ac.jp/japanese
tel: 022-795-7754

Semiconductor-Metal-Semiconductor Transition of C_{60}-Fullerene Thin-Films toward PS-Molecule Application

○Nobuyuki Aoki[1,2], Wataru Akiyama[1], Naoto Nakamura[1], Katsuhiko Miyamoto[1], Takashige Omatsu[1,3], Jonathan P. Bird[1,4], and Yuichi Ochiai[1]

[1] *Graduate School of Advanced Integration Science, Chiba University, Chiba, 263-8522 Japan*
[2] *JST-PREST, 4-1-8 Honcho Kawaguchi, Saitama 332-0012, Japan*
[3] *JST-CREST, 4-1-8 Honcho Kawaguchi, Saitama 332-0012, Japan*
[4] *Department of Electrical Engineering, University at Buffalo, SUNY, Buffalo, NY 14260-1920, USA*

If major components of electronics, such as metal, semiconductor and insulator, can be comprised of one kind molecule and all the materials can be recycled after the use, it would be an ideal material for a future green electronics. We defined such molecules as "pluripotent stem (PS) molecules" and found the potentials in C_{60} fullerene molecules.

Recently, we have succeeded to observe a transition of transport properties of C_{60} thin film from semiconducting to metallic by photo-polymerization using optical vortex laser light [1]. Metallic-C_{60} polymer having rhombohedral structure has been realized by application of high pressure at high temperature condition [2]. However it has not been achieved by photo-irradiation. Because the inter-molecular distance is shorten and the free rotation of the molecule stops after forming the dimer [3]. Consequently the polymerization no longer continues by using a usual light source. In this study, we are interested in a use of an optical vortex laser (OV) for the photo-polymerization of C_{60} molecules. Since the beam has a helical wavefront, not only a gradient force in the redial direction but also an optical torque along the tangential direction can be expected toward the C_{60} molecules. Therefore a successive polymerization takes a progress by providing the molecules under the beam. It would provide a unique photo-polymerization mechanism in a C_{60} thin film which can never achieved by usual light sources. Actually we had reported that we observed formation of additional two-dimensional films on the surface of the C_{60} thin film after the irradiation of OV and the film shows a metallic transport property (independent to the gate voltage). Recently, optimizing the irradiation condition, we have succeeded to observe a transition of the transport properties of a C_{60} thin-film field effect transistor from semiconducting to metallic in a *same* sample by applying excess dose of a green OV laser. Moreover we also confirmed that the property returned to semiconducting after annealing the sample at high temperature. Therefore, a reversible transition of electrical property has been achieved in the same sample. It indicate that the transition is not due to an irreversible destruction of C_{60} molecules to be amorphous carbon but due to a high level of photo-polymerization of the molecules. These result is pave a way to realize a reusable electronics composed of PS-molecules.

[1] T. Omatsu *et al.*, Opt. Express **18**, 17967 (2010).
[2] Y. Iwasa *et al.* , Science **264**, 1570 (1994).
[3] T. L. Makarova *et al.*, Semiconductors, **35**, 243 (2001).

Corresponding Author: N. Aoki
Tel: +81-43-290-3430, Fax: +81-43-290-3427,
E-mail: n-aoki@faculty.chiba-u.jp

Development of Ion Trap Ion Mobility Measurement System for Nano Materials

○Toshiki Sugai, Yasuhiro Hiroshiba, Hironobu Matsubayashi, Wataru Ohkawa, Takuma Ito, and Ryota Jinnouchi

Department of Chemistry, Toho University, Miyama 2-2-1 Funabashi, 274-8510, Japan

Ion mobility measurements have revealed varieties of novel information on nano materials. Structures of metallofullerenes show significant dependence on the number of metal atoms and the cage size and their novel structures have been also clarified[1]. Our newly developed ion trap mobility measurement system can hold the ionized particles for more than 2 hours realizing observations on long term transitions. However those measurements mainly performed on a single particle and restricted to micro particles. To apply these measurements to nano systems and to have statistical information, we have developed new system.

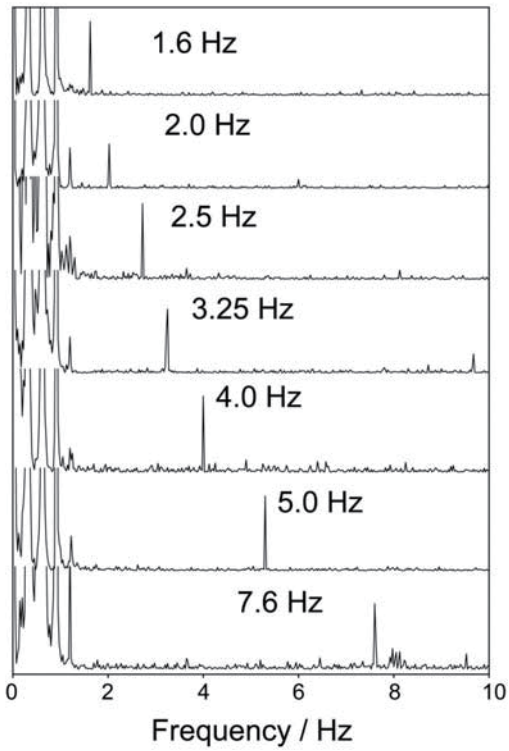

Fig. 1 Detected signal from trapped particles.

The system consists of a laser ionization source for polystyrene particles and electrodes for the trap. The produced ionized particles were trapped and moved in air for several minutes. The movement of every particle was observed by a microscope and position dependent fiber optics to evaluate its mobility. The detection sensitivity is enhanced by utilizing motion synchronized signal processing.

Figure 1 shows the Fourier transformed optical signal from the fibers. Peaks are found at the exact frequency of the motion showing the much enhanced S/N. We are going to apply the methods to various nano materials.

[1] T. Sugai *et al.*, *J. Am. Chem. Soc.* ***123***, 6427 (2001).
[2] T. Sugai *et al.*, 42nd *Fulluerene-nanotue-graphene conference.* 3-13

TEL: +81-47-472-4406, E-mail: sugai@chem.sci.toho-u.ac.jp

Electron Microscopic Imaging of Acceleration-Voltage-Dependent Molecular Motion on a Carbon Nanohorn

○Koji Harano[1], Ricardo M. Gorgoll[1], Emrah Yücelen[2], Akihito Kumamoto[3], Naoya Shibata[3] and Eiichi Nakamura[1]

[1] *Department of Chemistry, The University of Tokyo, Tokyo 113-0033, Japan*
[2] *FEI Company, Europe Nanoport, 5651 GG Eindhoven, The Netherlands*
[3] *Institute of Engineering Innovation, Graduate School of Engineering, The University of Tokyo, Tokyo 113-8656, Japan*

Although σ-bond rotation and the ensuing conformational changes are the fundamental subject of chemistry, the possibility of visually observing such events at atomic resolution has long eluded the ability of chemists. We recently tested the utility of transmission electron microscopy (TEM) and acquired in situ atomic resolution movies of the conformational changes of single organic molecules attached to the surface of a carbon nanohorn (CNH, a tapered variant of a single-walled carbon nanotube)[1–3]. However visually impressive, the movies themselves are insufficient as a research tool in the absence of a method to change and quantify the magnitude and frequency of the motions. We report here that the frequency of the molecular motions can be increased by lowering the electron accelerating voltage (from 120, 80 to 60 kV) as a consequence of large scattering cross section, and that the motions can be quantified using cross-correlation analysis between the neighboring frames of the movie [4]. As a platform for this study, we examined biotin derivatives **1** and **2** attached to the surface of a CNH through two different linkers (Figure a) whose motions were observed as they happened during several minutes on a TEM stage at the three different voltages. Molecule **1** is rather static at 80 and 120 kV, but vibrates frequently at 60 kV. In contrast, the more flexible molecule **2** is mobile enough at 80 kV to show us visually the process of stepwise energy relaxation by sequential rotations of σ-bonds in vacuum (Figure b)—a piece of information so far unobtainable by experimental methods but only by theoretical simulations.

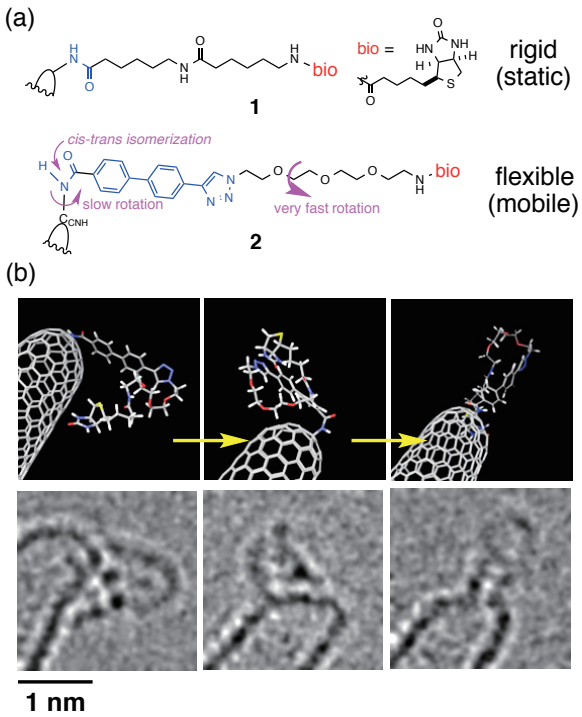

Figure. Biotinylated molecules **1** and **2** on CNH. (a) Molecular designs. (b) TEM images of rapidly moving **2** at 80 kV.

[1] E. Nakamura *et al. J. Am. Chem. Soc.*, **130**, 7808 (2008).
[2] K. Harano *et al. Nat. Mater.*, **11**, 877 (2012). [3] K. Harano *et al. J. Am. Chem. Soc.*, **136**, 646 (2014).
[4] R. M. Gorgoll *et al. J. Am. Chem. Soc.*, **137**, 3474 (2015).

Corresponding Author: E. Nakamura
Tel: +81-3-5841-1475, Fax: +81-3-5841-1475,
E-mail: harano@chem.s.u-tokyo.ac.jp

Recent progress in nanodiamond research & development

○Eiji Osawa, Shuichi Sasaki, Ryoko Yamanoi

NanoCarbon Research Institute, Asama Research Extension Center, Faculty of Textile Science and Technology, Shinshu University, Ueda, Nagano 386-8567, Japan

Size. The most practical criterion for the quality of primary particles of detonation nanodiamond (PPDND) is the size distribution obtained by DLS under certain conditions. The latest value for our product is 2.8±0.5nm. Available evidence indicates that this value is close to the true size. Structure of PPDND (Fig. 1) will be discussed in some detail.

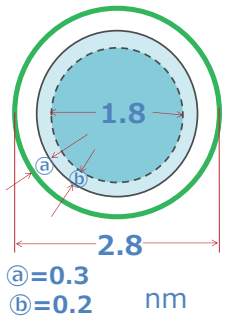

Figure 1

Unique properties. Our PPDND particles differ from other known products in the following features: (1) No COOH group is present above the detection limit of $1.4 \cdot 10^{-5}$ eq. This result is supported by XAS observation [1]. (2) Graphene patches are confirmed to exist on the surface by TEM and XAS [1]. (3) Zeta potential is about +60 mV [1]. (4) Colloidal stability of aqueous solution changes with concentration of PPDND, showing a peculiar trend 'aggregation by dilution, and dispersion by concentration,' against chemical common sense. The enigmatic trend is interpreted in terms of 'colloid crystal' or 'periodic colloid' [2].

Applications. The unusual properties in PPDND as given above suggest high prospects for major applications. We are currently developing three of them: (i) nano-composites with crystalline solid materials, (ii) nanospacer lubricants, and (iii) drug carrier in an open DDS for cancer. Application (ii) takes advantage of the quasi-spherical shape of PPDND and demonstrates a possibility of replacing traditional oil lubrication, which has been serious environmental hazard since industrial revolution. As shown in Table 1, dispersion of 2% PPDND to lubrication liquids like water and ethylene glycol reduced absolute friction coefficients to nearly one tenth in both cases. According to our preliminary experiments, the sphericity of PPDND particles can be increased by improved self-abrasion.[3] Spherical PPDND dispersed in appropriate lubrication liquids will eventually lead to an ideal lubrication free from friction and contribute to suppress CO_2 emission.

Table 1. Effect of ND addition to lubrication liquid on absolute friction coefficients.[1]

LL[2]	H_2O	H_2O+2%PPDND	EG[4]	EG+2%PPDND
AFC[3]	0.65	0.07	0.19	0.03

[1]Sapphire ball (Φ1mm)/polished SUS304 surface, 20Hz, 120m, 20mN, 40,000 measurements. [2]Lubrication liquid, [3]Absolute friction coefficient. [4]Ethylene glycol.

[1] Petit, T. *et al.*, *J. Phys. Chem. Lett.* **2015**, *6*, 2909. [2] Mchedlov-Petrossyan, N. O. *et al.*, *Phys. Chem. Chem. Phys.*, 2015, *17*, 16186. [3] Yamanoi, R. *et al.*, 48th FNTG General Symp., Univ. Tokyo, Feb. 21-23, **2015**, Oral 1P-39.

Corresponding Author: E. Osawa, Tel: +81-0268-75-8381, Fax: +81-0268-75-8551, E-mail: osawa@nano-carbon.jp

ポスター発表
Poster Preview

1P – 1 ～ 1P – 49
2P – 1 ～ 2P – 49
3P – 1 ～ 3P – 48

Raman spectroscopic measurement of C_{60} fullerene nanowhiskers

○Toshio Konno, Chika Hirata, Takatsugu Wakahara, Kun'ichi Miyazawa

Fullerene Engineering Group, Materials Processing Unit, National Institute for Materials Science (NIMS), 1-1, Namiki, Tsukuba, Ibaraki, 305-0044, Japan

Raman spectroscopy is a powerful tool to investigate the structural and electronic properties of C_{60} molecules. The $A_g(2)$ mode has been often used to characterize C_{60} solids, since it is known that the peak position of $A_g(2)$ mode well reflects the physical state of C_{60} molecules [1].

C_{60} nanowhiskers (C_{60}NWs) are the thin needle-like crystals composed of C_{60} molecules and have diameters less than 1000 nm, and have many applications such as field-effect transistors, solar cells, photocatalysts, photosensors, scaffolds for cell growth, superconductors, templates for chemical synthesis and so forth [2].

In our past researches [3,4], the Raman measurement in air was performed to characterize various C_{60}NWs synthesized by the liquid-liquid interfacial precipitation (LLIP) method [5], using the $A_g(2)$ mode as the probe to monitor the vibrational and electronic states of C_{60} molecules. However, the measured $A_g(2)$ mode Raman shift of C_{60}NWs is ranging from 1458 cm^{-1} to 1468 cm^{-1} in our previous research. Since the down shift of $A_g(2)$ mode Raman shift reflects the change of the environment where the C_{60} molecules are located, the current paper intends to conduct the precise measurement of the $A_g(2)$ mode Raman shift of C_{60}NWs that can be used as the standard value in air to monitor the physical state of C_{60} molecules in the solution-grown C_{60}NWs. The Raman shift measurement of a vacuum-deposited C_{60} thin film was also conducted and compared with the case of C_{60}NWs in order to validate the measurement method.

The C_{60}NWs dried in vacuum at 120 °C showed a Raman shift of 1469.95 ± 0.42 cm^{-1} with a coverage factor $k = 2.0$ for a level of confidence of 95 % in the air that was very close to the value of 1469.81 ± 0.38 cm^{-1} (k = 2.0, level of confidence of 95%) of a vacuum-deposited C_{60} thin film.

The value of 1469.95 ± 0.42 cm^{-1} can be used as a standard $A_g(2)$ Raman shift of the C_{60}NWs composed of monomer C_{60} molecules.

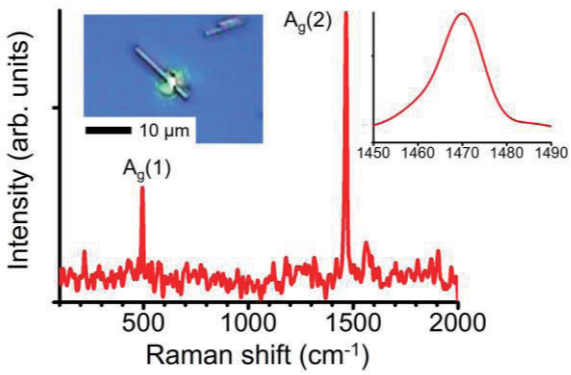

Fig.1. A Raman spectrum of the C_{60}NWs using laser beam power density of 5.7×10^3 mW / mm^2.

[1] H. Kuzmany *et al. Philos. Trans. R. Soc. Lond. A* **362**, 2375, (2004).
[2] K. Miyazawa *Sci. Technol. Adv. Mater.* **16**, 013502 (2015).
[3] K. Miyazawa *et al. J. Nanopart. Res.* **13**, 5739 (2011).
[4] M. Sathish *et al. Molecules* **17**, 3858 (2012).
[5] K. Miyazawa *et al. J. Mater. Res.* **17**, 83 (2002).

Corresponding Author: K. Miyazawa
Tel: +81-(0)29-860-4528, Fax: +81-(0)29-860-4667,
E-mail: miyazawa.kunichi@nims.go.jp

Energetics and electronic structures of molecular complexes of fullerenes and cyclohydrocarbons

○Yuya Nagasawa and Susumu Okada

Graduate school of Pure and Applied Sciences, University of Tsukuba
Tennodai, Tsukuba 305-8571, Japan

Fullerenes and polycyclic aromatic hydrocarbons are known to be constituent units for the various molecular complexes and molecular solids in which the constituent units are bound each other via weak intermolecular interaction. According to the weak interaction, the physical properties of the molecular complexes basically retain those of each constituent. However, on the other hand, the small intermolecular hybridization makes the complexes being unique in their properties which are absent in each unit. Recently, molecular complexes consisting of C_{60} and cyclohydrocarbons have experimentally synthesized, such as C_{60} with cycloparapyhenylene and cyclochrysenylen belts, which are regarded as the shortest armchair and chiral C_{60}-peapods, respectively. By the analogy with large fullerene peapods, similar inclusion complexes are expected to be synthesized by assembling appropriate large fullerenes and cyclohydrocarbons, possessing interesting electronic structures. In the present work, we explore the possibility of novel inclusion complexes of large fullerenes and cyclohydrocarbons using the density functional theory with local density approximation. We consider the cycloparaphenylene (CPP) and cyclacene (CA) for the belt unit of the complexes, which incorporate C_{78}(C_{v2}') fullerene.

Figure 1 shows the inclusion energy of C_{78} in cyclohydrocarbons as a function of their diameter. The inclusion energy, ΔE, is evaluated by the reaction: CPP(CA) + C_{78} → CPP-C_{78}(CA-C_{78}) - ΔE. Our calculations show that the inclusion of C78 fullerene in CPP and CA with appropriate diameter is exothermic with the energy gain of up to 1.2 and 1.5 eV for CPP and CA, respectively. The fact indicates that the inclusion complexes of C_{78} and CA/CPP are energetically stable as the case of C_{60} inclusion complexes. Electronic structure of the inclusion complexes strongly depend on that of the cyclohydrocarbons and the interunit spacing.

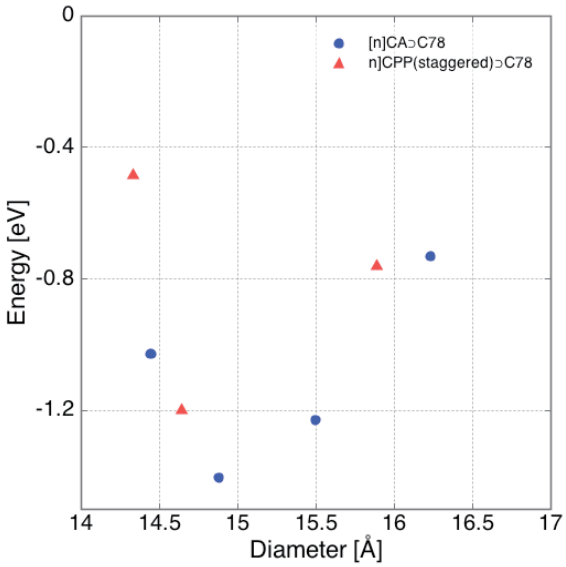

Fig. 1 Inclusion energy of C_{78} in CPP and CA as a function of their diameter

Corresponding Author: Y. Nagasawa
Tel: +81-29-853-5600(ext.; 8233), Fax: +81-29-853-5600,
E-mail: ynagasawa@comas.frsc.tsukuba.ac.jp

1P-3

ESR spectra of Gd and Y di-metallofullerenes

○Takahisa Yamaguchi[1], Natsumi Nakatori[3], Takuji Mitani[3], Koichi Kikuchi[3], Takeshi Kodama[3], Ko Furukawa[4], Tatsuhisa Kato[1,2]

[1]*Graduate School of Human and Environmental Studies, Kyoto University, Kyoto 606-8501, Japan*
[2]*Institute for Liberal Arts and Sciences, Kyoto University, Kyoto 606-8501, Japan*
[3]*Department of Chemistry, Tokyo Metropolitan University, Tokyo 192-0397, Japan*
[4]*Department of Chemistry, Niigata University, Niigata 950-2181, Japan*

Endohedral metallofullerenes show their chemical stability in the particular combination of metal with fullerene cage. In other words the metallofullerenes indicate diversity relied on the number and the type of metal and the cage structure. We succeeded to isolate Gadolinium (Gd) and Yttrium (Y) di-metallofullerenes as anion forms, those are $(Gd_2@C_{80})^-$, $(Y_2@C_{80})^-$, $(Gd_2@C_{78})^-$ and $(Y_2@C_{78})^-$, by using an ion-pair chromatography separation method. UV-vis-NIR absorption measurements showed that their C_{80} and C_{78} cage are I_h and D_{3h} symmetry. Their characteristic spin states were investigated by ESR spectroscopy. It was confirmed that their spin states and dynamics depend upon the cage structure.

X-band and Q-band ESR measurements were carried out with Bruker E500 and E680 spectrometer. Cryogenic temperatures were obtained with an Oxford 900 helium cryostat. Spectral simulations were performed by using EasySpin package with MATLAB program.

Observed electron spin echo field scan (ESEFS) and simulated spectra for $(Gd_2@C_{80})^-$and $(Gd_2@C_{78})^-$are shown in Fig 1. Both spin states were characterized by the high spin of S=15/2 and the fine structure with zero-field splitting constants of D and E tabulated in Table 1. It is noticeable that 14 electrons on 4f shells of two Gd ions and an excess reducing electron are all coupled in ferromagnetic manner and that $(Gd_2@C_{80})^-$ exhibits much larger E value than that of $(Gd_2@C_{78})^-$ in spite of the higher I_h symmetry of cage. On the other hand, the spin states of both $(Y_2@C_{80})^-$and $(Y_2@C_{78})^-$ were assigned as the doublet state of S=1/2 with the hyper-fine structure (HFS). And tetragonal (axial symmetric) HFS constants and g tensor were obtained regardless of cage structure.

Table 1. ESR parameters of $(Gd_2@C_{78})^-$and $(Gd_2@C_{80})^-$

	S	g	D /mT	E /mT	Lw /mT
$(Gd_2@C_{80})^-$	15/2	1.99	36.5	11	2.5
$(Gd_2@C_{78})^-$	15/2	1.985	53.75	0.25	2.2

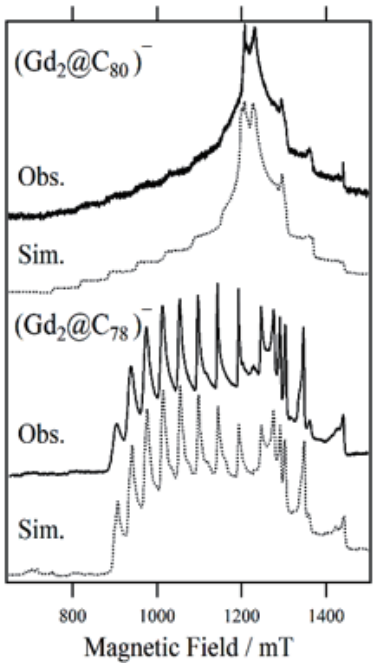

Fig 1. Q-band ESEFS spectra (Obs.) of $(Gd_2@C_{80})^-$ and $(Gd_2@C_{78})^-$observed at 6K. Simulated spectra (Sim.)

Corresponding Author: Tatsuhisa Kato
Tel: +81-75-753-6695, Fax: +81-75-753-6695,
E-mail: kato.tatsuhisa.6e@kyoto-u.ac.jp

Isolation and Characterization of the hidden metallofullerene: $Y_2@C_{78}$

○Natsumi Nakatori[1], Takuji Mitani[1], Takahisa Yamaguchi[2], Ko Furukawa[3], Tatsuhisa Kato[2, 4], Koichi Kikuchi[1], Yohji Achiba[1], Takeshi Kodama[1]

[1]*Department of Chemistry, Tokyo Metropolitan University, Hachioji 192-0397, Japan*

[2]*Graduate School of Human and Environmental Studies, Kyoto University, Kyoto 606-8501, Japan*

[3]*Department of Chemistry, Niigata University, Niigata 950-2181, Japan*

[4]*Institue for Liberal Arts and Sciences, Kyoto University, Kyoto 606-8501, Japan*

Although $Y_2@C_{80}$ has long been notified as a "hidden" or "missing" metallofullerene, recently, we have succeeded in the isolation and characterization of $Y_2@C_{80}$ using the method combining the ion-pair chromatography with the mixed solvent extraction [1]. Like $Y_2@C_{80}$, $Y_2@C_{78}$ has also been the one of the plausible candidates of such a "hidden" metallofullerene, because $La_2@C_{78}$ has well been known as a stable metallofullerene [2]. In this study, we isolated $Y_2@C_{78}$ by almost the same method as for $Y_2@C_{80}$, and characterized it.

Y-metallofullerenes were produced and extracted by the method previously reported [1]. $Y_2@C_{78}$ was isolated by two-stage HPLC, in which we used acetone with an ion-pair reagent, tetrabutyl-ammonium bromide, as an eluent. A Buckyprep column was used in both two stages.

Fig.1 shows the UV-vis-NIR absorption spectrum of the isolated $(Y_2@C_{78})^-$ and it is very similar to that of $Ce_2@C_{78}(D_{3h})$. Since the shape of UV-vis-NIR absorption spectra of the metallofullerenes is mainly characterized by the electronic state of the fullerene cage, the similarity in the absorption spectra of $(Y_2@C_{78})^-$ and $Ce_2@C_{78}(D_{3h})$ indicates that $(Y_2@C_{78})^-$ has $C_{78}(D_{3h})$ cage and an excess electron of $(Y_2@C_{78})^-$ is located on Y_2 dimer. Fig. 2 shows the ESR spectra of $(Y_2@C_{78})^-$ and $(Y_2@C_{80})^-$. They have a very similar pattern: three peaks with intensity ratio 1:2:1, which comes from the nuclear spin of Y (I=1/2). This pattern and the large hyperfine coupling constant (hfc) indicate that an excess electron exists on Y_2 dimer of $(Y_2@C_{78})^-$ as well as $(Y_2@C_{80})^-$. The smaller hfc of $(Y_2@C_{78})^-$ compared to that of $(Y_2@C_{80})^-$ suggests $(Y_2@C_{78})^-$ has the lower electron spin density on the Y nucleus than $(Y_2@C_{80})^-$.

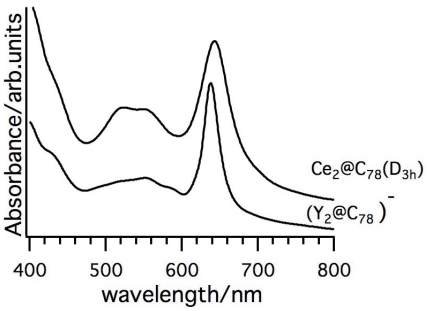

Fig.1 UV-vis-NIR absorption spectra of $(Y_2@C_{78})^-$ and $Ce_2@C_{78}(D_{3h})$.

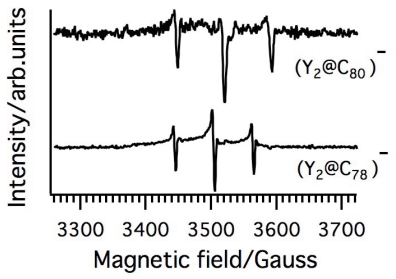

Fig.2 X-band ESR spectra of $(Y_2@C_{78})^-$ and $(Y_2@C_{80})^-$ at 4K.

[1] N. Nakatori, et al. *The 49th Fullerenes-Nanotubes-Graphene General Symposium* 46 (2015).

[2] B. Cao, et al. *J. Am. Chem. Soc.* **126,** 9164-9165 (2004).

Corresponding Author: Takeshi Kodama

E-mail: kodama-takeshi@tmu.ac.jp

Tel:+81-42-677-2530, Fax:+81-42-677-2525

Photoreactions of Trimetallic Nitride Template Endohedral Metallofullerenes with Digermirane

○Kyosuke Miyabe[1], Yuichi Sato[1], Masahiro Kako[*,1], Masanori Yasui[1], Kumiko Sato[2], Naomi Mizorogi[2], Wei-Wei Wang[3], Shigeru Nagase[3], Takeshi Akasaka[2,4,5]

[1]*Department of Engineering Science, The University of Electro-Communications, Chofu, Tokyo 182-8585, Japan*
[2]*Life Science Center of Tsukuba Advanced Research Alliance, University of Tsukuba, Tsukuba, Ibaraki 305-8577, Japan*
[3]*Fukui Institute for Fundamental Chemistry, Kyoto University, Kyoto 606-8103, Japan*
[4] *Department of Chemistry, Tokyo Gakugei University, Tokyo 184-8501, Japan*
[5] *Foundation for Advancement of International Science, Ibaraki 305-0821, Japan*

Endohedral metallofullerenes (EMFs) have been attracting much interest because of their fascinating properties regarding electron transfer from the endohedral metal atoms to the carbon cages. Many studies of the exohedral functionalization of EMFs have been performed to realize various applications such as organic electronic devices and biological diagnostic agents [1]. The functionalization of EMFs with electron-donating silyl and germyl groups is useful for modifying its electronic characteristics. Recently, it was observed that bis-germylation of $Lu_3N@I_h$-C_{80} proceeded more efficiently, and that germyl groups shifted the oxidation potential of $Lu_3N@I_h$-C_{80} slightly more cathodically than silyl groups [2].

In our continuing study of the functionalization of EMFs, we now report the bis-germylation of $Sc_3N@I_h$-C_{80} using digermirane **1**. The photoreaction of $Sc_3N@I_h$-C_{80} and **1** was conducted in a mixed solvent of 1,2-dichlorobenzene (ODCB) and toluene using two 500W halogen lamps with an aqueous $NaNO_2$ solution filter (cutoff < 400 nm). Separation of the reaction mixture afforded the corresponding 1,4-adduct **2** in 66% yield (Scheme 1). The 1,4-adduct **2** was fully characterized by spectroscopic, electrochemical, and theoretical studies, and was structurally established by single-crystal X-ray crystallography. The difference in reactivity between $Sc_3N@I_h$-C_{80} and $Sc_3N@D_{5h}$-C_{80}, the latter of which does not react with **1**, is also described.

Scheme 1.

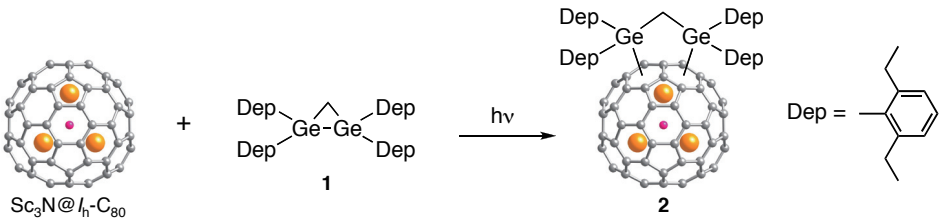

[1] L. Dunsch *et al.* Chem. Rev. **134**, 5989-6113 (2013).
[2] M. Kako, *et al.* Chem. Eur. J. **21**, 16411-16420 (2015).
Corresponding Author: Masahiro Kako Tel: +81-42-442-5570 E-mail: kako@e-one.uec.ac.jp

Mixed Valence transitions in Rare-earth Fullerides

Takeshi Nakagawa[a, *], Yasuhiro Takabayashi[a], Kosmas Prassides[a,b]

[a] *WPI-Advanced Institute for Materials Research (WPI-AIMR), Tohoku University, Sendai, 980-8577, Japan.*

[b] *JST ERATO Isobe Degenerate π-Integration Project, Tohoku University, Sendai, 980-8577, Japan.*

The family of rare-earth fullerides $RE_{2.75}C_{60}$ (RE = Sm and Yb) have been reported to show mixed-valence phenomena associated with the highly correlated narrow-band behaviour of the 4*f* electrons. Temperature- and pressure-induced abrupt or continuous valence transitions have been observed [1-3]. On the contrary, no anomalous behaviour is observed for the isostructural and isoelectronic $Ca_{2.75}C_{60}$, which lacks an electronically active 4*f* sublattice. We have now investigated Ca substitution effects in $Sm_{2.75}C_{60}$ with the synchrotron X-ray diffraction technique in an effort to obtain direct information on the electronic changes following the dilution of the Sm sublattice. Here we present the results of the temperature-dependent crystallographic studies, which probe the evolution of the negative thermal expansion effects with Ca^{2+}-doping in the $(Sm_{1-x}Ca_x)_{2.75}C_{60}$ ($0 \leq x \leq 1$) series.

[1] J. Arvanitidis, *et al.*,Nature **425**, 599 (2003)
[2] J. Arvanitidis, *et al.*,Dalton Trans. 3144 (2004).
[3] S. Margadonna, *et al.*, Chem. Mater. **17**, 4474 (2005).
Corresponding Author: T. Nakagawa
Tel: +81-22-217-5953, Fax: +81-22-217-5994,
E-mail: takeshi.nakagawa.b5@tohoku.ac.jp

μ^+SR study of fulleride superconductors across the superconductivity dome

○ Melita Menelaou[1,2], Yasuhiro Takabayashi[1], Ruth H. Zadik[3], Peter J. Baker[4], Kosmas Prassides[1,2]

[1] *WPI-Advanced Institute for Materials Research (WPI-AIMR), Tohoku University, Sendai, 980-8577, Japan.*
[2] *JST ERATO Isobe Degenerate π-Integration Project, Tohoku University, Sendai, 980-8577, Japan.*
[3] *Department of Chemistry, Durham University, Durham DH1 3LE, United Kingdom.*
[4] *The ISIS Facility, Rutherford Appleton Laboratory, Didcot OX11 0QX, United Kingdom.*

The electronic phase diagram of fullerides [1,2] exhibits striking similarities to those of many unconventional superconductors such as the cuprates. Superconductivity emerges from an antiferromagnetic strongly correlated Mott insulating state upon tuning a parameter such as pressure. The Mott insulator-metal transition may be traversed and the entire superconductivity dome tracked by applying chemical pressure by substituting the smaller Rb^+ cation for Cs^+ in the parent insulator, Cs_3C_{60} to generate the $Rb_xCs_{3-x}C_{60}$ ($0 < x \leq 3$) superconductors (Fig. 1) [3]. Here we report the results of transverse-field muon spin rotation (TF-μ^+SR) measurements to investigate the superconducting properties of $Rb_xCs_{3-x}C_{60}$ across the superconductivity dome – from underexpanded ($x = 2$) through optimally expanded ($x = 1$) to overexpanded ($x = 0.5$) compositions. This allows us to follow the evolution of the magnetic-field penetration depth, λ, which in turn is related to the superconducting carrier density, n_s and the effective mass, m^* across the dome as the importance of correlations increase and the superconductivity evolves from weakly- to strongly-coupled.

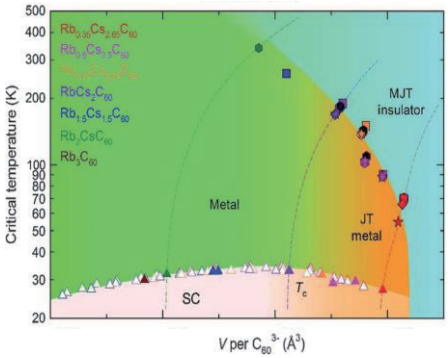

Fig. 1 Global electronic phase diagram of *fcc* $Rb_xCs_{3-x}C_{60}$ [3].

[1] Y. Takabayashi *et al.*, Science **323**, 1585 (2009).
[2] A. Y. Ganin *et al.*, Nature **466**, 221 (2010).
[3] R. H. Zadik *et al.*, Sci. Adv. **1**, e1500059 (2015).
Corresponding Author: M. Menelaou
Tel: +81-70-1140-1980, Fax: +81-22-217-5994,
E-mail: menelaou.melita.b1@tohoku.ac.jp

Energetics and electronic structure of CNT embedded in Si

○Taketo Kochi and Susumu Okada

University of Tsukuba, 1-1-1 Tennodai, Tsukuba, Ibaraki, 305-8571 Japan

Nanoscale vacancies in semiconducting materials can be regarded as negative clusters and molecules which exhibit interesting electronic properties depending on their sizes and shapes. Due to the low dimensionality and nanoscale size of vacancies, the vacancies in semiconductors are applicable for electronic, optical, and optoelectronic devices. Indeed, vacancies in GaAs filled by C_{60} have been synthesized experimentally, which acts as quantum dots. However, it is still uncertain whether the electronic property of the hybrid of vacancies and nanomaterials is the simple sum of those of constituent units or not. In the present work, we aim to explore the fundamental properties of the one-dimensional nanoscale tunnel in Si, which is filled by a carbon nanotubes (CNTs), as the possible hybrid consisting of negative and positive nanostructures using density functional theory with local density approximation. In this works, we construct the tubular vacancies with diameters of 10, 11, 12, and 13 Å along the [130] direction in the Si slabs with H-terminated (001) surfaces, which are filled by (8,0), (9,0), (10,0), and (11,0)CNTs. Figure 1 shows the electrostatic potential of the pristine tunnel and the CNT-filled tunnels. In the case of the pristine tunnel, inhomogeneous potential profile is observed, owing to the Si dangling bonds at the wall of the tunnel. Interestingly, although the dangling bond states retain upon CNT doping, we observed the almost flat potential profile inside the tunnel. We further observe the electronic structure modulation of CNTs within the tubular vacancies due to the substantial hybridization.

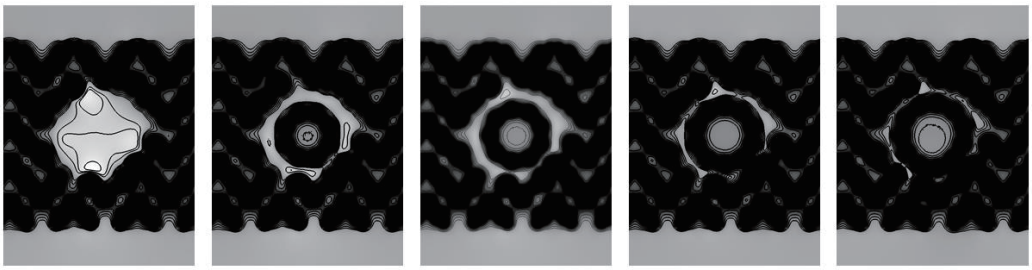

(a) (b) (c) (d) (e)

Fig. 1 Counter plots of the electrostatic potential of (a) a tubular vacancy with 13Å diameter in Si and the vacancies filled by (b) (8,0), (c) (9,0), (d) (10,0), and (e) (11,0) CNTs.

Corresponding Author: T. Kochi

Tel: +81-029-853-5600(ext.; 8233) , E-mail: tkochi@comas.frsc.tsukuba.ac.jp

Crossover from Quantum to Classical Transport in Carbon Nanotubes

○Keisuke Ishizeki [1], Kenji Sasaoka [2], Takahiro Yamamoto [1]

[1] *Department of Electrical Engineering, Tokyo University of Science*
[2] *Organization of Advanced Science and Technology, Kobe University*

Due to their quasi-one-dimensional structures, single-walled carbon nanotubes (SWNTs) are known to exhibit various remarkable electrical, optical, and thermal properties. In particular, electronic transport in SWNTs has attracted great attention because it is directly contributed to electrical device application for next-generation LSI technologies. An SWNT shorter than the mean free path (MFP) shows the quantum resistance originating from quantum ballistic transport in one dimension. This can be explained in terms of Landauer's transport theory. On the other hand, an SWNT longer than the MFP follows classical Ohm's law that the electrical resistance is proportional to the system length. This can be understood in terms of Boltzmann's transport theory.

In this work, we have developed a new quantum-transport simulation method that can seamlessly treat a whole regime from quantum ballistic to classical ohmic transport regimes. We have applied the method to armchair SWNTs with various lengths. Figure 1 shows the nanotube-length dependence of electrical resistance of a (5,5)-SWNT at 300K. We can clearly find crossover behavior from the quantized resistance (the broken line in Fig. 1) to ohmic resistance (the dotted line in Fig. 1). The MFP of a (5,5)-SWNT at 300K is given as 272 nm from the crossing point between the broken line and the dotted line in Fig. 1.

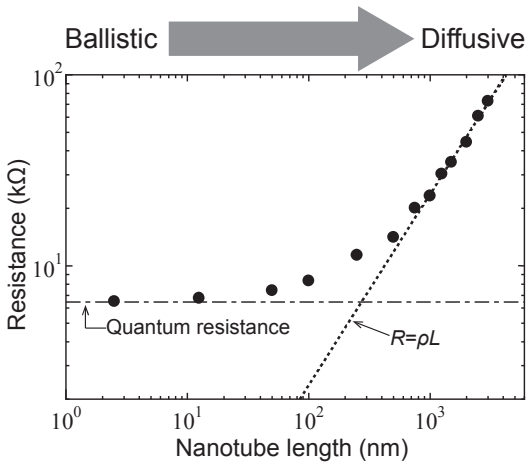

Fig. 1. Nanotube-length dependence of electrical resistance of a (5,5)-SWNT at 300 K.

By performing similar calculations at several temperatures, we estimated the temperature dependence of MFP of a (5,5)-SWNT. As seen in Fig. 2, the MFP is inversely proportional to the temperature. In addition, we have performed similar calculations for (3,3)-, (8,8)- and (10,10)-SWNTs. As shown in the inset of Fig. 2, the resistivity of armchair SWNTs is also inversely proportional to the diameter. The diameter dependence of MFP for thicker SWNTs is in agreement with previous experimental and theoretical results based on the continuum approximation [1,2].

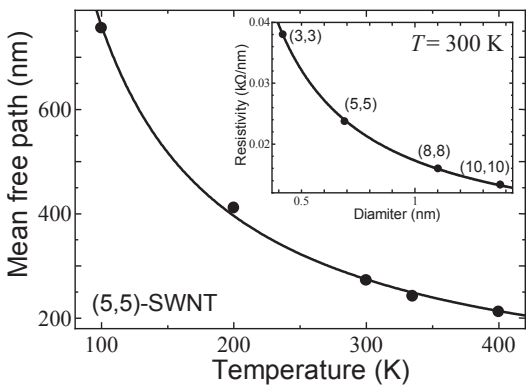

Fig. 2. Temperature dependence of mean free path of a (5,5)-SWNT. The inset represents diameter dependence of the resistivity of armchair SWNTs at 300 K.

[1] H. Suzuura and T. Ando. PRB. **65**, 235412 (2002).
[2] M. S. Purewal *et al*. PRL **98**, 186808 (2007).

Corresponding Author: T. Yamamoto
Tel: +81-3-5876-1492 E-mail: takahiro@rs.tus.ac.jp

1P-10

Photoluminescence spectral shift of chemically-modified single-walled carbon nanotubes by external stimuli

Hisashi Onitsuka[1], Tomohiro Shiraki[1,2], Naotoshi Nakashima[1,2]

[1]*Department of Applied Chemistry, Kyushu University, Fukuoka 819-0395, Japan*
[2] *WPI-I2CNER, Kyushu University, 744 Motooka, Fukuoka 819-0395, Japan*

Semiconducting single-walled carbon nanotubes (SWNTs) have unique optical properties exemplified by near-infrared photoluminescence (NIR PL), by which new materials for bio-sensing and imaging applications have been developed [1]. Typically, PL quantum yields of the SWNTs are low; however, a very small amount of chemical modification on the SWNTs has recently been reported to dramatically enhance their quantum yield by appearance of a new red-shifted PL (E_{11}*) compared to PL (E_{11}) of the pristine SWNTs [2]. After the finding, several compounds have been examined for the chemical modification of the SWNTs, suggesting suitable molecular design of such molecules leads to the preparation of novel functional SWNTs.

In this study, we synthesized a phenyl boronic acid derivative, which has a binding site with saccharides through the formation of boronate esters [3]. After the reaction using the newly-synthesized compound, the new E_{11}* PL was observed around 1150 nm although absorption spectrum of the resulting SWNTs were hardly changed in comparison with that of the pristine SWNTs, indicating a limited modification of the SWNTs. Interestingly, peak shift of the E_{11}* was observed by adding a saccharide solution to the SWNT solution. The spectral shifting behavior and molecular interactions will be discussed at the meeting.

[1] M. S. Strano, et al., *ChemSusChem.* **2011**. *4*. 848.

[2] Y. Wang et al., *Nat. Chem*. **2013**, *5*, 840

[3] N. Fujita, S. Shinkai, T. D. James, *Chem. Asian J.* **2008**, *3*, 1076.

Corresponding Author: Naotoshi Nakashima
Tel: +81-92-802-2840, Fax: +81-92-802-2840
E-mail: nakashima-tcm@mail.cstm.kyushu-u.ac.jp

Morphology Dependence on Thermal Transport Properties of Single-walled Carbon Nanotube Films

○Shuhei Yoshida[1], Ya Feng[1], Taiki Inoue[1], Rong Xiang[1], Shohei Chiashi[1], Esko Kauppinen[2], Shigeo Maruyama[1, 3]

1. Department of Mechanical Engineering, University of Tokyo, Tokyo 113-8656, Japan
2. Department of Applied Physics, Aalto University School of Science, 15100, FI-00076 Aalto, Finland
3. National Institute of Advanced Industrial Science and Technology (AIST), Tsukuba 305-8564, Japan

Single-walled carbon nanotubes (SWNTs) have gotten much attention as a highly promising material for the use of thermal management such as thermal interface materials owing to its superior thermal conductivity. According to the previous studies, isolated individual SWNTs have thermal conductivity as high as 2000 W/mK at room temperature [1]. On the other hand, many studies showed the apparent thermal conductivity of individual SWNTs inside of vertically aligned SWNT films is not as high as that of isolated one [2]. The cause of this discrepancy is not fully understood whereas it is discussed in many articles.

In this study, we measured the thermal conductivity of high quality random network SWNT films, whose optical transmittance are 86.4, 80.9, 63.7 and 53.5 %, made by floating catalyst chemical vapor deposition [3]. Micro Raman spectroscopy was employed, and thermal conductivities of the films were determined from excitation laser power dependence of G^+ band Raman shift [4]. The results agree with the measurement by using steady state method with IR camera. In addition, optical absorbance spectra were used to investigate SWNT bundle network structure of the films. It was observed that the level of optical anisotropy is decreased when the thickness of SWNT films is increased, and the effect of the anisotropy to their thermal transport properties is discussed. Figure 1 shows the positive correlation between film transmittance and normalized thermal conductivity. This trend suggests that thermal conductivity of SWNTs can be drastically reduced by phonon scattering at tube-tube interface. It should be noted that no phonon life time reduction around Γ point was confirmed based on Raman spectra line-width.

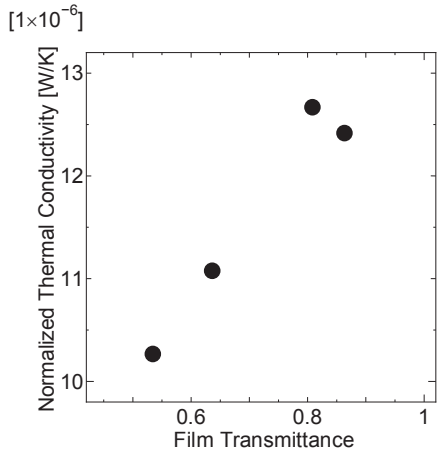

Fig. 1: Relationship between film transmittance and normalized thermal conductivity of SWNT films.

References:
[1] J. Hone, *et al.*, Phys. Rev. B, **59,** 2514 - 2516 (1999).
[2] J. Hone, *et al.*, Appl. Phys. Lett. **77**, 666 - 668 (2000).
[3] A Kaskela, *et al.*, Nano Lett., **10**, 4349-4355 (2015).
[4] W. Cai, *et al.*, Nano Lett. **10**, 1645 - 1651 (2010).
Corresponding Author: Shigeo Maruyama
Tel: +81-3-5841-6421, Fax: +81-3-5841-6421
E-mail: maruyama@photon.t.u-tokyo.ac.jp

Photothermoelectric Effect in Single Wall Carbon Nanotube Thin Films with Precisely Controlled Seebeck Coefficients

○Masatoshi Nakamura, Yoshimasa Kitamura, Yuki Oshima, Hideki Kawai, Yutaka Maniwa, Kazuhiro Yanagi

Department of Physics, Tokyo Metropolitan University, Tokyo 192-0397, Japan

Photo-thermoelectric effect is generation of photo-voltage using thermoelectric properties of materials through light induced local electron heating. To efficiently generate photo-induced voltage by photo-thermoelectric effect, it is necessary to use materials with weak electron-phonon interactions and to control spatial distribution of Seebeck coefficients in a device. Single wall carbon nanotubes (SWCNTs) are known to be a material with very weak electron-phonon interactions, and photo-voltage through such photo-thermoelectric effects have been reported in several studies.[1] However, it is very important to precisely control spatial distribution of Seebeck coefficient in order to efficiently generate voltage. Recently we developed a technique that enables precise control of the values and the signs (P or N) of Seebeck coefficients of SWCNTs using electric double layer carrier injection techniques.[2,3] Therefore, in this study, we investigated how efficiently we can generate photo-voltage through photo-thermoelectric effects in metallicity selected and Seebeck effect controlled SWCNT networks.

Figure 1(a) shows a picture of a device. Thin films of Semiconducting or metallic SWCNTs with diameter of 1.4 nm, which were purified through density-gradient centrifugation processes, were used as channels. The Seebeck coefficient of the half part of the channel was controlled to be negative (N-type) using electric double layer carrier injections, but the other half was non-controlled and was left to be P-type (Fig. 1(a)). The device was fabricated on a palylene layer for thermal isolation. Then, we illuminated laser light with wavelength of 488 nm on a center region between N and P Seebeck coefficient regions. We found clear generation of photo-voltage by illumination of laser light in both metallic and semiconducting SWCNT networks. Even in the case of metallic SWCNTs, we observed photo-voltage generation, suggesting voltage generation by photo-thermoelectric effect. The generated photo-voltage in the case of semiconducting SWCNTs is shown in Fig. 1(b). Photo-voltage was generated by irradiation of laser light (488 nm). The generated voltage was 16 mV/W. Although the value is lower than the reported efficiency, more precise tuning will improve the efficiency.

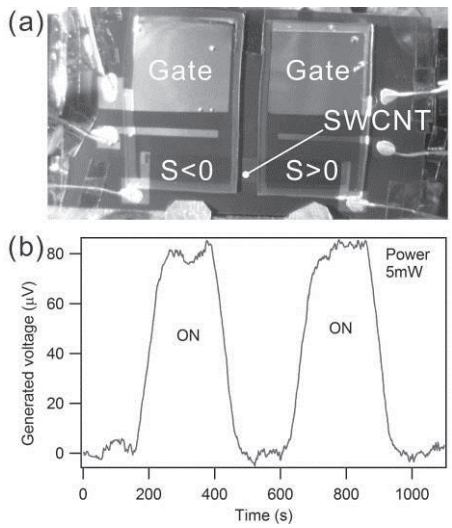

Fig. 1(a) A picture of a device, (b) generated voltages through photo-thermoelectric effects by light illumination

[1] X. He et al, *ACS Nano* 7, 7271 (2013)
[2] K. Yanagi et al., *Nano Lett.* 14, 6437 (2014)
[3] Y. Oshima, Y. Kitamura, Y. Maniwa, K. Yanagi, *Appl. Phys. Lett.* 107, 043106 (2015)

Corresponding Author: Kazuhiro Yanagi
Tel: +81-42-677-2494
E-mail: yanagi-kazuhiro@tmu.ac.jp

Carbon nanotube sheet as a transparent electrode for semi-transparent organic solar cell

○Senku Tanaka [1], Naoya Urakawa [1], and Kanzan Inoue [2]

[1] *Graduate School of Science and Engineering, Kinki University, Osaka 577-0818, Japan*
[2] *LINTEC OF AMERICA, Nano-Science & Technology Center, Texas 75081, U.S.A.*

Organic electronics devices, such as organic light emitting diodes, organic solar cells (OSC), and organic transistors, have attracted much interest because of its unique potentials of lightweight, flexible and low-cost processing. To use these unique characteristics, it needs appropriate electrodes for transporting carriers to an external circuit. Carbon nanotube (CNT) sheet produced from the CNT forest [1] is one of the potential candidates of electrode for the organic electronics devices. The characteristics of CNT-sheet (light weight, strong, flexible, transparent, conductive and stable) are suitable for using as the electrode of organic devices. We have studied the applicability of CNT-sheet as a top electrodes of OSC [2]. The transparency of CNT-sheet meets a requirement for a semi-transparent OSC. However the performance of OSC is limited by low conductivity of the CNT-sheet. To improve the conductivity of CNT-sheet, we studied a combination of silver with the CNT-sheet. These combination satisfied both of high transparency and high conductivity.

A semi-transparent OSC was fabricated on an ITO substrate. As an electron transport layer, a ZnO layer was deposited on the ITO by using a sol-gel method. As a photoactive layer, we used a bulk-heterojunction of poly (3-hexyl thiophene-2,5-diyl) (P3HT) and 6,6-phenyl C_{61} butyric acid methyl ester (PCBM). The CNT-sheet (cSilk, Lintec-NSTC) was attached on to the photoactive layer as the top electrode. In addition, silver and a conductive polymer solution were used to improve conductivity and adhesiveness. All the fabrication processes were done under atmospheric pressure. In addition, all the processes were done below 150 °C. The structure of the fabricated device was ITO/ZnO/P3HT:PCBM/modified CNT-sheet (from bottom to top). The device showed an average transmittance of approximately 51% in the wavelength range of 650–900 nm. (Fig. 1 (a). A photograph of semi-transparent OSC is shown in inset.) A typical photocurrent density-voltage characteristics was shown in fig.1 (b). The power conversion efficiency of approximately 1.7 % was obtained by the illumination from the ITO side under light with air mass of 1.5 (100mW/cm^2). Detailed results and properties of the semi-transparent OSC will be discussed.

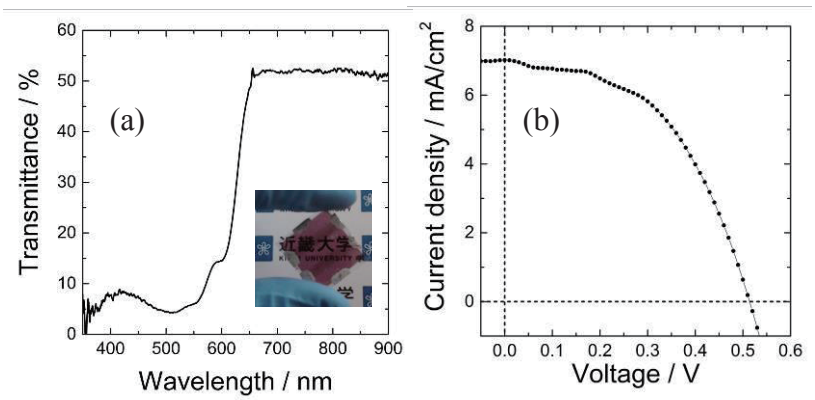

Fig. 1. (a) Transmittance and (b) Photocurrent density-voltage characteristics of a semi-transparent organic solar cell. The inset shows a fabricated semi-transparent organic solar cell.

[1] M. Zhang *et al.*, Science, **309** 1215 (2005).
[2] S. Tanaka *et al.* Synthetic Metals, **159** 2326 (2009).

Corresponding Author: S. Tanaka
Tel: +81-6-4307-4327
E-mail: senku@ele.kindai.ac.jp

In-situ TEM study on self-oscillations of carbon nanotube during field emission

○Tomonori Kato, Hitoshi Nakahara, Koji Asaka and Yahachi Saito

Department of Quantum Engineering, Nagoya University, Furo-cho, Nagoya 464-8603

Oscillations of carbon nanotube (CNT) during field emission (FE) under an application of DC voltage have been observed [1], but the origin of the oscillations is not well understood. In order to clarify the mechanism of the oscillations, we investigated the phenomena under various geometrical conditions of CNTs using transmission electron microscopy (TEM).

In previous studies, a mechanism for oscillating has been proposed as follows: a CNT bends to an anode by the electrostatic force, and then returns to the opposite direction by the elastic restoring force because of the decreased electrostatic force by FE (i.e., discharge) [2]. According to this hypothesis, it is required that the initial direction of the CNT is inclined from the surface normal of the anode to a certain extent. It is also required that the electric resistance of the CNT itself is larger than the resistance in FE [3].

We checked whether these conditions are satisfied or not by experiment using multi-wall carbon nanotube (MWCNT). FE experiments changing the inclination angle of a MWCNT showed that oscillations were observed without any dependence of the angle, even nearly vertical to the anode surface (Figs. 1(a), (b)). Also we measured current-voltage (*I-V*) characteristics of a MWCNT measured by two terminal method (Fig. 2(a)) and *I-V* of FE (Fig. 2(b)). From the slope of the *I-V* at the current value of 0.1 μA (the current when the oscillation started), we found that the resistance of MWCNT is smaller than that in FE. From these results on the angle independence and the relation between the resistances, we consider that the oscillation mechanism of MWCNT during FE in TEM cannot be explained by the idea previously reported.

We also investigated the effects of MWCNT length and radius, distance to anode, and found a relationship between amplitude of oscillation and FE current, but the mechanism remains unclear. In addition to these observations, the effect of Lorentz force will be discussed.

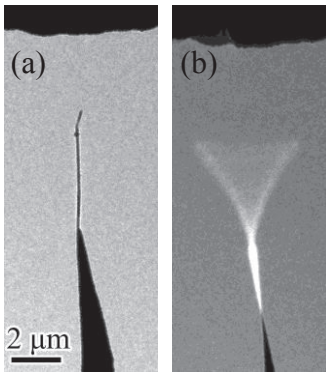

Fig. 1 TEM images of a MWCNT emitter and an anode. (a) Before applying voltage, and (b) during FE with oscillation.

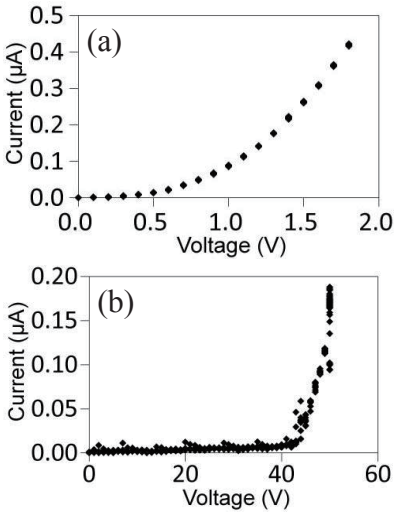

Fig. 2 *I-V* characteristics of (a) a MWCNT and (b) FE.

[1] Y. Saito *et al.,* Diamond & Related Materials 14, 1843-1847 (2005)
[2] Jeffrey A. Weldon *et al*., Nano Lett. 10, 1728-1733 (2010)
[3] A. Lazarus *et al.*, Int. J. Mech. Sci. 52, 1396-1406 (2010)

Corresponding Authors: Tomonori Kato, Yahachi Saito
Tel: +81-52-789-3714, Fax: +81-52-789-3703,
E-mail: t-kato@surf.nuqe.nagoya-u.ac.jp, ysaito@nagoya-u.jp

Transparent, stretchable all-carbon nanotube thin-film transistors for wearable electronics

○Takeo Onishi[1], Jun Hirotani[1], Shigeru Kishimoto[1], and Yutaka Ohno[1,2]

[1]*Graduate School of Engineering, Nagoya University, Nagoya 464-8603, Japan*
[2]*Institute of Material and Systems for Sustainability, Nagoya University, Nagoya 464-8603, Japan*

Flexible and stretchable electronics offer a wide variety of wearable electronics applications such as electronic-skins and healthcare/medical devices. Among various conductive materials for wearable electronics, carbon nanotube (CNT) thin films are advantageous in flexibility/stretchability, conductivity, and transparency. In addition, CNT thin films can be used both as a channel material for high-performance transistors [1] and as a metallic conductor for interconnections [2]; i.e. integrated circuits can be constructed by fully using CNT thin films [3]. A stretchability is one of essential functions for the wearable devices which are able to be directly attached to body. In this work, we have realized stretchable and transparent all-carbon devices.

The CNT thin-film transistors (TFTs) were realized on a poly(dimethylsiloxane) (PDMS) substrate. After the device fabrication was completed on a Si substrate, the devices were transferred on the PDMS substrate. The transfer process is applicable for a wide variety of substrates. Purified semiconducting CNTs were used as the channel material. The CNT electrodes were formed by the dry transfer process [4] and subsequent photolithography process. The fabricated device is transparent and attachable to human body as can be seen in Fig. 1. The all-carbon devices provide a new possibility to realize wearable devices without feeling its presence.

Acknowledgments: The semiconducting CNTs were provided by TASC. This work was partially supported by Grant-in-Aid by MEXT, JST/SICORP, JST/ALCA, and NEDO.

[1] D.-M. Sun, *et al.*, *Nature Nanotechnol.* **6**, 156 (2011).
[2] N. Fukaya, *et al.*, *ACS Nano* **8**, 3285 (2014).
[3] D.-M. Sun, *et al.*, *Nature Commun.* **4**, 2302 (2013).
[4] A. Kaskela, *et al.*, *Nano Lett.* **10**, 4349 (2010).

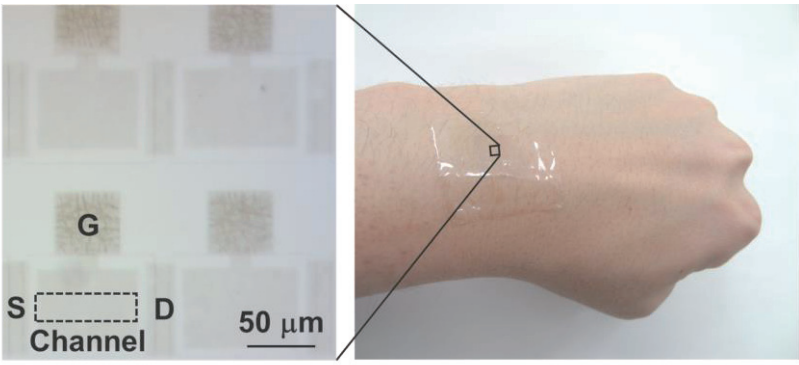

Fig. 1 Fabricated device images

Corresponding Author: Yutaka Ohno, Tel & Fax: +81-52-789-5387, E-mail: yohno@nagoya-u.jp

Mechanical and Electric Properties of Continuous Polymer-Free Carbon Nanotube Fibers

○Xueli Wu[1], Takahiro Morimoto[2,1], Ken Mukai[3,1], Kinji Asaka[3,1], Toshiya Okazaki[2,1*]

[1] *Technology Research Association for Single Wall Carbon Nanotubes (TASC), Tsukuba 305-8565, Japan,*
[2] *Nanotube Application Research Center, National Institute of Advanced Industrial Science and Technology (AIST), Tsukuba 305-8565, Japan,*
[3] *Inorganic Functional Materials Research Institute, National Institute of Advanced Industrial Science and Technology (AIST), Osaka, 563-8577, Japan*

Single-walled carbon nanotubes (SWCNTs) have been potentially applied in wide fields because they have a series of unique properties including electrical and mechanical properties since their discovery in the early 1993 [1]. One of the major obstacles for their applications is the poor dispersibility in solvents or polymers. Because strong van der Waals attractions cause SWCNTs to bundle, dissociation is increasingly difficult for long pristine SWCNTs. For instance, wet spinning from carbon nanotube (CNT) dispersions has attracted considerable interest for producing CNT fibers. The most important process of the method is the preparation of "good" CNT dispersions.

Surfactants have usually been used as supports for the CNTs dispersed in water since surfactants have adsorbed on the nanotube surface by hydrophobic or π-π interactions. The surfactant-stabilized CNT aqueous dispersions can be spun to fibers by coagulation. Recently, polymer-free CNT fibers were produced by a novel wet spinning method without a polymer coagulating solution or strong acid solvent [2]. CNT dispersions with different dispersing time were injected into 2-propanol to be coagulated as fibers.

Nevertheless, there are very few reports on the relation between CNT fiber properties and the character of the CNT dispersions, so far [3]. In this work, we have produced wet-spinning CNT fibers by using Super-Growth- and eDIPS-SWCNTs with different dispersing conditions. The prepared SWCNT dispersions were characterized by the far-infrared (FIR) and resonance Raman spectroscopy. The lengths and qualities of SWCNTs in dispersions were estimated from the FIR peak positions and the G/D values in the Raman spectra [4]. Interestingly, the mechanical and electrical properties of these fibers are closely related to the effective SWCNTs length and the quality of SWCNTs in the dispersions. The present finding suggests that it is very important to disperse CNTs without damage for preparing high performance CNT fibers.

This paper is based on results obtained from a project commissioned by the New Energy and Industrial Technology Development Organization (NEDO).

[1] S Ijima, T Ichihashi, Nature 363, 603 (1993).
[2] K. Mukai, K. Asaka, T. Murakami, C. Ito, T. Saito, M. Yumura, The 46th Fullerene-Nanotube-Graphene General Symposium, 3-1, p. 30 (2014).
[3] N Behabtua, M J Greena, M Pasquali, Nano Today 3, 24 (2008).
[4] T. Morimoto, S.-K. Joung, T. Saito, D. N. Futaba, K. Hata, T. Okazaki, ACS Nano, 8, 9897-9904 (2014).

Corresponding Author: Toshiya Okazaki
Tel: +81-29-861-4173, Fax: +81-3-123-4567, E-mail: toshi.okazaki@aist.go.jp

1P-17

Production and electrical properties of CNT-Cu composite wires

○Rajyashree Sundaram[1], Atsuko Sekiguchi [1,2], Takeo Yamada[1,2], Kenji Hata[1,2]
[1] *Technology Research Association for Single Wall Carbon Nanotubes (TASC), Central 5, 1-1-1 Higashi, Tsukuba 305-8565, Japan*
[2] *National Institute of Advanced Industrial Science and Technology (AIST), Central 5, 1-1-1 Higashi, Tsukuba 305-8565, Japan*

Carbon nanotube-copper (CNT-Cu) composites, which can potentially combine the advantages of CNTs and Cu, have garnered much attention as promising materials for applications requiring high electrical and thermal conductivities, high current carrying capacity, and low coefficient of thermal expansion [1-2]. Here, we report the preparation of CNT-Cu composite wires by two-stage electrodeposition of dry-spun multiwalled CNT wires. Our findings indicate that various process parameters, such as plating current, time, environment, solution concentration, etc. affect the Cu filling and distribution, which in turn affect the electrical properties of the wires. CNT-Cu composite wires prepared under optimum conditions show uniform Cu distribution along the length and cross section, indicating a continuous CNT-Cu interface.

This presentation is based on results obtained from a project commissioned by the New Energy and Industrial Technology Development Organization (NEDO).

[1] C. Subramaniam *et al*. Nat. Comm. **4**, 2202 (2013).
[2] C. Subramaniam *et al*. Nanoscale 6(5), 2669 (2014).

Corresponding Author: A. Sekiguchi
Tel: +81-29-861-4551, Fax: +81-29-861-4851
E-mail: atsuko-sekiguchi@aist.go.jp

Polymer Length effect on Selective Separation of Semiconducting Single-Walled Carbon Nanotubes

○Fumiyuki Toshimitsu [1] and Naotoshi Nakashima [1,2,3]

[1] *Department of Engineering, Kyushu University, Fukuoka 819-0395, Japan*
[2] *WPI-I²CNER, Kyushu University, Fukuoka 819-0395, Japan*
[3] *JST-CREST, Chiyoda-ku, Tokyo 102-0075, Japan*

Polyfluorene and their derivatives (PFOs) have been intensely investigated as dispersants for single-walled carbon nanotubes because they exhibit selectively sorting abilities for the semiconducting single-walled carbon nanotubes (sem-SWCNTs). The mechanism of selective extraction of PFOs, however, has not been fully clarified yet, including very fundamental issue such as effects of main-chain lengths of fluorene-based dispersants The studies investigating chain-length dependence of fluorene-based dispersants have been very limited [1],[2], because the conventional preparation methods for PFOs with different main-chain length could not eliminate the molecular weight distribution problem and not monodisperse.

In this study, we synthesized fluorene oligomers with different main-chain lengths (**FOn**, n: the number of fluorene repeating unit, see Fig. 1) using precise combination of monomers and obtained monodisperse **FOn**s with n=6, 9, 12, 15, 18, 21, 24, 27 [3]. Sorting abilities of **FOn**s on SWCNT solubilization showed obvious dependency on main-chain length of **FOn**s (Fig. 2); namely, SWNT dispersions was observed when the main-chain length was longer than n = 12 and shorter **FOn**s (n=12 and 15) did not show the sem-SWCNT selectivity, which was also confirmed from their Raman spectra. The chiral selectivity was further investigated by the experimental photoluminescence spectroscopy mapping together with molecular mechanics simulations, which revealed that the mechanism of chiral selectivity and molecular length of **FOn**s. The present study demonstrated importance of the main-chain length of the oligofluorenes on selected sem-SWNT sorting, which is useful for designing fluorene-based compounds that sort sem-SWNTs with a specific chirality.

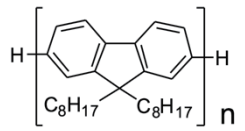

Figure 1. Chemical structures of **FOn**s.

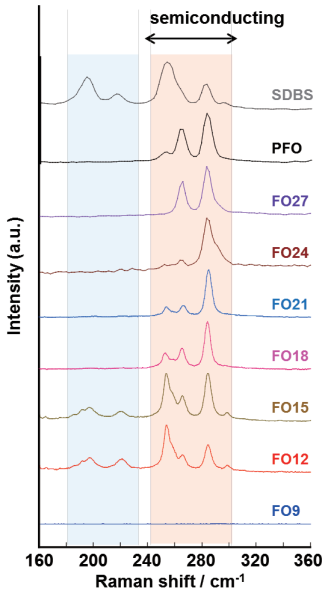

Figure 2. Raman spectra of solubilized SWCNTs with eight different **FOn**s and SDBS.

[1] P. Imin *et al.*, *Polym. Chem.* **2**, 1404 (2011)
[2] F. Jakubka *et al.*, *ACS Macro Lett.* **1**, 815 (2012)
[3] T. Shiraki *et al.*, *Polym. Chem.*, **6**, 5103 (2015)

Corresponding Author: N. Nakashima
Tel: +81-92-802-2845, Fax: +81-92-802-2845,
E-mail: nakashima-tcm@mail.cstm.kyushu-u.ac.jp

Chirality Control of In-Plane Oriented Single-Walled Carbon Nanotubes Using Free Electron Laser

○Daiki Kawaguchi, Miu Kobayashi, Shinnosuke Harumiya,
Tomoko Nagata, Nobuyuki Iwata and Hiroshi Yamamoto

College of Science & Technology, Nihon University
7-24-1 Narashinodai, Funabashi, Chiba 274-8501 Japan

Single-walled carbon nanotube (SWNT) has many advantages for application, such as high electric conductivity, high allowable current density and mechanical strength. For nano-scale field effect transistor using single-walled carbon nanotubes, metal and semiconductor separation as well as their chirality are required to be controlled. In addition growth position / density and *in-plane* orientation of the SWNTs are also required. In our previous study, the growth of all semiconducting SWNTs had been achieved by irradiation of the free electron laser (FEL) during growing process on SiO_2/Si substrate [1]. The irradiation of the FEL may enhance the growth of SWNTs having specific bandgap, which corresponds to the photon energy of the FEL. The purpose of this study is selective growth of *in-plane* oriented SWNTs with specific chirality using FEL irradiation during growth.

Co nano-particles were deposited on ST-cut quartz substrate by evaporation methiod. A chemical vapor deposition (CVD) was carried out for growth of the SWNTs for 10 min. The 800 nm FEL was irradiated during growth. Surface image revealed the growth of *in-plane* oriented SWNTs in both cases with FEL and without FEL. Fig.1 shows the Raman spectra of SWNTs grown with 800 nm FEL and without FEL. Without FEL, the RBM peaks were observed in 785 nm, 632 nm and 532 nm excitation laser. The calculated diameter was 1.05~1.14 nm (785 nm, ○), 1.55 nm (785 nm, ●), 1.76 nm (632 nm, ○), 1.08 nm (532 nm, ●). With FEL irradiation, the RBM peaks were observed only in Raman spectrum using 785 nm excitation laser. The calculated diameter was 1.05~1.14 nm (785 nm, ▽), 1.57 nm (785 nm, ▼). The notation of ▽, ○ and ▼, ● indicates semiconductor and metal peaks, respectively. These results indicate the FEL irradiation controls the bandgap.

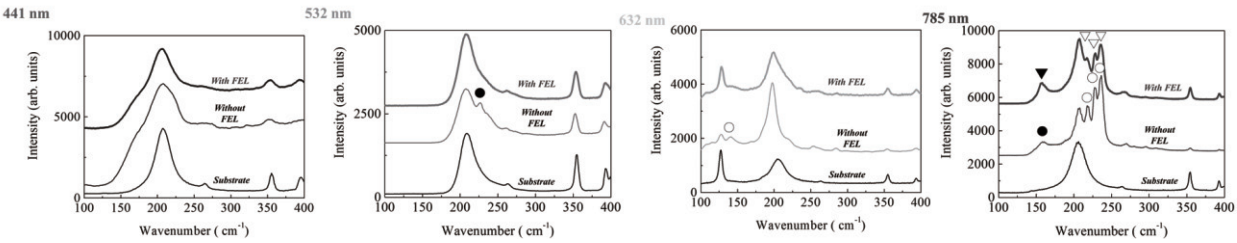

Fig. 1 Raman spectra using excitation lasers of 785, 632, 532 and 441nm. The notation of ▼, ▽ and ● and ○ indicates RBM peaks with FEL and without FEL, respectively. The open (▽, ○) and closed (▼, ●) symbols indicate semiconductor and metal. The bottom line of each Raman spectrum is of the substrate.

[1] K. Sakai *et al.* IEICE Trans. Electron. **E94-C**, 1861 (2011)

Corresponding Author: Nobuyuki Iwata
Tel: +81-47-469-5457, Fax: +81-47-469-5457, E-mail: iwata.nobuyuki@nihon-u.ac.jp

Catalyst Nucleation and Carbon Nanotube Growth from Flame-Synthesized Co-Al-O Nanopowders at 10 Second Time Scale

○Hiroyuki Shirae[1], Kei Hasegawa[1], Eongyu Yi[2], Richard M. Laine[2], Suguru Noda[1]

[1] *Dept. of Applied Chemistry, Waseda University, Tokyo 169-8555, Japan*
[2] *Dept. of Material Science and Engineering, University of Michigan, Ann Arbor, 48109, USA*

Carbon nanotubes (CNTs) are an attractive candidate material for electronic devices owing to their excellent electronic properties, excellent stability in ambient, flexibility, and compatibility with printing processes. Chemical vapor deposition (CVD) is widely used to produce CNTs, and improving catalyst technology is still important to establish efficient production of small diameter CNTs.

In this work, we investigated the use of Co-Al-O nanopowders by liquid-feed flame spray pyrolysis [1] as catalyst for small-diameter CNTs. Quick phase separation of Co from the mixed oxide would be the key in producing small Co particles, and thus we coated the nanopowders on SiO_2/Si substrate and heated them rapidly at a time scale ~10 s by electric current (Fig. 1) [2]. The nanopowders were reduced at 800−1200 °C with 3−10 vol% H_2/ 0−14 vol% CO_2/Ar at ambient pressure for 0−10 s. Then, CNTs were synthesized by adding 0.5 vol% C_2H_2 to the gas at the same temperature for 10 s. We examined the effect of Co mole fraction y in the $(CoO_x)_y$-$(Al_2O_3)_{1-y}$ nanopowder.

The nanopowders with low Co contents (y = 0.05, 0.10, and 0.25) were inert but that with a high Co content (y = 0.50) were active to yield single-wall CNTs (SWCNTs) as can be seen in the scanning electron microscope (SEM) and transmitting electron microscope (TEM) images (Fig. 2). And Raman spectra showed a split G-band peak and RBM peaks with small D-band peak at high temperatures (1000−1230 °C) (Fig. 3). We will show the results for different synthesis conditions and discuss the mechanisms for catalyst nucleation and CNT growth.

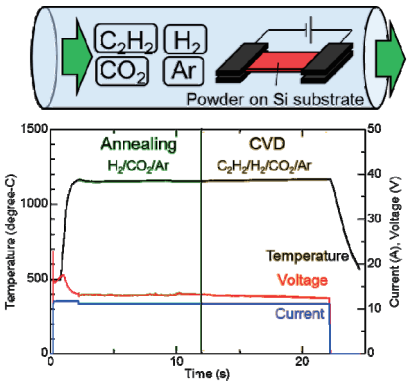

Fig. 1 Schematic of the reactor and typical temperature profile for electric current heating.

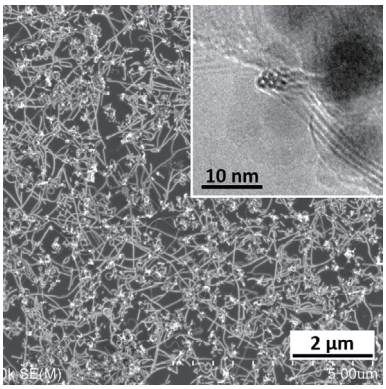

Fig. 2 Typical SEM image of the product. Inset shows a typical TEM image.

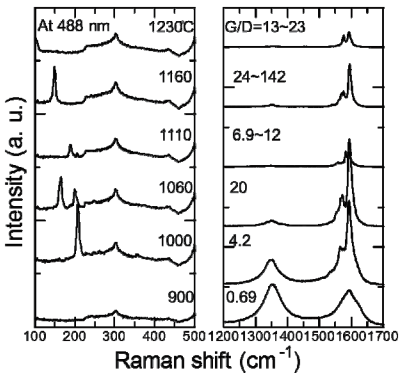

Fig. 3 Raman spectra of the CNTs synthesized by the nanopowder (y = 0.50) at various temperatures.

[1] J. Azurdia, *et al.*, *J.Am. Ceram. Soc.* **89**, 2749 (2006).
[2] K. Sekiguchi, *et al.*, Carbon **50**, 2110 (2012).

Corresponding Author: S. Noda, Tel&Fax: +81-3-5286-2769, E-mail: noda@waseda.jp

Chemical reaction analysis of cupper clusters by FT-ICR mass spectroscopy

○Ken Mizutani[1], Yoshinori Sato[1], Hiroya Minowa[1],
Taiki Inoue[1], Shohei Chiashi[1], Shigeo Maruyama[1,2]

[1] *Department of Mechanical Engineering, The University of Tokyo, Tokyo 113-8656, Japan*
[2] *Energy NanoEngineering Lab. National Institute of Advanced Industrial Science and Technology (AIST), Ibaraki. 305-8564, Japan*

To synthesize single walled carbon nanotubes (SWCNTs), chemical vapor deposition (CVD) method is one of the most common techniques. During CVD process, hydrocarbon molecules such as CH_4 or ethanol are decomposed on catalytic metal nanoparticles, and SWCNTs are formed from the carbon atoms at high temperature. As the catalytic metals, Fe, Ni and Co are often used, and Cu-Co alloy can be used especially for small diameter SWCNT growth [1]. Cu is also used for graphene growth. Although understanding the reaction characteristic of Cu clusters is beneficial for improving SWCNTs and graphene growth, it has not been researched well.

In this study, Cu clusters were investigated by using Fourier transform ion cyclotron resonance (FT-ICR) mass spectroscopy. Metal clusters are generated by laser vaporization, injected into FT-ICR cell and trapped. They do cyclotron motion in the magnetic field and their masses are calculated by the rotational frequency. Figure 1 (a) shows the mass spectrum of Cu_{12}^+ to Cu_{15}^+ clusters. We also detected chemisorption with remaining gas molecules in the chamber. The mass spectra of Co clusters are shown in Figure 1 (b). The comparison of these results indicates that Cu clusters have higher reactivity than Co clusters.

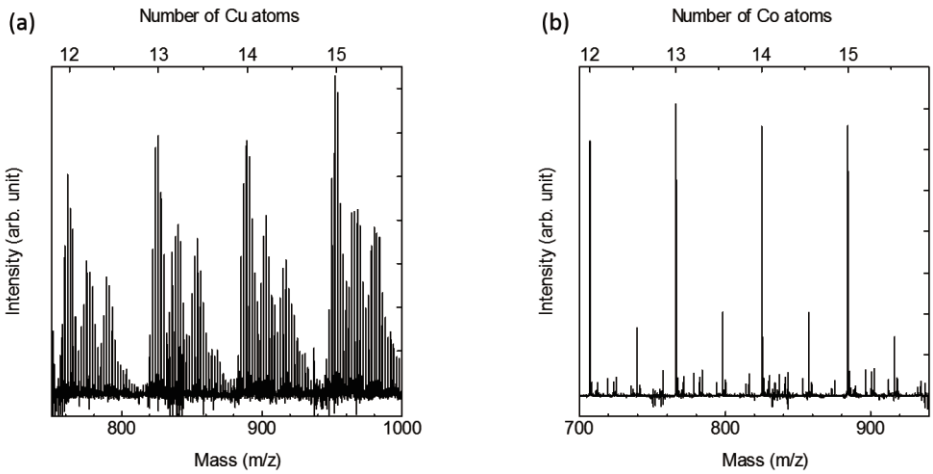

Fig.1 Mass spectra of (a) Cu and (b) Co clusters.

[1] K. Cui, *et al*., Nanoscale (2016) online.

[2] S. Maruyama *et al.*, Rev. Sci. Instrum., 61 (1990), 3686.

Corresponding Author: S. Maruyama
Tel: +81-3-5841-6421, Fax: +81-3-5841-6421,
E-mail: maruyama@photon.t.u-tokyo.ac.jp

Flow Rate Dependence of Production of Double-wall Carbon Nanotubes by High-temperature Pulsed-arc Discharge

○Yuto Hikichi, Ryota Jinnouchi, Toshiki Sugai

Department of Chemistry, Toho University, Chiba 274-8510, Japan

A high-temperature pulsed-arc discharge (HTPAD) has been developed to produce nanocarbon materials. The system utilizes width controlled pulsed arc discharge for the vaporization of electrode in temperature controlled ambient (~760 Torr) Ar. With this width and temperature control, novel materials have been produced by the system such as high-quality double wall carbon nanotubes(DWNW) with outer diameter of around 1.8 ± 0.2 nm[1]. However the production ratio of DWNT in all produced CNT with by-produced single-wall carbon nanotube (SWNT) is not high (~10%) and diameter of DWNT cannot be controlled so far. Recently, however, we have found that the ratio is enhanced up to 30% with low pressure (~300 Torr) operation[2]. Even in this low pressure condition, the diameter is still unchanged. To control the diameter and to achieve further enhancement of the ratio, here we present the effect of flow rate of Ar. The flow rate has been utilized to control the structures of carbon nanotubes, especially with laser vaporization (LV) method, where thick single-wall carbon nanotubes are produced in the low flow rate conditions[3].

The HTPAD system consists of a furnace with a ceramic tube inside, an Ar gas flow and pressure control system, an HV pulse voltage controller, and a water cooling trap. Electrodes made of graphite containing catalytic metals (Ni/Y 4.2/0.5 at. %:Toyo Tanso Co. Ltd.) were located in the ceramic tube. The pulsed arc discharges (0.6 ms, 50 Hz, and 100 A) vaporized the electrodes and produced nanotubes in the Ar gas at the temperature of 1250 ℃ and at the pressure of 300 Torr. The flow rate was change from 200 ml/min to 400 ml/min. The products were collected on the trap and were characterized by TEM observation.

Figure 1 shows the diameter distribution of SWNT and DWNT. Both of them shift to the larger diameters as the flow rate is decreased. This flow effects are very similar to those found in LV experiments[3]. Even though the diameter enlargement of SWNT is much more prominent than that of DWNT, the DWNTs produced in the condition of 200 ml/min with the average diameter of 2.3 nm is the thickest DWNT ever produced by HTPAD. Not only the diameter, but also the production ratio of DWNT is enhanced up to 60% in the 200 ml/min condition. These flow effects can be interpreted as that nascent production process of DWNT with HTPAD and that of SWNT with LV have some similarity.

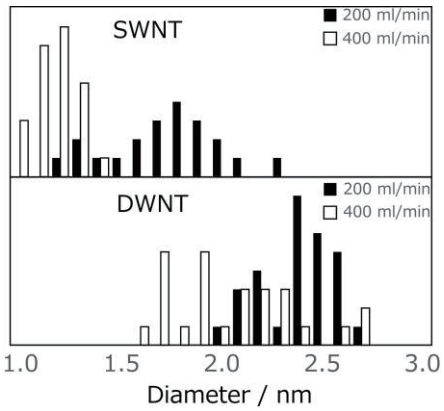

Fig. 1 Diameter dependence on flow rate

[1] T. Sugai *et al*., *Nano Lett*. **3**, 769 (2003).
[2] H. Kikuchi *et al*., 44th *Fulluerene-nanotue-graphene conference.* 1P-24
[3] R. Sen *et al*., *Chem. Phys. Lett.* **332**, 467 (2000).

Corresponding Author: T. Sugai Tel: 047-472-4406 E-mail: sugai@chem.sci.toho-u.ac.jp

Direct growth of patterned multi-layer graphene by precipitation method using patterned W capping layer

○Jumpei Yamada[1], Yuki Ueda[1], Takahiro Maruyama[2], and Shigeya Naritsuka[1]

[1]*Department of Materials Science and Engineering, Meijo University, Nagoya 468-8502, Japan*
[2]*Department of Applied Chemistry, Meijo University, Nagoya 468-8502, Japan*

Graphene is usually grown by CVD method using Cu or Ni catalyst. However, the transfer process of the graphene is a big problem for the mass production of devices. Not only the technical difficulties but also the degradation of their properties during the process are the problems which should be solved. In recent years, several group reported graphene growth of directly on a substrate as the alterative for the transfer process.

We also have been studied a direct growth of multi-layer graphene by precipitation method using W capping layer [1]. As a result, the high quality graphene was successfully grown directly on a sapphire substrate by precipitation method using W capping layer. In this study, we report the direct growth of patterned multi-layer graphene by precipitation method using a patterned W capping layer.

Amorphous carbon (a-C) and Nickel (Ni) layers were deposited on a sapphire substrate using electron-beam deposition. Thereon, patterned tungsten (W) capping layer was deposited. Patterned W (25 nm)/Ni (300 nm) /a-C (5 nm)/sapphire substrate was annealed at 900 ^{o}C for 30min in vacuum. Raman spectroscopy (532 nm) was performed to study the presence of the graphene on the substrate. Finally, the catalysts were removed by the dipping of the sample in aqua regia.

Figure 1 shows a differential interference micrograph and corresponding Raman spectra of the sample after the catalyst etching. Raman signal from point (1) shows the presence of graphene on the area while the signal from point (2) does the absence of graphene on the area. The result indicates that the multi-layer graphene successfully formed on the substrate where the W capping layer existed. On the other hand, graphene was observed on the bare Ni surface only before the catalyst etching. Therefore, the W capping layer has the function to switch the sides of the precipitation of the graphene. The mechanism will be discussed on the conference site.

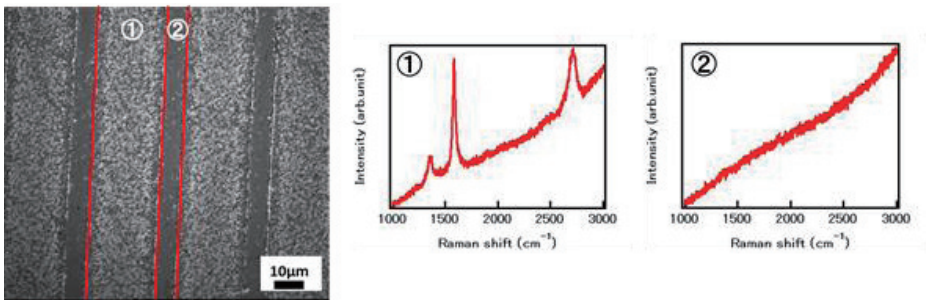

Figure 1. Differential interference microphotograph of substrate after etching, Raman spectra from point (1) and (2).

[1] J.Yamada et al. The 49th FNTG General Symposium, 3P-22, (2015).

Acknowledgement: This work was supported in part by JSPS KAKENHI Grant Numbers 2660089, 15H03558, 26105002, 25000011.

Corresponding Author: J.Yamada, E-mail: jjjjjjyyyyyy119@gmail.com

Fabrication and characterization of graphene nanoribbons by water-assisted anisotropic etching

Shun Ogawa[1], Ryosuke Inoue[1], Kenji Watanabe[2], Takasi Taniguchi[2], Yutaka Maniwa[1], Yasumitsu Miyata[1,3]

[1]*Department of Physics, Tokyo Metropolitan University, Hachioji 192-0397, Japan*

[2]*National Institute for Materials Science, Tsukuba 305-0044, Japan*

[3]*JST, PRESTO, Kawaguchi 332-0012, Japan*

Graphene nanoribbons (GNRs) have attracted much attention because of their unique structure-dependent electrical and magnetic properties. Even though various fabrication methods have been reported, anisotropic etching provides an effective way for the preparation of GNRs directly on insulating substrates. In previous reports, hydrogen plasma is used to fabricate zigzag-edge GNRs from graphene flakes [1]. In contrast, Luo *et al*. recently demonstrated the selective formation of armchair edges in graphite by annealing with water vapor [2]. This motivates us to prepare armchair-edge GNRs using water-assisted anisotropic etching.

Here, we report the fabrication and characterization of GNRs from graphene using water vapor. Graphene films were prepared by methane CVD on Cu foil, and annealed with water vapor at 800~900 °C on insulating substrates. As shown in atomic force microscope image (Fig.1a), the annealing process leads to the formation of hexagonal-shaped holes in graphene through anisotropic etching, and in some cases, a GNR was formed between the two holes. Height profile presents that the GNR has a width of 20 nm and monolayer thickness (Fig.1b). No change in Raman spectra was observed for the etched graphene, suggesting that the etching is proceeded preferentially at the edge (Fig.1c). These results indicate that the water-assisted etching would be an effective method to fabricate armchair-edge GNRs on insulating substrates.

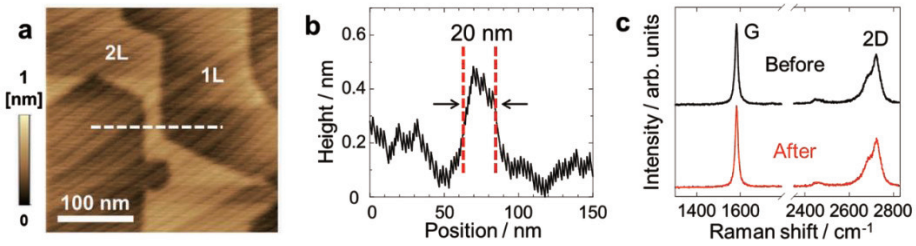

Fig. 1(a) AFM image of graphene after the annealing under water vapor. (b) Height profile of the dotted line in (a). (c) Raman spectra of graphene before and after the etching.

[1] R. Yang, *et al*., Adv. Mater. 22, 4014 (2010) , [2] D. Luo, *et al*. Small **10**, 2809 (2014)

Corresponding Author: Yasumitsu Miyata, Tel: +81-42-677-2508, E-mail: ymiyata@tmu.ac.jp

Study of non-catalytic CVD of graphene on sapphire substrate
----- Effect of growth temperature on nucleation -----

○Yuki Ueda[1], Jumpei Yamada[1], Itsuki Uchibori[1], Masashi Horibe[1], Shinichi Matsuda[1]
Takahiro Maruyama[2], and Shigeya Naritsuka[1]

[1] *Department of Materials Science and Engineering, Meijo University*
Nagoya 468-8502, Japan
[2] *Department of Applied Chemistry, Meijo University, Nagoya 468-8502, Japan*

In conventional, chemical vapor deposition (CVD) with a metallic catalyst is used to grow high-quality, large-area graphene. However, it is necessary to transfer the graphene from the surface of the catalyst to a certain substrate to fabricate graphene devices. The transfer process is not only complicated but also harmful for the graphene performances, such as electron mobility. Therefore, a direct growth of graphene on a substrate has been requested. In this study, non-catalytic CVD of graphene is investigated to directly grow the graphene on the requested substrate. The growth temperature is systematically changed to study its growth mechanism.

A c-plane sapphire was used as a substrate for the graphene growth. Ethanol was supplied to the growth chamber as a source material with bubbled by N_2 at a flow rate of 10 sccm. The growth temperature was systematically changed between 980-1180 ^{o}C while the flow rate of N_2 carrier gas, the growth time, and the pressure of the growth chamber were fixed at 600 sccm, 60 min, and $5x10^3$ Pa, respectively.

Figure 1 shows the Raman spectra of the samples grown at between 980 and 1180 ^{o}C, which indicates that the graphene was successfully grown above 1030 ^{o}C because D, G and G' peaks were observed. On the other hand, Fig.2 (a) and (b) show the AFM images of the samples grown at 1080 ^{o}C and 1180 ^{o}C. The size of the circular islands increased with the growth temperature while their density decreased. It is probably because the nucleation of the graphene was decreased by the thermally-enhanced diffusion of the carbon adatoms.

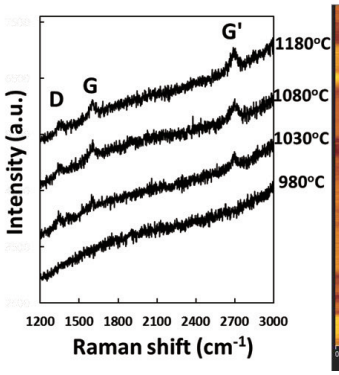

Fig.1 Raman spectra of samples grown at between 980-1180 ^{o}C.

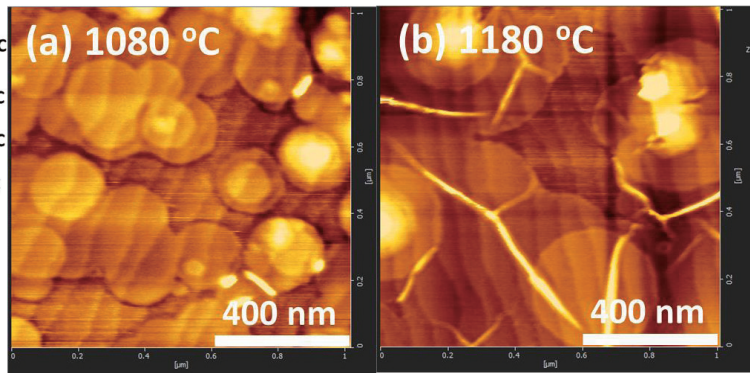

Fig.2 AFM surface images of graphene grown at 1080 ^{o}C (a) and 1180 ^{o}C (b), respectively.

Acknowledgment: This work was supported in parts by JSPS KAKENHI Grant Numbers 2660089, 15H03558, 26105002, 25000011.
Corresponding author: Y. Ueda Tel: +81-52-838-2387, E-mail: 153434003@ccalumni.meijo-u.ac.jp

Growth of Large-Grain Graphene and the Role of Oxygen

○Dong Ding,[1] Rozan Mohamad Yunus,[1] Pablo Solís Fernández,[2] and Hiroki Ago[1,2,3,*]

[1] *Interdisciplinary Graduate School of Engineering Sciences, Kyushu University, Fukuoka 816-8580, Japan*
[2] *Institute for Materials Chemistry and Engineering, Kyushu University, Fukuoka 816-8580, Japan*
[3] *PRESTO, Japan Science and Technology Agency, Saitama 332-0012, Japan*

Large-area graphene grown by CVD over Cu foil is generally polycrystalline with widely dispersed grains boundaries (GBs), which leads to a largely degraded electrical and mechanical properties of graphene. Recently, it was found that oxygen has a strong impact on the reduction of the graphene nucleation density [1]. Different roles of oxygen atoms in the graphene growth have been proposed [2-3], but the mechanism still remains unclear. In this study, we have investigated the roles of oxygen in the growth of large single-crystalline graphene [4]. The Cu foil was first pre-oxidized at 250 ℃ on a hot plate in air. Then, the Cu was heated up in pure Ar to 1070 ºC in 30 min, followed by annealing in Ar/H_2 at the same temperature for 30 min. After that, CH_4 was introduced to grow graphene. We observed that the grain density of graphene significantly decreases from ~ 2400 cm^{-2} to ~ 10 cm^{-2} by extending the pre-oxidation time from 0 to 10 min. This decrease in the nucleation density lead to the synthesis of isolated single-layer graphene grains with sizes up to 6 mm. As already reported, the gas used during the heating up of the Cu foil was found to be also essential [1]. Thus, the introduction of H_2 during this stage gave a high grain density (~ 5000 cm^{-2}) regardless of the pre-oxidation time.

Figure 1 shows the Raman spectra of Cu surfaces at different stages of the CVD procedure. The peaks corresponding to copper oxide became very weak after heating up in either Ar/H_2 or pure Ar, suggesting that the oxide layer on Cu foil disappeared from the Cu surface. However, the XRD, which reflects better the bulk of Cu, showed significant differences between both cases. While the Cu foil heated in Ar shows a diffraction peak corresponding to copper oxide (Cu_2O), this is absent in the sample heated in Ar/H_2. Heating in Ar also modified the crystal structure of the Cu, giving a stronger Cu(111) peak. These results suggest that surface oxide layer on the Cu foil decomposed during the heating up stage. However, heating in Ar seems to promote the diffusion of the O atoms into the Cu bulk, forming Cu_2O. We speculate that such stored O atoms diffuse back to the surface during the graphene growth, resulting in a reduced nucleation density. Our work highlights the growth mechanism of CVD graphene on oxidized Cu foil and will help the growth of giant single-crystalline graphene for realizing intrinsic physical properties of graphene.

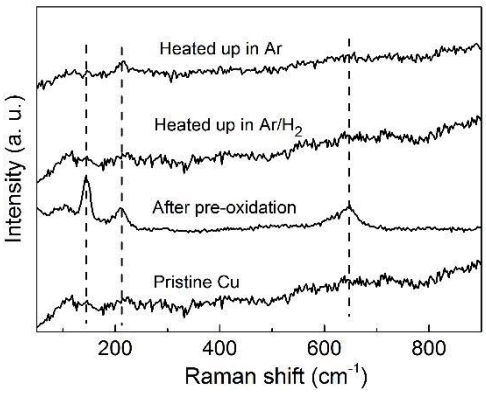

Fig. 1. Raman spectra of Cu surfaces at different stages. Dotted lines correspond to copper oxide peaks.

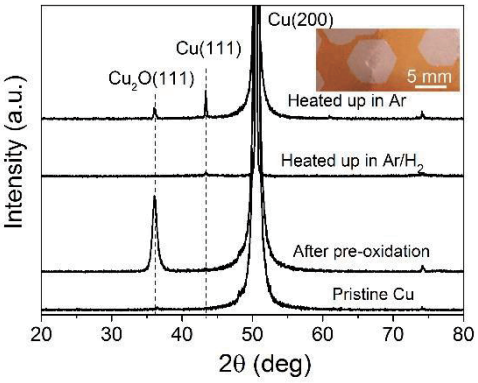

Fig. 2. XRD profile of the Cu foils at different stages. Inset shows 6 mm grain.

References: [1] Hao Y. et al., *Science* **342**, 720 (2013). [2] Gan L. and Luo Z., *ACS Nano* **7**, 10 (2013). [3] Eres G. et al., *ACS Nano* **8**, 6 (2014). [4] Ding D. et al., in preparation.

Corresponding author: Hiroki Ago (Tel&Fax: +81-92-583-7817 E-mail: ago@cm.kyushu-u.ac.jp)

Characterization of few-layered graphene obtained by exfoliation of Graphite Intercalation Compounds

○Takuya Yasutake, Taro Kinumoto, Tomoki Tsumura, Masahiro Toyoda

Department of Applied Chemistry, Faculty of Engineering, Oita University, 700 Dannoharu, Oita 870-1124, Japan.

INTRODUCTION

Graphene exhibits excellent mechanical, chemical and electrical characteristics such as conductivity. Graphene has been prepared by numerous methods. In the case of graphene prepared by the exfoliation of Grapite Intercalation Compounds (GICs) via desalination with alkyl halide solvents, the resulting graphene is expected to exhibit novel characteristics. In this study, Na-tetrahydrofuran-GICs (Na-THF-GICs) were used as the host material for the exfoliation through desalination of ternary GICs. Thus, obtained few-layered graphene was observed to exhibit no defects and some usual properties.

MATERIALS AND METHODS

Na-THF-GICs were prepared from natural graphite powder with grain size of 100 μm in (SN-100, SEC CARBON Ltd.) by a solution method. For exfoliation of the GICs by desalination was used 2-chloro-2-methylpropane (2CMP, Tokyo Chemical Industry Co., Ltd.) was selected as alkyl halide solvents.

RESULTS AND DISCUSSION

Fig. 1 shows TEM micrograph of few-layered graphene obtained by the exfoliation of the GICs. Fig. 1(a) shows micrograph of the graphene, whereas Fig. 1(e) shows its 002 lattice, and Fig. 1(f) shows its selected area electron diffraction (SAED) pattern. These results indicate that the obtained few-layered graphene exhibits a length at a few micrometers in planar direction and thickness of a few nanometers. Its SAED pattern shows the clear spots, thereby indicating that the few-layered graphene exhibits orderly stacking and does not contain defects induced by the exfoliation process. The obtained few-layered graphene contains special feature such as holes obtained thought the reaction between alkyl halide solvents and Na in GICs's interlayers. Further exaltations of the obtained few-layered graphene are currently under way.

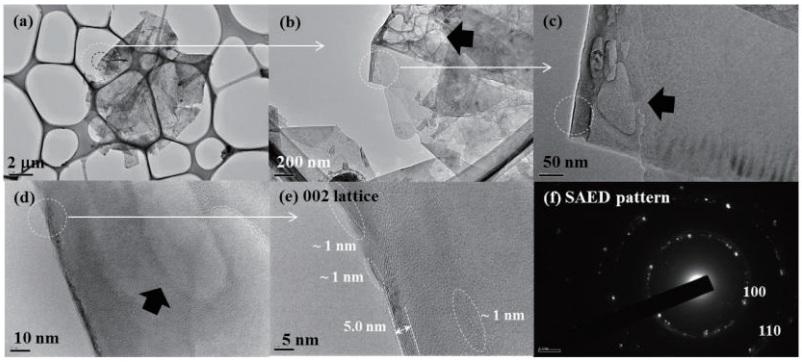

Fig. 1 TEM micrographs of (a)-(d) few-layered graphene was exfoliation by 2CMP, (e) its 002lattice and (f) its SAED pattern of black cycle in (a).

Corresponding Author:
M. Toyoda
Tel: +81-97-554-7094,
Fax: +81-97-554-7094,
E-mail: toyoda22@oita-u.ac.jp

The Use of Double-layered Graphene Oxides for Capturing Carbon Dioxides: A Computational Proposal

○Takashi Yumura[1], Ayumi Yamasaki [1]

[1] *Department of Chemistry and Materials Technology, Kyoto Institute of Technology, Matsugasaki, Sakyo-ku, Kyoto, 606-8585, Japan*

We have investigated whether double-layered graphene oxides (GO) can be utilized to trap CO_2 by using density functional theory (DFT) (PBE functional). Previously, we discussed migration of CO_2 within the interlayer space of anhydrous and hydrous GOs. The study is relevant to recent experimental reports in Refs. 1 and 2. Our previous DFT studies found important roles of water molecules in trapping CO_2 inside the interlayer space of GOs [3]. In short, migration of CO_2 within GOs is prevented by the repulsive interactions with the GO layers in hydrous forms to trap CO_2 inside the interlayer space (Fig. 1a). Such repulsive interactions cannot be operated within anhydrous GOs, and then CO_2 can be released from the GO interlayer.

For materials candidate for CO_2 capture and storage (CCS), aqueous alkanolamine absorbents and amine-modified solid porous materials have been well studied. In this direction, the current study proposes from DFT calculations another strategy for trapping CO_2 by GO structures encapsulating ethylenediamine. According to DFT calculations, ethylenediamine containing GOs have relatively larger interlayer spacings relative to the pristine and hydrous GO cases. Then, interactions between CO_2 and GO layers are attractive, being in contrast to hydrous GOs (Fig. 1a). In addition, CO_2 attractively interacts with a nitrogen atom of ethylenediamine with lone pair electrons (Fig. 1b). Therefore, CO_2 is captured by GO with the ethylenediamine guest through attractive CO_2-GO layer and CO_2-amine interactions. DFT calculations indicated that GO layered materials have different fashions to capture CO_2, depending on guest molecules. Then, GO interlayer spacings are key to differentiate the fashions for capturing CO_2 kinetically from thermodynamically.

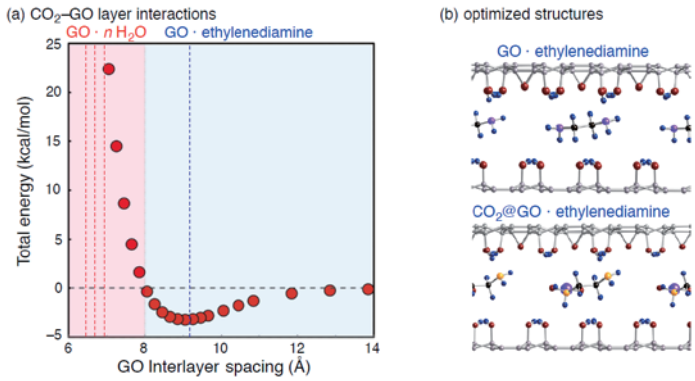

Fig. 1 Interactions between CO_2 and graphene oxide (GO) layers as a function of GO interlayer spacings.

[1] S. Eigler, C. Dotzer, A. Hirsch, M. Enzelberger, P. Müller, Chem. Mater. **24**, 1276 (2012).
[2] D. Kim, D. W. Kim, H.-K. Lim, J. Jeon, H. Kim, H.-T. Jung, H. Lee, J. Phys. Chem. C **118**, 11142 (2014).
[3] T. Yumura, A. Yamasaki, Phys. Chem. Chem. Phys. **16**, 9656 (2014).

Corresponding Author: Takashi Yumura
Tel: +81-75-724-7571, Fax: +81-75-724-7571, E-mail: yumura@kit.ac.jp

Geometric and electronic structures of graphene nanoribbons under uniaxial pressure

○Kohei Narita and Susumu Okada

Graduate School of Pure and Applied Sciences, University of Tsukuba
1-1-1 Tennodai, Tsukuba 305-8571, Japan

Electronic structures of graphene nanoribbons (GNRs) are known to be ranging from a metal to a semiconductor depending on their edge shape and width due to the discretized condition on the two-dimensional metallic energy band of graphene. Recently, the ultra narrow GNR with edge roughness has been synthesized in nanometer tubular space of carbon nanotubes (CNTs) by origomerization or polymerization of coronene molecules ($C_{24}H_{12}$) [1,2]. Inside CNT, it is plausible to apply the uniaxial pressure on the GNRs with the use of the appropriate pressure medium, being expected to induce the structural transition into the novel one-dimensional structures. In this work, we aim to explore the high-pressure phases of GNRs with the edge roughness inside CNT and elucidate their electronic structures based on density functional theory with generalized gradient approximation. In the present work, we consider the narrow armchair and zigzag GNRs with edge roughness (Fig. 1).

By applying the uniaxial pressure on the GNRs, we find that the GNRs undergo the structural phase transition into different high-pressure phases shown in Fig. 2: The high-pressure phase of the armchair GNRs has a double-decker structure of armchair GNRs which are connected each other via sp C atoms. On the other hand, for the zigzag GNR, the high-pressure phase has a diamond nanowire structure sorely consisting of C atoms with the four-fold coordination. The double-decker armchair GNRs and diamond nanowire are a semiconductor and a metal, respectively.

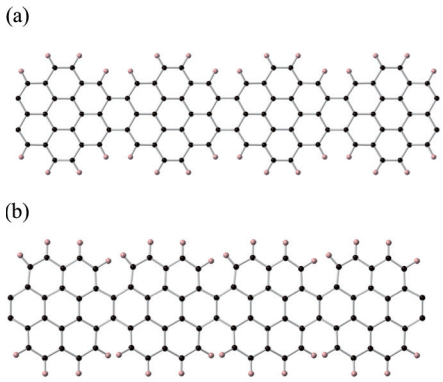

Fig. 1 Geometric structures of GNRs with (a) armchair and (b) zigzag edges with edge roughness.

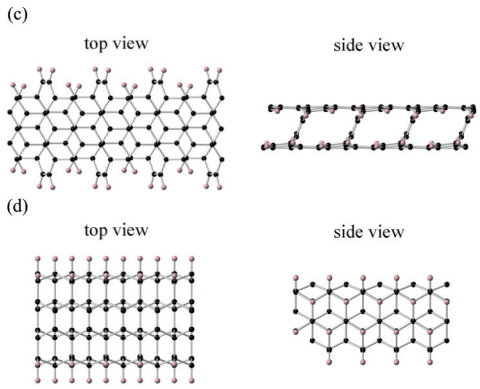

Fig. 2 Top and side views of optimized geometries of GNRs with (c) armchair and (d) zigzag edges with edge roughness under the uniaxial pressure.

[1] M. Fujihara, Y. Miyata, R. Kitaura, Y. Nishimura, C. Camacho, S. Irle, Y. Iizumi, T. Okazaki, H. Shinohara, J. Phys. Chem. C **116**, 15141 (2012).

[2] H.E. Lim, Y. Miyata, M. Fujihara, S. Okada, Z. Liu, Arifin, K. Sato, H. Omachi, R. Kitaura, S. Irle, K. Suenaga, H. Shinohara, ACS Nano, **9**, 5034 (2015).

Corresponding Author: K. Narita
Tel: +81-29-853-5921, Fax: +81-29-853-5924,
E-mail: sokada@comas.frsc.tsukuba.ac.jp

Adsorption of Dps onto graphene using carbon nano-horn binding peptide

○Yuki Hashima[1], Yasuaki Ishikawa[1], Mutsunori Uenuma [1], Naofumi Okamoto[1], Ichiro Yamashita[1] and Yukiharu Uraoka[1]

[1], Graduate School of Material Science, Nara Institute of Science and Technology, 8916-5 Takayama, Ikoma, Nara 630-0192, Japan

Graphene exhibits excellent physical and chemical properties for sensing such as high carrier mobility, ambipolar effect, low noise level, good compatibility, and stability [1]. Graphene sensors that take advantage of those features are becoming a hot spot. We introduced a Dps, the surface of which was genetically modified with peptides, as sensing key component in graphene sensors. Dps is a cage-shaped protein. It is possible to encapsulate inorganic materials in the inner cavity by bio-mineralization. Additionally, N^- and C^- termini are protruding outside and two-types of peptides can be genetically added on their outer surface.

In this presentation, we designed and mass-produced Dps displaying carbon nano-horn binding peptide and Ti binding peptide which was named CDT-1. Carbon nano-horn binding peptide had been reported to bind to the carbon nanotube [2]. However, adsorption to the graphene was not yet confirmed. Therefore, we studied adsorption ability of CDT-1 onto graphene.

Experimentally, CDT-1 solution (0.5 mg/ml Fe-oxide cored CDT-1, 50 mM MES-Tris buffer pH 6.0) was dropped on CVD graphene on Cu substrate. Then un-binding proteins were washed away. After the process, samples surface was observed by SEM.

The SEM image is shown in Fig. 1. The white dots in Fig. 1 are the Fe-oxide core in CDT-1 with 4.5 nm diameter adsorbed onto the graphene surface. The measured adsorption density for CDT-1 was 7.0×10^{10} dots/cm^2. Based on the SEM images, it was proved that carbon nano-horn binding peptides anchored Dps onto the graphene surface.

As a result, we successfully demonstrated that the spherical shell protein adsorbed to graphene using carbon nano-horn peptide.

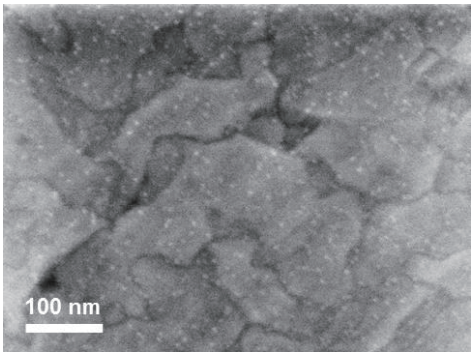

Fig 1. A SEM image of CDT-1 adsorbed on graphene.

The white dots is Fe-oxide core in CDT-1.

[1] C. Zheng *et al. ACS applied materials & interfaces* **7**, 16953–16959 (2015).

[2] M. Kobayashi *et al. Chem.Commun*., 47, 3475-3477 (2011)

Corresponding Author: Yasuaki Ishikawa

Tel: +81- 743-72-6064, Fax: +81- 743-72-6069,

E-mail: yishikawa@ms.naist.jp

1P-31

Silicon Thin-Film Solar Cells with Graphene Transparent Electrode

○Ryousuke Ishikawa, Tomoya Oya, Takahiro Nomoto, and Nozomu Tsuboi
Faculty of Engineering, Niigata University, Niigata 950-2181, Japan

Transparent electrode is a key component in the multi-junction solar cells, working as window and intermediate electrodes. It requires high transparency for wide range and suitable electrical junctions. We focused on graphene, a single atomic layer of sp^2 graphitic carbon, as a promising material for transparent conducting electrode in multi-junction solar cells because of its high electrical conductivity and optical transparency over a wide range of wavelengths [1]. Here, we investigated the potential of graphene electrode in silicon thin-film solar cells.

High quality graphene was fabricated by CVD growth technique using Cu foil as catalyst substrate. Monolayer of graphene was grown at 1000 ^{o}C for 30 min under 22 sccm of CH_4 and 44 sccm of H_2. After CVD growth, deposited graphene was then transferred by polymethyl methacrylate (PMMA) assisted process onto glass substrates. By repeating this step on the same substrate, trilayered graphene films can be prepared that exhibit enhanced electrical and optical properties. The p-i-n single-junction solar cells of hydrogenated amorphous silicon carbide (a-SiC_x:H), hydrogenated amorphous silicon (a-Si:H), and hydrogenated microcrystalline silicon oxide (μc-SiO_x:H) were fabricated on the graphene films by plasma enhanced chemical vapor deposition (PECVD) in a multi-chamber system. The schematic image of solar cells structure using graphene window electrode is shown in Fig. 1. The photovoltaic characteristics of the solar cells with the cell area of 0.086 cm^2 were measured under AM 1.5 G (100 mW/cm^2) at 25 ^{o}C.

Figure 2 shows the photovoltaic characteristics of the solar cells including the data of those using sputtered ZnO:Al as window electrodes as comparison. As can be seen from the figure, higher V_{oc} has been obtained with the cell using graphene window electrode. This result is probably due to the lower Schottky barrier at the graphne/p-layer interface and this can increase the built-in potential of the cell. Actually, the *I-V* characteristics of graphene/p-layer exhibited the perfect ohmic contact, whereas that of ZnO:Al/p-layer showed the Schottky diode characteristics. Further investigation is needed to elucidate the origin of the ohmic contact. Higher cell performance would be expected by further cell optimization.

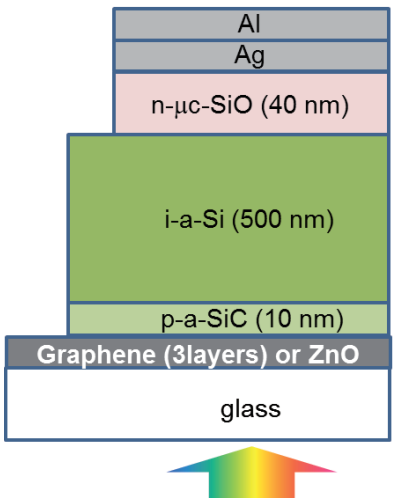

Fig. 1 The schematic images of fabricated solar cells

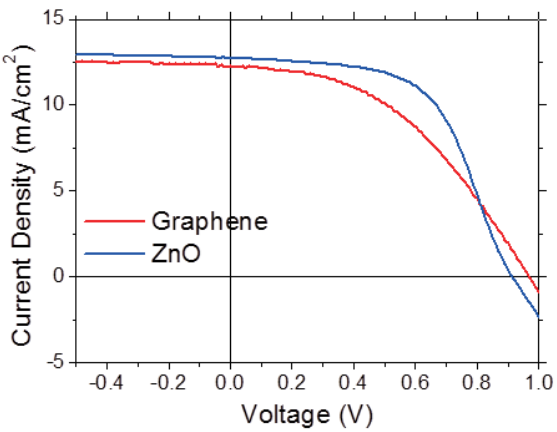

Fig. 2 The photovoltaic characteristics of the solar cells.

[1] R. Ishikawa et al. Jpn. J. Appl. Phys., **51** 11PF01 (2012).
Corresponding Author: R. Ishikawa, Tel & Fax: +81-25-262-6736, E-mail: ishikawa@eng.niigata-u.ac.jp

Substrate dependence of graphene oxide in amidation and esterification reactions

○Haruya Okimoto, Yasutaka Yoshii, and Masahito Sano
Department of Polymer Science and Engineering, Yamagata University, Yonezawa, 992-8510, Japan

Chemical functionalization of graphene oxide (GO) fixed on a solid substrate is a topic of paramount importance, for it allows fine-tuning of the chemical and physical properties of GO. In practice, GO film can be easily prepared on various substrates by wet processes. Therefore it is important to understand the influence of a substrate upon GO functionalization. Especially, amidation and esterification have been applied frequently to modify GO, which have significant amounts of hydroxyl and carboxyl groups. In this study, we demonstrate that the substrate influences the reactivity of the top surface of GO using quantitative reactions with fluorescent dyes.

An aqueous dispersion of GO was splay cast on octadecyltrichlorosilane (OTS) modified SiO_2/Si or 3-aminopropyltriethoxysilane (APTES) modified SiO_2/Si. A thin GO film that partially covers the substrate surface and a multilayered thick film that completely covers were made for comparison. These films were amidated with 5-aminofluorecein or esterified with 1-pyrenbutiric acid, respectively. The amount of reacted dye was quantified by hydrolysis of the products.

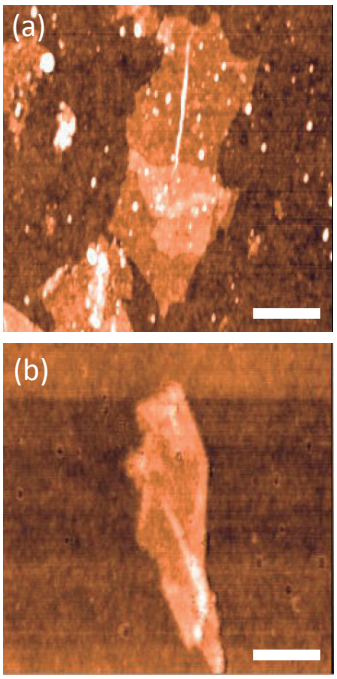

Fig. 1 AFM image of isolated GO film on (a) APTES/SiO_2 and (b) OTS/SiO_2.

Figure 1 shows AFM image of thin GO on each substrate. The GO on APTES/SiO_2 (hydrophilic surface) spreads flat on the surface, while the GO on OTS /SiO_2 (hydrophobic surface) appears folded. This indicates that wetting of GO on a solid substrate has strong influences on the morphology. Figure 2 shows the reacted amounts for thin and thick GO films for the esterification reaction. It has been reported that the reactivity of graphene is enhanced by strain on graphene films. Since the folded GO on OTS/SiO_2 is strained stronger than the flat GO on APTES/SiO_2, the observed reactivity difference can be explained by the film morphology. For the thick GO films, the reactivity does not differ as much as that of the thin film. This shows that the influence of substrate is limited to the GO that are immediate vicinity of the substrate surface. The amidation reaction gives a similar result.

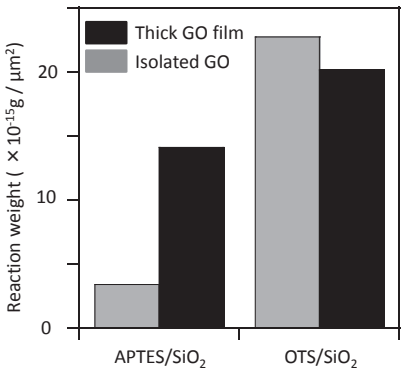

Fig 2 Reaction weight of fluorescent agent for GO film on the substrate.

In summary, we demonstrate that the reactivity of GO films on the solid substrate is strongly influenced by the morphology of GO which is determined by wettability.

Corresponding Author: H. Okimoto Tel/FAX: +81-238-26-3074 E-mail: haruya@yz.yamagata-u.ac.jp

1P-33

Indirect angle resolved photoemission spectra in graphene

○ Pourya Ayria[1], Shin-ichiro Tanaka[2] , Ahmad R.T. Nugraha[1], and Riichiro Saito[1]

[1]*Department of Physics, Tohoku University, Sendai 980-8578, Japan*

[2]*The Institute of Scientific and Industrial Research, Osaka University, 8-1 Mihogaoka, Ibaraki, Osaka 567-0047, Japan*

Angle-resolved photoemission spectroscopy (ARPES) can be used to detect the electron-phonon coupling (EPC) in solids [1]. Most of the previous studies of ARPES in graphene have explored EPC effects on ARPES spectra by the direct observation of the energy bands near the *K* point. Recently, several ARPES experiments observed the indirect transition of ARPES spectra far from the energy bands around the Γ point and near Fermi energy, where there is no available energy band [2, 3].

In order to explain the evidence of the indirect transition observed in graphene (or graphite) [2, 3], we theoretically investigate the indirect transition of ARPES spectra as a function of the incident light polarizations and the photon energy. The electron-photon and electron-phonon matrix elements are calculated by the dipole approximation [4] and the rigid-ion approximation [5], respectively, where in the both of the calculations we utilize first-principles calculation [6]. Our calculation shows that the transverse optical TO-phonon mode has the strongest EPC for the photo-excited electron at the K point to the Γ point by the K point phonon mode. This signal is strong for the photon energy $\hbar\omega = 11$ eV, which corresponds to the lowest unoccupied electron state near the K and K' points. We compare the calculated results of ARPES spectra with the experimental results of graphite.

[1] A. Damascelli *et al*., Rev. Mod. Phys. **75**, 473 (2003).
[2] Y. Liu *et al*. Phys. Rev. Lett. **105**, 136804 (2010)
[3] S. Tanaka *et al*., Sci. Rep. **3**, 3031 (2013).
[4] P. Ayria *et al*., Phys. Rev. B **92**, 195148 (2015).
[5] G. Grimvall, Electron-phonon interaction in metals, North-Holland, (1980).
[6] P. Giannozzi *et al*., J. Phys. Cond. Matt. **21**, 395502 (2009).
Corresponding Author: P. Ayria, E-mail: pourya@flex.phys.tohoku.ac.jp

Raman Spectroscopy of Ti-Cleaned Single-Layer Graphene and Transfer on Paper Substrate

○Akira Fujimoto[1,2], Masafumi Sakita[3], Ren Kaneko[4], Ryosuke Nakano[3], Kazuo Satoh[5]
Shuichi Murakami[5], Yoshiyuki Harada[1,2], Toshihiko Maemoto[2,4], Mitsuaki Yano[2,3]

[1]*Applied Physics, Faculty of Engineering, Osaka Institute of Technology, Osaka 535-8585, Japan*
[2] *Nanomaterials Microdevices Research Center, Osaka Institute of Technology, Osaka 535-8585, Japan*
[3]*Department of Electronics Information and Communication Engineering, Faculty of Engineering, Osaka Institute of Technology, Osaka 535-8585, Japan*
[4]*Department of Electrical and Electronic Systems Engineering, Faculty of Engineering, Osaka Institute of Technology, Osaka 535-8585, Japan*
[5]*Technology Research Institute of Osaka Prefecture, Izumi, Osaka 594-1157, Japan*

Chemical-vapor-deposited (CVD) graphene is good for fabricating devices on a large scale. However, the charge-neutral point (CNP) appears at a relatively high back-gate voltage (V_G) because of molecular adsorption and impurities on the graphene surface. In this work, we used a Ti-cleaning process for the transferred graphene surface [1] and examined the optical characteristic using Raman spectroscopy. Ti-cleaning process is as follows. 2 nm of Ti was deposited on the graphene and allowed to oxidize to Ti oxide upon exposure to air. The Ti oxide was then removed with HF. Owing to Ti cleaning, the CNP shifted to a lower V_G, and the mobility increased [2]. We found that Ti-cleaned graphene showed the same CNP and the electrical characteristic was maintained for several months. In order to confirm these phenomena, we examined Raman spectra for Ti-cleaned graphene samples for a few months. As a result, the peak positions of G and 2D do not shift apparently as time passes. The results of Raman spectroscopy by Lee *et al*.[3] show that the 2D peak position for suspended graphene are 2676.9 ± 0.7 cm^{-1}. However, 2D peaks of our samples are larger by about 20 cm^{-1} than that of Lee's data, resulting from a compressive strain according to Lee's analysis method.

Currently organic electro-luminescence starts to be applied to flexible substrates such as polyethylene terephthalate (PET), graphene also has a potential to be used on such substrates. We also tried to transfer CVD-graphene onto paper substrates and evaluated the optical characteristic. Figure 1 shows Raman spectra for graphene on Si/SiO_2 and paper substrates measured at room temperature. We confirmed that G and 2D peaks appear for a graphene sample on paper substrate, which indicates that the graphene transfer onto paper is carried out well. In the presentation these details will be discussed together with electric characteristics.

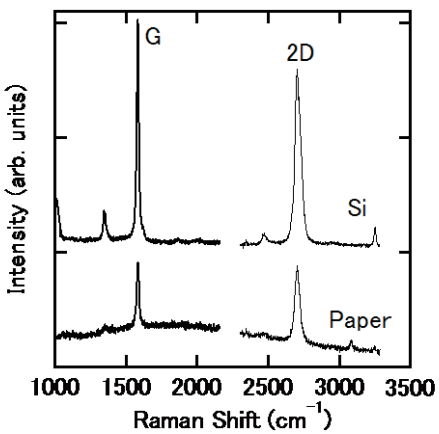

Fig.1 Raman spectra for graphene on Si/SiO_2 and paper substrates.

[1] C. A. Joiner *et al*., Appl. Phys. Lett. **104**, 223109 (2014).
[2] A. Fujimoto *et al*., J. Phys. Conf. Series **603**, 012021 (2015).
[3] J. E. Lee *et al*., Nature Commun. **3** 1024 (2012).

Corresponding Author: A. Fujimoto
Tel: +81-6-6954-4377, Fax: +81-6-6957-2137,
E-mail: akira.fujimoto@oit.ac.jp

1 H-1T' phase transition and heterojunction formation in CVD-grown monolayer $Mo_{1-x}Re_xS_2$

○Shohei Mori[1], Shogo Sasaki[1], Yu Kobayashi[1], Liu Zheng[2,3], Shoji Yoshida[4], Takahiro Takeuchi[4], Hidemi Shigekawa[4], Kazutomo Suenaga[3], Yutaka Maniwa[1], Yasumitsu Miyata[1,5]

[1]*Department of Physics, Tokyo Metropolitan University, Hachioji, 192-0397, Japan*
[2]*Inorganic Functional Materials Research Institute, AIST, Nagoya, 463-8560, Japan*
[3]*Nanomaterials Research Institute, AIST, Tsukuba, 305-8565, Japan*
[4] *Faculty of Pure and Applied Sciences, University of Tsukuba, Tsukuba 305-8573, Japan*
[5]*JST, PRESTO, Kawaguchi, 332-0012, Japan*

Semiconductor heterojunctions based on atomic layers have attracted much attention because of their potential applications in electronics and optoelectronic. So far, such heterojunctions have been fabricated by using chemical vapor deposition (CVD) of various transition metal dichalcogenides (TMDCs) such as monolayer MoS_2, WS_2 and $Mo_{1-x}W_xS_2$ alloys [1-3]. In contrast, the junctions with different polytypes have been also observed for exfoliated MoS_2 flakes [4], and for the laser- and electron-beam-irradiated samples [5,6]. However, the direct growth of polytype-based heterojunctions still remain as an unsolved issue. In this study, we report the growth and characterization of heterojunction of 1H and 1T' phase monolayer $Mo_{1-x}W_xS_2$ alloys grown by CVD.

Monolayer $Mo_{1-x}Re_xS_2$ alloys were formed on graphite and quartz substrate substrates by CVD of sulfur, molybdenum oxide, and rhenium oxide. Growth of hexagonal-shaped monolayer grains was confirmed from atomic force microscope (AFM) observation (Fig.1a). Interestingly, the coexistence of 1H and 1T' phases was found within a single grain through scanning transmission electron microscope (STEM) image (Fig.1b), Raman spectrum (Fig.1c), and scanning tunneling microscope (STM) observations. In particular, the STEM image indicates that the 1T' phase has higher Re concentrations than the 1H phase. In the presentation, we will report the details of their phase-transition conditions and electronic state.

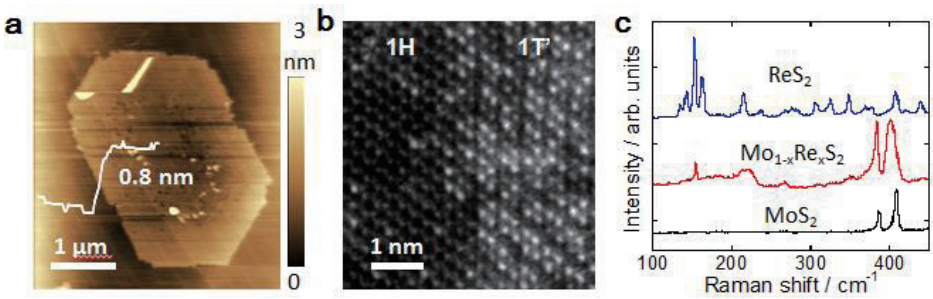

Fig.1 (a) AFM and (b) STEM images of $Mo_{1-x}Re_xS_2$. (c) Raman spectra of MoS_2, ReS_2, and $Mo_{1-x}Re_xS_2$.

[1] Y. Gong, *et al*. Nat. Mater., 13, 1135 (2014). [2] Y. Kobayashi *et al*., Nano Res., 8, 3261 (2015).
[3] S. Yoshida, *et al*. Sci. Rep., 5, 14808 (2015). [4] Y. Lin, *et al*. Nat. Nanotechnol., 9, 391 (2014).
[5] S. Cho, *et al*. Science, 349, 625 (2015). [6] G. Eda, *et al*. ACS Nano, 6, 7311 (2012).

Anisotropic optical absorption and Raman spectrum in GaTe

○Yuki Tatsumi[1], Shengxi Huang[2], Xi Ling[2], Huaihong Guo[3], Teng Yang[4], Mildred S. Dresselhaus[2], Riichiro Saito[1]

[1] *Department of Physics, Tohoku University, Sendai 980-8578, Japan*
[2] *Department of Electrical Engineering and Computer Science, Massachusetts Institute of Technology, Cambridge, Massachusetts 02139 USA*
[3] *College of Science, Liaoning Shihua University, Fushun, 113001, China*
[4] *Institute of Metal Research, CAS, Shenyang 110016, China*

Gallium telluride (GaTe) is a newcomer of atomic layer families, whose primitive unit cell contains 6 Ga and 6 Te atoms [Fig. 1 (a)]. In the bulk form, GaTe is a direct energy gap semiconductor with the gap energy E_{gap}~1.65eV [1]. We can expect GaTe as an application for photodetectors since recent experiment [2] reports that GaTe has high photoresponsivity (10^4 A/W) and short response time (6 ms) compared with other atomic layer materials. Optical properties of GaTe is still not apparent and in this work, we focus on the anisotropy of optical absorption and Raman spectroscopy depending on the polarization of incident photons. In order to investigate the polarization dependence of electron-photon interaction, we perform two step calculations: (1) DFT calculation for obtaining the electronic energy bands and eigenfunction, (2) Calculation of matrix elements for electron-photon interaction based on dipole approximation. We also analyze the polarization of optical transition by group theory analysis.

Figure 1 (b) shows a polarization dependence of optical absorption for x and y polarized light. We can find that x polarized light is absorbed more than y polarized light. We verify the origin of this anisotropy by group theory analysis. GaTe belongs to C_{2h}^3 space group and we can discuss the selection rule of optical transition at symmetric point in Brillouin zone [Z and P point in Fig.1 (c)] by the symmetry of wave function. Figure 1 (c) illustrates the bands symmetry assignment near the Fermi energy at Z and P point. Selection rule shows that the transition near the gap energy is polarized to x direction and x polarized light is mainly absorbed. We will present the analysis of anisotropic Raman spectrum, too.

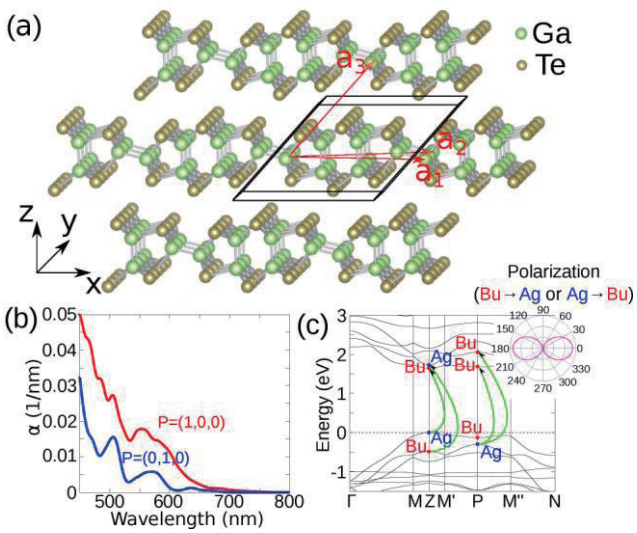

Fig.1: (a) Atomic structure of GaTe. $\boldsymbol{a_1}$, $\boldsymbol{a_2}$, and $\boldsymbol{a_3}$ are primitive lattice vectors. (b) Polarization dependence of absorption spectrum in bulk-GaTe on incident photon energy. $\boldsymbol{P}$ is polarization vector for incident photon. (c) Bands Symmetry assignment for C_{2h}^3 space group at P and Z point of Brillouin zone. Permitted transition is shown by arrow. Inset is polarization dependence for matrix element for these transitions. 0 (90) degree corresponds to x (y) direction.

[1] P. Hu, *et al.* Nano Res., 7, 694 (2014)
[2] F. Liu, *et al.* ACS Nano, 8, 752 (2014)

Corresponding Author: Yuki Tatsumi
Tel: +81-22-795-6442, Fax: +81-22-795-6447,
E-mail: tatsumi@flex.phys.tohoku.ac.jp

Observation of Biexciton States in high-quality Tungsten Disulfide Atomic Layers from 80 K to Room Temperature

○Mitsuhiro Okada[1], Yuhei Miyauchi[2], Kenji Watanabe[3], Takashi Taniguchi[3], Kazunari Matsuda[2], Hisanori Shinohara[1], Ryo Kitaura[1]

[1] *Department of Chemistry & Institute for Advanced Research, Nagoya University, Nagoya 464-8602, Japan*
[2] *Institute of Advanced Energy, Kyoto University, Uji 611-0011, Japan*
[3] *National Institute for Materials Science, Tsukuba 305-0044, Japan*

Group-VI transition metal dichalcogenides (TMDC) have attracted a great deal of attention due to their unique physical properties including exciton-dominated photoluminescence (PL), high performance in field effect transistors and valley-contrast properties. To explore these fascinating properties of TMDC , the preparation of high-quality samples is needed, which are ideally free from defects, surface roughness and the over extrinsic effects arising from substrates. For this purpose, we have focused on chemical vapor deposition growth of TMDC directly onto hexagonal boron nitride (hBN). We report here the growth of high quality WS_2 on hBN and detailed PL properties including the observation of biexcitons at 80 K under low excitation power of 24 W/cm^2. This condition is much milder than that in a previous report (4 K, 50 kW/cm^2) [1].

Figure 1 shows a proposed structure model of WS_2/hBN. PL spectra of WS_2 grown on hBN show very strong and sharp PL emission with a FWHM of 21.5 meV, where PL intensity of WS_2 on hBN is 300 times as stronger as those grown on sapphire. Figure 2 shows PL spectra observed at 80 K, which shows additional peaks at the lower energy region. The excitation power dependence of the PL peak at 2.00 eV shows a linear relation with an alpha of 1.54, and the lifetime measurement of this emission is two times as shorter as that of excitons. The present results clearly show that the PL peak can be attributed to biexcitons, which has been observed with low excitation power down to 24 W/cm^2. PL emission from biexcitons has been observed even at room temperature under a high excitation power of 50 kW/cm^2. And we think minimal substrate effects and amount of trapping site in WS_2/hBN sample are key factors for the current observation of biexciton states.

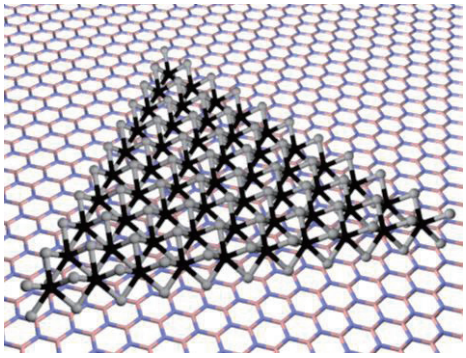

Fig. 1: Schematic view of WS_2/hBN. Hexagonal sheet under WS_2 is hBN.

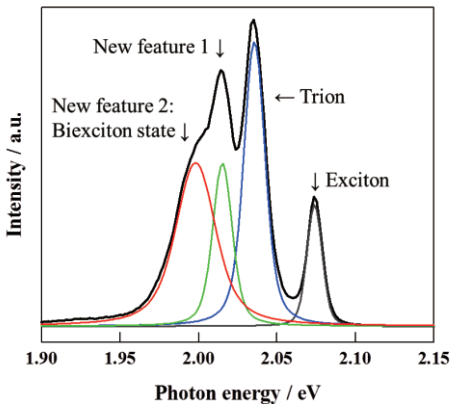

Fig. 2: PL spectra of WS_2 on hBN at 80 K.

[1] G.Plechinger *et al.*, ***Phys. Status Solidi RRL***. **9**, 457 (2015).

Corresponding Author: R.Kitaura and H.Shinohara
Tel: +81-52-789-2477, Fax: +81-52-747-6442,
E-mail: r.kitaura@nagoya-u.jp and noris@nagoya-u.jp

1P-38

Visualization of local transport properties of MoS_2 transistors by scanning gate

○Ayaka Higuchi[1], Masahiro Matsunaga[1], Guanchen He[2], Jonathan P. Bird[2], Yuichi Ochiai[1] and Nobuyuki Aoki[1, 3]

[1] *Graduate School of Advanced Integration Science, ChibaUniversity, Chiba 263-8522, Japan*
[2] *Department of Electrical Engineering, University at Buffalo, SUNY, Buffalo, New York 14260-1920, USA*
[3] *JST-PRESTO, Kawaguchi, Saitama 332-0012, Japan*

In recent studies, molybdenum disulfide, MoS_2, which has layered structure has been attracted lots of interests because of its properties. Typically, it exhibits semiconducting properties having a band gap of 1.8 eV in the monolayer structure. Therefore, it has been studied so as to be utilized as field effect transistor (FET). In our study, we use scanning gate microscopy (SGM) to examine characteristic of MoS_2. SGM can visualize local transport properties in semiconducting materials using a metallic coated cantilever as a mobile top gate.

In our previous report [1], we reported local gate responses within MoS_2 FET by SGM. The results indicated that the SGM response attributed to the transport properties of the MoS_2 FET, which is dominated by the properties of ohmic contact at injection side. Combining electrostatic force microscopy (EFM) observation, we can evaluate the potential discussion within the channel.

In our study, single layer MoS_2 crystals which were directly grown on SiO_2/Si substrates by chemical vapor deposition and provided by the Ajayan group at Rice University [2]. Source and drain electrodes (Cr/Au) were patterned by electron beam lithography.

As results of these measurements, we found SGM responses observed inside the MoS_2 channel, away from the electrode in the same sample. In addition, EFM image we obtained indicated that a huge potential drop was at the same position where the SGM response observed. Interestingly, some groups reported that a crystalline structure of MoS_2 can be transformed from semiconducting (2H-structure) to metallic (1T-structure) by several ways [3, 4]. Considering our results of the SGM and the EFM, a Schottky potential barrier could process. It suggests that a possibility of a partial-structural transition from 2H to 1T might be introduced by EB lithography.

[1] M. Matsunaga *et al*, The 49th FNTG General Symposium 3P-36 (2015).

[2] Y. Zhan *et al*., Small **8**, 966-971 (2012).

[3] R. Kappera *et al*., Nature Mater. **13**, 1128 (2014).

[4] Y. C. Lin *et al*., Nature Nanotech. 9, 391 (2014).

Corresponding Author: N. Aoki
Tel:+81-43-290-3430, Fax:+81-43-290-3427
E-mail:n-aoki@faculty.chiba-u.jp

Extremely Thin and Flexible Single-Layer WS_2 Phototransistors

○Adha Sukma Aji,[1] Toshiaki Shiiba,[1] Kenjiro Fukuda,[2,3] Hiroki Ago[1,3,4,*]

[1]*Interedisciplinary Graduate School of Engineering Sciences, Kyushu University*
[2]*Thin-Film Device Laboratory, RIKEN*
[3]*PRESTO-JST*
[4]*Institute for Materials Chemistry and Engineering (IMCE), Kyushu University*

The discovery of graphene has expanded the research field of two-dimensional (2D) materials [1]. The 2D materials show unique physical properties, such as high carrier mobility in graphene and direct band gap in single-layer MoS_2 and WS_2, which can be developed to novel electronic and photonic applications. Moreover, their atom-thick structures make devices very thin, flexible, and transparent.

In the present work, we demonstrate an extremely thin, flexible, and soft phototransistors using WS_2 and graphene as channel and electrodes, respectively. Single-layer WS_2 used as a channel was synthesized on sapphire substrates by ambient pressure CVD using WO_3 and S powder. All the source, drain, and gate electrodes were made by multi-layer graphene which had been grown by CVD on Cu-Ni foil. We synthesized relatively thick graphene (~12 nm thick), because it gave much lower sheet resistance (100 Ω/□) than that of monolayer graphene (600 Ω/□). After patterning WS_2 and graphene, we assembled all these 2D materials on 1 μm-thick parylene substrate, as illustrated in Figure 1a.

The transport property of the all-2D device was measured in vacuum at room temperature. Interestingly, the device worked by directly contacting probe tips to graphene electrodes, without using metals, such as Au and Ti. Moreover, as shown in inset in Figure 1b, the WS_2 channel and graphene electrode showed near Ohmic behavior, suggesting graphene can form a good contact to 2D materials. Figure 1b presents the transfer curves in dark and under illumination of visible light. The on/off ratio and electron mobility are 2×10^4 and 2 cm^2/Vs, respectively, in dark. The all-2D device showed a clear optical response, with photoresponsitivity as high as 70 μA/W at V_g=30 V. The internal quantum efficiency (IQE) were calculated to be 9%. These values indicate good photon to electron conversion even though the device is nearly transparent. Our result would enrich 2D material applications for transparent and flexible optoelectronic devices.

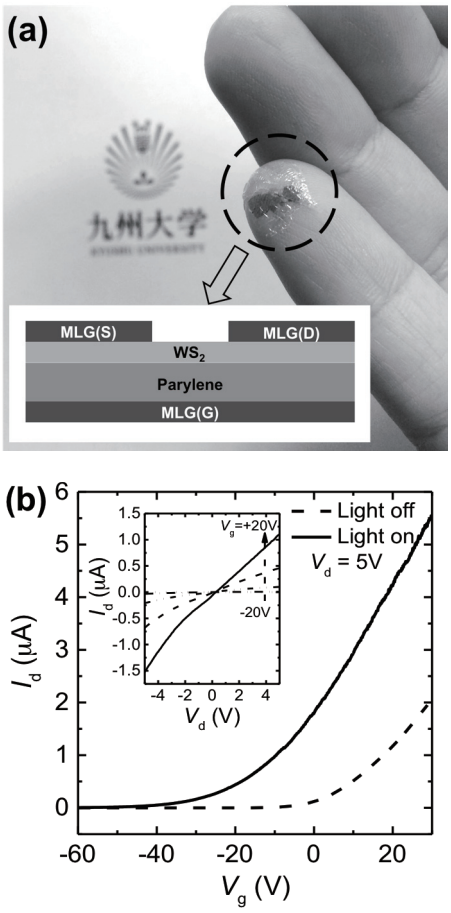

Fig 1. (a) Photograph of the all-2D device attached on a human finger. Inset: Schematic view of the device. (b) Transfer characteristic of the device.

Reference: [1] S. Z. Butler *et al.*, *ACS Nano*, **7** (2013) 2898.
Corresponding Author: Hiroki Ago (Tel&Fax: +81-92-583-7817, E-mail: ago@cm.kyushu-u.ac.jp)

Lattice Vibrations in Isotopic Diamond Superlattice

○Yuki Bando, Susumu Saito

Department of Physics, Tokyo Institute of Technology, Tokyo 152-8551, Japan

Isotopic Diamond Superlattice Structure where ^{12}C and ^{13}C diamond layers are stacked alternately was created by Watanabe *et al* [1]. In this system, the confinement of carriers to ^{12}C diamond layers was observed by cathodoluminescence experiments. It is expected that this phenomenon is caused by characteristic electron-phonon interaction in a diamond crystal [2]. However, details of the lattice vibrations and its effects on the electronic structure in isotopic diamond suprelattice have not been reported theoretically so far.

In our study, we computed lattice vibrations in isotopic diamond suprelattice using density functional perturbation theory [3] with a special combination of Fourier transformation for isotopic superlattice. As a result, the density of states of lattice vibrations (LV-DOS) of the superlattice alternately stacked 36 ^{12}C layers and 36 ^{13}C layers ((36, 36) superlattice) is found to be nearly equal to the arithmetic mean of LV-DOS of the 12C diamond and that of the ^{13}C diamond (Fig. 1). On the other hand, LV-DOS of the (2, 2) superlattice is nearly equal to LV-DOS of virtual $^{12.5}C$ diamond (Fig. 2).

(a) Comparison with $^{12.5}C$ (b) Comparison with arithmetic mean of ^{12}C and ^{13}C

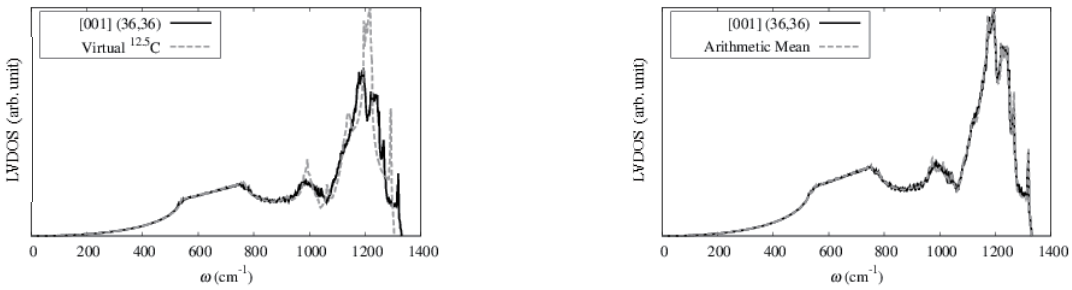

Fig 1. LV-DOS of (36, 36) superlattice stacked toward [001] direction

(a) Comparison with $^{12.5}C$ (b) Comparison with arithmetic mean of ^{12}C and ^{13}C

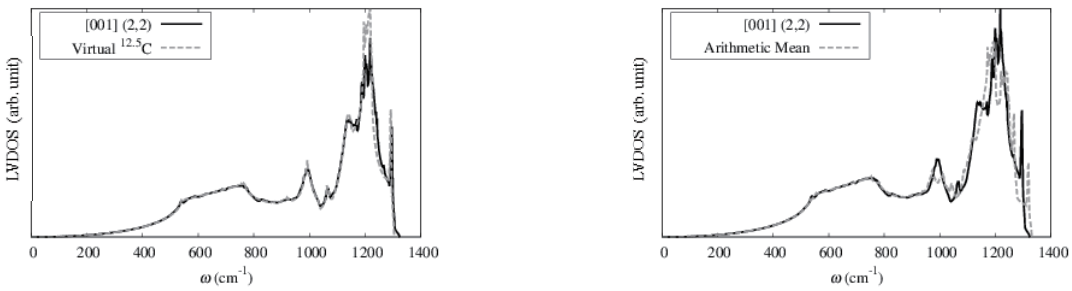

Fig 2. LV-DOS of (2, 2) superlattice stacked toward [001] direction

[1] H. Watanabe, C. E. Nebel, and S. Shikata, *Science* **324** 1425 (2009)
[2] F. Giustino, S. G. Louie and M. L. Cohen, *Phys. Rev. Lett.* **105** 265501 (2010)
[3] S. Baroni, S. de Gironcoli, and A. D. Corso, *Rev. Mod. Phys*. **73**, 515 (2001)

Corresponding Author: Y. Bando
Tel: +81-03-5734-2387, Fax: +81-03-5734-2739,
E-mail: y-bando@stat.phys.titech.ac.jp

Josephson effect in $NbSe_2/NbSe_2$ van der Waals junction

○Naoto Yabuki [1], Rai Moriya [1], Miho Arai [1], Yohta Sata [1], Sei Morikawa [1], Satoru Masubuhi [1], Tomoki Machida [1,2,3]

[1] *Institute of Industrial Science, University of Tokyo, Tokyo, Japan*
[2] *Institute for Nano Quantum Information Electronics, University of Tokyo, Tokyo, Japan*
[3] *CREST, Japan Science and Technology Agency, Japan*

We demonstrated the Josephson effect at the van der Waals (vdW) interface. Layered dichalcogenide superconductor $NbSe_2$ is mechanically exfoliated, and vdW contact between freshly cleaved surfaces has been built by using dry transfer technique [Fig. 1(a)]. By optimizing exfoliation and transfer condition, we fabricated highly transparent vdW junction between $NbSe_2$ crystals with resistance-area product RA=16 Ω-μm^2. Cross-sectional TEM images reveal atomically flat vdW interface without significant oxidation.

Current-voltage characteristics exhibited zero bias current accompanying apparent hysteresis [Fig. 1(b)]; thus suggesting the Josephson current flow across vdW junction. By applying magnetic field parallel to the junction, the periodic modulation of the Josephson current (Fraunhofer pattern) is observed [fig. 1(c)]. The ratio between subgap and normal-state resistance R_{qp}/R_N = 20 already comparable to that of modern Nb-based Josephson junction. Furthermore, we demonstrate $R_N I_c$ product of 1.04 mV; this is close to the maximum value expected from the Ambegaokar-Baratoff theory. These results indicate that high quality vdW Josephson junction has been fabricated in vdW interface [1].

[1] Naoto Yabuki , Rai Moriya *et al.*, Nature Communications, in press.

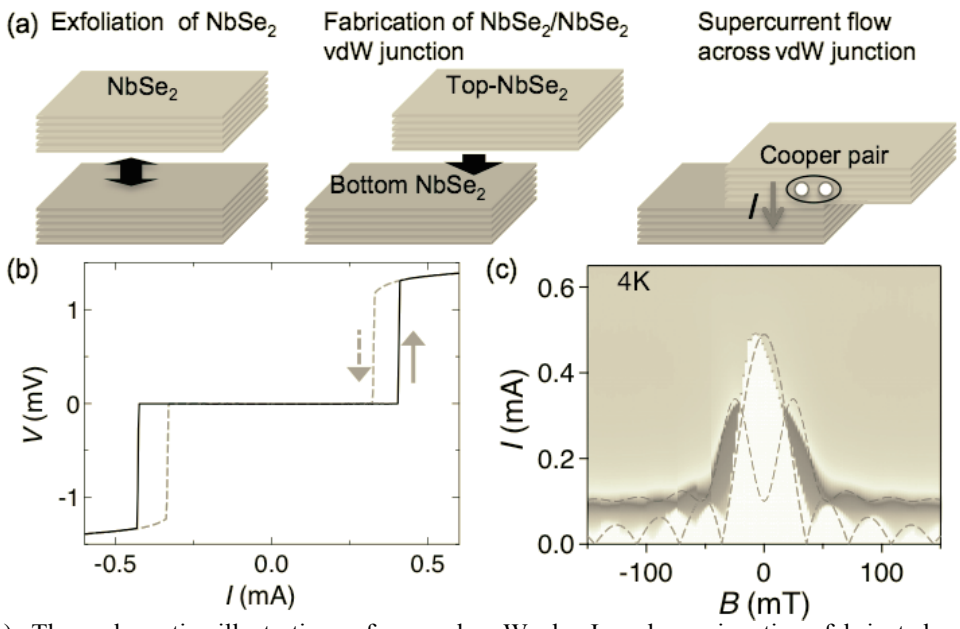

Fig.1 (a) The schematic illustration of van der Waals Josephson junction fabricated with $NbSe_2$. (b) Current-voltage characteristics of the junction at 4.5 K. (c) In-plane magnetic field dependence of *I-V* curves showing Fraunhofer pattern at 4 K. Dashed line indicates the theoretical calculation.

Corresponding Author: N. Yabuki
Tel: +81-3-5452-6158, Fax: +81-3-5452-6157,
E-mail: yabuki@iis.u-tokyo.ac.jp

Functional carbon nanohorn complexes for multi-dimensional cancer elimination

○Eijiro Miyako[1*], Svetlana Chechetka[1], Minfang Zhang[2], Masako Yudasaka[1]

[1] *Department of Materials and Chemistry, Nanomaterial Research Institute (NMRI), National Institute of Industrial Science and Technology (AIST), Central 5, 1-1-1 Higashi, Tsukuba 305-8565, Japan*

[2] *Department of Materials and Chemistry, CNT-Application Research Center, AIST, Central 5, 1-1-1 Higashi, Tsukuba 305-8565, Japan*

We have developed multi-componential nanomaterials that are based on folic acid (FA) and polyethylenimine (PEI)-functionalized carbon nanohorn conjugates that encapsulate magnetite nanoparticles (FA-PEI-MAG-CNH_{ox}) (Fig. 1)[1,2]. The nanoconjugates were characterized using a variety of experimental setups, including dynamic light scattering, thermogravimetric analysis, Fourier transform infrared spectrometry, and ultraviolet–visible–near-infrared (UV–Vis–NIR) spectroscopy. An NIR laser and a radio frequency-induction heating system were used to evaluate the heat-generating capability of the nanoconjugates. Aqueous solutions containing the nanoconjugates exhibited a significant increase in temperature after laser irradiation and/or radio frequency induction compared with controls. The intercellular distribution of the nanoconjugates was quantitatively analyzed using UV–Vis–NIR spectroscopy with two cell lines: human epidermal carcinoma (KB) and human embryonic (FHs173We) cells. The interaction between the FA-modified nanoconjugates and KB cells was enhanced through overexpression of FA receptors on the surface of the KB cells. A stronger interaction between the nanoconjugates and KB cells was observed in the presence of a magnet. Furthermore, laser- and/or radio frequency-induced nanoconjugates in combination with external magnetic application reduced the viability of KB cells. Therefore, the present study will open a new direction for the development of multi-dimensional cancer therapy.

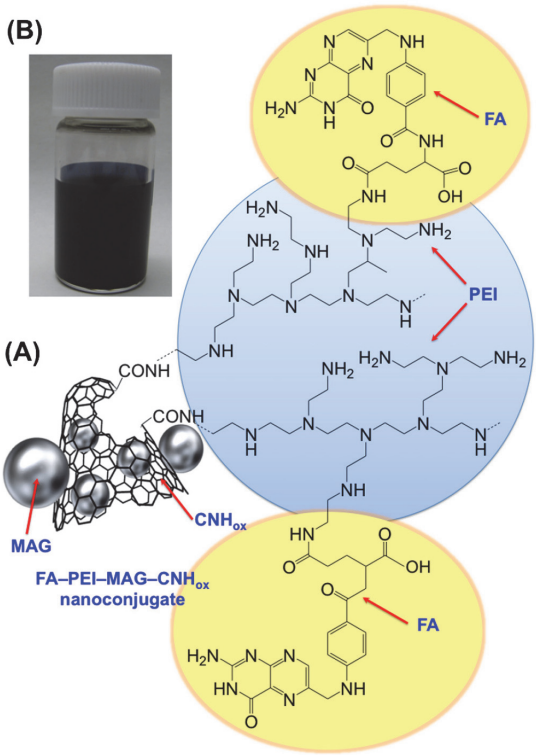

Fig. 1 Chemical structure and water-dispersibility of FA-PEI-MAG-CNH_{ox} conjugates. (A) A schematic illustration of the chemical structure of FA-PEI-MAG-CNH_{ox}. (B) FA-PEI-MAG-CNH_{ox} in an aqueous solution. The FA-PEI-MAG-CNH_{ox} was dispersed in HEPES buffer (100 mM, pH 7.4) at a concentration of 300 μg/mL.

[1] S. Chechetka et al. *Carbon* **97**, 45-53 (2016).

[2] S. Chechetka et al. *Chem. Asian J.* **10**, 160-165 (2015).

*Corresponding Author: E. Miyako

Tel: +81-87-869-3574, Fax: +81-29-861-4413, E-mail: e-miyako@aist.go.jp

Characterization and Supercapacitor Properties of Fibrous Aggregates of Single-Walled Carbon Nanohorns

○Ryota Yuge[1], Fumiyuki Nihey[1], Kiyohiko Toyama[1], and Masako Yudasaka[2, 3]

[1]*Smart Energy Research Laboratories, NEC Corporation, Tsukuba 305-8501, Japan*
[2]*National Institute of Advanced Science and Technology (AIST), Tsukuba, 305-8565, Japan*
[3]*Graduate School of Science and Technology, Meijo University, Nagoya 468-8502, Japan*

Single-walled carbon nanohorns (SWCNHs) [1], a type of nano-carbon materials, are attractive having high dispersibility in solutions and large specific surface area. Recently, we have succeeded in preparing fibrous aggregates of SWCNHs (fib-CNHs), which also have large surface area and, different from SWCNHs, their electrical conductivity is high [2]. As well known, the large surface area and high electrical conductivity are fundamental properties for the electrodes materials of supercapacitors, but it is not easy for one substance to have these two properties. It seems that the fib-CNHs could be an ideal material to make the electrode of supercapacitor. In this study, the supercapacitors were fabricated by using fib-CNHs electrodes and the capacitance and quick discharge properties were evaluated.

Fib-CNHs were prepared by CO_2 laser ablation of an iron-containing graphite target at room temperature. The CO_2 laser was operated in the continuous-wave mode. The gas pressure in the growth chamber was sustained at 760 Torr by controlling the evacuation rate while the flow rate of buffer gas of N_2 was kept at 10 L/min. The conventional SWCNHs of spherical structure (sph-CNHs) were also prepared using an iron-free graphite target, which is used as a reference sample. Composite-pellet for the supercapacitor electrode was prepared by sph-CNHs and/or fib-CNHs with polytetrafluoroethylene binder (PTFE). The supercapacitor was assembled with 1 M $(CH_3(CH_2)_3)_4N{\cdot}BF_4$/propylene carbonate electrolyte, glass separator, and the composite-pellet electrodes. Galvanostatic charge/discharge measurements were carried out in the range of 0 to 2.5 V at 20ºC

The specific surface areas of fib- and sph-CNHs after hole-opening by the oxidation treatment were 1580 m^2/g and 1690 m^2/g, respectively. Their capacitances were 20 and 21 F/g, which mean that the capacitance depends strongly on the specific surface area. The supercapacitor with hole-opened fib-CNHs indicated the higher capacitance, *i.e.*, less capacitance drop at high power operation. The capacitance retention of hole-opened fib-CNHs at the discharge current at 5 A/g was 40% higher than that of sph-CNHs.

[1] S. Iijima *et al*. Chem. Phys. Lett. **309**, 165 (1999).

[2] R. Yuge *et al*. The 49th FNTG Symposium, 65 (2015).

Corresponding Author: R. Yuge

Tel: +81-29-850-1566, Fax: +81-29-856-6137,

E-mail: r-yuge@bk.jp.nec.com

Electrical conductivity of carbon nanomaterials under compression

○K. Mizui[1], T. Ohiro[1], Y. Suda[1], T. Harigai[1], H. Takikawa[1], H. Ue[2]

[1] *Department of Electrical and Electronic Information Engineering, Toyohashi University of Technology, Toyohashi, Aichi 441-8580, Japan*
[2] *Fuji Research Laboratory, Tokai Carbon Co., Ltd., Oyama, Shizuoka 410-1431, Japan*

1. Introduction

Carbon black, nanometer-size carbon particles, is commercially used as the catalyst support in fuel cell owing to its high surface area, porosity, electric conductivity, low density, and low cost. In the previous work, we have used various carbon nanomaterials as catalyst supports for direct methanol fuel cell (DMFC) [1]. In this study, we measured the powder conductivity of carbon nanomaterials with different geometries and graphitic structures. Under compression it is shown that the electrical conductivity of carbon black did not only depend on its intrinsic morphological properties, which determine the degree of packing of the material and hence the change in density, but also on such extrinsic factors as the applied pressure and the ambient humidity.

2. Experimental

The carbon nanomaterials were characterized using scanning electron microscopy (SEM; S-4500II and SU8000, Hitachi) and compressive conductivity measurements. We used four samples of carbon nanoballoon (CNB), Vulcan XC-72R (Vulcan), vapor-grown carbon fiber (VGCF-H), ketjen black (KB). The powder conductivity of compressed carbon nanomaterials is the result of a combination of the number of factors, including the resistivity of the individual particles, the degree of contact between the particles, and their packing density.

3. Results

Fig. 1 shows the variation of the conductivity with applied pressure. The effect of the increase in pressure on conductivity was very strong for all the samples. Because the contact area between the carbon particles increase for the denser carbons.

CNB which was prepared by heat treatment of Arc black (AcB) showed comparable powder conductivity to commercial Vulcan and KB. Moreover, VGCF-H showed the highest conductivity.

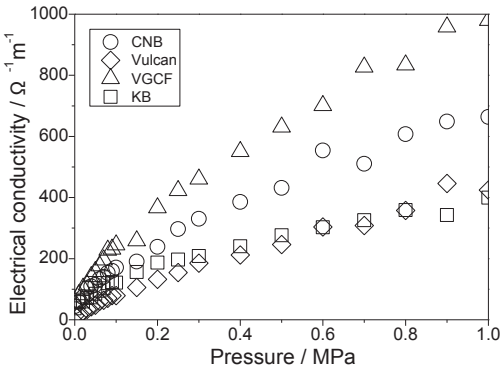

Fig. 1. Electrical conductivity versus pressure

This work has been partly supported by the EIRIS Project from Toyohashi University of Technology (TUT); JSPS KAKENHI Grant Number 24360108 and 15K13946; and the Toyota Physical and Chemical Research Institute, “Scholar Project”.

[1] Yoshiyuki Suda, Yoshiaki Shimizu, Masahiro Ozaki, et al. Materials Today Communications, 3 (2015) 96-103

Corresponding Author: Y. Suda
Tel: +81-532-44-6726, Fax: +81-532-44-6757
E-mail: suda@ee.tut.ac.jp

Laser Power Dependence in LDI MS of Detonation Nanodiamonds

○Masayoshi Fukaya[1], Yoshiki Otsubo[1], Toshihiko Tanaka[1], Ryoko Yamanoi[2], Eiji Osawa[2]

[1] *Department of Chemistry and Biochemistry, National Institute of Technology, Fukushima College, 30 Aza-nagao, Tairakamiarakawa, Iwaki, Fukushima, 970-8034, Japan*
[2] *Nano Carbon Research Institute Ltd., Asama Research Extension Centre, Faculty of Textile Science and Technology, Shinshu University 3-15-1 Tokita, Ueda, Nagano, 386-8567 Japan*

Primary particles of detonation nanodiamonds (PPDND) should have strong electric polarization and it possibly accounts for their enigmatic properties including a successful drug delivery for cancer therapy.[1] The structure of PPDND is therefore essential there and was simulated by a density functional method.[2] Moreover it has been investigated by some experiments such as TEM, Raman, NMR, and dynamic light scattering (DLS).[3-5] Furthrtmore, mass analysis would reveal their sizes as well as their charges with respect to ionization.

We report herein the laser power dependence in laser desorption ionization mass spectra (LDI MS) of the nanodiamonds (NDs) deposited on a stainless plate from the aqueous solution of highly dispersible PPDND. We reported previously that a positive 12k Da peak (Fig.1) is attributable to the diamond core of PPDND.[6] However, abundant oligomeric peaks under 5k Da suggested that appreciable decomposition takes place through the ionization of PPDND. Hence, we should take into consideration whether the core becomes thin or fat there during LDI.

Figure 2 demonstrates that the ion from diamond core became thin through decomposition in the LDI process: peak m/z decreases with the laser power. The other 2 sorts of ion (~39k, ~120k) also became thin. Through the ionization, the core therefore should decompose by the laser exposure and the original size of the core should be larger than 12k Da. Plausible decomposition reactions as well as possible methods for measuring original core sizes will be discussed here.

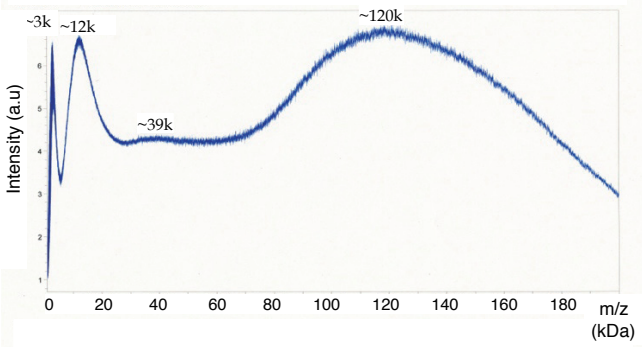

Fig.1. LDI MS of NDs.

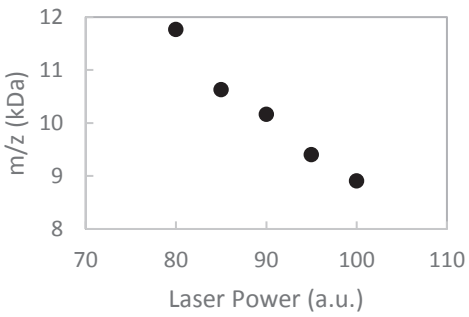

Fig.2. Laser power dependence in peak m/z near 12k.

[1] E. Osawa, D. Ho, H. Huang, M. V. Korobov, N. N. Rozhkova; *Dia. Rel. Mat.* 18, 904(2009).
[2] A.S.Barnard, E.Osawa; *Nanoscale* 6, 1188 (2014).
[3] E. Osawa; *Dia. Rel. Mat.* 16, 2018 (2007).
[4] V. I. Korepanov, H. Witek,H. Okajima, E. Osawa, and H. Hamaguchi; *J. Chem. Phys.* 140, 41107 (2014).
[5] A. M. Panich, H-M. Vieth, A. I. Shames, N. Froumin, E. Osawa,|A. Yao; *J. Phys. Chem. C* 114, 774 (2010).
[6] T. Tanaka, R.Yamanoi, E.Osawa; *FNTG* 48, Proceedings 19(2015).

Corresponding Author:Toshihiko Tanaka / Tel: +81-246-46-0810 / E-mail: ttanaka@fukushima-nct.ac.jp

Polymer-derived Nanoporous Carbon Monolith: High Electrochemical Capacitive Behaviors

○Yanqing Wang[1], Bunshi Fugetsu[2], Ichiro Sakata[1, 2], Zhipeng Wang[3], Wei Gong[1], Mauricio Terrones[4], Morinobu Endo[3], Mildred Dresselhaus[5]

[1]Nano-Agri Laboratory, School of Engineering, The University of Tokyo, Bunkyo-ku, Tokyo 113-0032, Japan.

[2]Nano-Agri Laboratory, Policy Alternative Research Institute, The University of Tokyo, Bunkyo-ku, Tokyo 113-0032, Japan.

[3]Institute of Carbon Science and Technology, Shinshu University; 4-17-1 Wakasato, Nagano 380-8553, Japan.

[4]Department of Physics, Department of Chemistry, Department of Materials Science and Engineering and Center for 2-Dimensional and Layered Materials, The Pennsylvania State University, University Park, PA 16802, USA.

[5]Research Laboratory of Electronics, Department of Electrical Engineering and Computer Science, Department of Physics, Massachusetts Institute of Technology, 77 Massachusetts Avenue, Cambridge, MA 02139-4307, USA.

The development of mesoporous carbon materials with well-defined continuous interconnected pore structure has been growing remarkably in recent years. A monolith, or a single piece of three-dimensional (3D) porous material was first reported in 1990s and has now become an essential part of polymer chemistry and materials chemistry. Polyacrylonitrile (PAN) is widely used as fibers in various industries. PAN fibers are also used as good precursors for carbon fibers. PAN monolith with controlled shape/morphology and pore sizes can be fabricated through thermal induced phase separation technique and acts as the precursor for activated carbon monolith (ACM), which has large potential in capacitors and batteries applications. As illustrated in Fig. 1, mesoporous PAN monoliths with 3D continuous network structure were fabricated successfully. The shape of monoliths can be easily tailored in different ways according to the vessels they are used. The conditions such as DMSO/H_2O composition, temperature, holding time, etc. have an important effect on the PAN 3D networks, including the skeleton structure and pore diameter. Leaf-, ribbon-, skeleton like monolith structures with surface area ranging from 40 to 200 m^2/g and the pore diameters from 8 to 22 nm were created by controlling the parameters. A monolith with an average skeleton size around 18 nm and the average mesopore diameter around 11.2 nm was carbonized followed by two steps: pretreatment at 200℃ in air and 600～900℃ heat treatment in mixture of Ar and CO_2. The surface area of the monoliths increased by 2～5 times after carbonization process. As shown in Fig. 1, PAN monolith with continuous interconnected network structure still keeps in the ACM (Fig. 2). All carbon monoliths showed good rectangular cyclic voltammetry (CV) curves at scan rates 10 mV/s, indicating effective EDL capacitance as electrode. The capacitance of 26-2, 26-1 and 25-2 was ca. 135 F/g, 21 F/g, 93 F/g, respectively. The galvanostatic charge/discharge curves of carbon monoliths-based electrodes exhibited symmetric triangular shape, revealing a typical characteristic of EDL capacitor.

Fig. 1. Fabrication process of PAN-based carbon monolith.

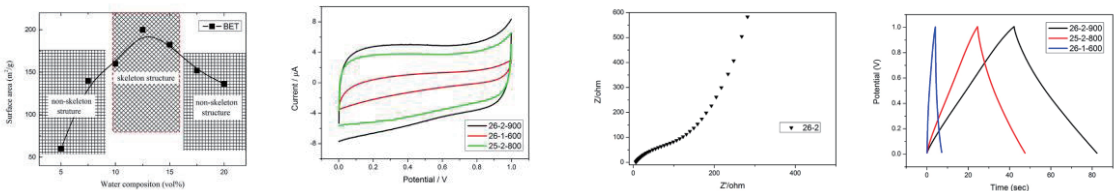

Fig. 2. Electrochemical capacitive behaviors of PAN-based carbon monolith.

Corresponding Author: Y. Q. Wang
Tel: +81-3-5841-7461, E-mail: wang2011@ees.hokudai.ac.jp

Polyyne formation by laser-induced breakdown in argon-diluted propane gas flow

○Yuki Taguchi[1], Hitomi Endo[1], Takeshi Kodama[1], Tomonari Wakabayashi[2], Yohji Achiba[1], Haruo Shiromaru[1]

[1] *Department of chemistry, Tokyo Metropolitan University, Tokyo 192-0397, Japan*
[2] *Department of Chemistry, Kindai University, Osaka 577-8502, Japan*

Polyynes are linear carbon chains composed of alternating single and triple bonds, and are typically terminated by hydrogen atoms. The conventional method of generating polyynes is laser ablation of graphite powder in organic solvent [1]. Recently, we reported that polyynes are produced by laser ablation of graphite in argon/propane mixed gases and the increase of polyyne yield is observed for higher ratio of propane gas [2]. Both experiments employ graphite powder as a source of the carbon chain. In the present study, we examined polyyne formation without graphite, by laser-induced breakdown in argon/propane mixed gas flow. The experimental setup is shown Figure 1. The mixed gases (propane gas ratio is 0.1 %~100 %, 50 mL/min) were introduced to the glass cell, where the Nd; YAG laser (30 Hz, 532 nm) with the power of 150 mJ/pulse was irradiated for one minute. The laser was tightly focused to the center of the glass cell by the lens of focal length 70 mm, to induce breakdown. The products were carried by the gas flow, and captured in the hexane at -80 degrees. Liquid propane coexists with the products at this temperature. After irradiation, liquid propane was evaporated at room temperature. The soluble products were analyzed by UV absorption spectra.

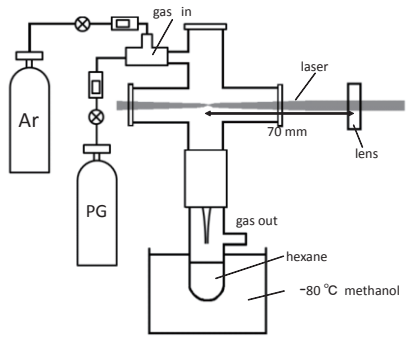

Figure 1 Schematic drawing of the laser-induced breakdown setup.

A typical UV spectrum of the sample solution is shown in Figure 2, where polyynes $C_{2n}H_2$(n=3~7) and methyl polyyne $CH_3C_{16}H$ are clearly observed. The yields of polyynes show a saturation behavior with respect to the ratios of the propane gas. The quantitative analysis of the polyyne yield curves is now under way.

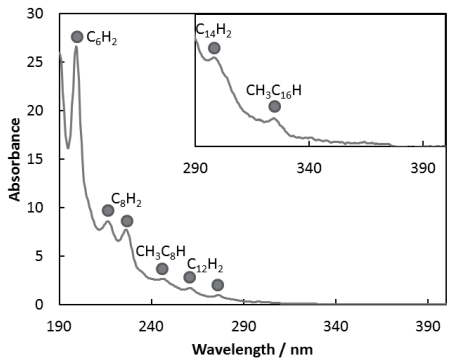

Figure 2 The UV spectrum of the sample solution obtained from 100 % propane breakdown. The peaks of polyynes $C_{2n}H_2$(n=3~7) and methyl polyyne $CH_3C_{16}H$ are indicated by filled circles.

[1] M. Tsuji et al., Chem. Phys. Lett. 355 (2002) 101.
[2] Y. Taguchi et al., CARBON 94 (2015) 124.

Corresponding Author: Yuki Taguchi
Tel: +81-42-677-1111, Fax: +81-42-677-2525
E-mail: taguchi-yuuki@ed.tmu.ac.jp

Polyyne formation by laser ablation of PAH/graphite composite disk in vacuum

○Ryouichi Moriguchi,[1]Yuki Taguchi,[1]Hitomi Endo,[1]
Tomonari Wakabayashi,[2] Takeshi Kodama,[1]Yohji Achiba,[1]and Haruo Shiromaru[1]

[1] *Department ofChemistry,Tokyo Metropolitan University, Tokyo 192-0397, Japan*
[2]*Department of Chemistry,Kindai University,Osaka 577-8502, Japan*

Polyynes and PAHs play an important role in evolution of interstellar molecules in carbon-rich environment, and long chains up to 8 carbonsterminated with H and those up to 10 carbons terminated with H and CN have been identified in space [1,2]. In contrast to the reactions in space, experimental studies on polyyne formation have been conducted in organic solvent [3] or in hydrocarbon gas flow of atmospheric pressure [4], initiated by laser ablation of graphite. The laboratory studies indicate that a choice of proper surroundings is important for efficient production of polyynes. In the present study, we conducted laser ablation of model compounds of PAHs in vacuum and confirmed that polyynes were efficiently formed without the aid of surrounding gases/solvents.

The experimental setup is shown in Fig.1. A mixed powder of anthracene and graphite with wt.-ratios of 1:1 or 1:3 was compressed to prepare a composite disk, which was amodel compound of PAHs with different degrees of unsaturation. The disk was set to face its surface to the exit of the ablation cell.The ablation products directed to the exit were captured by hexane solvent in a glass bottle, which was cooled down to near the freezing temperature. The ablation cell and solvent bottle were evacuated by a rotary pump. Loosely focused 2nd harmonic of pulsed Nd:YAG laser (10 Hz, 0.8 J/cm^2) was irradiated to the disk for three minutes. The soluble ablation products were analyzed by HPLC and UV absorption.

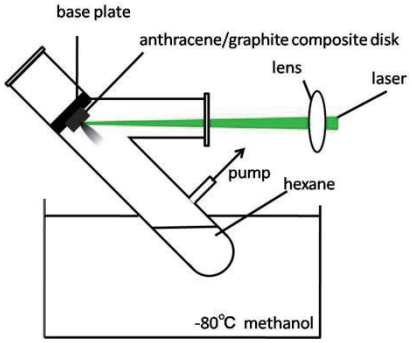

Fig. 1 Experimental setup

The absorption spectra of the solutions measured at known retention times of various lengths of polyynes are shown in Fig. 2, where characteristic peaks of polyynes are clearly seen up to $C_{14}H_2$. The polyynes are identified both for 1:1 and 1:3 disks, while the yield is lower for the 1:3 disk. Considering that the ablation products are rapidly diffused in vacuum, the result suggests that chain-form carbon clusters are efficiently terminated by hydrogen formed in a same ablation event.

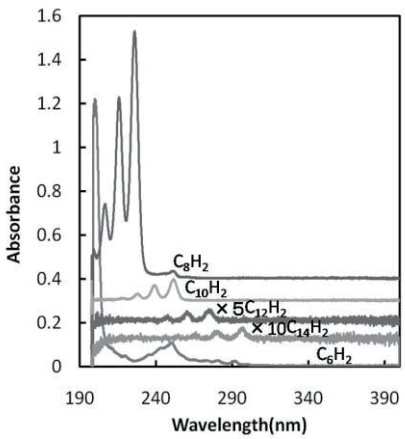

Fig. 2UV absorption spectra of the ablation products from anthracene/graphite 1:1 disk, measured after HPLC analysis.

[1] M. Guelin*et al.*, *A&A***309** L27 (1996).[2] M. B. Bell*et al.*,*ApJ***483**, L61 (1997). [3] M. Tsuji*et al.*, *Chem. Phys. Lett.*355,101 (2002). [4] Taguchi *et al.*, *Carbon***94**, 124 (2015).Corresponding Author:H. Shiromaru, Tel: +81-42-677-1111, Fax: +81-42-677-2525, E-mail:shiromaru-haruo@tmu.ac.jp

Observation of Size Dependence of Charge State of Nano-level Particles by Ion Trap Ion Mobility Measurement

○Yasuhiro Hiroshiba, Hironobu Matsubayashi, Takuma Ito,
Ryota Jinnouchi, Toshiki Sugai

Department of Chemistry, Toho University, Chiba 274-8510, Japan

Structural observation techniques have been a key to investigate nano materials. Various methods, such as TEM and STM, have been developed so far. Those traditional methods are powerful enough for most of stable nano materials such as carbon nanotubes and metal particles. To track structural changes of floppy or unstable materials, however, those traditional methods may not be mighty. We have been working on the development of ion mobility spectrometry (IMS) system for the structural observation of nano materials and have found novel metallofullerene structures by IMS[1]. Furthermore we have succeeded to develop ion trap ion mobility to trap and observe long-term structural change of μm size particles up to 2 hours[2]. IMS can cover materials with wide-range size but the results depend not only on their structures but also on their charges[3]. To cover materials with wide-range sizes, here we present the observation of size dependence of charge state of particles with radii from 250 nm to 10 μm.

Fluorescent polystyrene particles with precisely size control (Bay bioscience and Estapor) were ionized by a Nd:YAG laser (266 nm) ablation. They were introduced and trapped in the IMS system. The trapped particles were repeatedly drove to have up-down motion in air and their motion were monitored with an eradiation semiconductor laser (532 nm) and digital camera. Their mobility and charge states were calculated with the motion and Stokes' law[2,3].

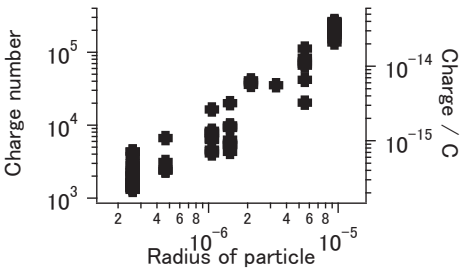

Fig. 1 Size dependence of charge of polystyrene particles.

Figure 1 shows log-log plot of the size and the amount of charge. We have succeeded to observe down to nano-level particles with the radius of 250 nm. The charge increases as the particle size increases. The amount of charge distributes even if the particle size is unchanged. However, the slope of figure 1 shows that the maximum amount of charge is proportional to the radius. Those results suggest that the system can be utilized to nano materials and may reveal their size only by mobility measurement without checking their charge states.

[1] T. Sugai *et al.*, *J. Am. Chem. Soc.* ***123,*** 6427 (2001).
[2] T. Sugai *et al.*, 42nd *Fulluerene-nanotue-graphene conference.* 3-13
[3] T. Sugai, *J. Mass Spectrom. Soc. Jpn.* **58**, 47, (2010).

Corresponding Author: T. Sugai, Tel: +81-47-472-4406, E-mail: sugai@chem.sci.toho-u.ac.jp

Regioselective Addition of Grignard Reagents to Azafulleroids

○Naohiko Ikuma, Koji Nakagawa, Ken Kokubo, Takumi Oshima

Division of Applied Chemistry, Graduate School of Engineering,
Osaka University, Suita 565-0871, Japan

Multiple functionalization of fullerene C_{60} is an important technique in the application for the material chemistry because the introduced groups are able to control their electronic properties and enhance the solubility for wet-processing. However, C_{60} has many reaction sites and would often give a mixture of multiadducts with low selectivity. In order to prepare the regioselective multifunctionalized fullerenes, we have interested in the intrinsic reactivity of azafulleroids which have one bridged nitrogen atom and two highly twisted bridgehead double bonds. Previously, we have reported the high regioselectivity of azafulleroids on the acidic arylation [1] and the oxidative deamination with peracids [2]. Here we report the regioselective nucleophilic addition of Grignard reagents to azafulleroids due to the coordination between bridged nitrogen and magnesium.

For alkyl azafulleroids, Grignard reagents preferably attacked the Cα–carbon following by acidic quench leading to Cβ-hydrogen adduct. This Cβ-hydrogen adduct was further transformed to alkyl adduct by alkyliodide under basic condition (KOtBu). On the other hand, for tosyl azafulleroid, Grignard reagents seem to attack the Cβ-carbon to give 1-amino-2-arylfullerenes via the cleavage of C-N bond. The change of reaction site in alkyl/tosyl azafulleroids is well consistent with the transition state calculations.

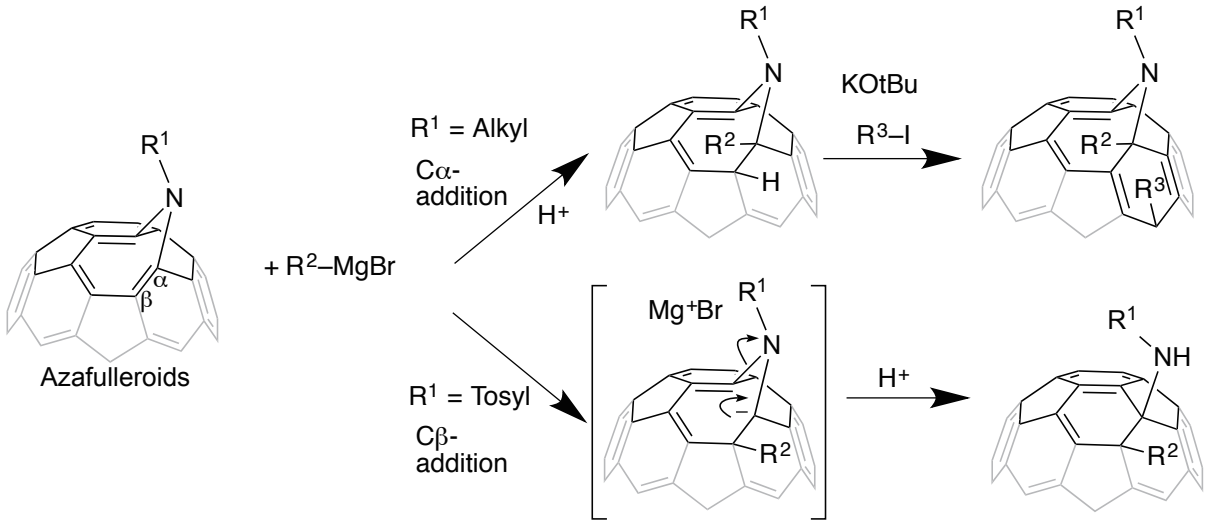

[1] N. Ikuma, Y. Doi, K. Fujioka, T. Mikie, K. Kokubo, T. Oshima, *Chem. Asian J.* **2014**, *9*, 3084–3088.
[2] N. Ikuma, K. Fujioka, Y. Misawa, K. Kokubo, T. Oshima, *Org. Biomol. Chem.* **2015**, *13*, 5038–5043.

Corresponding Author: N. Ikuma
Tel: +81-6-6879-4592, Fax: +81-6-6879-4593,
E-mail: ikuma@chem.eng.osaka-u.ac.jp

Solid properties in hydroxylated carbon materials studied by ^{1}H NMR

○Yoshiaki Sano[1] and Hironori Ogata [1, 2]
[1]*Graduate School of Engineering, Hosei University, Koganei, Tokyo 184-8584, Japan*
[2]*Research Center for Micro-Nano Technology, Hosei University, Koganei, Tokyo, 184-0003, Japan*

Polyhydroxylated Fullerenes (fullerenol: $C_{60}(OH)_x$) have been thought to have potential applications in proton conductive materials. It has been reported that $C_{60}(OH)_{12}$ solids by Oleum method[1] have proton conductivity in a dry atmosphere. On the other hands, $C_{60}(OH)_{24}$ solids by NaOH/TBAH method[2] did not show ionic conductivity at all [3]. On the other hands, it has not reported on the proton conductivity in hydroxylated carbon nanotubes(CNT-OH). Detailed proton conduction mechanism of hydroxylated carbon solids has not been fully elucidated.

We previously reported the synthesis and characterization of hydroxylated single-walled carbon nanotubes (SWNT-OH)[4]. In this study, we systematically investigated the proton dynamics in fullerenol ($C_{60}(OH)_{12}$ and $C_{60}(OH)_{44}$) and SWNT-OH by using wide-line ^{1}H-NMR spectroscopy.

Figure 1 shows the temperature dependence of the spin-lattice relaxation time (T_1) of ^{1}H-NMR at 400 MHz for $C_{60}(OH)_{12}$, $C_{60}(OH)_{44}$ and SWNT-OH. Solid lines are fitting from high temperature regions. Detailed results on the properties of proton motions in these materials will be presented.

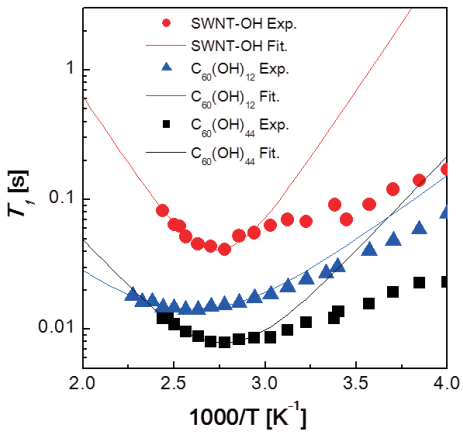

Figure 1 Temperature dependence of the spin-lattice relaxation time (T_1) of ^{1}H-NMR at 400 MHz for $C_{60}(OH)_{12}$, $C_{60}(OH)_{44}$ and SWNT-OH

References:

[1] L. Y. Chiang et al., Org. Chem. **59**, (1994) 3960
[2] J. Li et al., J. Chem. Soc. Chem. Commun. (1993)1784
[3] K. Hinokuma *et al., Chem. Phys. Lett.,* **341**, (2001) 442.
[4] Y. Sano *et al.*, Proc.of the 49th Fullerene-Nanotubes-Graphene General Symposium (3P-6)

Corresponding Author: H. Ogata
Tel: +81-42-387-6229, Fax: +81-42-387-6229, E-mail: hogata@hosei.ac.jp

Synthesis of Fullerene Derivatives Having Cyclic Structure through Cationic Intermediate for Organic Solar Cells Application

○Keisuke Ogumi [1], Hiroshi Okada [2], Takafumi Nakagawa [2], Yutaka Matsuo [2]

[1] *Tokyo Metropolitan Industrial Technology Research Institute, 2-4-10, Aomi, Koto-ku, Tokyo 135-0064, Japan*
[2] *Department of Chemistry, School of Science, The University of Tokyo, 7-3-1 Hongo, Bunkyo-ku, Tokyo 113-0033, Japan*

Introduction

Fullerene cation serves as a versatile platform for functionalization of fullerene [1]. Its utility attracts attention, however, fullerene cation is difficult to be generated because of the electronegative nature of fullerene moiety. Previous works indicated utility of fullerene cation by efficient method of dihydromethanofullerene [2] and regioselective synthesis of 1,2-di(organo)fullerene derivatives [3]. These reactions involve regioselective generation of fullerene cation followed by intramolecular annulation. This method established new synthesis method of fullerene derivatives having cyclic structure adjoins fullerene moiety.

This work

In this work, fullerene derivatives bearing cyclic structure containing oxygen were obtained from corresponding fullerene dimer precursors. Scheme 1 shows mechanism for 7-membered ring fullerene derivative **1**. First fullerene radical was generated from cleavage of fullerene dimer by heating. Then I_2 oxidized fullerene radical to give fullerene cation. The annulation reaction was completed by C–O bond cleavage and another C–O bond formation with demethylation.

Scheme 1. Proposed mechanism for fullerene-cation-mediated cyclization.

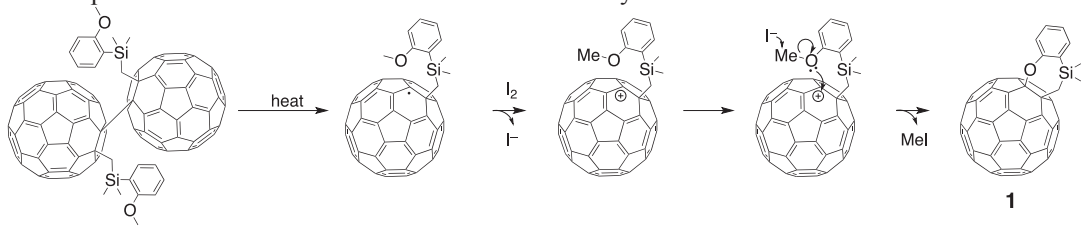

This method reaches a 7-membered ring fullerene derivative **1** which is expected as an interesting organic semiconductor material for its electrochemical property and flexibility due to conformation of the 7-membered ring. Photovoltaic devices using **1** were fabricated. The device showed higher V_{OC} value than that of a device using PCBM because of shallow LUMO level. Device performance depended on annealing temperature. In the case of 80 ºC, PCE was the best, 1.74%. This work shows first time a behavior of 7-membered ring fullerene derivatives as acceptors in organic solar cells and expands fullerene materials in organic semiconductor field.

[1] (a) Kitagawa, T.; Sakamoto, H.; Takeuchi, K. *J. Am. Chem. Soc.* **1999**, *121*, 4298–4299.
(b) Murata, Y.; Cheng, F.; Kitagawa, T.; Komatsu, K. *J. Am. Chem. Soc.* **2004**, *126*, 8874–8875.
[2] Zhang, Y.; Matsuo, Y.; Li, C.-Z.; Tanaka, H.; Nakamura, E. *J. Am. Chem. Soc.* **2011**, *133*, 8086–8089.
[3] Zhang, Y.; Matsuo, Y.; Nakamura, E. *Org. Lett.* **2011**, *13*, 6058–6061.

Corresponding Author: Y. Matsuo
Tel: 03-5841-1476, Fax: 03-5841-1476, E-mail: matsuo@chem.s.u-tokyo.ac.jp

Investigation of catalytic activity for reduction of 4-nitrophenol with [C_{60}]fullerene nanowhisker-silver nanoparticle composites

○Jeong Won Ko[1], Hwa Jeong Chae[1], Weon Bae Ko[1,2]

[1]*Department of Convergence Science, Graduate School, Sahmyook University, Seoul 139-742, South Korea,* [2] *Department of Chemistry, Sahmyook University, Seoul 139-742, South Korea*

Silver nanoparticles solution was prepared for adding silver nitrate ($AgNO_3$), trisodium citrate dihydrate ($C_6H_5Na_3O_7 \cdot 2H_2O$), sodium borohydride($NaBH_4$), cetyltrimethyl ammonium bromide ($(C_{16}H_{33})N(CH_3)_3Br$) and ascorbic acid($C_6H_8O_6$) into distilled water and then, the resulting solution was irradiated for 3 h under ultrasonic irradiation. Silver nanoparticle-[C_{60}]fullerene nanowhisker composites were prepared using C_{60}-saturated toluene, silver nanoparticles solution and isopropyl alcohol by liquid-liquid interfacial precipitation(LLIP) method. The product of silver nanoparticle-[C_{60}]fullerene nanowhisker composites was confirmed by X-ray diffraction, Raman spectroscopy, scanning electron microscopy and transmission electron microscopy. Catalytic activity of silver nanoparticle-[C_{60}]fullerene nanowhisker composites as a catalyst was characterized by the reduction of 4-nitrophenol by UV-vis spectroscopy.

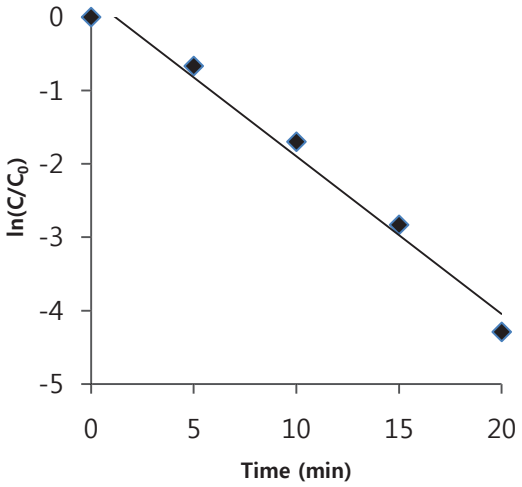

Fig.1 Kinetics study for reduction of 4-nitrophenol with the silver nanoparticle-[C_{60}]fullerene nanowhisker composites

[1] S. K. Hong, J. H. Lee, J. M. Kim and W. B. Ko, *J. Nanosci. Nanotechnol.*, **11,** 734 (2011).
[2] K. Miyazawa, *J. Nanosci. Nanotechnol.*, **9,** 41(2009).

Corresponding Author: W. B. Ko
Tel: +82-2-3399-1700, Fax:, +82-2-979-5318,
E-mail: kowb@syu.ac.kr

Chemical reduction of Metallofullerene using Various Amine

○Yuta Sato, Kosuke Tanaka, Kazuhiko Akiyama, Shiro Kubuki

Department of Chemistry, Tokyo Metropolitan University, Hachioji, 192-0397, Japan

Endohedral metallofullerene(EMF) is well known to have many characteristic properties, such as encapsulation structure, charge transfer from inside metal atom to cage, and small band gap energy. These unique characters are expected to apply metallofullerenes to a medicine, an electronic device, and so on. However, in practice, there are very much difficulties for the application of metallofullerenes such as small amount of production yield and difficulties in a separation/purification. Recently, efficient separation methods using smaller electrochemical band gap character of metallofullerenes than those of empty species were reported. Among these separation methods, the separation methods using chemical oxidation and reduction of metallofullerenes are promising from the view point of total cost [1,2]. However, the separation mechanisms of these methods, especially for the chemical reduction, have not been made clear yet. To obtain the knowledge about the chemical reduction of metallofullerenes by some electron donors, we investigated the reduction tendency of alkylamine. In this study, we report the chemical reduction of La@C_{82} in chlorobenzene (CB) by alkylamine measured by UV/vis/NIR absorption spectroscopy.

La@C_{82} was produced by general arc discharge method. Purified La@C_{82} was dissolved into CB solution with the concentration of 10^{-5} M. An alkylamine was added to this solution as the increase of volume falling within a few percent.

Figure 1 shows vis-NIR spectra of La@C_{82} in CB with (a) propylamine (PA) and (b) triethylamine (TEA). In both case, it was found that the absorption peak of La@C_{82} at 1000nm was decreased with increase of alkylamine concentration and also the absorption peak of [La@C_{82}]$^-$ at 932 nm was increased. On the other hands, the time dependent spectral change was smaller than those observed in the alkylamine concentration dependence. These results suggested that the chemical reduction by alkylamine was a kind of equilibrium reaction such as contact charge transfer.

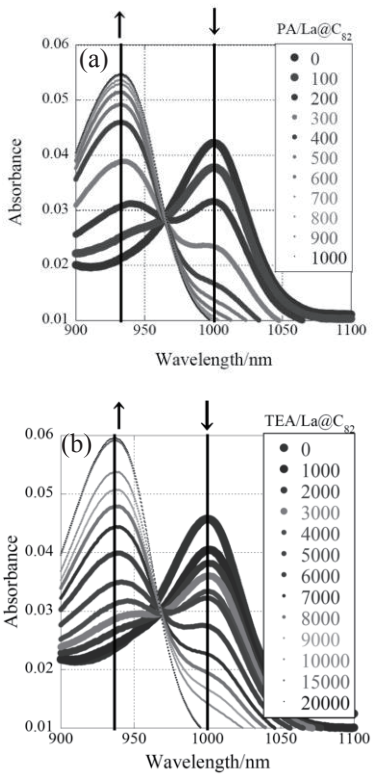

Fig 1, vis-NIR absorption of La@C_{82} (1000 nm) and [La@C_{82}]$^-$ (932 nm) in CB with (a)Propylamine, and (b)Ttietylamine/La@C_{82}.

[1] K. Akiyama, *et al.*, *J. Am. Chem. Soc.,* **2012**, 134, 9762
[2] T. Kodama, *et al.*, *Chem. Lett.* **2005**, *34*, 464

Corresponding Author: Y. Sato
Tel: +81-42-677-1111, EX, 3587,
E-mail:kakiyama@tmu.ac.jp

Isolation and characterization of $Gd_2@C_{80}$ anion whose spin state is S=15/2

○Takuji Mitani[1], Natsumi Nakatori[1], Takahisa Yamaguchi[2], Tatsuki Kobayashi[3], Ko Furukawa[4], Tatsuhisa Kato[2, 5], Koichi Kikuchi[1], Yohji Achiba[1], Takeshi Kodama[1]

[1]*Department of Chemistry, Tokyo Metropolitan University, Hachioji 192-0397, Japan*
[2]*Graduate School of Human and Environmental Studies, Kyoto University, Kyoto 606-8501, Japan*
[3]*School of Science, Kitasato University, Sagamihara 252-0373, Japan*
[4]*Department of Chemistry, Niigata University, Niigata 950-2181, Japan*
[5]*Institue for Liberal Arts and Sciences, Kyoto University, Kyoto 606-8501, Japan*

Recently, Nakatori et al. have succeeded in the isolation of $Y_2@C_{80}$[1] which has long been considered to be one of the hidden metallofullerenes notified by their characteristic properties such as "those expected to be formed but never isolated". The key points of the success were due to 1) the extraction of $Y_2@C_{80}$ as an anion form directly from the raw soot with a mixed solvent of triethylamine (TEA) and acetone, 2) the isolation of $Y_2@C_{80}$ by an ion-pair chromatography by which $Y_2@C_{80}$ is safely kept as an anion form throughout the procedures.

In order to confirm such a hidden property of $M_2@C_{80}$ more generally, we chose $Gd_2@C_{80}$ as the next target in the present work. In the anion state of $Gd_2@C_{80}$ if it exists, an excess electron (S=1/2) is expected to be located on Gd_2 dimer and thus, the clarification of the actual spin state of $(Gd_2@C_{80})^-$ is definitely of quite interesting. In 2011, Fu et al. isolated $Gd_2@C_{79}N$, which seems to have similar electronic configuration to that of $(Gd_2@C_{80})^-$, and concluded that the spin state is S=15/2 by ESR spectroscopy[2]. Here, we report for the first time the isolation and characterization of $(Gd_2@C_{80})^-$.

The isolation of $Gd_2@C_{80}$ was accomplished by almost the same method as $Y_2@C_{80}$. Soot containing Gd-metallofullerenes was produced by a direct-current arc discharge, and the raw soot was extracted with a mixed solvent of TEA and acetone. $Gd_2@C_{80}$ was isolated by two-stage HPLC using acetone with an ion-pair reagent, tetrabutyl-ammonium bromide, as an eluent.

As shown in Fig.1, the UV-vis-NIR absorption spectrum of the isolated $(Gd_2@C_{80})^-$ is very similar to those of $(Y_2@C_{80})^-$ and $(Ce_2@C_{80}(I_h))^-$, where the latter is generated electrochemically. Therefore, it is suggested that the $Gd_2@C_{80}$ also has $C_{80}(I_h)$ cage. ESR studies revealed that the spin state of $(Gd_2@C_{80})^-$ is S=15/2 as expected by $Gd_2@C_{79}N$.

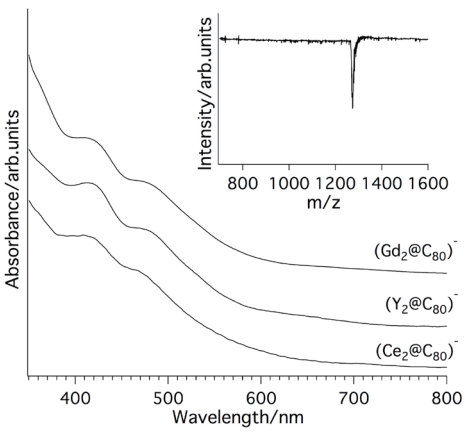

Fig.1 UV-vis-NIR absorption spectra of $(Gd_2@C_{80})^-$, $(Y_2@C_{80})^-$ and $(Ce_2@C_{80}(I_h))^-$. The inset shows the negative LD-TOF-MS spectrum for $(Gd_2@C_{80})^-$.

[1] N. Nakatori, et al. *The 49th Fullerenes-Nanotubes-Graphene General Symposium* 46 (2015).
[2] W. Fu, et al. *J. Am. Chem. Soc.* **133**, 9741-9750 (2011).
Corresponding Author: Takeshi Kodama
E-mail: kodama-takeshi@tmu.ac.jp
Tel:+81-42-677-2530, Fax:+81-42-677-2525

Reactions of Endohedral Metallofullerenes with Silacyclopropanes: Mono-silylation and Carbosilylation of $Lu_3N@I_h$-C_{80}

○Kazuya Minami[1], Masahiro Kako[*,1], Kumiko Sato[2], Naomi Mizorogi[2], Shigeru Nagase[3], Takeshi Akasaka[2,4,5]

[1]*Department of Engineering Science, The University of Electro-Communications, Chofu, Tokyo 182-8585, Japan*
[2]*Life Science Center of Tsukuba Advanced Research Alliance, University of Tsukuba, Tsukuba, Ibaraki 305-8577, Japan*
[3]*Fukui Institute for Fundamental Chemistry, Kyoto University, Kyoto 606-8103, Japan*
[4] *Department of Chemistry, Tokyo Gakugei University, Tokyo 184-8501, Japan*
[5] *Foundation for Advancement of International Science, Ibaraki 305-0821, Japan*

Much attention has been devoted to endohedral metallofullerenes (EMFs) owing to their unique structures and properties. The exohedral derivatization of EMFs has been developed as an effective method to functionalize EMFs for use in applications such as molecular electronics, nanomaterials sciences, and biochemistry [1]. Recent studies have indicated the high efficiency of organic photovoltaic devices based on $Lu_3N@I_h$-C_{80}, which is a result of the relatively higher lowest unoccupied molecular orbital energy of $Lu_3N@I_h$-C_{80} compared with that of C_{60} [2]. Moreover, we reported that the addition of silylene to $Lu_3N@I_h$-C_{80} afforded monosilylated adducts that exhibited remarkable redox properties as potential acceptor materials for organic photovoltaic devices [3]. This result prompted us to gain more insight into the effects of monosilylation and carbosilylation on the properties of $Lu_3N@I_h$-C_{80}.

In this study, we report the reactions of $Lu_3N@I_h$-C_{80} with silacyclopropanes **1a**, **1b**, and **2** as silylating reagents. Upon the heating of $Lu_3N@I_h$-C_{80} with **1a** (or **1b**) in *o*-dichlorobenzene at 150°C in a sealed Pyrex tube, adducts **3a** and **3b** were obtained by the addition of silylenes Dmt_2Si and Mes_2Si, respectively. The structures of **3a** and **3b** were determined to be silylene adducts at the [6,6] ring junction of $Lu_3N@I_h$-C_{80} based on the nuclear magnetic resonance (NMR) and visible–near-infrared (vis–NIR) spectra. In contrast, photoirradiation of $Lu_3N@I_h$-C_{80} with **2** in toluene afforded three adducts **4a**–**4c** as carbosilylated $Lu_3N@I_h$-C_{80}. Both **4a** and **4b** are structurally assigned to [5,6]-adducts of $Lu_3N@I_h$-C_{80}, while **4c** is considered to be the corresponding [6,6]-isomer from spectral data.

Scheme 1.

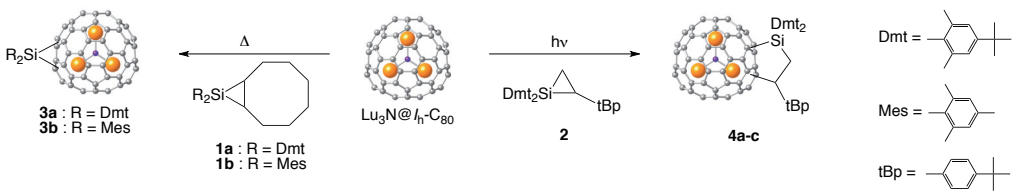

[1] M. Yamada, T. Akasaka Bull. Chem. Soc. Jpn. **87**, 1289–1314 (2014). [2] (a) R. B. Ross *et al.* Nat. Mater. **8**, 208–212 (2009). (b) R. B. Ross, *et al.* Adv. Funct. Mater. **19**, 2332–2337 (2009). [3] K. Sato *et al.* J. Am. Chem. Soc. **134**, 16033–16039 (2012).

Corresponding Author: Masahiro Kako Tel: +81-42-442-5570 E-mail: kako@e-one.uec.ac.jp

Electrostatic interaction of fullerenes under an external electric field

○Jun-ya Sorimachi, Susumu Okada

Graduate school of Pure and Applied Sciences, University of Tsukuba, Tsukuba 305-8571, Japan

It is known that fullerenes and their derivatives are the constituent materials for photovoltaic devices and electronic devices. For such applications, the external electric field is essential to inject carrier and control the functions of the devices. For the fundamental aspect, in addition, it is known that electric structures of fullerenes and their derivatives depend on an external electric field. Therefore, it is important to clarify the physical properties of fullerenes under an external electric field. In this work, we investigate the energetics of fullerenes up to C_{78}, all of which satisfy the isolated pentagon rule (IPR), under the constant electric field between two parallel planar electrodes using density functional theory (DFT) with the effective screening medium (ESM) method (Fig. 1).

Figure 2 shows the total energy of C_{60} and C_{74} as a function of the electric field. In the case of C_{60}, the energy is proportional to the square of the electric field, and do not depend on molecular direction with respect to the field. Thus, the electron system of C_{60} fullerene can be regarded as the spherical electron system, since the total energy of dielectric spherical shell is proportional to the square of the parallel external electric field. In contrast, the total energy of C_{74} is substantially stabilized under the non-zero electric field. By further investigation, we find that C_{74} cage has polarization with respect to the molecular direction. We further investigate the total energy of fullerenes up to C_{78} with various molecular orientations under the electric field.

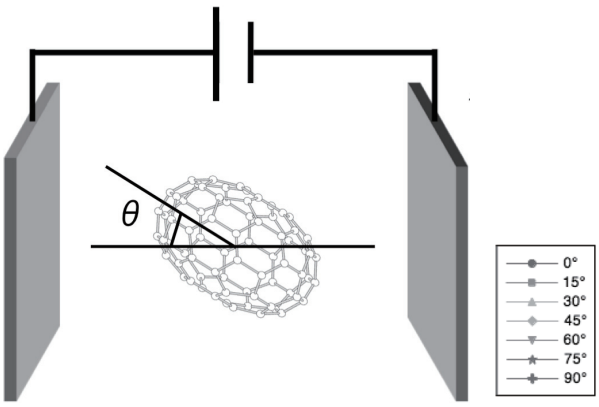

Fig. 1; A structural model of fullerenes under the electric field. Gray slabs represent the parallel electrodes simulated by ESM.

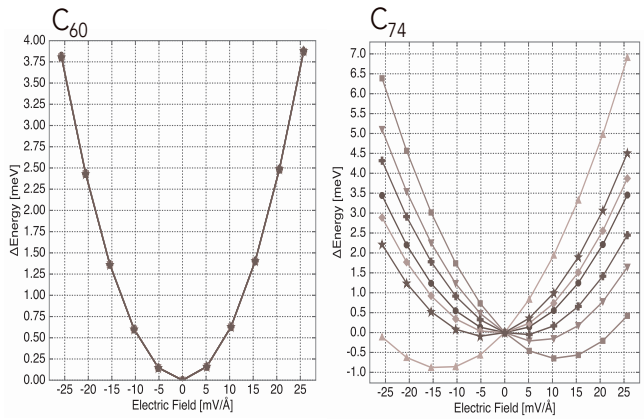

Fig. 2; Total energy of C_{60} and C_{74} as a function of the electric field.

Corresponding Author: J. Sorimachi
Tel: +81-29-853-5600(ext.; 8233)
E-mail: jsorimachi@comas.frsc.tsukuba.ac.jp

2P-9

Solid-State NMR Studies on the Aggregated Structures of Organic Bulk Heterojunction Solar Cells with Solvent Additives (III)

°Saki Kawano[1] and Hironori ogata[1,2]

[1] Grad. School of Sci. and Engin. , Hosei Univ. , [2]Res.Center for Micro-Nano Technol., Hosei Univ.

E-mail: hogata@hosei.ac.jp

Bulk heterojunction (BHJ) organic solar cells are an emerging technology that has the potential to provide a low cost photovoltaic devices. It is well known that the nanomorphology of the polymer:fullerene BHJ is a critical factor which affects the solar cell performance. The addition of processing additives such as 1,8-diiodooctane (DIO) is widely used approach to increase power conversion efficiencies for many organic solar cells[1-2]. Solid-state solar NMR spectroscopy offers several techniques for the investigation of the morphological, structural, and dynamics properties of BHJ organic solar cells.

We have explored the effects of DIO addition of P3HT/PCBM BHJ films on the local crystallinity and morphology by using solid-state NMR spectroscopy. In this study, we investigated the change in the crystallinity, morphology, and the properties of molecular motions of P3HT/PCBM BHJ film by adding another solvent additives(1,8-Octanedithiol(ODT) and 1-Chloronaphthalene(CN)) and also investigated the mixing effect of two additives by using ^{13}C and ^{1}H solid-state NMR spectroscopy.

Mixed solution of P3HT/PCBM of 1:1(w/w) was prepared by mixing P3HT and PCBM into chlorobenzene at a concentration of 1 wt% for 50 hrs in a glove box under argon atmosphere. A 3% by volume of additive DIO, ODT or CN was then dropped into the solution and then stirred for 1 hr. The solution was filtered using 0.45μm filter before making films to remove undissolved materials. P3HT/PCBM BHJ films were prepared by dropping the solution in a glass plate and dried in a glove box under argon atmosphere for 40 hrs and then put in the vacuum for 24hrs. Dried film were removed from the glass plate and sealed into 4 mm zirconia NMR rotor. Solid-state NMR spectra were collected on Bruker AVANCE300 spectrometer.

Figure 1 shows the ^{13}C-CP/MAS NMR spectra of (a)P3HT/PCBM BHJ film with DIO+CN additive, (b) with CN additive and (c)P3HT/PCBM BHJ. The detailed results of the change of morphology and the properties of molecular conformations of P3HT/PCBM BHJ films by CN or ODT addition will be presented.

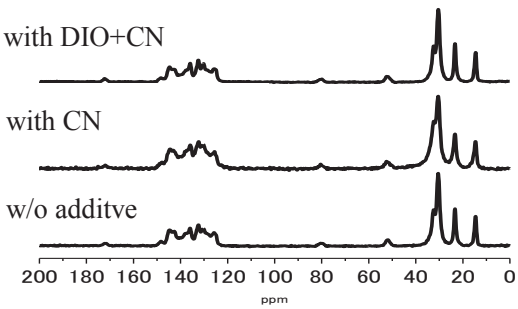

Fig.1 ^{13}C-CP/MAS NMR spectra of (a)P3HT/PCBM BHJ film with DIO+CN additive, (b)with CN (c)w/o additive

References:

1) J. K. Lee et al., *J.Am.Chem.Soc.*,**130**(2008)3619.

2) B.R.Aïch *et al, Organic Electronics*,**13** (2012)1736.

2P-10

Concentration Dependence of Photoluminescence of (*n*,*m*) Single-Wall Carbon Nanotubes

○Xiaojun Wei, Takuya Hirakawa, Yohei Yomogida, Atsushi Hirano, Shunjiro Fujii, Takeshi Tanaka and Hiromichi Kataura

Nanomaterials Research Institute, National Institute of Advanced Industrial Science and Technology (AIST), Tsukuba, Ibaraki 305-8565, Japan

Semiconducting single-wall carbon nanotubes (SWCNTs) show bright photoluminescence (PL) which can be used for estimation of a pair of optical transitions, E_{11} and E_{22}. In PL measurement, the emission intensity is also important to know the abundance of specific species in a mixture or chirality-sorted sample. For the reliable estimation, however, chirality dependent quantum efficiency and self-absorption effect should be considered [1]. In order to reveal the PL characteristics of SWCNTs, we investigated the SWCNT concentration dependence of PL intensity in a fixed surfactant concentration.

In this study, roughly chirality selected semiconducting SWCNTs suspended in 1% sodium cholate (SC) solution were prepared by gel chromatography. To change the SWCNT concentration, the sample was diluted by adding 1% SC solution. We confirmed that the absorbance increased linearly with increasing SWCNT concentration for all chiralities, while the emission intensity exhibited a nonlinear change. Figure 1 shows the results of the emission intensity and emission wavelength shift for (6,5) and (7,5) as a function of each absorbance. In the low absorbance (SWCNT concentration) region, the emission intensity increased with increasing the absorbance, and the emission wavelength did not change for both chiralities. In the high absorbance region, however, the emission intensity decreased after showing a maximum and the E_{11} emission wavelength red-shifted gradually. This intensity change can be explained by a self-absorption effect. The emission wavelength shift is probably due to a change of local electric field. Importantly, these concentration effects don't depend on the total SWCNT concentration but each chirality concentration. Since the concentrations of (6,5) and (7,5) are different in a solution, each experimental PL efficiency is different. As a result, PL intensity cannot be used for purity estimation. We will show results of more species of SWCNTs to discuss chirality dependence of the local environmental effects.

This work was supported by KAKENHI No. 25220602.

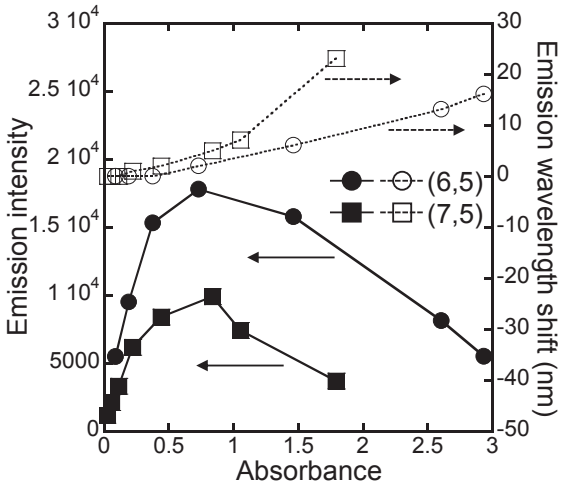

Figure 1. The plots of the emission intensity (solid line) and emission wavelength shift (dashed line) as a function of each absorbance for (6,5) and (7,5) SWCNTs.

[1] D. A. Tsyboulski *et al*., *Nano Lett.* **7,** 3080–3085 (2007).

Corresponding Author: H. Kataura
Tel: +81-29-861-2551, Fax: +81-29-861-2786, E-mail: h-kataura@aist.go.jp

Chirality-Selective Metal Enhanced Fluorescence of DNA-Dispersed Single-Walled Carbon Nanotubes

○Min Lyu, Qinghua Zhao, Juan Yang, Yan Li

College of Chemistry and Molecular Engineering, Peking University, Beijing 100871, China

The near-infrared fluorescence of single-walled carbon nanotubes (SWNTs) possesses a great prospect in biological imaging [1], but its low quantum yield hinders its further applications. Single-strand DNA (ssDNA) was reported to be able to well disperse SWNTs in aqueous solution [2]. In addition, certain DNA sequence motifs can be used for structure-specific recognition and seperation of carbon nanotubes [3]. We find that ssDNA might serve as a superior molecular spacer between gold nanoparticles (AuNPs) and SWNTs to achieve a good metal-enhanced fluorescence (MEF) effect of the SWNTs.

In this work, we prepare ssDNA-SWNTs-AuNPs hybrids to achieve the chirality-selective metal-enhanced fluorescence of carbon nanotubes. In addition to the overal fluorescence enhancement of about 10-fold, a higher enhancement for (7,5) than for other chiralities is observed when we use the reported (7,5) recognition DNA $(ATT)_4AT$. This method may lead to further in-situ study of metal enhanced fluorescence of SWNTs on substrate.

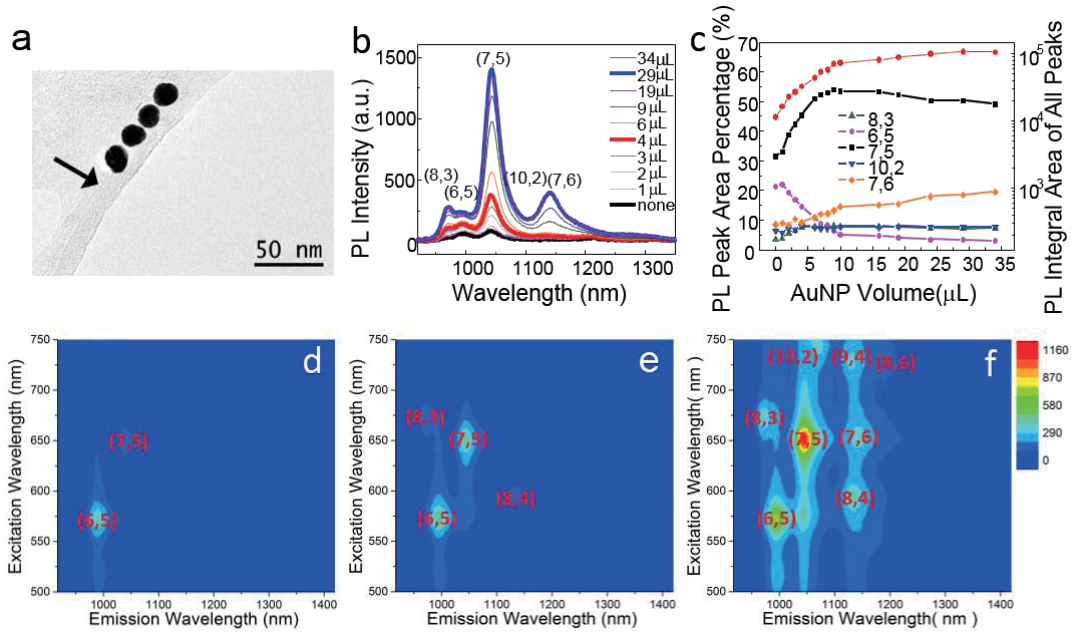

Figure 1. (a) TEM images of the AuNP-$(ATT)_4AT$-SWNT nano hybrids. (b)PL emission spectra at excitation of 650 nm of the hybrid with addition of AuNPs from 0 to 34 μL. (c) PL integral area of all peaks (red dots) and the PL peak area percentage of (8,3), (6,5), (7,5), (10,2), and (7,6) in (a). PLE maps of the original $(ATT)_4AT$-SWNT solution (d) and with addition of 4 μL (e) and 29 μL AuNPs (f). The PL intensities for (d)-(f) are in the same color scale.

[1] M. Zheng *et al*. Nat. Mater. **2**, 338 (2003).
[2] Dai *et al*. Nat. Photon. **8**, 723 (2014).
[3] M. Zheng *et al*. Nature, **460**, 250 (2009)

Corresponding Author: Juan Yang
Tel:+86-10-62755357, Fax: +86-10-62755357,
E-mail: yang_juan@pku.edu.cn

Substituent effects on defunctionalization of alkylated single-walled carbon nanotubes

○Yuya Takehana, Mitsuaki Suzuki, Michio Yamada, Yutaka Maeda

Department of Chemistry, Tokyo Gakugei University, Tokyo 184-8501, Japan

Much attention has been attracted to the introduction of functional groups onto the single-walled carbon nanotubes (SWNTs) because it affects not only their dispersibility but also their optical and electronic properties. However, SWNTs lose their intrinsic properties by excessive functionalization because of disconnection of the π-conjugated system. Thus, control of degree of functionalization of SWNTs is important. Recently, we studied the substituent effects on two-step reductive alkylation of SWNTs and revealed that the degree of functionalization can be well controlled by the bulkiness of alkyl groups of RLi and RBr [1]. In addition, thermal treatment of alkylated SWNTs is effective to remove the substituent partially [2]. Weisman et al reported the diameter selective thermal defunctionalization of hexylated SWNTs [3]. Herein, we report substituent effects on thermal defunctionalization of alkylated SWNTs.

Dialkylated SWNTs (^{n}Bu-SWNTs-R) were prepared according to the previously reported method using HiPco SWNT, ^{n}BuLi, and RBr (R = ^{n}Bu, ^{sec}Bu, ^{t}Bu). Order of degree of functionalization for ^{n}Bu-SWNTs-Bu (^{n}Bu-SWNTs-^{t}Bu > ^{n}Bu-SWNTs-^{n}Bu > ^{n}Bu-SWNTs-^{sec}Bu) was estimated by Raman spectroscopy and thermogravimetric analysis. After thermal treatment under a nitrogen flow, characteristic absorption and Raman peaks assigned to large diameter SWNTs were recovered predominantly. Spectral changes of ^{n}Bu-SWNTs-Bu before and after the thermal treatment indicate that defunctionalization takes place following order: ^{n}Bu-SWNTs-^{t}Bu < ^{n}Bu-SWNTs-^{n}Bu < ^{n}Bu-SWNTs-^{sec}Bu.

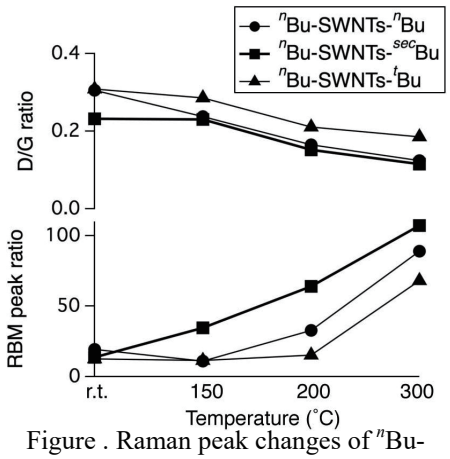

Figure . Raman peak changes of ^{n}Bu-SWNTs-Bu after the thermal treatment.

[1] Y. Maeda *et al*. J. Am. Chem. Soc. **134**, 18101 (2012).
[2] Y. Maeda *et al*. Chem. Commun. **51**, 13462 (2015).
[3] S. Ghosh *et al*. ACS Nano **9**, 6324 (2015).

Corresponding Author: Y. Maeda
Tel: +81-42-329-7512, Fax: +81-42-329-7512
E-mail: ymaeda@u-gakugei.ac.jp

Electronic structure of CNTs under an external electric field

○U Ishiyama and Susumu Okada

Graduate School of Pure and Applied Sciences, University of Tsukuba, Tennodai, Tsukuba 305-8577, Japan

Carbon nanotubes (CNTs) are attracting much attention because of it unique geometric and electronic structures those allow them being an emerging material for semiconductor electronic devices in the next generation. It has been shown experimentally that CNTs work as a conducting channel of field-effect transistors (FETs). In the FET devices, CNTs form hybrid structures with foreign materials, other CNTs, and defects, which seriously affect the physical properties of the FET device. However, it is still unclear whether the defects and CNT intersections affect the fundamental properties of CNTs under an electric field. In this work, we aim to elucidate the electronic properties of various CNT hybrids under the external electric field. To explore the electronic structures of CNT hybrids under the external electric field, we used the density functional theory combined with the effective screening medium method and the local density approximation. An ultrasoft pseudopotential is adopted to describe the interaction between valence electrons and ions. Here, we consider (10,0), (11,0), and (12,0) CNTs with monovacancies, divacancies, C_2 adatoms, and Stone-Wales defects as for the individual CNT with defects. In addition to the single CNT, we also consider the thin films of CNTs consisting of (11,0), (13,0), and (14,0) CNTs forming CNT bilayer structure with respect to the electrode.

Our calculations show that the local electrostatic potential of CNTs substantially affects the carrier accumulations by the external electric field. In the CNTs with defects, we find that the gate voltage for accumulating electrons and holes strongly depends on the defect species and their relative positions in the CNTs with respect to the electrode (Fig.1). The gate voltage variation is ascribed to the internal electric field in the CNTs induced by the inhomogeneous electron density around the defects. In addition to the inhomogeneity of the charge density, the work function of each CNT forming thin films affects the carrier accumulation in CNT thin films by the electric field. Gate voltages to inject carriers depend on CNT arrangement with respect to the electrode. Further analysis unraveled that the unusual electric field is induced between CNTs under the low electron concentration

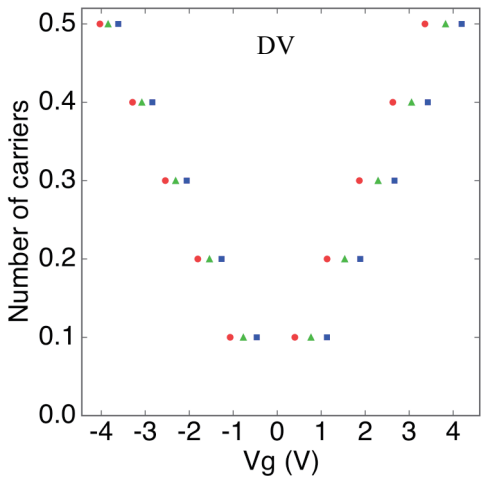

Fig. 1: Gate voltages that induce carrier accumulations of 0.1-0.5 electrons and hole in the (11,0) CNT with divacancy (DV). The circles, triangles, and squares denote defect arrangements of θ = 0˚, 90˚, and 180˚, respectively.

Corresponding Author: U Ishiyama
Tel: +81-29-853-5600 (ext. 8233), Fax: +81-29-853-5924,
E-mail: yishiyama@comas.frsc.tsukuba.ac.jp

Chemical Bond Formation between Multi-walled Carbon Nanotube and Polystyrene Side Chain through Photo-induced Radical Formation

○Takuma Baba[1], Tomoya Takada [2]

[1] *Graduate School of Photonics Science, Chitose Institute of Science and Technology, Chitose 066-8655, Japan*
[2]*Department of Applied Chemistry and Bioscience, Chitose Institute of Science and Technology, Chitose 066-8655, Japan*

Modification of polymers with carbon nanotubes (CNTs) is important for fabrication of functional materials containing CNTs. In this work, we prepared polystyrene having chloromethyl groups on its side chains and attempted to achieve chemical bond formation of the side chains with multi-walled carbon nanotubes (MWCNTs) by UV light irradiation.

The polymer was synthesized by radical polymerization of p-(chloromethyl)styrene (p-CMSt). The polymer and MWCNTs were mixed in 1-methyl-2-pyrrolidone and irradiated with UV light (250-385nm) from a xenon light source at room temperature for 24 hours. Polymer films were made by solution casting, and X-ray photoelectron spectra (XPS) and Raman spectra of them were recorded. The XPS were recorded using the equipment installed in the Laboratory of XPS analysis, Hokkaido University. Similar UV irradiation and characterization using MWCNTs treated with hydroxylammonium chloride to enhance their dispersion in solvent were also carried out in the same manner. To observe the temperature change of the samples induced with infrared light (IR), the samples were irradiated with IR from a xenon light source for 5 min. Their temperature changes during and after the irradiation were observed by using a thermal imaging camera.

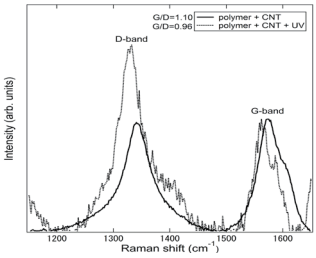

Fig.1 Raman spectra of polymer-MWCNT films.

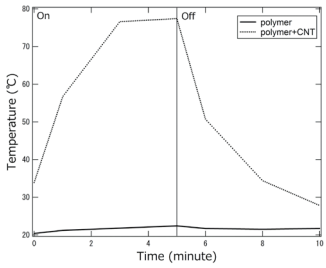

Fig.2 Temperature change induced by IR irradiation.

From the result of elemental analysis based on XPS, it was found that the content of Cl in the samples decreased after the UV irradiation. Also, on the basis of the Raman spectra (Fig. 1), surface deformation of MWCNTs was observed after the UV irradiation. The similar spectral features were also observed also in the case of MWCNTs treated with hydroxylammonium chloride. These results support the radical formation from polymer side chains and the chemical bond formation between the radicals and MWCNTs. While polymer film fabricated without MWCNTs did not show obvious temperature change during IR irradiation, temperature of the film containing MWCNTs rose with IR irradiation (Fig. 2). This result indicates that the polymer-MWCNT films fabricated in the present way can be used as photothermal conversion materials.

This work was supported by Nanotechnology Platform Program of the MEXT, Japan, and JSPS KAKENHI.

Corresponding Author: T. Takada
Tel: +81-123-27-6056, Fax: +81-123-27-6056, E-mail: t-takada@photon.chitose.ac.jp

Highly Packed CNT-Cu composite by the Spark Plasma Sintering

○Shinichiro Chiku, Masanobu Nomura, Hiroshi Nishikawa and Takashi Hasegawa

Murata Manufacturing Co., Ltd., Nagaokakyo 617-8555, Japan

Carbon nanotube (CNT)-copper composite is reported to exhibit notable properties such as high current density and low temperature coefficient of the resistivity[1]. But, as they tried, it is difficult to combine hydrophobic CNTs with metallic copper in liquid phase. We examined the fabrication process through the synthesis of CNT-Cu powder in solvents and the sintering the powder under the high temperature and the high pressure.

Multi-walled CNTs (MWCNTs) were dispersed without any dispersing agent in the solution of copper (II) acetate in *N*-methyl-2-pyrrolidone (NMP) by the supersonic treatment. Hydrazine hydrate was added to reduce Cu^{2+} ions for the growth of copper nanoparticles on the MWCNTs' surfaces. Figure 1 shows an FE-SEM micrograph of dried MWCNT-Cu powder in which we can recognize some copper second particles penetrated by separated MWCNTs.

MWCNT-Cu powder was sintered by the spark plasma sintering (SPS) method in vacuum atmosphere. Figure 2 (low magnification) and Figure 3 (high magnification) show FE-SEM micrographs of a dicer cut face of a sintered composite. In Figure 2, copper forms a continuous sintered compact and there is no distinct pore nor MWCNT large cohesion. Dark points are MWCNT small cohesions. In Figure 3, a few MWCNTs appear separately at the cross section generally homogeneous. The carbon content of the composite was analyzed to be 4wt% (equivalent to 15vol% when CNT density is 2.1g/cm^3). The packing fraction was calculated to be 99%.

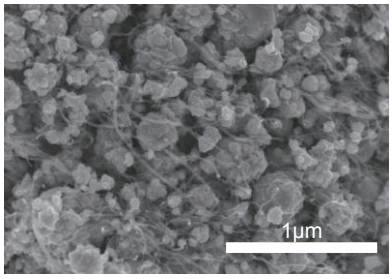

Fig.1 FE-SEM micrograph of MWCNT-Cu powder

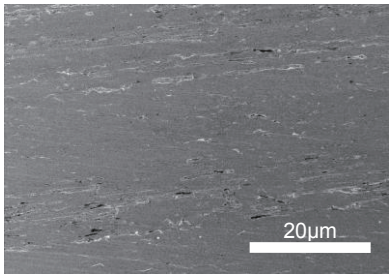

Fig.2 FE-SEM micrograph of a MWCNT-Cu compound's cross section (low magnification)

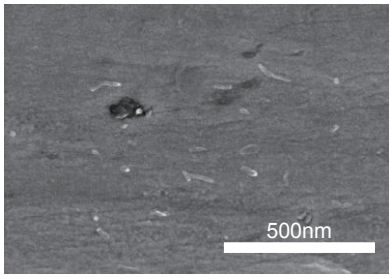

Fig.3 FE-SEM micrograph of a MWCNT-Cu compound's cross section (high magnification)

[1] C. Subramaniam *et al*. Nature Commu. **4**, article number 2202 (2013).

Corresponding Author: S. CHIKU
Tel: +81-77-586-8712, Fax: +81-77-587-6782,
E-mail: tiku@murata.com

Characterization of carbon nanotube interdigitated electrode for electrochemical biosensors

○Takuya Ushiyama[1], Nguyen Xuan Viet[1], Shigeru Kishimoto[1], and Yutaka Ohno[1,2]

[1]*Graduate School of Engineering, Nagoya University, Nagoya 464-8603, Japan*
[2]*Institute of Materials and Systems for Sustainability, Nagoya University, Nagoya 464-8603, Japan*

Carbon nanotube (CNT) is promising electrode material for electrochemical biosensors because of its wide potential window, rapid electron transfer kinetics, [1] and excellent anti-fouling properties. [2] Previously, we reported the amplified steady-state voltammetry, utilizing redox cycling process in CNT interdigitated electrode (CNT-IDE). The high amplification factor of ~14 and the anti-fouling property better than gold IDE have been shown. We also demonstrated the detection of dopamine at LOD of ~50 nM. [3] The amplification factor of the redox cycling process is mainly determined by relation of the geometry of IDE and diffusion length of analyte. In this work, we have investigated the effects of width of a microband electrode and of gap width between the electrodes on electrochemical characteristics of CNT-IDEs.

We fabricated CNT-IDEs with clean surface on a PEN substrate, using the dry transfer and micro-fabrication process as our previous work. [3] The electrochemical property of the CNT-IDEs was evaluated by measuring cyclic voltammetry of $K_4[Fe(CN)_6]$. Figure 1 shows signal current as functions of (a) gap width between generator and collector electrodes (W_g) and (b) width of a microband electrode (W_e). The signal current increased with decreasing W_g. This behavior can be explained by enhancements in concentration gradient of the analyte and collection efficiency of the redox cycle with decreasing W_g, as reported previously for the case of metal-based IDEs. [4,5] Although similar behavior is expected for W_e dependence, the signal current decreased in the present device with decreasing W_e as shown in Fig. 1(b). This is probably due to *IR* drop in CNT microband electrodes, i.e., the resistance of each CNT microband electrode increased with decreasing W_e.

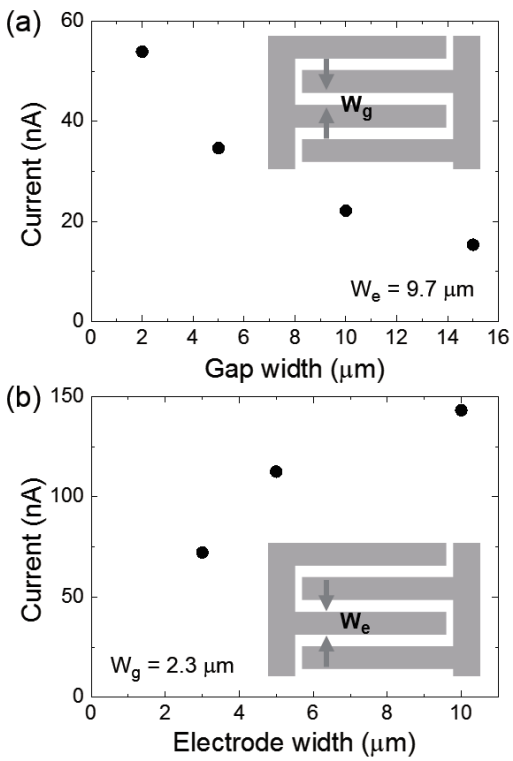

Fig. 1 Signal current versus (a) gap width and (b) electrode width.

[1] I. Dumitrescu *et al.*, Chem. Commun., **45**, 6886 (2009)
[2] W. Harreither *et al.*, Anal. Chem., **85**, 7447 (2013)
[3] T. Ushiyama *et al.*, The 49th FNTG General Symp. 1P-13 (2015)
[4] K. Aoki *et al.*, J. Electroanal. Chem., **256**, 269 (1988)
[5] N. Osamu *et al.*, Anal. Chem., **62**, 447 (1990)

Corresponding Author: Y. Ohno, Phone & Fax: +81-52-789-5387, E-mail: yohno@nagoya-u.jp

Charging-discharging phenomena of CNT electrical double layer capacitors

○Karolina Laszczyk[1], Atsuko Sekiguchi [2], Takeo Yamada [2], Kenji Hata[2]

[1] *Technology Research Association for Single Wall Carbon Nanotubes (TASC), Tsukuba 305-8565, Japan*
[2] *National Institute of Advanced Industrial Science and Technology (AIST), Tsukuba 305-8565, Japan*

The growing demand for portable (small, light-weight) power sources enabling to achieve high energy and power have caused the numerous of researchers around the world to work on principles behind the electrochemical energy storage (EES) mechanism. Its understanding would lead to low-cost and efficient EES electrodes design, e.g. for supercapacitors. However, since the discovery of the electrical double layer (EDL) mechanism, there are still a lot of questions to answer, especially as the model is suitable for anode-electrolyte-cathode system omitting other phenomena taking place in porous EES electrodes. On the other hand still new anomalous phenomena have been discovered which analytical solutions have not predicted before [1,2].

Here, we would like to present the experimental data on dependence of the cell performance upon various electrodes' designs and configurations, i.e. the aspect ratio between length and width of the cells' electrodes is changed. The cell were made of porous CNT mesh film using developed lithography-based process [3]. As result about 100 cells (ave. 25 cells per particular design) were released, measured and compared about their performance.

The measurements were done using cyclic voltammetry and potentiostatic electrochemical impedance spectroscopy (PEIS). We found the interesting trend in cells' performance expressed in capacitance retention and efficiency to discharge the energy (Fig. 1).

We believe the obtained results will contribute and support the development of electro-physical model of EDL systems, that find use not only in EES domain but in sensing, water desalination, power and energy harvesting and storage, biomedicine, fluidics, and many others.

This presentation is based on results obtained from a project commissioned by the New Energy and Industrial Technology Development Organization (NEDO).

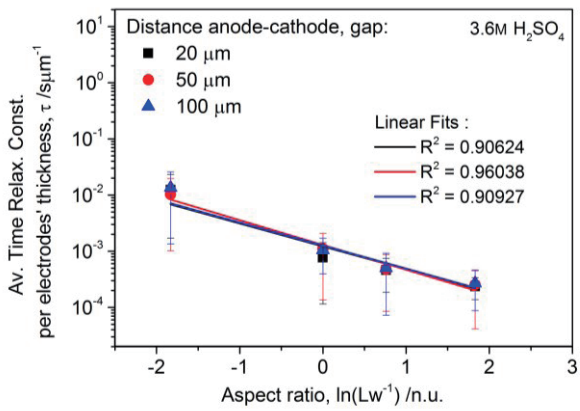

Fig.1 Time relaxation dependence on cell designs possessing the same volume of CNT electrodes, where *L* and *w* are denoted to the length and width of an electrode, respectively.

[1] J. Chmiola *et al*. Science. **313**, 5794 (2006).
[2] N. Miljkovic *et al* .Nat. Comm. **4**, 2517 (2013).
[3] K. Laszczyk *et al.*, Adv. En. Mat. **5**, 18 (2015)

Corresponding Author: A. Sekiguchi ,
Tel: +81-29-861-4611, Fax: +81-29-861-4851,
E-mail: atsuko-sekiguchi@aist.go.jp

Fabrication of Pt nanocluters on polymer warpped multi-walled carbon nanotubes and their use as fuel cell catalyst

○Yuki Hamasaki[1,2], Tsuyohiko Fujigaya[1,2,3], Naotoshi Nakashima[1,2]

[1] *Department of Applied Chemistry, Kyushu University, Fukuoka 819-0395, Japan*
[2] *WPI-I2CNER, Kyushu University, Fukuoka 819-0395, Japan*
[3] *PRESTO, JST, Saitama, 332-0012, Japan*

Platinum (Pt) shows excellent catalytic activity for both hydrogen oxidation and oxygen reduction reaction (ORR) in proton-exchange polymer electrolyte fuel cells (PEFCs). For the wide spread of PEMFCs, reduction of Pt amount is a strong social demand due to its high cost. One way to solve this issue is the reduction of particle size of Pt in the catalyst. [1-4].

In this study, we fabricate highly dispersed Pt nanoclusters on polybenzoimidazole (PBI)-wrapped multi-walled carbon nanotubes (MWNTs) with low damage (Fig. 1). The PBI and MWNTs work as an anchoring polymer for Pt-coordination and catalyst support, respectively [3,4].

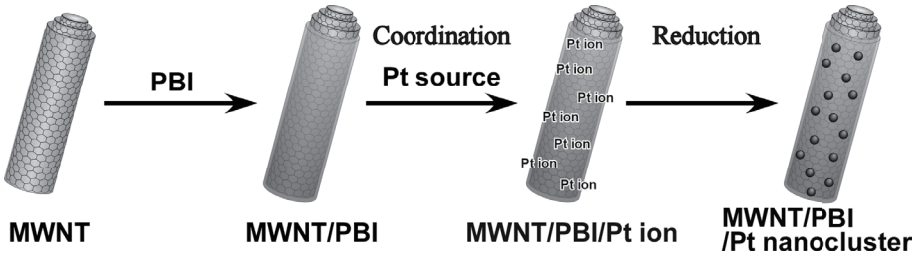

Fig. 1 Schematic illustration of the preparation of the MWNT/PBI/Pt nanocluster

MWNT/PBI composites were prepared according to a previous paper, then dispersed them in water by sonication, to which a Pt precursor solution was added. After stirring, the composite solution was washed with water to remove any excess Pt precursor. Then, the solid product was collected by filtration, which was dried under vacuum. The obtained material was characterized by transmission electron microscope (TEM), thermogravimetric analyses (TGA) and X-ray photoelectron spectroscopy (XPS). We examined the ORR activity of the catalyst in oxygen saturated 0.1 M $HClO_4$, and the result will be reported at the meeting.

[1] J. Chen *et al*. Energy Environ. Sci. **3**, 1286 (2010).
[2] I. N. Leontyev *et al*. J. Phys. Chem. C **115**, 5429 (2011).
[3] N. Nakashima *et al*. Small **5**, 735 (2009).
[4] N. Nakashima *et al*. Sci. Rep. **4**, 6295 (2014).

Corresponding Author: N. Nakashima
Tel & Fax: +81-92-802-2840
E-mail: nakashima-tcm@mail.cstm.kyushu-u.ac.jp

2P-19

Film-making of single-wall carbon nanotubes by using limonene in two immiscible aqueous solution phases

○Ryo Ishida[1], Marin Ohtsuka[1], Naoki Kanazawa[1], Hiroshi Nagasawa[2], Akira Ono[3], Shinzo Suzuki[1],

[1]*Department of Physics, Kyoto Sangyo University, Kyoto 603-8555, Japan*
[2]*Kankyo Resilience Co. Ltd., Yokohama 240-8501, Japan*
[3]*Department of Engineering, Kanagawa University, Yokohama 221-8686, Japan*

In the previous symposium, we reported about the application of Raman spectroscopy for evaluating the ratio of metal/semiconductive single-wall carbon nanotubes in two immiscible solution phases by changing excitation photon energy (532 nm and 633 nm) [1, 2]. This separation technique by using two immiscible solution phases (e.g., in polyethylene glycol (PEG) and dextran (DX) solution) has been first reported by C.Y. Khripin et al. in 2013 [3], where metal/semiconductive SWNTs of large diameter (> 1.2 nm) were shown to be successfully separated. This technique has been extensively applied for those dispersed in DNA solution as well, by using slightly modified combination of two immiscible aqueous solution phases [4, 5].

In this symposium, we reported about the application of Raman spectroscopy in order to show how metal/semiconductive single-wall carbon nanotubes are separated in these immisible solution phases. Additionally, in certain experimental condition, where limonene is further added to two immiscible solution phases, film of carbon nanotubes could be clealy seen in the solution. Further experimental findings are presented and discussed.

References:

[1] N. Kanazawa et al., *Proc. of the 46th Fullerene-Nanotube-Graphene General Symposium.* 1P-27(2014).
[2] R. Ishida, et al., *Proc. of the 49th Fullerene-Nanotube-Graphene General Symposium.* 1P-16(2015).
[3] C.Y. Khripin et al., *J. Am. Chem. Soc.*, **135**, 6822-6825(2013).
[4] G. Ao et al., *J. Am. Chem. Soc.*, **136**, 10383-10392(2014).
[5] H. Gui et al., *Nano Lett.*, **15**, 1642-1645(2015).

Corresponding Author: Shinzo Suzuki
Tel: +81-75-705-1631, Fax: +81-75-705-1820,
E-mail: suzukish@cc.kyoto-su.ac.jp

Creation of "floating supported catalyst" from metalorganic vapors and gas-phase synthesis of carbon nanotubes

○Yusuke Sugino[1], Kei Hasegawa[1], Toshio Osawa[1], Takayuki Tsukada[2], Suguru Noda[1,*]

[1] *Department of Applied Chemistry, Waseda University, Tokyo 169-8555, Japan*
[2] *Hodogaya Chemical, Tokyo 104-0028, Japan*

Carbon nanotubes (CNTs) have attracted much interest but further progress is needed for large-scale, low-cost production of high quality CNTs to realize their applications. Chemical vapor deposition (CVD) is most commonly used for their production because of its scalability and high productivity. CNTs are grown from catalyst nanoparticles either floating in gas [1] or supported on substrates/powders [2]. Floating catalyst CVD effectively use three-dimensional reaction space and realized mass-production of carbon fibers and multi-wall CNTs with large diameters (~100 nm) at ~100 ton/y. It also yields high-quality single-wall CNTs (<10 nm), however, at much smaller production scale due to the small mass of such CNT and the rapid aggregation of small floating catalysts. Small catalyst particles can be supported densely on flat substrates, however, reaction space is limited to the two dimensional substrate surface.

In this work, we propose "floating supported catalyst" in which each sub-micrometer-sized oxide particle supports hundreds of catalyst nanoparticles and grows hundreds of CNTs (Fig. 1). Ferrocene and aluminum isopropoxide were used as precursors for catalyst (Fe) and support (Al_2O_3), respectively, and fed as vapors with 4 vol% H_2/Ar flow at 300 sccm into a reactor (40 mm in inner diameter and 600 mm in heating zone length) at 800 °C. Floating supported catalyst (Fe/Al_2O_3) were successfully produced and many CNTs grew from each particle using carbon in metalorganics (Fig. 2).

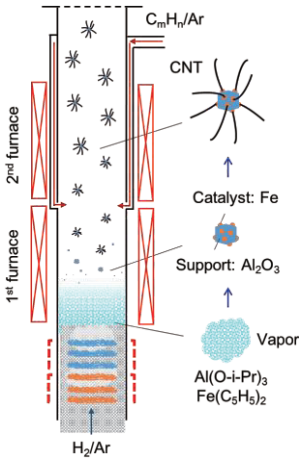

Fig. 1 Schematic of the CVD reactor.

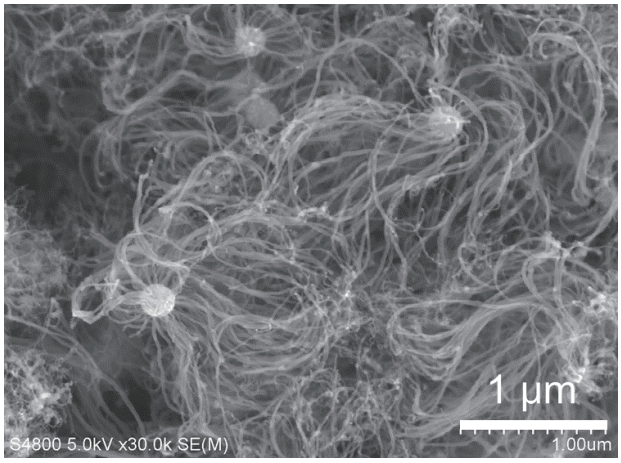

Fig. 2 Typical SEM image of the product.

[1] T. Saito, *et al*., *J. Nanosci. Nanotechno.* **8**, 6153 (2008)

[2] K. Hata, *et al.,* Science **306**, 1362 (2004).

Corresponding Author: S. Noda, Tel&Fax: +81-3-5286-2769, E-mail: noda@waseda.jp

Growth of Horizontally Aligned Chirality-Specific Single-Walled Carbon Nanotubes

○Feng Yang, Yan Li

Beijing National Laboratory for Molecular Science, College of Chemistry and Molecular Engineering, Peking University, Beijing 100871, China

High-performance and integrated circuits essentially require SWNT samples with well-aligned arrays of pure chirality [1]. Recently, employing tungsten-based intermetallic catalyst with high melting points and consequently are able to maintain their specific crystal structure during the chemical vapor deposition (CVD) process, which regulates the chirality of the grown SWNTs [2,3]. We have developed herein an approach for the growth of horizontally aligned chirality-specific SWNTs using uniform W_6Co_7 nanoparticles as catalysts on the sapphire surface.

Using the uniform W_6Co_7 nanoparticles as structural templated catalysts, we are able to grow the high abundance of the (13,6) SWNT arrays on the sapphire surface at the optimized growth condition. Our findings open up the possibility of the wafer-scale growth of aligned chirality-specific SWNTs by using uniform intermetallic nanoparticles as catalysts for practical nanoelectronics applications.

[1] A. D. Franklin. Nature **498**, 443 (2013).
[2] F. Yang, Y. Li *et al*. Nature. **510**, 522 (2014).
[3] F. Yang, Y. Li *et al*. J. Am. Chem. Soc. **137**, 8688 (2015).
Corresponding Author: Yan Li
Tel: +86-10-6275-6773, Fax: +86-10-6275-6773,
E-mail: yanli@pku.edu.cn

2P-22

Diameter-controlled ACCVD growth of SWNTs using water vapor

○Hiroki Takezaki [1], Shinnosuke Ohyama [1], Taiki Inoue [1], Rong Xiang [1], Shohei Chiashi [1] and Shigeo Maruyama [2]

[1] *Department of Mechanical Engineering, The University of Tokyo, Tokyo 113-8656, Japan*
[2] *Energy NanoEngineering Lab. National Institute of Advanced Industrial Science and Technology (AIST), Ibaraki. 305-8564, Japan*

The method of chirality-controlled synthesis of single-walled carbon nanotubes (SWNTs) is required to realize the application of SWNTs. It is important to understand the influence of water in synthesis of SWNTs such as preferential etching of metallic SWNTs using water vapor [1] and water-assisted CVD [2]. Here, we studied effects of water vapor both during the catalyst reduction stage and the growth stage to obtain the knowledge for chirality-controlled growth of SWNTs.

Co/Mo catalyst was reduced by Ar/H_2 gas, and then ethanol vapor was introduced as a carbon source to grow SWNTs at 650 – 800 °C, while water vapor (30 – 1500 Pa) was added in the reduction stage and/or the growth stage. SWNTs were characterized by scanning electron microscope (SEM) and Raman scattering spectroscopy with four different excitation lasers. Figure 1 shows RBM peaks of SWNTs grown with or without water vapor before and during growth. By introducing water vapor before CVD growth, smaller diameter SWNTs were grown. The diameter of SWNTs was further reduced by reducing the temperature of SWNTs growth. At the same time, we found that the ratio of near-zigzag SWNTs was drastically decreased as indicated by arrows in Fig. 1.

[1] P. Li, et al., *J. Mater. Chem.*, **21** (2011) 11815.
[2] K. Hata, et al., *Science*, **306** (2004) 1362.

Corresponding Author:Shigeo Maruyama
E-mail: maruyama@photon.t.u-tokyo.ac.jp
TEL: +81-3-5841-6421

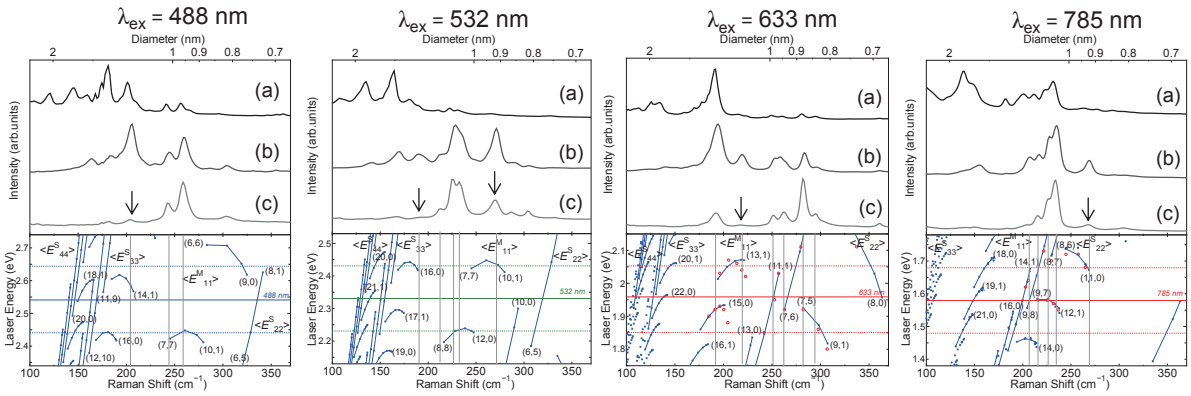

Fig. 1 RBM peaks of SWNTs (a) grown at 800 °C without water vapor before and during growth, (b) grown at 800 °C introducing water vapor before growth and (c) grown at 700 °C introducing water vapor before growth.

Molecular structure of chalcogen encapsulated in single-walled carbon nanotubes studied by molecular dynamics simulations and First-Principles DFT calculations

○[1]Yutaka Sato, [1]Eita Yokokura, [1]Yousuke Kataoka and [1,2,3]Hironori Ogata
[1] *Graduate School of Science and Engineering, Hosei University, Koganei 184-8584, Japan*
[2]*Department of Faculty of Bioscience and Applied Chemistry, Hosei University, Koganei, 184-8584, Japan*
[3]*Research Center for Micro-Nano Technology, Hosei University, Koganei 184-0003, Japan*

Single-walled carbon nanotubes(SWNTs) have a hollow space in the nanometer size that can be encapsulated various functional molecules. Recently, sulfur encapsulated SWNTs and selenium encapsulated DWNTs are synthesized and one-dimensional conductive sulfur chain structure and double-helices selenium structure were reported[1,2]. However, the tube diameter dependence of the local structure and properties of the encapsulated chalcogens have not yet been investigated systematically. In this study, we report the effects of chirality and tube diameter of CNTs on the local structures and molecular mobility of the chalcogen by using molecular dynamics(MD) simulations and first-principles DFT calculations.

In our MD simulations using scigressVer2.6.1(Fujitsu). We applied the GEAR method of the fifth order in the numerical integration method and the speed scaling method in the temperature control method. By placing the CNT and arbitrary number of slufur atoms or selenium atoms in rectangular cell, and using NTV ensemble. First, we calculated the relaxation structure at 1K. Then, stable structure at 300 K was calculated with the NVT ensemble after the relaxation calculation at 800 K. In the First-Principles DFT calculation, we have calculated solid-state ^{33}S NMR parameters(chemical sift and electric field gradient (EFG) tensor). All of the calculations were done using a code package PWscf and GIPAW in Quantum ESPRESSO. We used the pseudo potential method.

Figure1 shows the structure of sulfur encapsulated in (a) (7,0) and (b) (6,6) carbon nanotubes at 298K. Sulfur encapsulated in SWNT took one-dimensional linear or zig-zag chain structure. Detailed results including DFT calculations will be presented.

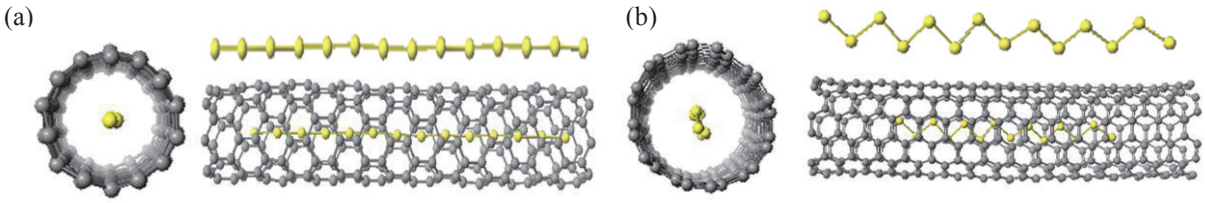

Fig.1 Structure of (a)S@(7,0)SWNT , (b)S@(6,6)SWNT

[1] Toshihiko Fujimori et al. Nature Communications4(2013)2162.
[2]Frank H.Stillinger et al. J.Phys.Chem85, 6460 (1986)
[3]Frank H.Stillinger et al. J.Phys.Chem.1987, 91 (19), pp4899-4907

Length-Selective Loading of Gold into the Interior of Carbon Nanotubes

○R.V. Bekarevich [1], M. Toyoda [1], S. Baba [2], T. Nakata [2], K. Hirahara [1]

[1] *Department of Mechanical Engineering, Osaka University, Suita 565-0871, Japan*
[2] *Research & Development Group, Hitachi, Ltd., Yokohama 244-0817, Japan*

Creation of metal – carbon nanotube (CNT) hybrid structures opens new horizons for such applications as optical resonant antennas or pen-tip injectors for additive nanomanufacturing. Such applications require controlled-loading of metals into the interiors of individual CNTs. Recent results report the Joule-heat induced filling the inner channel of the CNT bridged between two metal electrodes. [1-2] In this situation a strong temperature gradient directed toward the electrode pushes metal melts in the same direction. This may prevent metal loading into the CNT and may lead to its destruction. To eliminate the negative effects, we proposed to connect the CNT not to electrode directly but to the double-walled CNT (DWCNT) decorated with gold nanoparticles. Such configuration shifts the point of highest temperature during Joule heating on the supportive DWCNT. This enables us to create a temperature gradient that is always directed toward the open end of the host CNT, ensuring that thermophoresis promotes rather than hinders the metal loading process. This arrangement also prevents the Joule heat-induced damage of the host CNT. After establishing a contact between the host CNT and the supportive DWCNT, voltage was applied and increased until the gold nanoparticles began to coalesce on the DWCNT and reach diameters roughly matching the inner diameter of the host CNT. Then we slightly adjusted the positioning of the open tip of the host CNT so that it was located in front of a gold nanoparticle. The voltage was then increased until molten gold particles entered inside the host CNT driven by the impact of thermal gradient. At this step, a gold nanowire with a length of 6–8 nm encapsulated in CNT was formed. The length of the encapsulated nanowire can be precisely controlled by the number of serial contacts with other gold nanoparticles located on the supportive DWCNT (Fig. 1). The accuracy of the loading strongly depends on the diameter of loaded nanoparticles and can be vary within 0.5 – 5 nm, what allows the loading of selective portion of gold into the interior of CNT.

The gold loading process could not be explained by only one mechanism; instead, the gold loading was attributed to a combination of multiple mass-transport effects, with the primary mechanisms being thermophoresis and the coalescence of gold nanoparticles caused by grain boundary diffusion. The effect of electromigration was determined to be negligible compared to the above mechanisms. The results of this study provide a reliable method for length-selective filling the interiors of CNTs with metal, which can be applied to the fabrication of novel structures.

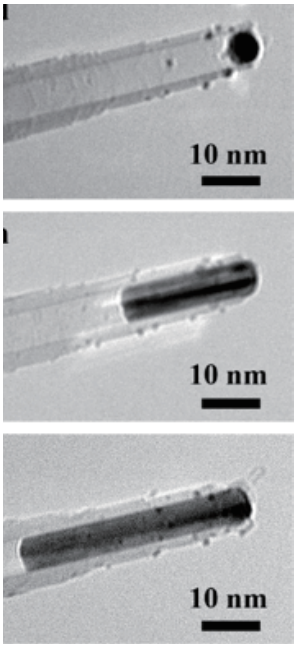

Fig.1 Length-selective growth of the gold nanowire.

[1] R. Zou, *et al*. Adv. Mater. **25**, 2693 (2013).
[2] Z. Fan, *et al*. Carbon **86**, 280 (2015)

Corresponding Author: R. Bekarevich
Tel/Fax: +81-6-6879-7815,
E-mail: bekarevich@ne.mech.eng.osaka-u.ac.jp

Local structure and properties of the cesium iodide crystals encapsulated in single-walled carbon nanotubes studied by molecular dynamics and First-Principles DFT calculations

○Eita Yokokura [1], Yutaka Sato[1], Yosuke Kataoka [1] and Hironori Ogata[1,2]

[2] *Graduate School of Engineering, Hosei University, Koganei, 184-8584, Japan*
[3] *Research Center for Micro-Nano Technology, Hosei University, Koganei, 184-0003, Japan*

Single-walled carbon nanotubes (SWNTs) have a hollow space in the nanometer size that can be encapsulated various functional molecules. The confined molecular assemblies may exhibit unique low-dimensional structures and solid state properties that can not be realized in the bulk. Synthesis and structure of several kinds of alkali halide encapsulated SWNTs have been reported [1-3]. However, the tube diameter dependence of the local structure of the encapsulated alkali halides have not yet been reported. In this study, we report the effects of the diameter and chirality of SWNTs on the local structures of the encapsulated alkali halides including temperature dependence by using molecular dynamics (MD) and DFT simulations.

In the MD simulation, we used the Born-Mayer-Huggins-Tosi-Fumi intermolecular potential between the alkali halide ions and the Dreiding potential between carbon atoms in SWNT. We have investigated on the armchair and zigzag nanotubes with diameters ranging from 1.1 to 1.6 nm systematically. One SWNT and alkali halide ion pairs (Cs-I) around SWNT were set in a rectangular cell as initial configuration. Stable structure at 300 K was calculated with the NVT ensemble after the relaxation calculation at 1000 K. We have demonstrated that structural phase transition is observed at 410 K in CsI@(9,9)SWNT.

In the First-Principles DFT calculation, we have calculated solid-state ^{133}Cs and ^{127}I NMR parameters(chemical sift and electric field gradient (EFG) tensor). All of the calculations were done using a code package PWscf and GIPAW in Quantum ESPRESSO. We used the pseudo potential method. We have demonstrated that ^{133}Cs-NMR spectrum is a useful in which reflect the differences in the local structure of encapsulated CsI sensitively. The detailed results will be also presented.

References:

[1] J. Sloan, M.C. Novotny, *Chem. Phys. Lett.*, **329** (2000)61.

[2] M. Wilson, P.A. Madden, *J. Am. Chem. Soc.,* **123** (2001)2101.

[3] Ryosuke Senga, Hannu-Pekka Komsa, Zheng Liu, Kaori Hirose-Takai, Arkady V. Krasheninnikov and Kazu Suenaga, *Nature Materials,*13(2014)1050.

Corresponding Author: H. Ogata Tel: +81-42-387-6229, Fax: +81-42-387-6229, E-mail: hogata@hosei.ac.jp

Recrystallization of polycrystalline Cu-foil for CVD-grown graphene

○Yui Ogawa[1], Satoru Suzuki[1], Koji Onomitsu[1], Hiroki Hibino[2], Hideki Yamamoto[1]
[1] *NTT Basic Research Laboratories, Nippon Telegraph and Telephone Corporation, Kanagawa 243-0198, Japan*
[2] *School of Science and Technology, Kwansei Gakuin University, Hyogo 669-1337, Japan*

A chemical vapor deposition (CVD) method for graphene using copper (Cu) catalyst and hydro-carbon gases, e.g. methane, has been widely studied as a promising growth technique for an inexpensive and large-scale growth[1]. Aligned CVD-grown graphene could be obtained performing epitaxial growth between grapehen and single crystalline Cu[2-4]. Subsequently, the scalable growths of aligned graphene on commercial Cu-foils has been reported, and the pre-treatments, such as annealing and electropolishing approaches, were performed to enhance a recrystallization of Cu and to get single crystalline Cu from the polycrystalline Cu-foils[5,6]. However, various Cu-foils show different trends in the recrystallization process and these mechanisms are not understood well yet.

Here, we report recrystallization (preferentially-appeared orientation and plane, and grain size of the crystal) of three types of Cu-foil by annealing processes, and CVD growth of graphene. Results of secondary ion mass spectrometry (SIMS) and inductively coupled plasma mass spectrometry (ICP-MS) indicate that each Cu-foil has signature of impurities: aluminum (Al), silver (Ag), and calcium (Ca) in A-foil, B-foil-B, and C-foil, respectively. A-foil shows lowest impunity concentration. Graphene grown on all type of Cu-foils is mainly single layer with less defects according to the characterizations of optical microscopy (OM), Raman spectroscopy, and low energy electron microscopy (LEEM). For the recrystallization of the polycrystalline Cu-foil, A-foil and C-foil are sensitive against hydrogen (H_2) concentration during the annealing before CVD growth of graphene. In contrast, B-foil did not show any dependence on the annealing condition and could always give large Cu grain in centimeter scale. In case of A-foil, beyond 90 % area was recrystallized with Cu(111) plane in a centimeter scale, which was confirmed by OM, electron back scattering diffraction (EBSD), and X-ray diffraction (XRD) as shown in Fig. 1, when H_2 concentration was over 5 % in argon (Ar). Also, C-foil provided Cu(001) and Cu(120) planes. As results, impurities contained in Cu-foil and H_2 annealing are considered as important factors to control grain size and crystal plane of Cu-foil in the recrystallization process.

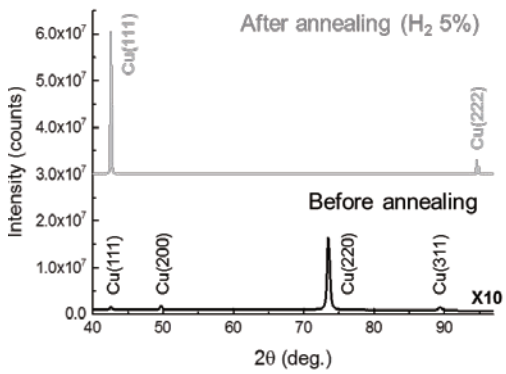

Fig. 1 XRD patterns of A-foil after (gray) and before (black) H_2 annealing.

Acknowledgement: A part of Cu-foil is provided by JX Nippon Mining and Metals co.

References:
[1] S. Bae *et al.*, *Nat. Nanotechnol.* **5**, 574 (2010).
[2] L. Gao *et al.*, *Nano Lett.* **10**, 3512 (2010).
[3] B. Hu *et al.*, *Carbon*, **50**, 57 (2012)
[4] Y. Ogawa *et al.*, *J. Phys. Chem. Lett.* **3**, 219 (2012).
[5] L. Brown *et al.*, *Nano Lett.* **14**, 5706 (2014).
[6] V. L. Nguyen *et al.*, *Adv. Mater.* **27**, 1376 (2015).

Corresponding Author: Yui Ogawa
Tel: +81-46-240-3423, Fax: +81-46-240-4718, E-mail: ogawa.yui@lab.ntt.co.jp

Efficient fabrication of graphene/BN heterostructures by metal melting transfer

○Ryosuke Inoue[1], Kenji Watanabe[2], Takashi Taniguchi[2], Yutaka Maniwa[1], Yasumitsu Miyata[1,3]

[1]*Department of Physics, Tokyo Metropolitan University, Hachioji, 192-0397, Japan*
[2] *National Institute for Materials Science, Tsukuba 305-0044, Japan*
[3]*JST, PRESTO, Kawaguchi, 332-0012, Japan*

Chemical vapor deposition (CVD) is widely used for the growth of large-area, uniform monolayer graphene films. Generally, CVD graphene is grown on metal substrates such as Cu and Ni foil, and thus graphene films should be transferred from metal substrates to insulating substrates such as SiO_2 and boron nitride (BN) for electronics applications. Conventional polymer-assisted transfer process, however, includes several unavoidable issues such as remaining polymer and solvent on the graphene surface and at the graphene/substrate interface. To solve this problem, we have developed a novel transfer method using metal melting under an inert atmosphere at high temperature [1].

In this study, we have improved the meta-melting transfer process to obtain large-area graphene/BN heterostructures with high yield. This improvement can be achieved by the use of large-area BN flakes with a size of over 100 μm (Fig.1a). For sample preparation, graphene was grown on Cu foil, and then was fixed on BN substrates. For the transfer, the samples were annealed at 1150~1200°C to melt Cu foil under Ar/H_2 atmosphere. During the Cu melting, the graphene films can be directly transferred on the BN substrates. The graphene on BN has highly-clean surface like BN surface and one-atom-thick height profile (Fig.1b,c). Furthermore, we found that the melting-transfer samples have less frequency variations of G and 2D bands than the conventional polymer-transfer samples (Fig. 1d). This result indicates that the present graphene has less lattice strain and charged impurities [2]. In the presentation, we will report the details of transfer process and electric transport properties of graphene/BN heterostructures.

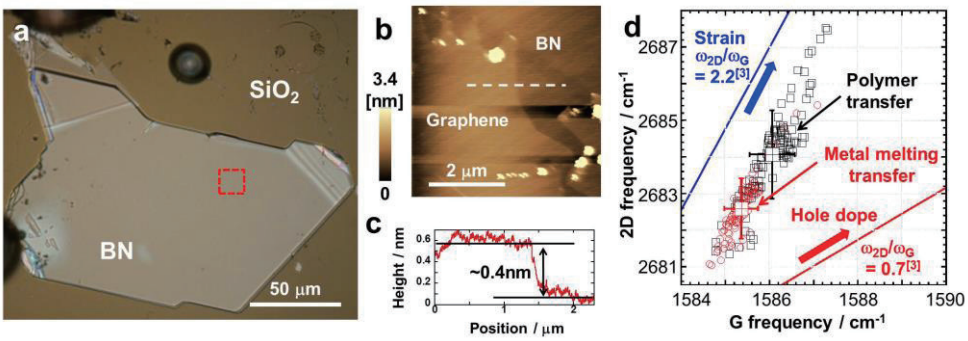

Fig.1 (a) Optical microscope and (b) AFM images, and (c) height profile of the graphene transferred on BN. (d) Correlation between the frequencies of the G and 2D Raman modes of polymer-transfer and metal-melting-transfer graphene films.

[1] R. Inoue, *et al*. 49th FNTG symposium. [2] J. E. Lee *et al*., Nat. Commun **3**, 1024 (2012).
Corresponding Author: Yasumitsu Miyata, Tel: +81-42-677-2508, E-mail: ymiyata@tmu.ac.jp

Suppression of graphene nucleation by turning off hydrogen supply just before atmospheric chemical vapor deposition growth

○Seiya Suzuki, Yoshifumi Terada, Masamichi Yoshimura

Graduate school of Engineering, Toyota Technological Institute 468-8511, Japan

Chemical vapor deposition (CVD) is a promising method to produce high quality large-size single-crystal graphene, and further increase in domain size is desirable for electro/optic applications. Suppression of the nucleation of graphene is a crucial technique to obtain large-size domains of graphene, and several effective methods have been established such as prolonged annealing [1], wrapping Cu foils [2], and high pressure annealing [3]. However, the long processing time of these methods becomes a significant disadvantage for graphene fabrication on an industrial scale. Here we report an effective method of suppressing graphene nucleation in atmospheric CVD of Cu (100 μm thickness) by turning off hydrogen supply just before the growth process. Using this method, we reduced the annealing time down to 20 minutes and achieved growing isolated graphene domains with ~500 μm in diameter.

Figure 1(a) shows a schematic diagram of the CVD growth process. Hydrogen flow was turned off for 5 minutes just after the annealing process. Figures 1(b) and 1(c) show optical micrographs of Cu after CVD with and without turning off hydrogen flow, respectively. It was found that the density of graphene domains was reduced from 95.3 to 51.6 cm^{-2} by turning off hydrogen.

To reveal the effect of the turning off hydrogen process, we measured the annealed Cu surfaces (after A and B shown in Fig. 1(a)) by X-ray photoelectron spectroscopy (XPS), where the amount of oxygen increased ~5% in atomic ratio by the turning off process. This indicates that the Cu surface was oxidized by residual oxygen in the CVD chamber during the turning off hydrogen. The surface oxidation would be attributed to suppress the graphene nucleation by passivation of nucleation sites [4].

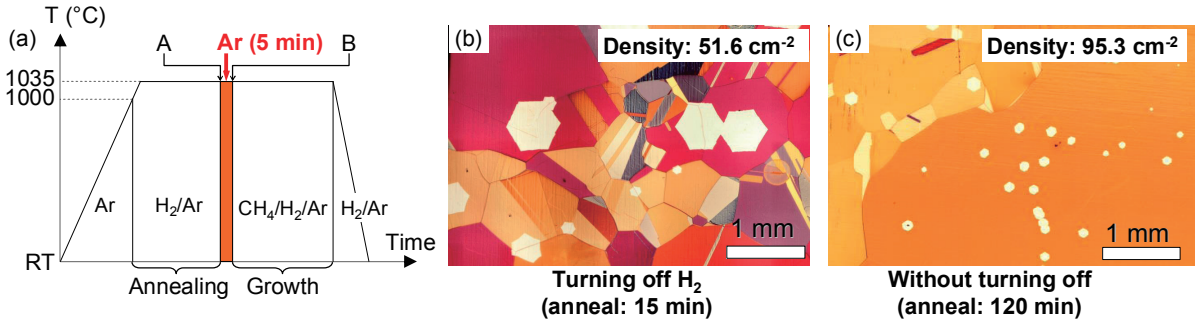

Fig. 1. (a) Schematic diagram of CVD process. (b,c) Optical micrographs of Cu foils after CVD with and without turning off hydrogen, respectively. The Cu foils were heated around 200 ºC to visualize the graphene domain (shown in white contrast).

[1] H. Wang et al., J. Am. Chem. Soc. **134,** 3627 (2012).
[2] S. Chen et al., Adv. Mater. **25,** 2062 (2013).
[3] S. Suzuki et al., Jpn. J. Appl. Phys. **53,** 095101 (2014).
[4] Y. Hao et al., Science **342,** 720 (2013).

Corresponding Author: S. Suzuki
Tel: +81-52-809-1852,
E-mail: seiya09417@gmail.com

Evaluation of spin magnetism and chemical activity for graphene derivatives

○Tomoki Yamashina[1], Takuya Isaka[1], Kentaro Tajima[2], Yoshiaki Matsuo[3], Kazuyuki Takai[1,2,]

[1] *Graduate School of Science and Engineering, Hosei University, Tokyo 184-8584, Japan*
[2] *Department of Chemical Science and Technology, Hosei University, Tokyo 184-8584, Japan*
[3] *Graduate School of Engineering, University of Hyogo, Hyogo 671-2280, Japan*

The introduction of functional groups, edges, defects or strain is typical method for giving chemical activity to graphene. For example, the edge structure gives graphene the half-filled edge states with a large density of states near the Fermi level, where the spin magnetism and chemically activity emerge as the singly occupied molecular orbital (SOMO) of aromatic molecules. The oxygen containing functional groups also give graphene a catalytic activity in various reaction systems [1], where the stabilized radical states take an important role. In this study, the correlation between the spin magnetism and chemical activity for graphene oxide (GO) and activated carbon fibers (ACFs) which is an edge-riched nanographene assembly material was investigated by XRD, XPS, the magnetic susceptibility, ESR and GC-MS. GO samples were synthesized by Brodie [2] and Hummers [3] methods (BGO and HGO). Chemical activities were evaluated by a coupling reaction of aromatic amine using ACFs and GO as catalyst. The spin susceptibilities N_{spin} estimated by ESR intensities are summarized in **Fig.1** for GO and ACFs samples. N_{spin} are very close to those obtained from the static magnetic susceptibility (SQUID). The g-value is lower than 2.0023 for ACFs having π–electron with shielding effect, while BGO and HGO show $g > 2.0023$, suggesting sp^3-carbon spin system. The absence of π-electron in GO by oxidation is also supported by XPS. GC-MS yields for the reaction from benzylamine to *N*-benzylidenebenzylamine are shown in **Fig.1** for BGO, ACFs and HGO as catalyst. The spin magnetism is dominant factor for catalytic activity but other factors such as the presence of π-electron influences the results.

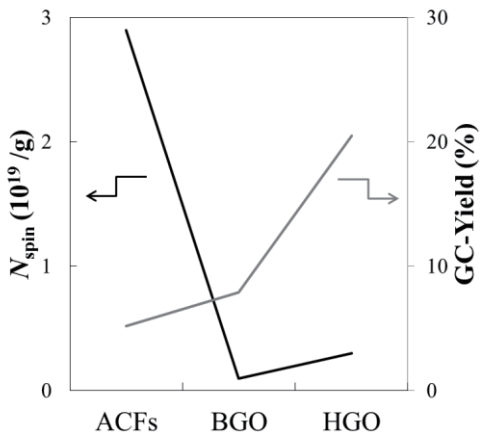

Fig.1 Spin densities and GC yields for BGO, HGO and ACFs

[1] C.Su, M.Acik, K.Takai et al, *Nat. Commun.*, **3**, 1298 (2012)
[2] B. C. Brodie, *Phil. Trans. R .Soc. Lond.*, **149**, 249-259 (1859)
[3] D. C. Marcano et al, *ACS Nano*, **4**, 8, 4806–4814 (2010)

Corresponding Author: Kazuyuki Takai
Tel: +81-42-387-6138, Fax: +81-42-387-7002,
E-mail: takai@hosei.ac.jp

Environmentally Stable Carrier Doping into Graphene Films by Extraordinary Molecular Lewis Acid

○T. Miyauchi[1], N. Tanaka[2], Y. Shoji[2], K. Funahashi[3], K. Kanahashi[3], M. Ishihara[4], M. Hasegawa[4], T. Fukushima[2] and T. Takenobu [1,3,5]

[1] *Department of applied Physics, Waseda University, Shinjuku 169-8555, Japan*
[2] *Chemical Resources Laboratory, Tokyo Institute of Technology, 4259 Nagatsuta, Midori-ku, Yokohama 226-8503, Japan*
[3] *Department of Advanced Science and Engineering, Waseda University, Shinjuku, Tokyo 169-8555, Japan*
[4] *Carbon-Based Thin Film Materials Group, Nanomaterials Research Institute, National Institure of Advanced Industrial Science and Technology (AIST), Ibaraki 305-8565, Japan*
[5] *Kagami Memorial Laboratory, Waseda University, Shinjuku, Tokyo 169-0051, Japan*

Graphene films are one of the most promising materials for the future flexible transparent electrode due to their high transparency, excellent transport properties, and high flexibility, which is difficult for commonly-used indium tin oxide (ITO) films. However, sheet resistance (*R*s) of graphene films is higher than them of ITO and, therefore, many researchers on charge charrier doping into Graphene with very diverse dopants (HNO_3, $AuCl_3$, *etc*) have been reported, resulting in poor air stability [1]. Very recently, we found that the combination of the super Lewis acid, diarylborinium ion (Mes_2B^+; Mes (mesityl) = 2, 4, 6-trimethylphenyl) and counter anion, tetrakis (pentafluorophenyl) borate ($[(C_6F_5)_4B]^-$) (Fig.1) [2] leads to air-stable carrier doping in carbon nanotubes. Therefore, we apply this material into graphene films.

We prepared few-layer graphene films by CVD method and transferred on plastic substrates. These films were films were immersed into the saturated *o*-dichlorobenzene solution of dopant, Mes_2B^+ $[(C_6F_5)_4B]^-$. Before and after the above doping processes, we characterized these films by four-probe resistance measurements and confirmed the carrier doping into graphene films by R_S reduction of -26% (Fig.2). Importantly, the doped films were air-stable for one month.

In conclusion, we succeeded in chemical doping of graphene films by the novel dopants, Mes_2B^+ and $[(C_6F_5)_4B]^-$. This researches promotes the use of graphene films as new flexible electrode.

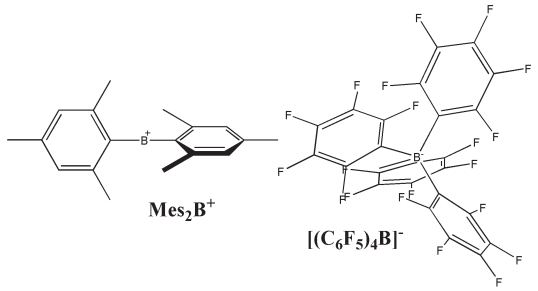

Fig. 1 Novel dopant; cation, Mes_2B^+ and counter anion, $[(C_6F_5)_4B]^-$

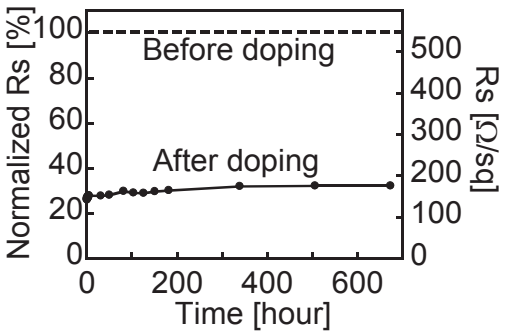

Fig. 2 Time evolution of *R*s increase in graphene film doped by novel dopant

[1] F. Günes *et al., ACS Nano* 4, 4595 (2010). [2] Y. Shoji *et al., Nature Chemistry* 6, 498–503 (2014).
Corresponding Author: T. Takenobu, Tel&Fax: +81-3-5286-2981, E-mail: takenobu@waseda.jp

Evaluation of Graphene Oxide Catalyst regarding Organic reaction in Aqueous media

○Takuya Isaka[1], Tomoki Yamashina[1], Kentaro Tajima[2], Yutaka Ohta[2], Kazuyuki Takai[1,2]

[1]*Graduate School of Science and Engineering, Hosei University, Tokyo 184-8584, Japan*
[2]*Department of Chemical Science and Technology, Hosei University, Tokyo 184-8584, Japan*

Graphene oxide (GO) having oxygen-containing groups is promising as metal-free and environment-compatible catalyst due to its amphiphilic and Brönsted acid nature [1], although the detail mechanism for catalytic activity is not clear yet. In this study, the change in the chemical structure of graphene oxide as catalytic activity is investigated before / after the synthesis of a xanthene derivative in water solvent in order to clarify the mechanism of the catalytic activity.

GO was synthesized from natural graphite flake by Hummers methods. The following reaction using GO as catalyst was conducted in water medium (Scheme 1). A mixture of benzaldehyde (**1**)

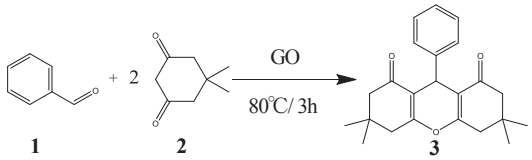

Sheme 1 Synthesis for xanthene dericative using GO in water

(2 mmol), dimedone (**2**) (4 mmol) and GO catalyst (4.9 wt%) dispersed in water was stirred at 80℃ for 3h. After separation of GO catalyst from the reaction media by filtration and washing with dichloromethane, the water solvent was evaporated. The obtained product was characterized by GC-MS. The chemical structure of GO before / after the reaction was evaluated by XPS.

The GC-MS peak for 3,3,6,6-tetramethyl-9-phenyl-3,4,5,6,7,9-hexahydro-1H-xanthene-1,8(2H)-dione (**3**) (m/z = 350) appears in the product of the reaction using GO catalyst in spite of the absence of the peak on the condition without GO (Fig. 1), indicating catalytic activity of GO as Brönsted acid. The yield and conversion are 22.6% and 86.4% respectivity from GC-MS. However, the C/O ratio of GO estimated by XPS decreases after the reaction. Taking the fact that C/O ratio also decreases in the control experiment without reactants, the C/O decreasing is mainly attributed to the heat-induced reduction during the reaction. The intensity ratio among C1s peaks for oxygen-containing functional groups [2] is almost same for GO after the reaction and that for control experiment (Fig. 2). Any unique contribution of specific functional group in the reaction is not found.

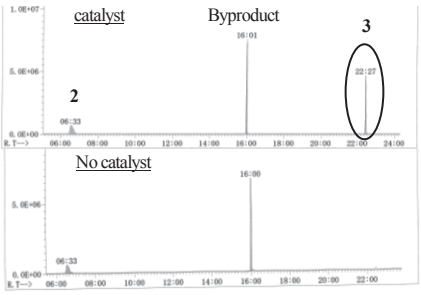

Fig. 1 MS spectra for product

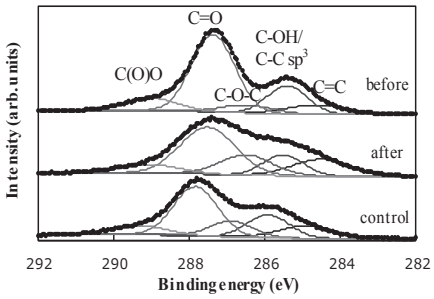

Fig. 2 The change of XPS C1s peaks for GO before / after the reaction

[1]Shaabani, A.; Mahyari, M.; Hajishaabanha, F. *Res. Chem. Intermed*. **2013**, 40, 8, 2799-2810
[2]Rodriguez-Postor, I.; Ramos-Fernandez, G.; Varela-Rizo, H.; et al. *Carbon*. **2015**, 84, 299-309

Corresponding Author: Kazuyuki Takai,
Tel: +81-42-387-6138, Fax: +81-42-387-7002, E-mail: takai@hosei.ac.jp

Electrocatalytic properties toward methanol oxidation of Pt-based nanoparticles on surface-modified carbon nanomaterials

○[1] Haruhiko Yoshitake , [3]Eiichi Inami, [2]Wang Zhipeng and [1,3]Hironori Ogata

[1] *Graduate School of Science and Engineering, Hosei University Koganei 184-8584, Japan*
[2] *Institute of Carbon Science and Technology, Shinshu University, Nagano 380-8553, Japan*
[3]*Research Center for Micro-Nano Technology,Hosei University,Koganei 184-0003,Japan*

Direct methanol fuel cells (DMFCs) are one of the most promising transportable power sources which can be used in mobiles, laptops, and small power generation. The basic operation principle of DMFCs involves methanol oxidation and oxygen reduction on the precious metal catalysts, which are loaded on the support surfaces. As is well-known, the dispersion of Pt-based alloys on carbon supports as well as catalyst particle size and shape plays a dominant role in the electrochemical performance for fuel cells. We have explored the electrocatalytic properties of Pt-based nanoparticles supported on the carbon materials by electrodeposition systematically. In this study, we investigated the effects of the radio frequency(RF) O_2 plasma treatment on the dispersion state and electrocatalytic properties of Pt-based nanoparticles supported on the carbon material (CNSs , SWNTs) by electrodeposition method. Figure 1 shows the XPS for CNSs before and after RF O_2 plasma treatment and table.1 summarizes their electrochemical characteristics of methanol oxidation. The detailed results on the shape and dispersion state of Pt-based nanoparticles and their electrocatalytic performance for methanol oxidation will be presented.

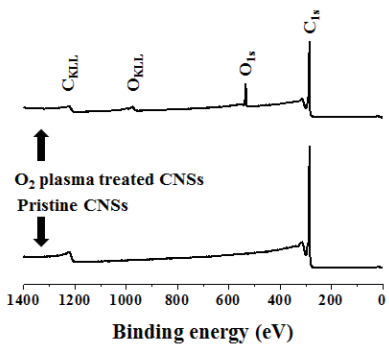

Figure 1. X-ray photoelectron spectra(XPS) for CNSs

	S_{Pt} [cm^2]	J_F [mA/cm^2]	I_f/I_b	V_F [V]
Pristine CNS	**1.45×10^3**	**21.0**	**1.21**	**0.646 (±0.005)**
O_2 plasma treated CNS	**1.70×10^3**	**33.3**	**0.76**	**0.676 (±0.005)**

Table 1. Electrochemical characteristics

References:
(1)J.M.Sieben *et al., J. Appl. Electrochem.***38**(2008)483-490.
(2)Zhipeng Wang, Mao Shoji and Hironori Ogata, *Appl. Surf. Sci.***259**(2012)219-224.
(3)M.Tsai *et al., ElectroChemistry. Communication* **8**(2006)1445-1452.
(4)S.H.Ahn *et al., Chem. Eng .J. ,* (2012)**181-182** , 276-280.
Corresponding Author: Hironori Ogata,
Tel: +81-42-387-6229, Fax: +81-42-387-6229, E-mail: hogata@hosei.ac.jp

Electrochemical Interaction at the Interface between Graphene and Electrolyte

○Daisuke Suzuki[1], Kazuyuki Takai [1, 2]

[1] *Graduate School of Science and Engineering, Hosei University, Tokyo 184-8584, Japan*
[2]*Department of Chemical Science and Technology, Hosei University, Tokyo 184-8584, Japan*

In electric storage devices, phenomena at the interface between electrode and electrolyte play the most important roles. Electric double-layer capacitors depend on physical adsorption of electrolyte, and battery utilizes an electrochemical reaction at electrodes. Carbon materials like graphite and its derivatives are widely used in electric storage devices such as negative electrode in a battery, where degradation mechanism of electrode and SEI (Solid electrolyte interphase) formation are crucial in device performance. However phenomena at the interface between carbon materials and electrolyte in battery devices are still unclear because of complicated structure of conventional carbon electrode materials. In this study, the electrochemical interaction at the interface between graphene electrode as a model structure of carbon electrode materials and electrolyte solution is investigated in order to clarify the phenomena in battery devices.

Gate voltage dependence of the conductivity was measured for graphene FET on SiO_2 substrate with the bipolar electrochemical configuration, where the graphene channel and Pt wire in the electrolyte were applied as working and counter electrodes, respectively. 1 M KCl aqueous solution and 1 M LiCl aqueous solution, and 1 M $LiBF_4$ organic solution (EC / DMC) were used as electrolyte solution. Raman spectroscopy was carried out using excitation wavelength of 532 nm under an atmospheric condition.

Similar results were obtained in the case of KCl and LiCl aqueous solution. A reversible behavior of the transfer curve upon the cycle of applying top gate voltage (Pt counter electrode) was observed for smaller voltage region, where the electrochemical current between top electrode and graphene channel is negligible. This is attributed to the physisorption of electrolyte on the graphene surface. Appling larger gate voltage, irreversible gate-voltage dependence appears with electrochemical currents due to electrolysis of water at electrodes. However, no change in Raman spectra after larger voltage applying suggests less structural change for graphene. With $LiBF_4$ organic electrolyte solution (Fig.1), the observed electrochemical current at more than 2 V resembles actual battery reactions between carbon and lithium. On the other hand, the typical behavior due to formation of SEI that occurs between 2 - 3 V is absent in the graphene-based device, suggesting significant roles of stacking structure and non-ideal structure of graphene such as edges and defects of carbon electrode in actual battery devices.

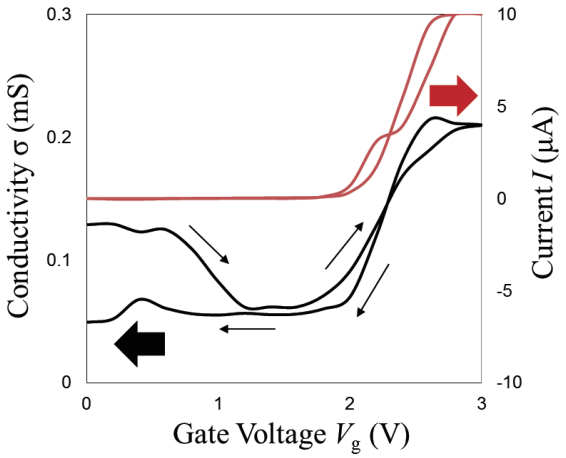

Fig.1 Gate voltage dependence of Conductivity in FET with $LiBF_4$ organic electrolyte solution

[1] H. Wang *et al*, ACS. Nano. **4**, 7221 (2010)

Corresponding Author: Kazuyuki Takai,
Tel: +81-42-387-6138, Fax: +81-42-387-7002,
E-mail: takai@hosei.ac.jp

Electron confinement in bilayer graphene

○Yuya Inoue[1], Riichiro Saito[1]

[1]*Department of Physics, Tohoku University, Sendai 980-8578, Japan*

Graphene is a material attracting wide-range of attentions for applications due to its great physical properties such as high mobility. However, the weakness of graphene is that it can not be used as field effect transisitor (FET) unless the band gap is made artificially. The reason for the weakness is well known as the Klein tunneling phenomena that the electron on the monolayer graphene can not be confined by applying any potential [1].

Some previous works show that FET using bilayer graphene can be realized by applying electric field perpendicular to the bilayer graphene, which breaks the symmetry between the two layers and results in opening the energy gap [2,3].

In this work, we also focus on the bilayer graphene (AB stacking), which has the property that complete reflection against the potential barrier is realized due to the Klein tunneling effect for bilayer graphene [1]. The present work shows that changing the potential height and width in the tunneling processes can be applied to make current switch. Fig. 1 shows the resonance condition, where electron in bilayer graphene can go through the potential barrier with height V_0 and width D. If the resonance (T=1) does not occur, electron can be confined between two such barriers. We calculate the time development of wave packet and show the possibilities of electron confinement and propose a switching device.

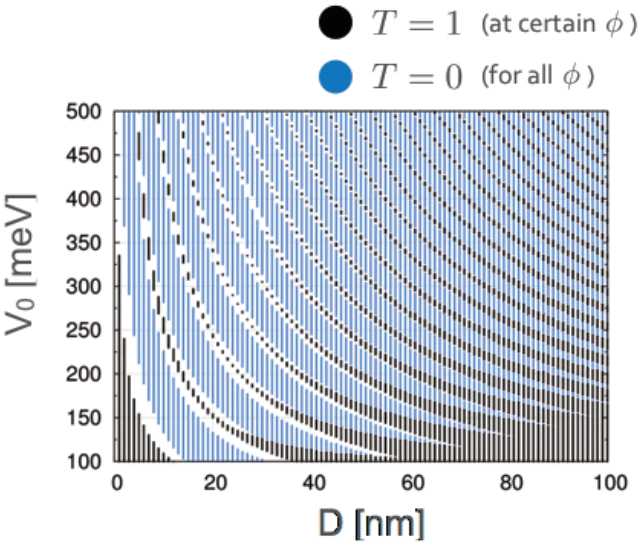

Fig.1: Resonance tunneling condition in bilayer graphene. T is transmission probability, V_0 is the potential height, D is the potential width, and ϕ is the angle for the incident electron. The energy of incident electron is ~ 17meV.

[1] M. I. Katsnelson *et al*. Nature Physics **2**, 620 (2006).
[2] Y. Zhang, *et al*. Nature **459**, 820 (2009).
[3] S-L. Li *et al*. Acs Nano **5**, 500 (2011).
Corresponding Author: Y. Inoue
Tel: +81-22-7 95-6442, Fax: +81-22-795-6447,
E-mail: inoue@flex.phys.tohoku.ac.jp

Electric field and charge modulation spectroscopy of monolayer WS_2 on graphite

○Keiichiro Matsuki [1], Jiang Pu [1], Daichi Kozawa [1], Yu Kobayashi [2], Shogo Sasaki [2], Yasumitsu Miyata [2], Lain-Jong Li [3], Yutaka Maniwa [2], Taishi Takenobu [1,4]

[1] *Department of Advanced Science and Engineering, Waseda University, Shinjuku 169-8555*
[2] *Department of Physics, Tokyo Metropolitan University, Hachioji 192-0397, Japan*
[3] *Physical Sciences and Engineering Division, KAUST, Thuwai 23955-6900, Saudi Arabia*
[4] *Kagami Memorial Laboratory, Waseda University, Shinjuku, Tokyo 169-0051, Japan*

Transition metal dichalcogenide (TMDCs) monolayers are known as direct bandgap semiconductors with ultimately thin thickness (< 1 nm), leading to ideal quantum wells (QWs) and stable charged excitons (trions). Due to their quantum-well structures, electric field and/or charge modulation of optical properties, such as the quantum confined Stark effect and many body effect, are expected and it has been already investigated by other groups [1]. However, the solid evidenced of the quantum confined Stark effect and many body effect have not yet been observed because an additional peak of trions masks the spectral modulations. To overcome these problems, we focus on the recently reported monolayer WS_2 on graphite, in which the effect of trions is negligible [2].

As shown in fig. 1, we fabricated electric double layer capacitors. Monolayer WS_2 was synthesized on exfoliated graphite by chemical vapor deposition methods [2] and Au electrodes were thermally deposited on graphite as a working electrode and on quartz as a gate electrode. For electrolyte, ion gel which is mixture of ionic liquid ([EMIM] [TFSI]) and organic polymer (PS-PMMA-PS) was spincoated on the sample. We applied gate voltage (V_G) at room temperature. Figure 2 shows PL spectra of monolayer WS_2 on graphite at various gate voltages. We have successfully observed clear V_G-dependent spectral change and these spectra are well explained by single Lorentz fitting analysis, resulting in peak redshift, broadening and intensity decrease. Importantly, the redshift is proportional to square of V_G, strongly suggesting the quantum confined Stark effect. Moreover, through quantitative analysis based on the basic theory of quantum confined Stark effect, we found the clear threshold gate voltage, which separates the simple field modulation and the multiple modulation by both electric field charge accumulation, possibly leading to the evidence of many body effect.

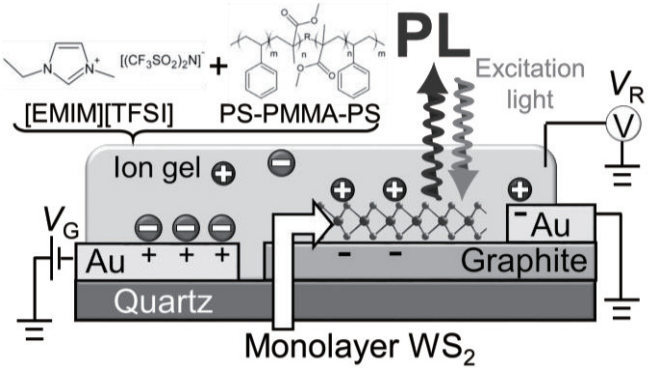

Fig. 1 Device structure of EDLC

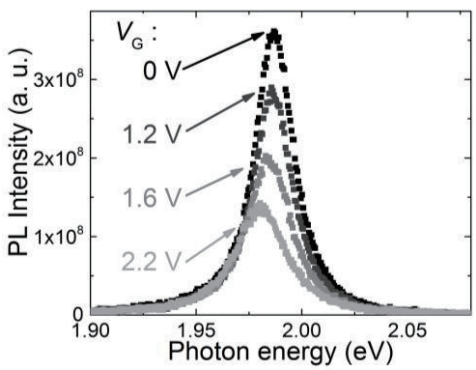

Fig. 2 Gate voltage dependence of PL spectra in Monolayer WS_2 on graphite

[1] A. M. Jones *et al*. Nature Nanotech., **8**, 634 (2013)
[2]Y. Kobayashi, S. Sasaki, Y. Miyata *et al*. ACS NANO, **9**, 4056 (2015)

Corresponding Author: Taishi Takenobu, Tel&Fax: +81-3-5286-2981, E-mail: takenobu@waseda.jp

Behavior of Graphene Oxide in Aqueous Solution

○Meng Wang, Yang Niu, Zhenyu Zhang, Yan Li

College of Chemistry and Molecular Engineering, Peking University, Beijing, 100871, China

Graphene oxide (GO), which possesses a range of oxygen-containing functional groups, such as carboxylic acid groups, hydroxyl and epoxy groups, has very good water solubility without further functionalization [1]. Considering the structure of GO, it might show similar properties to the polyelectrolyte in aqueous solution. Here, different sizes of GO sheets were separated by a centrifugation-based process, and the size distribution of the obtained GO solutions were studied by atomic force microscopy (AFM) and static light scattering (SLS). The aggregation behaviors of GO dispersions in water and under the condition of adding salt were also studied by SLS. GO solutions were destabilized by adding excess NaCl and $MgCl_2$, but when adding excess $AlCl_3$, the GO solution remained stable attributed to the inversion of surface charges of GO sheets.

[1] Dreyer, Daniel R., *et al.* Chem. Soc. Rev.**39**, 228-240 (2010).

Corresponding Author: Yan Li

Tel: +86-10-62756773, Fax: +86-10-62751708.

E-mail: yanli@pku.edu.cn

Host-Guest interactions between nanographene host and magnetic guest molecule

○Akira Suzuki[1], Kazuyuki Takai[1, 2]

[1] *Graduate School of Science and Engineering, Hosei University, Tokyo 184-8584, Japan*
[2]*Department of Chemical Science and Technology, Hosei University, Tokyo 184-8584, Japan*

Activated Carbon Fibers (ACFs) consisting of 3D random network of nanographenes is interesting host material because of its nanopores and localized spins originating in zigzag-edges [1]. In this study, we introduced Ferrocene ($FeCp_2$) having localized *d* -electron as guest molecule to ACFs host in order to clarify host-guest magnetic interaction between nanographene and magnetic molecule.

The guest molecule was introduced by vapor transfer ($FeCp_2$-ACFs). The introduction of the guest molecule is confirmed by Fe_{2p} peaks in XPS. The increment in shake-up peak intensity of C_{1s} spectrum indicates the increase of conducting electrons (**Table 1**). The emergence of charge transfer host-guest interaction is suggested in $FeCp_2$-ACFs, which is also supported by red-shift of G-band in Raman spectrum. The larger spin concentration of $FeCp_2$-ACFs than that of ACFs indicates the presence of cationized $FeCp_2$ in which chemical form spin magnetism of 3*d* electron appears (**Fig. 1**). Although it has been reported $FeCp_2$-doped ACFs showed ferromagnetism [2], our sample doesn't show that. Assuming the simple dipolar interaction between nanographene's edge and ferrocenium cation spins, ESR linewidth is expected to increase 5 times as large as that of ACFs. Actually, the ESR linewidth of $FeCp_2$-ACFs doped at 80°C are much broadened comparing with that of ACFs and the ESR peak disappears.

Table 1 Relative intensities for $FeCp_2$ - ACFs and ACFs in XPS

XPS peak	ACFs	$FeCp_2$-ACFs
C_{1s} (C-C)	1	1
C_{1s} (C-O)	0.26	0.26
C_{1s} (C=O)	0.60	0.50
C_{1s} (shake-up)	0.14	0.18
Fe_{2p}	0	0.03

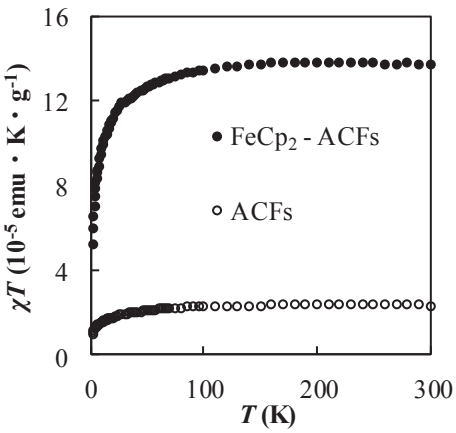

Fig.1 Temperature dependence of magnetic susceptibility for $FeCp_2$-ACFs and ACFs

[1] T. Enoki and K. Takai Solid State Comm. **149**, 1144-1150 (2009)

[2] A. Nakayama *et al.* Synt. Met. **86**, 2335-2336 (1997)

Corresponding Author: Kazuyuki Takai

Tel: +81-42-387-6138, Fax: +81-42-387-7002

E-mail: takai@hosei.ac.jp

2P-38

Asymmetric Kohn anomaly in G' band of graphene

Eddwi H. Hasdeo, Ahmad R. T. Nugraha, and Riichiro Saito
Department of Physics, Tohoku University, Sendai 980-8578, Japan

The existence of the gapless linear energy bands (Dirac cones) in graphene modifies phonon energy, spectral broadening, and spectral lineshape of the Raman spectra. One of the well-known phenomena is the Kohn anomaly effect, in which the phonon energy (lifetime) becomes lower (shorter) due to second-order perturbation by electron-phonon interaction [1]. Peak position (linewidth) of the G band Raman spectra (~1600 cm^{-1}), the first order Raman scattering, symmetrically increases (decreases) as a function of absolute value of Fermi energy [2,3]. We shall call these phenomena as symmetric Kohn anomaly. On the other hand, the Kohn anomaly effect of the G' band (~2700 cm^{-1}), the second order Raman process, shows two controversial experimental results. Araujo et al. show that G' band gives symmetric Kohn anomaly effect yet opposite compared to that of the G band, namely peak position (linewidth) symmetrically decreases (increases) as a function of absolute value of Fermi energy [2]. Meanwhile, Das et al. show asymmetric Kohn anomaly of the peak position of G' band, namely peak position is barely changed on negative Fermi energy but decreases on positive Fermi energy [4]. In this work, we perform calculation of phonon self energy that responsible to explain the change of both phonon energy and linewidth as a function of Fermi energy. The calculation results show that at certain phonon wave vector, asymmetric Kohn anomaly effect is expected. Since the G' band spectra comes from integration of all possible phonon wavevector depending on laser energy, we will discuss symmetric or asymmetric Kohn anomaly as a function of laser energy.

[1] M. Lazzeri and F. Mauri, Phys. Rev. Lett. 97, 266407, (2006)
[2] D. L. Mafra et al., Phys. Rev. B 86, 195434, (2012)
[3] P. T. Araujo et al., Phys. Rev. Lett. 109, 046801, (2012)
[4] A. Das et al., Nature Nanotech. 3, 210, (2008)
Corresponding Author: E. H. Hasdeo
TEL: +81-22-795-6442, FAX: +81-22-795-6447, E-mail: hasdeo@flex.phys.tohoku.ac.jp

2P-39

Electronic structure of bilayer graphene with defect under an external electric field

○Ken Kishimoto and Susumu Okada

Graduate school of Pure and Applied Sciences, University of Tsukuba, Tsukuba 305-8571, Japan

Electronic structure of graphene is fragile against the formation of the hybrid structure with foreign materials, such as insulating substrate, defect, adsorbent, and other graphene layers. By adsorbing the graphene with atomic defects on pristine graphene, the resultant bilayer graphene no longer possesses a pair of linear dispersion bands at Fermi level. The bilayer graphene one of which layer possesses the defect has a finite energy gap of 0.3 eV in their pi electron states [1]. Thus the bilayer graphene with defects may exhibit different properties to the pristine graphene under the carrier injection due to the finite energy gap and the defect induced states. In this work, we aim to reveal the influence of defects on the electronic structure of bilayer graphene under an external electric field using the density functional theory combining with the effective screening medium method.

By applying negative and positive gate voltage, injected electrons and holes substantially modulate the electronic energy band of the bilayer graphene with the defect (Fig. 1): In the neutral case, the Fermi level crosses the three flat dispersion bands arising from the defect. For the case of hole doping, the Fermi level located just below the defect states, but the relative position of the defect-induced states is deeper by 0.1 eV than the state without the excess carrier [Fig. 1(b)]. In contrast, the defect-induced states substantially shift upward by the electron doping [Fig. 1(c)]. Furthermore, the carrier doping also modulates the bandwidth of the defect-induced states. The width is narrower and wider than that for the neutral case by hole and electron doping, respectively. Thus, the bilayer graphene with defect does not exhibit rigid band nature under the carrier doping by the contour electrode. The physical mechanism of the shift with respect to the carrier density will be discussed.

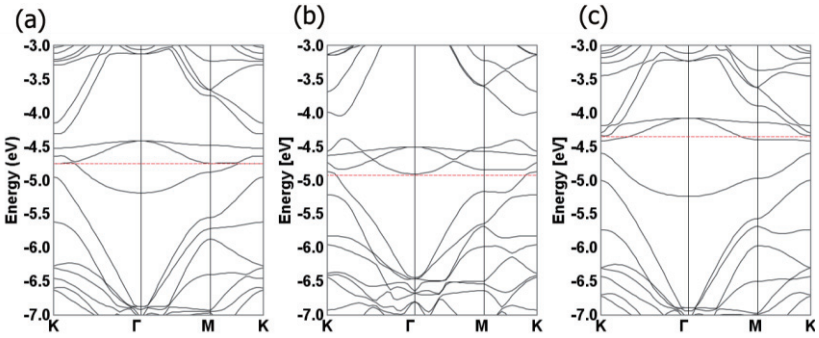

Fig. 1, (a) Electronic structures of bilayer graphene one of which layers possesses monovacancies. Electronic structures of bilayer graphene one of which layers possesses monovacancies under (b) hole and (c) electron doping. Red horizontal dotted lines denote the Fermi level.

[1] K. Kishimoto and S. Okada, Sur. Sci. **644**, 18, (2016).

Corresponding Author: K. Kishimoto

Tel: +81-29-853-5600(ext.; 8233)

E-mail: kkishimoto@comas.frsc.tsukuba.ac.jp

Halide-assisted CVD and characterization of monolayer Nb-doped WS_2

○Shogo Sasaki[1], Yu Kobayashi[1], Zheng Liu[2, 3], Kazutomo Suenaga[3]
Yutaka Maniwa[1], Yasumitsu Miyata[1, 4]

[1] *Department of Physics, Tokyo Metropolitan University, Hachioji 192-0397, Japan*
[2] *Inorganic Functional Materials Research Institute, AIST, Nagoya, 463-8560, Japan*
[3] *Nanomaterials Research Institute, AIST, Tsukuba, 305-8565, Japan*
[4] *JST, PRESTO, Kawaguchi 332-0012, Japan*

Atomic-layer transition metal dichalcogenides (TMDCs) are attractive components for two-dimensional layered heterostructures because of their tunable electronic properties. To control their bandgap and carrier densities, there are several approaches such as chemical doping and alloying. In our previous works, we reported the growth of bandgap-tunable $Mo_{1-x}W_xS_2$ alloys [1] and highly-conductive $Nb_{1-x}W_xS_2$ alloys [2] using thin-film sulfurization. However, it is difficult to obtain large-area crystals using thin film sulfurization probably due to the limitation of nucleation densities. To solve this issue, we have developed a growth method of large-area, monolayer TMDC alloys using chemical vapor deposition (CVD) because of its tunability of supplying rate of precursors.

In this presentation, we report the growth and characterization of monolayer Nb-doped WS_2. Nb-doped WS_2 were grown on SiO_2/Si substrates by halide-assisted CVD method [3] using WO_3, Nb and NaCl powders at 800 ~ 850 °C under argon/sulfur atmosphere. Figure 1a shows an optical image of typical triangle-shaped crystals with a size of 20 μm on the SiO_2/Si substrate. Scanning transmission electron microscope (STEM) image indicates that a Nb atom is substitutional doped at W site (Fig. 1b). The crystals have two characteristic small Raman peaks at 380 cm^{-1} and 400 cm^{-1} between WS_2-E' and WS_2-A_1' peaks (Fig. 1c). These results suggest that the present approach enables large-area growth of Nb-doped WS_2 monolayers, and could provide an effective way to produce carrier-controlled TMDC-based heterostructures.

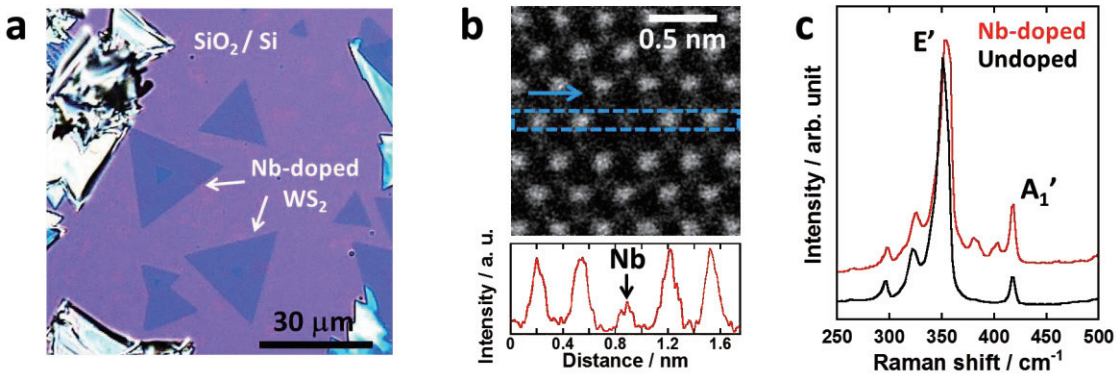

Fig. 1 (a) Optical image of typical monolayer Nb-doped WS_2 crystals grown on a SiO_2/Si substrate. (b) STEM image of monolayer Nb-doped WS_2. Transmitted electron intensity along the cross direction of blue box in the STEM image. (c) Raman spectra of undoped and Nb-doped WS_2 monolayers.

[1] Y. Kobayashi *et al.*, Nano Res. **8**, 3261-3271, (2015).
[2] S. Sasaki *et al.*, The 48th FNTG symposium.
[3] S. Li *et al.*, Applied Materials Today **1**, 60-66, (2015).
Corresponding Author: Yasumitsu Miyata, Tel: +81-42-677-2508, E-mail: ymiyata@tmu.ac.jp

Fabrication and manipulation of slidable atomic layers

○Yu Kobayashi[1], Takashi Taniguchi[2], Kenji Watanabe[2],
Yutaka Maniwa[1], Yasumitsu Miyata[1,3,*].

[1]*Department of Physics, Tokyo Metropolitan University, Hachioji 192-0397, Japan*
[2]*National Institute for Materials Science, Tsukuba 305-0044, Japan*
[3]*JST-PRESTO, Kawaguchi 332-0012, Japan*

Development of novel fabrication and manipulation techniques of atomic-layer heterostructures is one of the most important challenges to control their emergent electrical and optical properties. So far, the heterostructures have been prepared mainly by two major methods including transfer and direct-growth processes of graphene, boron nitride (BN), and transition metal dichalcogenides (TMDCs). As-prepared heterostructures are usually fixed and are used without any structural modification. If each layer could be slidable, we can control interlayer coupling by changing stacking orientation and create various heterostructures such as lateral and vertical junctions. However, there has been no report of such slidable atomic layers as yet probably due to large interlayer frictional force.

Here, we report the preparation and manipulation of slidable atomic layers in clean heterostructure systems. In this work, TMDC crystals were grown on exfoliated graphite and BN by chemical vapor deposition as reported in our previous work [1]. We found that such systems have very small interlayer frictional force because of their clean interface and atomically-flat van der Waals surfaces. For example, a WS_2 crystal can be smoothly moved on graphite by manipulation with a tip (Fig.1). Furthermore, this sliding process also allows us to suspend and tear atomic layers, and to prepare vertically-stacked and lateral heterostructures by connecting it to another crystal (Fig. 1c). Our findings provide a novel, effective way to realize a wide variety of atomic-layer heterostructures.

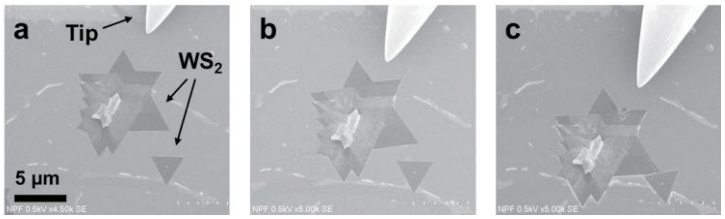

Fig.1 (a-c) SEM images of moving WS_2 crystals grown on graphite by prober-tip.

A part of this work was conducted at the AIST Nano-Processing Facility, supported by "Nanotechnology Platform Program" of the Ministry of Education, Culture, Sports, Science and Technology (MEXT), Japan.

[1] Y. Kobayashi *et al.*, ***ACS Nano***, 9, 4056 (2015).

Corresponding Author: Yasumitsu Miyata, Tel: 042-677-2508, E-mail: ymiyata@tmu.ac.jp

2P-42

Interlayer excitons in high-quality MoS_2/WS_2 vertical heterostructures

○Tetsuki Saito[1], Yu Kobayashi[1], Kenji Watanabe[2], Takashi Taniguchi[2], Yutaka Maniwa[1], Yasumitsu Miyata[1,3]

[1]*Department of Physics, Tokyo Metropolitan University, Hachioji, 192-0397, Japan*
[2] *National Institute for Materials Science, Tsukuba 305-0044, Japan*
[3]*JST, PRESTO, Kawaguchi, 332-0012, Japan*

Heterostructures of transition metal dichalcogenides (TMDCs) have attracted attention because of their emergent optical and electronic properties. As a representative example, the presence of interlayer excitons has been reported for TMDC-based vertical heterostructures [1,2]. However, in previous studies, an observed photoluminescence (PL) peak relating to the interlayer excitons has relatively-large linewidth probably due to the presence of inhomogeneous broadening. To solve this issues, we have developed the CVD process of TMDCs with highly-uniform optical spectra and their heterostructures [3,4]. Here, we report on the observation of sharp PL peaks in high-quality MoS_2/WS_2 vertical heterostructures.

Vertical MoS_2/WS_2 heterostructures are grown on boron nitride (BN) substrates by two-step CVD. The presence of a monolayer WS_2 grain on a triangle-shaped monolayer MoS_2 was confirmed from an atomic force microscope (AFM) image (Fig.1a) and Raman/PL maps. This heterostructure shows three PL peaks between 1.4~1.7 eV (Fig.1b). These fine structures of PL have never been observed in the previous CVD-grown MoS_2/WS_2 heterostructure [2], and can be tentatively assigned to the direct and indirect optical transitions as shown in Fig.1c. Interestingly, only I3 PL peak has redshift with increase in temperature. Compared to the band structures considering thermal expansion, I3 peak can be assigned to the interlayer-derived direct transition at K point. The present results indicate that the high-quality heterostructures are an ideal system for the precise understanding of interlayer coupling.

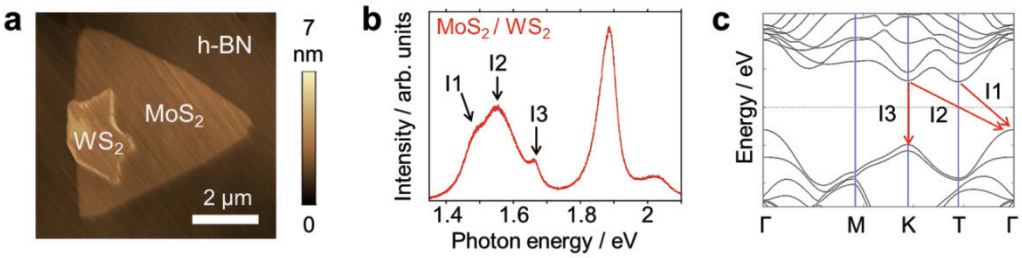

Fig.1 (a) AFM image and (b) PL spectrum of the MoS_2/WS_2 vertical heterostructure on BN. (c) Band structure of the MoS_2/WS_2 vertical heterostructure obtained from first-principles calculations.

[1] P. Rivera, *et al*., Nat. Commun. 6. 6242 (2015), [2] Y. Gong, *et al*., Nat. Mater. 13, 1135 (2014).
[3] Y. Kobayashi, *et al*., ACS Nano 9, 4056 (2015). [4] S. Yoshida. *et al*., Sci. Rep. 8, 14808 (2015).

Corresponding Author: Yasumitsu Miyata, Tel: 042-677-2508, E-mail: ymiyata@tmu.ac.jp

High-Performance Complementary Inverters of Large-Area Transition Metal Dichalcogenide Monolayers

○Jiang Pu [1], Kazuma Funahashi [1], Chang-Hsiao Chen [2], Ming-Yang Li [3,4], Lain-Jong Li [4], and Taishi Takenobu [1,5]

[1] *Department of Advanced Science and Engineering, Waseda Univ., Tokyo 169-8555, Japan*
[2] *Dept. of Automatic Control Engineering, Feng Chia University, Taichung 40724, Taiwan*
[3] *Research Center for Applied Sciences, Academia Sinica, Taipei 10617, Taiwan*
[4] *Physical Sciences and Engineering Division, KAUST, Thuwal 23955-6900, Saudi Arabia*
[5] *Kagami Memorial Laboratory, Waseda University, Tokyo 169-0051, Japan*

The ultra-thin thickness of transition metal dichalcogenide (TMDC) monolayers ensures an ultimately thin transistor active channel, which offers more efficient electrostatic controllability than bulks and results in a high on/off current ratio of > 10^6 and a low subthreshold swing *S* of 60 mV/dec [1]. Importantly, the large on/off ratio and small *S* are crucial for designing high-performance complementary metal-oxide-semiconductor (CMOS) inverters. Although excellent p-type and n-type transistors have been demonstrated in mechanical-exfoliated TMDC monolayers, it is still difficult to apply these devices for CMOS inverters. Firstly, a CMOS inverter must combine p-type transistors with n-type transistors and the method used for reproducible fabrication is crucial for realizing superior device performance. However, it is almost impossible for exfoliated samples to overcome and the switching performance of CMOS inverters is still limited, resulting in a low voltage gain and/or large power consumption [2]. Moreover, although CMOS inverters with low power consumption is recently reported, the typical film sizes of exfoliated samples are less than 10 μm^2, which are not suitable for scalable integration [3]. Considering these obstacles, we focus on the wafer-scale uniform TMDC monolayers grown by chemical vapor deposition (CVD) methods, and it is mandatory to demonstrate high-performance CMOS inverters.

Here, we demonstrated CMOS inverters using CVD-grown large-area WSe_2 and MoS_2 monolayers [4,5]. In particular, ion gels, i.e., gelated ionic liquids, are adopted for use as a gate electrolyte to tune the material polarities via efficient switching control due to high specific capacitance. By combining p-type WSe_2 and n-type MoS_2 transistors, we realized CMOS inverters with the highest voltage gain (> 100) among the 2D materials. Furthermore, in order to address the practical applications, we also demonstrated the optimized inverter characteristics which involved excellent total noise margin (> 95%), low power consumption (~200 pW), and good switching speed (~1 kHz) without compromising proper gain (Fig. 1).

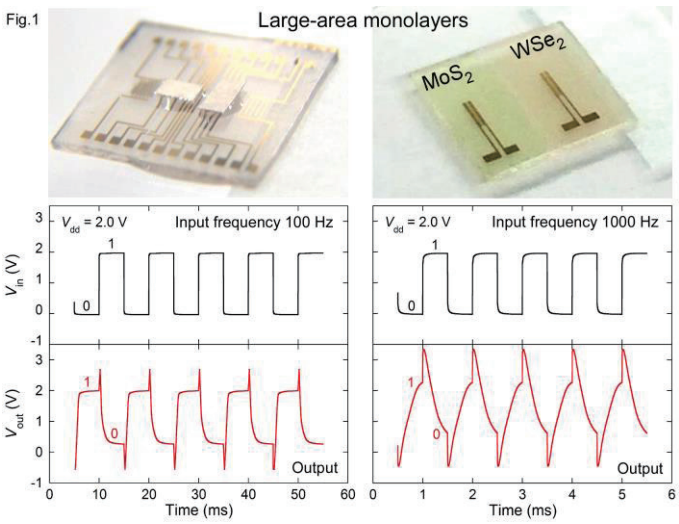

[1] G. Fiori *et al*., *Nat. Nanotechnol.* **9**, 768 (2014).
[2] M. Tosun *et al*., *ACS Nano* **8**, 4948 (2014).
[3] P. J. Jeon *et al*., *ACS Appl. Mater. Interfaces* **7**, 22333 (2015).
[4] J. K. Huang, J. Pu, *et al*. *ACS. Nano.* **8**, 923 (2014).
[5] Y. H. Chang, J. Pu, *et al*. *ACS. Nano.* **8**, 8582 (2014).

Corresponding Author: J. Pu, T. Takenobu
Tel/Fax: +81-3-5286-2981
E-mail: hokoh.apple@fuji.waseda.jp
takenobu@waseda.jp

Photoluminescence Quantum Yield and Exciton Radiative Lifetime in Monolayer WSe_2

○N. Baizura Mohamed, Koirala Sandhaya, Feijiu Wang, Hong En Lim, Shinichiro Mouri, Yuhei Miyauchi and Kazunari Matsuda

Institute of Advanced Energy, Kyoto University, Uji, Kyoto 611-0011, Japan

The discovery of intriguing and unique properties of graphene has opened new research fields in atomically thin-layered two-dimensional (2D) materials [1]. The atomically thin semiconducting transition metal dichalcogenides (TMDs), MX_2 (M = Mo, W; X = S, Se, Te), with a few nanometer thickness of its monolayer, have attracted great research interest in recent years due to novel fundamental physics and potential applications of optoelectronic devices [2,3]. It is essential to obtain the radiative lifetimes of excitons (electron-hole pair) and its radiative photon emission efficiency, i.e. photoluminescence (PL) quantum yield, both from viewpoint of fundamental research and optical device applications [4].

In this study, we have experimentally evaluated the PL quantum yield and intrinsic exciton radiative lifetimes of semiconducting monolayer WSe_2. Figure 1(a) shows the excitation power dependence of PL spectra of monolayer WSe_2 at room temperature. The PL intensity linearly increases at lower excitation conditions below 60 W/cm^2. The PL quantum yield of WSe_2 was estimated using the data of PL intensity at lower excitation condition and absorbance as about 0.04 %, evaluated by the relative-method using highly fluorescent dye as a standard reference [5]. We also conducted the time-resolved PL spectroscopy at room temperature, as shown in Fig. 1(b). The exciton radiative lifetime of ~ 1.2 μs was evaluated from the PL quantum yield and PL decay time of ~ 500 ps. Our experimental result of considerably long exciton radiative lifetime was about three-orders of magnitude larger compared to the theoretically predicted values of ns at room temperature [6]. The very long exciton radiative lifetime of monolayer WSe_2 can be explained by contribution of the dark states and finite exciton coherence length (coherence area in 2D system).

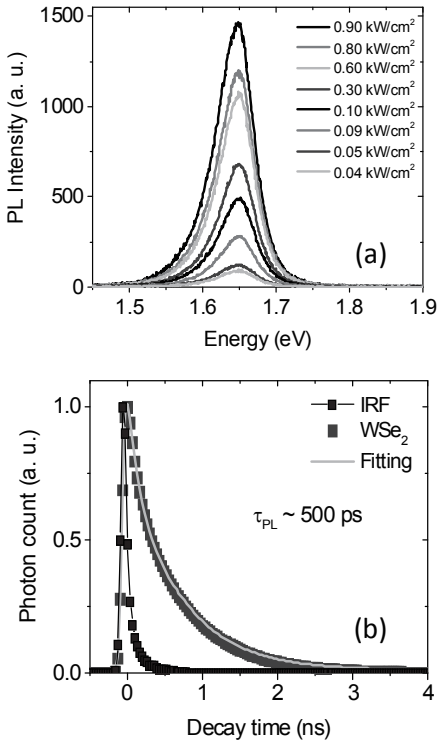

Figure 1: (a) Excitation power dependence of PL spectra for WSe_2, (b) PL decay profile at 2.25 eV excitation photon energy.

[1] A. K. Geim *et al.*, *Nat. Mat.* **6**, 183 (2007).
[2] A. Splendiani *et al.*, *Nano Lett.* **10**, 1271 (2010).
[3] G. Eda *et al.*, *ACS Nano* **7**, 5660 (2013).
[4] H. Wang *et al.*, arXiv:1409.3996v1 (2014).
[5] A. Wakamiya *et al.*, *Angew. Chem. Int. Ed.* **46**, 4273 (2007).
[6] M. Palummo *et al.*, *Nano Lett.* **15**, 2794 (2015).

Corresponding Author: N. Baizura Mohamed
Tel: +81-774-38-3460
Fax: +81-774-38-3460
E-mail: nur.mohamed.26v@st.kyoto-u.ac.jp

Optical Absorption Spectra of MoS_2 Monolayer Crystals under Tensile Strain

○Musashi Fukumura, Kotaro Homma, Junji Nozaki, Yutaka Maniwa, Kazuhiro Yanagi

Department of Physics, Tokyo Metropolitan University, Tokyo 192-0397, Japan

Monolayer transition metal dichalcogenides (TMDCs) are atomically thin materials, and they have attracted a lot of interest because of their remarkable physical and electronic properties such as direct gap optical characteristics, electroluminescence, high carrier mobility, and valley spin polarization. Especially, remarkable piezoelectricity has been reported.[1] When strain is applied in the arm chair direction, charges of opposite polarity are induced at the zig-zag edges of a monolayer MoS_2 flake, and then piezoelectric voltage and current out put were observed with increasing strain.[1] Strains significantly influence on the electronic structures of MoS_2, thus in this study we investigated how their optical absorption spectra are influenced by strain.

MoS_2 monolayer thin films are synthesized using chemical vapor deposition (CVD) methods. In this study, we used Ar + H_2 gas flow for reduction of MoO_3 powders and N_2 gas for growth. Thus prepared MoS_2 monolayer crystals were transferred using a PMMA polymer to a silicone rubber sheet with very high optical transparency. Then we investigated their optical absorption spectra under strain.

Figure 1 (a) and (b) show photoluminescence (PL) images of MoS_2 on non-stretched and 5% stretched silicone rubber with conventional optical microscope using 532 nm laser excitation. As shown here, slight decrease of PL intensities was observed. Then we investigated their optical absorption spectra using a super-continuum light source. Figure 1 (c) indicates the optical absorption spectra of MoS_2 on non-stretched and 5% stretched silicone rubber. When we stretched the rubber, we found clear shift of the A peak optical absorption peak and slight decrease of its absorbance, suggesting significant influences of tensile strains on their electronic properties.

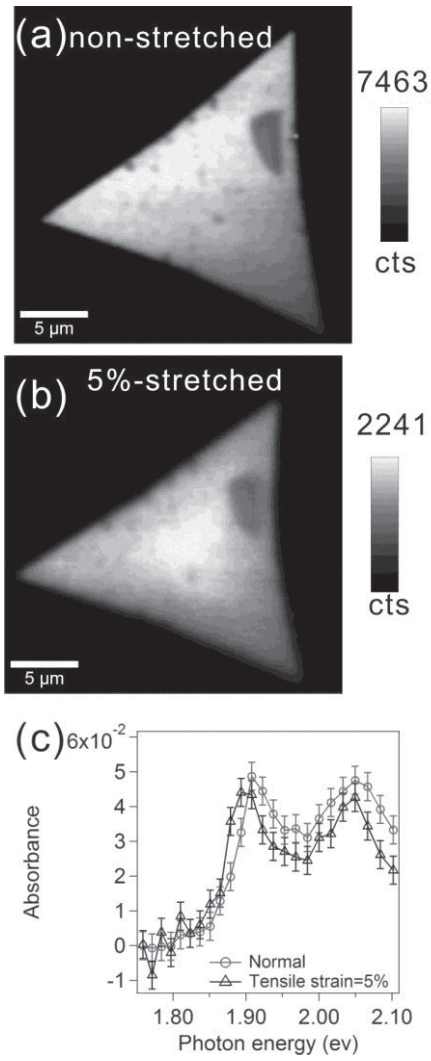

Figure 1. PL mapping images of MoS_2 on (a) non-stretched and (b) 5% stretched silicone rubber. (c) Optical absorption spectra

[1] W. Wu et al., Nature 514, 470 (2014).

Corresponding Author: Kazuhiro Yanagi
Tel: +81-42-677-2494
E-mail: yanagi-kazuhiro@tmu.ac.jp

2P-46

Fluorination and annealing effects on magnetism and structure of nanodiamond

○Kenta Kogane[1] ・Hidekazu Touhara[2] ・Yoshiyuki Hattori[2] ・
Vladimir Osipov[3] ・Nickolai Romanov[4] ・Kazuyuki Takai[1, 5]

[1]*Graduate School of Science and Engineering, Hosei University, Tokyo 184-8584, Japan*
[2]*Faculty of Textile Science and Technology, Shinshu University, Nagano 386-8567, Japan*
[3]*Ioffe Physical-Technical Institute, St.Petersburg 194021, Russia*
[4]*Peter the Great St.Petersburg Polytechnic University, St.Petersburg 195251, Russia*
[5]*Faculty of Bioscience and Applied Chemistry, Hosei University, Tokyo 184-8584, Japan*

Nanodiamond (ND) is featured with the large surface area as well as many excellent properties of bulk diamond, although it has a problem of aggregation [1]. Fluorination of ND is expected not only to stabilize the surface structure for disaggregation, but also to introduce functional groups on the surface, the conduction carriers, and so on [2]. In this study, we evaluate the structure and magnetic properties of ND and fluorinated nanodiamond (FND) in order to consider the change in the electronic states and the surface structure by fluorination by using X-ray diffraction (;XRD, Mo Kα), X-ray photoemission spectra (;XPS, Al Kα), infrared (;IR) absorption spectroscopy and electron spin resonance (;ESR, X-band).

FND was synthesized by the direct reaction between detonation nanodiamond and 1 atm of fluorine gas at the temperature of 623 K, 773 K and 873 K for several days. Hereafter, each sample is labeled as FND623K, FND733K, and FND873K according to the maximum temperature during synthesis, while Non-fluorinated one is referred to as ND. XRD profile reveals that well crystalline diamond core structure with a diameter of 3 – 4 nm in all samples and the fluorination only at the surface part in FNDs. According to XPS, the fluorine content increases up to F/C = 0.2 for FND873K with increasing fluorination temperature with formation of C-F bonding, supported by IR. For both of NDs and FNDs, ESR linewidth decreases and becomes a minimum upon annealing (fluorination) temperature, and eventually increasing with the further raising of the temperature (Fig. 1). This is mainly attributed to the structural relaxation by heat-treatment [3]. Subtracting the contribution of the heat-treatment effect, FNDs shows increasing in the linewidth of 0.05 – 0.1 mT. The hybridization of the spin state with the fluorine orbitals having the larger hyperfine coupling is responsible for the increment in the linewidth in FNDs.

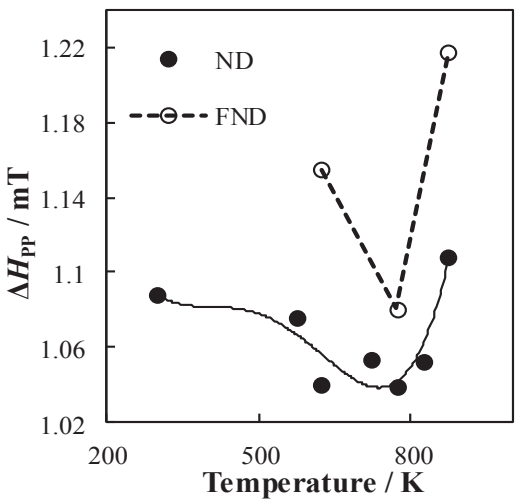

Fig. 1 Annealing temperature dependence of ESR linewidth

[1] Eiji Osawa, *Journal of the surface science society of japan*, **30**, 258-266 (2009).
[2] Hidekazu Touhara, Akiko Yonemoto, *Nanocarbon Handbook*, part**3**, chapter 4 (2007).
[3] J.W. Park, *Current Applied Physics*, **6**, 188–193 (2006).

Corresponding Author: Kazuyuki Takai
Tel: +81-42-387-6138, Fax: +81-42-387-7002
E-mail: takai@hosei.ac.jp

2P-47

Synthesis of carbon nanoballoon and evaluation of its catalytic activity in direct methanol fuel cells

○T. Ohiro[1], K. Mizui[1], Y. Suda[1] T. Harigai[1], H. Takikawa[1], H. Ue[2]

[1] *Department of Electrical and Electronic Information Engineering, Toyohashi University of Technology, Toyohashi, Aichi 441-8580, Japan*
[2] *Fuji Research Laboratory, Tokai Carbon Co., Ltd., Oyama, Shizuoka 410-1431, Japan*

1. Introduction

Carbon black, nanometer-size carbon particles, is commercially used as the catalyst support in fuel cell owing to its high surface area, porosity, electric conductivity, low density, and low cost. In the previous work, we have used various carbon nanomaterials as catalyst supports for direct methanol fuel cells (DMFC) [1]. In this study, we used carbon nanoballoon (CNB) as a catalyst support and measured the catalytic activity of CNB-supported PtRu catalyst.

2. Experimental

The twin-torch arc discharge apparatus was used for AcB synthesis. CNB was prepared by a heat treatment in Ar gas at 2600°C [2]. The particle shape of CNB is hollow. CNB is graphitic and has high conductivity. We prepared PtRu catalysts for the DMFC anode. The PtRu catalysts were loaded onto CNB by the reduction method using sodium boron hydrate ($NaBH_4$), and a counterpart employing the commercial Vulcan-supported PtRu catalyst was also prepared.

3. Results

Table 1 shows the electrical conductivity, the electrochemically active surface area (ECSA) and the peak current density during methanol oxidation reaction (MOR) of the PtRu catalysts. The catalyst activity of catalyst-supported CNB was better than that of catalyst-supported of Vulcan. This is mainly due to the higher electrical conductivity in the anode catalyst layers benefiting from the structure of CNB.

Table 1. Electrochemical properties of PtRu catalyst particles loaded on carbon nanoballoon and Vulcan

	Electrical conductivity /Ω^{-1} m^{-1}	ECSA/m^2 g^{-1}	Peak current density/mA cm^{-2}
PtRu/CNB	43.4	53.8	2.07
PtRu/Vulcan	17.5	16.8	0.39

This work has been partly supported by the EIIRIS Project from Toyohashi University of Technology (TUT); JSPS KAKENHI Grant Number 24360108 and 15K13946; and the Toyota Physical and Chemical Research Institute, "Scholar Project".

[1] Y. Suda *et al*. Materials Today Communications. Vol 3, pp. 96-103 (2015).
[2] T. Ikeda *et al*. Japanese Journal of Applied Physics Vol 50, 01AF13 (2011).

Corresponding Author: Y. Suda
Tel: +81 532 44 6726, Fax: +81 532 44 6757
E-mail: suda@ee.tut.ac.jp

Acceleration of separation velocity in electric-field-induced layer formation method by adjusting surfactant concentration

○Fusako Sasaki[1], Fumiyuki Nihey[2], Yuki Kuwahara[1,3], Hiroyuki Endoh[2], Shinichi Yorozu[2], Takeshi Saito[1,3*]

[1] *Technology Research Association for Single Wall Carbon Nanotubes, Tsukuba 305-8565, Japan*
[2] *Smart Energy Research Laboratories, NEC Corporation, Tsukuba 305-8501, Japan*
[3] *National Institute of Advanced Industrial Science and Technology, Tsukuba 305-8565, Japan*

The electric-field-induced layer formation (ELF) method had been recently proposed as an ionic-contamination-free method for separating metallic and semiconducting single-wall carbon nanotubes (m- and sc-SWCNTs) [1]. However, probably due to the low responsiveness of nonionic surfactant to electric field, the separation velocity in ELF method was relatively slow, which was still remained as an important issue. In this presentation, we report the effect of adjusting the surfactant concentration in ELF on the separation velocity.

In this work, SWCNTs synthesized by eDIPS [2] were dispersed in aqueous solutions of polyoxyethylene (100) stearyl ether (Brij S100) with the concentrations of 0.25 and 1 wt% by sonication and ultracentrifugation for ELF separation experiments. The typical optical absorption spectra of separated fractions (0.25 wt%) shown in Fig. 1 support the effective enrichment of m- and sc-SWCNTs. Figure 2 plots the condensing velocity of sc-SWCNTs layer that suggests the acceleration of separation process by reducing the Brij concentration. The other results will be reported in the presentation.

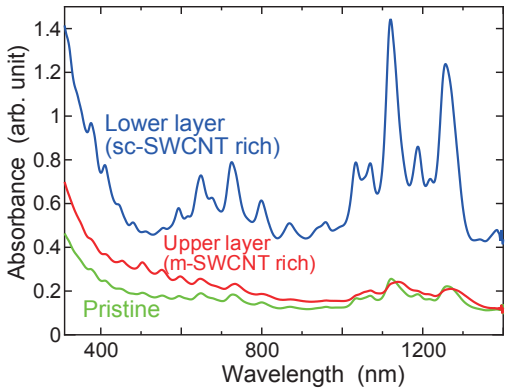

Fig. 1 Typical optical absorption spectra of separated m- and sc-SWCNTs.

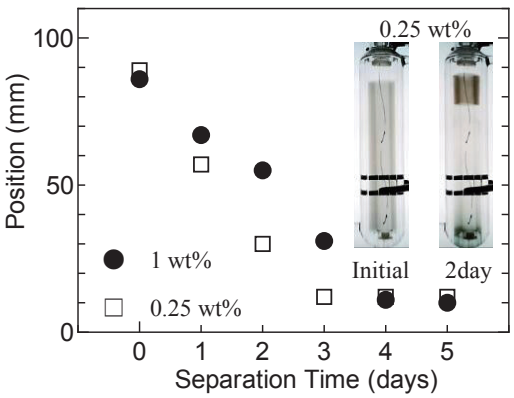

Fig. 2 The position (top face) of condensing sc-SWCNTs layer in the case of 0.25 wt% and 1 wt%.

Acknowledgment: This presentation is based on results obtained from a project subsidized by the New Energy and Industrial Technology Development Organization (NEDO).

References: [1] K. Ihara et al., J. Phys. Chem. C 115, 22827 (2011).
[2] T. Saito et al., J. Nanosci. Nanotechnol. 8, 6153 (2008).

***Corresponding Author:** Tel: +81-29-861-4683, Fax: +81-29-861-4413, E-mail: takeshi-saito@aist.go.jp

Carrier Injections on WS_2 Nanotube Networks by Electrochemical Doping Techniques

○Mitsunari Sugahara, Yoshimasa Kitamura, Yuki Oshima, Hideki Kawai, Kazuhiro Yanagi

Department of Physics, Tokyo Metropolitan University, Tokyo 192-0397, Japan

Thermoelectrics are one of very important technologies to efficiently convert waste heat to electric power. Hicks and Dresselhaus have proposed that the performance can be significantly enhanced using low-dimensional materials, and one-dimensional materials are the most promising for thermoelectric devices with highest performance.[1] Single wall carbon nanotubes are a model for one-dimensional materials, and we have investigated the Fermi level dependence of their thermoelectric properties. We found significant enhancement of their power factor,[2,3] however, the large thermal conductance in a single rope of SWCNT has been a week point for their thermoelectric applications. Therefore, it is also important to investigate other one-dimensional materials to realize the highest thermoelectric performance of one-dimensional materials. There are a plenty of one-dimensional materials, however, we have to use materials whose Fermi level will be well controlled because the thermoelectric performance strongly depend on the position of the Fermi level.[2,3] In this study, we investigated WS_2 multi-layered nanotubes because they have less dangling bonds on their surfaces, which will enable us to shift the Fermi level by electrochemical doping approaches. Previously, field effect transport characteristics of a single rope of WS2 nanotube were reported,[4] suggesting capability of control of electrical properties by carrier injection.

First we dispersed WS_2 nanotubes (NanoMaterials Co.) to toluene solutions and deposited on gold electrodes and investigated Raman intensities with carrier injections using ionic liquid gating. Here carriers were injected to WS2 nanotubes through formation of electric double layers on their surfaces by side-gating. Figure 1 shows the Raman spectra of WS_2 nanotube networks as a function of gate voltages. As shown in Fig. 1, the Raman peak originating from WS_2 nanotubes was significantly changed by the positive shift of the reference voltage. The results suggested that the electron injections on the WS_2 nanotube networks were possible. Then we fabricated their thin films and clarified their transport properties. The results suggested that optical and electrical properties of WS_2 nanotube network films were controllable by electro-chemical doping approaches.

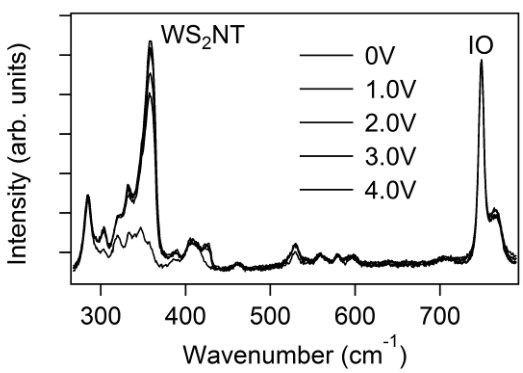

Figure 1. Raman spectra of WS_2 nanotube networks as a function of gate voltages. WS_2NT and IO indicate peaks originating from WS_2 nanotubes and ionic liquid we used.

[1] Hicks & Dresselhaus, Phys. Rev. B 47, 16631 (1993).
[2] K. Yanagi *et al.*, *Nano Lett.* 14, 6437 (2014)
[3] Y. Oshima, Y. Kitamura, Y. Maniwa, K. Yanagi, *Appl. Phys. Lett.* 107, 043106 (2015)
[4] R. Levi *et al.*, *Nano Lett.* 13, 3736 (2013)

Corresponding Author: Kazuhiro Yanagi
Tel: +81-42-677-2494
E-mail: yanagi-kazuhiro@tmu.ac.jp

Degradation of organic dyes under ultraviolet light condition with carbon nanocapsule encircled by nickel nanoparticle composites

○Jeong Won Ko[1], Hae Soo Park[1], Jiulong Li[1], Weon Bae Ko[1,2]

[1]*Department of Convergence Science, Graduate School, Sahmyook University, Seoul 139-742, South Korea,* [2] *Department of Chemistry, Sahmyook University, Seoul 139-742, South Korea*

In this work, we got a novel product of carbon nanocapsule encircled by nickel nanoparticle composites by the reaction of [C_{70}]fullerene and nickel hydroxide at 700 ℃ for 2 h. The carbon nanocapsule encircled by nickel nanoparticle composites were characterized by X-ray diffraction, scanning electron microscopy, transmission electron microscopy. It may be confirmed the structure of [C_{70}]fullerene changed into capsule like type of carbon nanomaterials and nickel nanoparticles were surrounded by carbon nanocapsules using TEM. The carbon nanocapsule encircled by nickel nanoparticle composites were evaluated as a photocatalyst in the degradation of organic dyes under ultraviolet light at 254 nm.

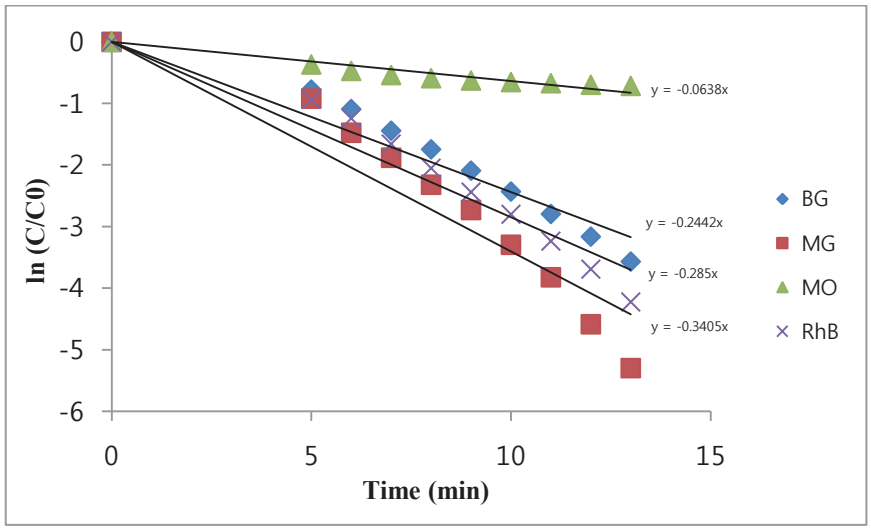

Fig.1 Photocatalytic activity for organic dyes degradation under ultraviolet light using carbon nanocapsule encircled by nickel nanoparticle composites

[1] S. K. Hong, J. H. Lee and W. B. Ko, *J. Nanosci. Nanotechnol*., **11,** 6049 (2011).
[2] H. S. Park and W. B. Ko, *J. Nanosci. Nanotechnol*., **15,** 8215 (2015).

Corresponding Author: W. B. Ko
Tel: +82-2-3399-1700, Fax:, +82-2-979-5318,
E-mail: kowb@syu.ac.kr

ESR measurement of molecular oxygen in openC_{60}

○Azusa Kato[1], Tsukasa Futagoishi [2], Yasujiro Murata[2], Tatsuhisa Kato [1,3]

[1] *Graduate School of Human and Environmental Studies, Kyoto University, Kyoto 606-8501, Japan*
[2] *Institute for Chemical Research, Kyoto University, Kyoto 611-0011, Japan*
[3] *Institute for Liberal Arts and Sciences, Kyoto University, Kyoto 606-8501, Japan*

Molecular oxygen (O_2) is a fundamental bi-radical molecule. The electron spin resonance (ESR) absorption of O_2 in the electronic ground state, $^3\Sigma_g^-$, has been studied in the gas phase, and the detailed analysis was well documented. However few observations have been described for O_2 in condensed phase because of the difficulty in stable trapping of the molecule. Some ESR measurements reported the spectrum of O_2 trapped in a few matrices at the temperature below 10K, and the line broadening mechanism led to the absence of the ESR signal above 10K. [1] We performed the molecular surgery synthesis of the endohedral fullerene of O_2@openC_{60}, in which O_2 is trapped in the inside of openC_{60} cage, and succeeded in obtaining clear ESR spectra of O_2 in frozen solution and powder forms at various temperatures.

X-band and W-band ESR measurements at cryogenic temperatures were carried out with Bruker E500 and E680 spectrometers equipped by Oxford 900 and CF935 helium cryostats respectively. Simulations of ESR spectra were carried out by using EasySpin package with MATLAB program.

X-band ESR spectra of O_2@openC_{60} powder were observed at temperatures from 4K to 64K, as shown in Fig. 1. The W-band ESR spectrum in toluene solution was also obtained at 10K. All spectra were recorded at the position of resonance field expected from the energy levels of the spin system with S=1, and well simulated by using ESR parameters in Table.1. The temperature dependence of signal intensity correctly obeyed the Boltzmann statistics in the energy levels without any unexpected broadening effect.

Table.1 ESR parameters of O_2@openC_{60}

g	D / cm^{-1}	E / cm^{-1}	ΔH / mT
2.0023	3.73	0.015	20

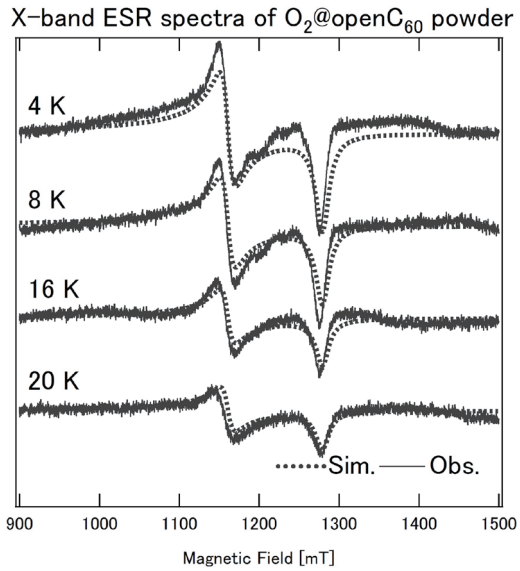

Fig.1 X-band ESR spectra of O_2@openC_{60} powder observed at 4K, 8K, 16K, and 20K (Obs.). And simulated spectra (Sim.).

[1] Hideo Kon, *J. Am. Chem. Soc.* **95**, 1045-1049 (1973).

Corresponding Author: Tatsuhisa Kato
Tel: +81-75-753-6695, Fax: +81-75-753-6695,
E-mail: kato.tatsuhisa.6e@kyoto-u.ac.jp

Macroscopic Preparation and Isolation of La@C_{60} as a Trifluoromethyl Derivative

○Katsuma Ishino[1], Shinobu Aoyagi[2], Haruka Omachi[1], Zhiyong Wang[1], Hiroyuki Niwa[1], Ayano Nakagawa[1], Ryo Kitaura[1], and Hisanori Shinohara[1]

[1] *Graduate School of Science, Nagoya University, Nagoya 464-8602, Japan.*
[2] *Department of Information & Biological Science, Nagoya City University, Nagoya 467-8501, Japan.*

The macroscopic preparation and isolation of M@C_{60}-type metallofullerenes has been a long-standing challenge in fullerene science, since M@C_{60} is one of the most interesting fullerenes due to its theoretically predicted fascinating properties like superconductivity. Although the first production of La@C_{60} can be traced back to a week after the discovery of C_{60} in 1985 [1], its complete separation/purification has not yet been achieved. Highly reactive La@C_{60} has led to readily form insoluble polymers in arc-processed soot. This has precluded so far the isolation of La@C_{60} from other fullerenes by liquid chromatographic techniques.

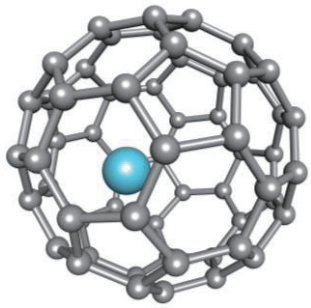

Fig. 1 A schematic view of La@C_{60}

Here we demonstrate the first isolation of the missing metallofullerene La@C_{60} as a trifluoromethyl derivative, which was prepared by using the *in situ* exohedral trifluoromethyl functionalization method we developed[2]. Solubilization of La@C_{60} by trifluoromethyl groups can lead to chromatographic separation. In laser desorption mass spectroscopy of the isolated derivative, an intense peak of La@$C_{60}(CF_3)_4$ was observed with their fragments (Fig. 2). Optical absorption analyses indicate that the HOMO- LUMO gap of La@$C_{60}(CF_3)_4$ is ca.1.7 eV, suggesting that this derivative is almost as stable as C_{60}.

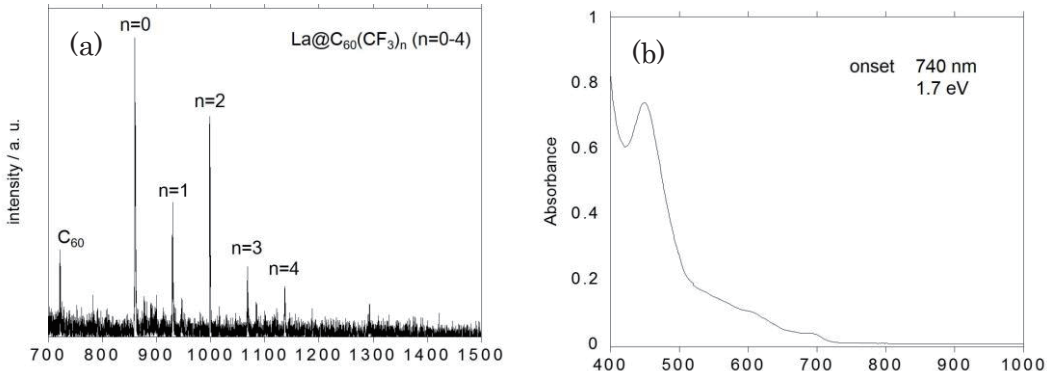

Fig. 2 MALDI-TOF mass spectrum (a) and optical absorption spectrum (b) of La@C_{60} derivative.

[1] J. R. Heath *et al.*, ***J. Am. Chem. Soc.***, 107, 7779 (1985). [2] (a) Z. Wang *et al.*, ***Angew. Chem. Int. Ed.***, 52, 11770 (2013). (b) Z. Wang *et al.*, ***Angew. Chem. Int. Ed.***, early view.

Corresponding Author: Hisanori Shinohara
Tel: +81-52-789-2482, Fax: +81-52-747-6442, E-mail: noris@nagoya-u.jp

Preparation, Structural Determination, and Characterization of Electronic Properties of Carbosilylated $Sc_3N@I_h$-C_{80}

○Takeshi Sugiura[1], Shinpei Fukazawa[1], Kyosuke Miyabe[1], Masahiro Kako[*,1], Masanori Yasui[1], Michio Yamada[2], Mitsuaki Suzuki[2], Yutaka Maeda[2], Takeshi Akasaka[2,3,4]

[1]*Department of Engineering Science, The University of Electro-Communications, Chofu, Tokyo 182-8585, Japan*
[2]*Department of Chemistry, Tokyo Gakugei University, Tokyo 184-8501, Japan*
[3]*Life Science Center of Tsukuba Advanced Research Alliance, University of Tsukuba, Tsukuba, Ibaraki 305-8577, Japan*
[4] *Foundation for Advancement of International Science, Ibaraki 305-0821, Japan*

The chemical functionalization of endohedral metallofullerenes (EMFs) has been extensively exploited from the synthetic viewpoints of various applications [1]. For example, the introduction of a silicon-based functionality into fullerene cages induces remarkable changes in the electronic characteristics of fullerenes. The photoreaction of disilirane with $Sc_3N@I_h$-C_{80}, which is the most abundant and well-studied trimetallic nitride template (TNT) EMF, has been reported to afford the corresponding bis-silylated adduct with significant electronic properties [1]. Conversely, the reaction of $Sc_3N@I_h$-C_{80} with silylene, which is a monosilylating reagent, provided trace amounts of silylated products, whereas the addition of silylene to $Lu_3N@I_h$-C_{80} afforded monosilylated adducts in moderate yields [2]. These results prompted us to study complementary bis-silylation and monosilylation reactions for the utilization of TNT EMFs as functional materials. Very recently, we reported the preliminary result that photoreaction of $Sc_3N@I_h$-C_{80} with silirane **1a** afforded two [5,6]-carbosilylated adducts **2a** and **3a**, and one [6,6]-adduct **4a** [3]. However, the characterization of **4a** was unsuccessful owing to its low product yield. Herein, we describe the details of the synthesis, characterization, and electronic properties of the carbosilylated $Sc_3N@I_h$-C_{80} obtained by photoreaction with **1b**.

Scheme 1.

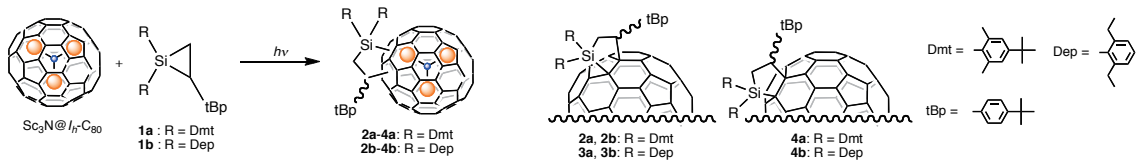

[1] M. Yamada, T. Akasaka Bull. Chem. Soc. Jpn. **87**, 1289–1314 (2014).
[2] K. Sato *et al.* J. Am. Chem. Soc. **134**, 16033–16039 (2012).
[3] M. Kako *et al.* Phosphorus, Sulfur, and Silicon and the Related Elements. in press.
Corresponding Author: Masahiro Kako Tel: +81-42-442-5570 E-mail: kako@e-one.uec.ac.jp

Pressure-induced transformations and light irradiation effects on ferrocene-doped C_{60} nanosheets

○Kyohei Kato[1], Hiromichi Gonnokami[1], Hidenobu Murata[1], Masaru Tachibana[1]

[1] *Department of Nanosystem Science, Yokohama City University, 22-2 Seto, Kanazawa-ku, Yokohama 236-0027, Japan*

Micro- and nano-crystals of fullerene C_{60} have attracted much interest due to their unique morphologies, structures and properties depending on solvents or dopants contained in C_{60} lattices. Recently, it was reported that ferrocene-doped C_{60} ($C_{60}(Fc)_2$) nanosheets with layer structure alternating C_{60} and ferrocene layers exhibited unique pressure-induced transformations, e.g. reversible polymerization of C_{60} at room temperature [1,2]. These are due to the charge transfer from ferrocene to C_{60} and the limited polymerization in 2D layer of C_{60} under pressure. We found that higher pressure gives rise to new polymeric phase of C_{60}. In addition, light irradiation led to not only the promotion of the pressure-induced transformations but also their modification. In this paper, we report the pressure-induced transformations of ferrocene-doped C_{60} nanosheets up to 12.5 GPa and their light irradiation effect.

$C_{60}(Fc)_2$ nanosheets were prepared by liquid-liquid interfacial precipitation method, in which an interface was formed between isopropyl alcohol and toluene [3]. For the high-pressure studies, a diamond anvil cell of CLOCK type generated pressrue and ruby luminescence method was used for pressure determination. Samples and ruby ball were loaded into a 300 μm diameter hole in a stainless-steel gasket. Silicone oil was used as pressure medium. The pressure-induced transformation of $C_{60}(Fc)_2$ were observed in in-situ Raman measurements at room temperature with a 532 nm Nd:YVO_4 as excitation. The excitation laser also served as the light irradiation.

The pressure dependence of the Raman spectra exhibits two main changes at 1.0 and 2.8 GPa, respectively. The former is the discontinuous change of the slope of the pressure dependence of the peak position of main Raman bands in C_{60} and ferrocene. The latter is the appearance of the shoulder, i.e. new peak, at the lower frequency than original $A_g(2)$ one of C_{60} by 10 cm^{-1}. These changes are associated with the orientation disorder-order transition and polymerization of C_{60}, respectively. It should be noted that higher compression at 12.5 GPa gives rise to new peaks at lower frequencies. These peak frequencies are much lower than original $A_g(2)$ one by 18 and 25 cm^{-1}, which are in good agreement with those of L-shape and 2D tetragonal polymeric phases, respectively, reported previously [4]. These polymeric phases are reversible with the pressure, which are different from those by light irradiation and high pressure and temperature reported previously [5]. These features of the pressure-induced polymers in $C_{60}(Fc)_2$ will be discussed comparing with the results by light irradiation.

[1] W. Cui *et al*., J. Phys. Chem. B **116**, 2643 (2012), [2] K. Kato *et al*., Trans. Mat. Res. Soc. Japan (in press), [3] T. Wakahara *et al*., J. Am. Chem. Soc. **131**, 9940 (2009), [4] D. Porezag *et al.,* Phys. Rev. B **52**, 14963 (1995), [5] A. M. Rao *et al*., Science **259**, 955 (1993).

Corresponding Author: M. Tachibana
Tel & Fax: +81-45-787-2307
E-mail: tachiban@yokohama-cu.ac.jp

Electronic and magnetic properties of pentaorgano[60]fullerenes under an external electric field

○Sho Furutani and Susumu Okada

Graduate school of Pure and Applied Sciences, University of Tsukuba
Tennodai, Tsukuba 305-8571, Japan

Due to the moderate chemical reactivity of fullerene molecules, fullerenes can form the various derivatives by attaching the functional groups onto the covalent network, which are constituent materials of photovoltaic and organic semiconductor devices. On the other hand, chemically functionalized fullerenes possess unusual electronic and magnetic properties due to the segmentation of their spherical π electron systems. Indeed, pentaorgano and decaorgano C_{60} molecules exhibit various spin polarized states as the ground states depending on the arrangement of functional groups attached to the cage. In the present work, we investigate the electronic and magnetic properties of pentamethyl C_{60} ($C_{60}(Me)_5$) and pentaphenyl C_{60} ($C_{60}(Ph)_5$) under an external electric field by using the density functional theory combined with the effective screening medium method.

Before examining the magnetic properties of $C_{60}(Me)_5$ and $C_{60}(Ph)_5$ under the electric field, we investigate the electrostatic properties of these pentaorgano C_{60}. Due to the asymmetric π electron network and the attached functional groups, the molecule has large potential difference between head and tail of 0.62 V arising form the dipole moment of the molecule. Five functional groups are attached to the C atoms surrounding one of twelve pentagons, leading to the spin polarization on the segmented pentagonal ring. Our calculation shows that the polarized electron spin on the pentagonal ring is robust against the carrier injection by the external electric field. Figure 1 shows the number of polarized electron spin, $\Delta\rho = \rho_{up} - \rho_{dn}$, as a function of the number of injected carrier. Injection of 1 hole into molecule leads to the triplet spin states with S=1 due to the doubly degenerated singly occupied states. On the other hand, the electron injection leads to the nonmagnetic ground states as the case of cyclopentadienyl anion. Furthermore, the number of polarized spin gradually decreases with increasing the electrons.

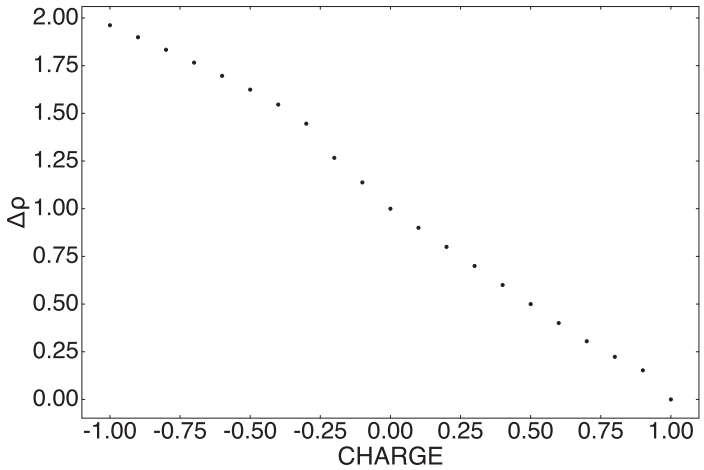

Fig.1: The number of polarized electron spin as a function of injected carriers.

Corresponding author: S. Furutani
Tel: +81-29-853-5600 (ext. 8233), Fax: +81-29-853-5924,
E-mail: sfurutani@comas.frsc.tsukuba.ac.jp

3P-7

Influence of deformations of carbon nanotubes on carrier accumulation under an electric field

Akiko Hasegawa and Susumu Okada

Graduate School of Pure and Applied Sciences, University of Tsukuba, Tennodai, Tsukuba 305-8571, Japan

It has been demonstrated that semiconducting carbon nanotubes (CNTs) can work as the conducting channel of field-effect transistors (FETs). In FET, it is plausible that the CNTs are deformed by the interaction with the substrates and other CNTs. However, it is still unclear how the carrier accumulation in CNT by the gate electrode depends on the structural deformation of CNTs in the FET structure. Thus, in the present work, we aim to investigate the influence of CNT deformation on carrier accumulation under the electric field by the gate electrode. All calculations are performed in the framework of the density functional theory (DFT) with local density approximation combining with the effective screening medium method to apply the external field on CNTs. In this work, we consider the structural model in which the deformed CNT is located above the planar gate electrode to simulate the CNT-FET device structure. As for the deformed CNTs, we consider (20,0) CNT with circular, squashed, and ellipsoidal cross sections.

Figure 1 shows the contour plot of the accumulated electrons by the external electric field. The injected electrons are mainly distributed at the electrode side of the CNTs. In addition to the electrode side of the CNT, we find the electron depletion and accumulation throughout the CNT, depending on their cross sections. For the circular CNT, charge oscillation occurs along their circumference [Fig. 1(a)]. In contrast, for the squashed and ellipsoidal CNTs, the electron density oscillates along the normal to the CNT walls [Figs. 1(b) and 1(c)]. In accordance with the carrier accumulation depending on CNT shapes, capacitance also depends on the cross section of CNTs.

Figure 2 shows the contour plot of the electrostatic potential and vector plot of the electric field of CNTs with the 0.2 electrons. We can find that the field concentration occurs around protruded areas with large curvature of circular and squashed CNTs [Fig. 2(a) and 2(b)]. On the other hand, the field does not concentrate for the CNT with the ellipsoidal shape [Fig.2 (c)].

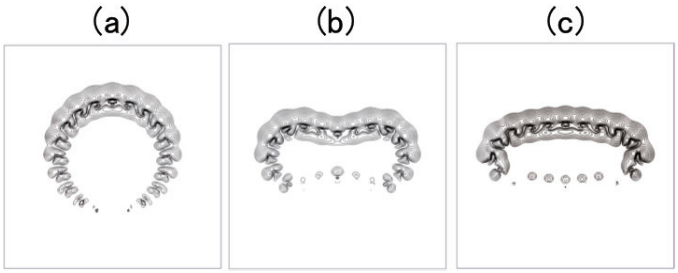

Fig.1: The contour plot of the charge redistribution of CNTs with (a) circular, (b) squashed, and (c) ellipsoidal cross section under the positive gate voltage injecting 0.2 electrons.

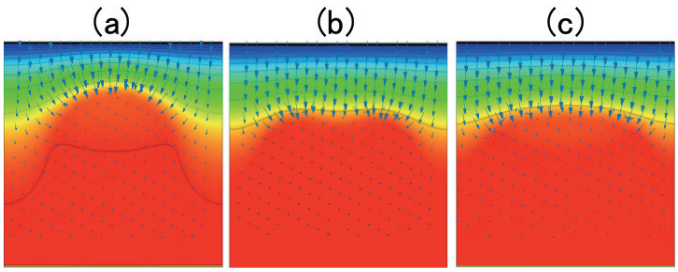

Fig.2: The contour and vector plots of electrostatic potential and electric field, respectively, of CNTs with (a) circular, (b) squashed, and (c) ellipsoidal cross sections under the positive gate voltage injecting 0.2 electrons.

Corresponding Author: A. Hasegawa
Tel: +81-29-853-5921, FAX: +81-29-853-5924
E-mail: sokada@comas.frsc.tsukuba.ac.jp

Exact Extraction of Transfer Length at Metal/Carbon Nanotube Contacts by Improved Transmission Line Method

○Noriyuki Tonouchi[1,3], Hiroyuki Endoh[1,3], Fumiyuki Nihey[1], Tomoyuki Yokota[2], and Takao Someya[2,3]

[1] Smart Energy Research Laboratories, NEC Corporation, Tsukuba 305-8501, Japan
Phone: +81-29-850-1157 E-mail: n-tonouchi@ab.jp.nec.com
[2] Department of Electrical Engineering, School of Engineering, The University of Tokyo, Tokyo 113-8656, Japan
[3] Institute for Nano Quantum Information Electronics, Tokyo 153-8505, Japan

To achieve high-frequency operation of carbon-nanotube thin-film transistors (CNT-TFTs), it is essential to reduce parasitic capacitances between device constituents such as a gate and a drain. Previously, we have reported high-frequency back-gated CNT-TFTs with narrow source/drain electrodes whose parasitic capacitances are greatly reduced. From a device design viewpoint, the electrode width (W_{el}) should be sufficiently larger than a transfer length (l_t) that scales a region required for electric carriers to be transferred from an electrode to an overwrapping CNT film at the electrode edge. In general, transmission line method (TLM) is used to obtain l_t by assuming that the sheet resistance of semiconductor channels that overwrap with electrodes (r_{sh2}) is the same as that in between the electrodes (r_{sh1}) as shown in Fig. 1. For CNT-TFTs, however, r_{sh2} should differ from r_{sh1} because of their very thin channels. Thus, it is necessary to evaluate r_{sh2} to obtain correct l_t. In this study, we propose improved transmission line method to extract the exact values of r_{sh2} and l_t.

We measured the voltage drop $V(W_{el})$ between the CNT film and the metal electrode at the opposite end of electrode. Figure 2 shows that $V(W_{el})$ depends exponentially on W_{el}, supporting the validity of our analytical method. Using the values of $V(W_{el})$ and contact resistance obtained by conventional TLM, we successfully extracted the exact values of r_{sh2} and l_t. They are different from those obtained by the conventional TLM by an order of magnitude. We revealed that it is necessary to deal r_{sh2} and r_{sh1} separately for the exact extraction of l_t and confirmed the effectiveness of our improved method.

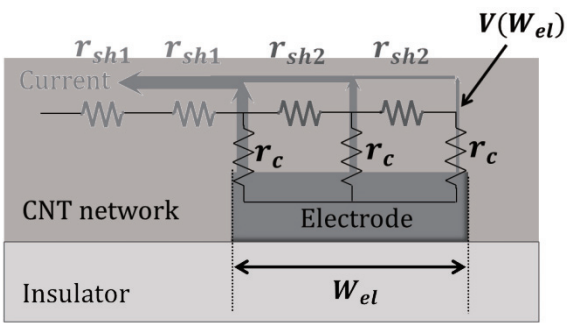

Fig. 1 Equivalent circuit around electrode

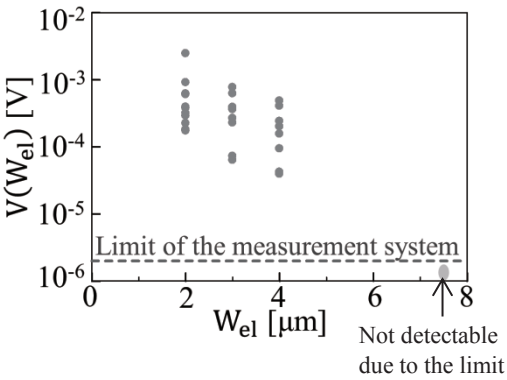

Fig. 2 Dependence of $V(W_{el})$ on W_{el}

Experimental investigation of thermal conductivity of single walled carbon nanotube thin film with infrared thermal imager

Ya FENG[1], Makoto WATANABE[1], Shuhei YOSHIDA[1], Taiki INOUE[1], Rong XIANG[1], Shohei CHIASHI[1], Shigeo MARUYAMA[1,2]

1. *Department of Mechanical Engineering, The University of Tokyo, Tokyo 113-8656, Japan*
2. *Energy NanoEngineering Lab., National Institute of Advanced Industrial Science and Technology, Tsukuba 305-8564, Japan*

In theory, single walled carbon nanotubes (SWNT) have been proven to be with extraordinarily high axial thermal conductivity owing to its unique quasi-one-dimensional structure[1], thus having been expected to mitigate the severe heat dissipation problem in the continuously shrinking electronic devices. In its bulk counterpart form, the ballistic phonon transfer is seriously impeded by the tube-tube interface scattering, but the remarkable thermal conductivity of single SWNT still boost the application of SWNT thin film as a thermal interface material[2]. Therefore, researches are extensively conducted, trying to precisely measure the thermal conductivity of carbon nanotube films grown in laboratory, which still remains quite a difficulty.

In the present work, we proposed a new method to directly measure the thermal conductivity of SWNT thin film. Two cantilevered silicon thin plates (thickness of 100μm) were joined with the SWNT thin film in between them, while the other ends were respectively bathed in different temperatures to form a steady state heat flow along. With the infrared thermal imager recording the temperature distribution along the targeted structure, the silicon plates with known thermal conductivity can work as a reference to calculate the heat flux transporting through the SWNT thin film. Repeating the experiment without the SWNT thin film, the effect of thermal radiation can be neatly deducted. Thereupon, the thermal conductivity of the SWNT thin film with 90% transparency is obtained through Fourier's law, which is around 22W/m K.

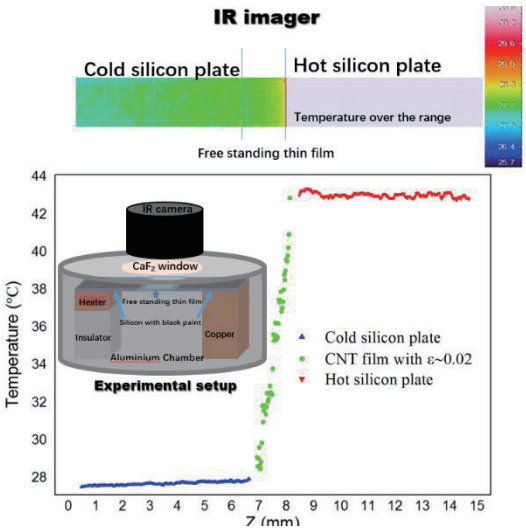

Fig. 1 The experimental setup and temperature profile.

[1] MS Dresselhaus *et al.* Adv. Phys. **49** (6), 705-814 (2000).
[2] Tong Tao *et al.* IEEE T Compon. Pack. T **30** (1), 92-100 (2007).

Corresponding Author: S. Maruyama
Tel: +81-3-5841-6421, Fax: +81-3-5800-6983
E-mail: maruyama@photon.t.u-tokyo.ac.jp

3P-10

Emergence of a New Red-Shifted PL from Chemically-Modified Single-Walled Carbon Nanotubes

Tomonari Shiraishi[1], Tomohiro Shiraki[1,2], Naotoshi Nakashima[1,2]

[1]*Department of Applied Chemistry, Kyushu University, Fukuoka 819-0395, Japan*

[2] *WPI-I2CNER, Kyushu University, 744 Motooka, Fukuoka 819-0395, Japan*

Single-walled carbon nanotubes (SWNTs) show photoluminescence (PL) in the NIR region based on the first sub-band transition in chirality-dependent electronic structures and are promising for a wide variety of applications such as optoelectronic, sensing, and imaging devices. Therefore, new techniques for controlling emission wavelength would expand SWNT research fields in not only fundamentals but also applications over the chirality-dependent features. Recently, a very limited amount of chemical modification with aryl functional groups on SWNT (Ar-SWNT) has been reported to create a new red-shifted PL labeled as E_{11}*, which shows superior PL properties to those of pristine (non-modified) SWNT in terms of quantum yields and longer wavelength emission [1]. The E_{11}* PL could be considered due to the band splitting of the degenerated electronic states of the SWNTs by the structural symmetry-breaking through the partial chemical modification [2]. Therefore, one can think that chemical modification would be a key factor to change PL properties with dependence on the chemical structures of the modified compounds.

In this study, the chemical modification using newly-synthesized compounds having two reactive groups (2Ar) was examined, resulting in appearance of a new red-shifted PL peak (E_{11}^{2}*) at the longer wavelength region compared to the emission of Ar-SWNT (E_{11}*). Importantly, the observed E_{11}^{2}* at 1255 nm has not been observed for pristine SWNT and Ar-SWNT. Based on the position of E_{11} in the pristine SWNT, the shifted value of E_{11}^{2}* was 270 nm (271 meV) in 2Ar-SWNT, which was much larger than 150 nm (165 meV) of E_{11}* in Ar-SWNT. From the absorption spectra of the 2Ar-SWNT, there was little change before and after the chemical modification indicating that small amount of the chemical modification using 2Ar induces the new E_{11}^{2}* emission. The detailed results and mechanism will be reported at the meeting.

[1] Y. Wang *et al.*, *Nat. Chem.* **5**, 840 (2013).

[2] N. Nakashima et *al.*, *J. Phys. Chem. C*, in press (2015).

Corresponding Author: Naotoshi Nakashima

Tel: +81-92-802-2840, Fax: +81-92-802-2840,

E-mail: nakashima-tcm@mail.cstm.kyushu-u.ac.jp

Rayleigh Scattering Spectroscopy of Single-Walled Carbon Nanotubes in Various Surrounding Environments

○Toru Osawa[1], Takeshi Okochi[1], Yoritaka Furukawa[1], Taiki Inoue[1],
Rong Xiang[1], Shohei Chiashi[1], Shigeo Maruyama[1, 2]

[1]*Department of Mechanical Engineering, The University of Tokyo, Tokyo 113-8656, Japan*
[2]*Energy NanoEngineering Laboratory, National Institute of Advanced Industrial Science and Technology (AIST), Ibaraki, 305-8564, Japan*

Single-walled carbon nanotube (SWNT) is one of the most promising materials for electronic devices such as a field effect transistor because of their high mobility and nanostructure. However, it is known that electronic structures of SWNTs depend not only on their chiralities, but also on their surrounding environment. Therefore, accurate and in-situ evaluation of their electronic structures is critical for high performance and reliability of electronic devices. Recently, Rayleigh scattering spectroscopy has attracted much attention as an efficient method to investigate the 1D electronic structure of SWNTs [1, 2].

In this study, we constructed the measurement system and observed Rayleigh scattering spectra and images of various SWNT samples. The attenuated continuum laser (the range of wavelength is 400 - 2500 nm) was focused on SWNTs. Scattered light was measured with CCD array and InGaAs detectors for spectroscopy and with 2D CCD camera for image. We measured Rayleigh scattering of dispersed SWNTs in the surfactant solutions [3], dry-deposited SWNT films [4], suspended SWNTs in a slit and horizontally aligned SWNTs on substrates [5]. As one example, Fig. 1 and 2 show Rayleigh scattering image and a spectrum of a suspended SWNT, respectively. From these experimental results, we compared characteristic features of SWNT electronic structures depending on surrounding environments.

[1] M. Y. Sfeir et al., Science **306**, 1540 (2004).
[2] K. Liu et al., Nat. Nonotechnol. **8**, 917 (2013).
[3] H. Liu et al., Nat. Commun. **2**, 309 (2011).
[4] A. Kaskela et al., Nano Lett. **10**, 4349 (2010).
[5] T. Inoue et al., J. Phys. Chem. C **117**, 11804 (2013).
Corresponding Author: S. Maruyama
Tel: +81-3-5841-6421, Fax: +81-3-5841-6421,
E-mail: maruyama@photon.t.u-tokyo.ac.jp

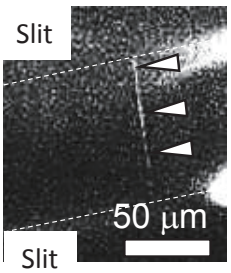

Fig. 1: Rayleigh scattering image of a suspended SWNT.

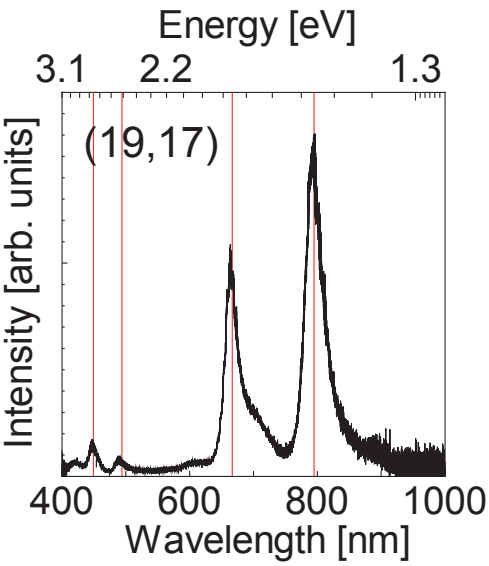

Fig. 2: Rayleigh scattering spectrum of a suspended SWNT.

Chemical Bond Formation between Multi-walled Carbon Nanotube and Polyvinyl Benzoate Side Chain through Photo-induced Radical Formation

○Tomoya Takada[1], Yuya Nishioka [1], Takuma Baba [2]

[1] *Department of Applied Chemistry and Bioscience, Chitose Institute of Science and Technology, Chitose 066-8655, Japan*
[2]*Graduate School of Photonics Science, Chitose Institute of Science and Technology, Chitose 066-8655, Japan*

Chemical hybridization of polymers and carbon nanotubes (CNTs) is an important technique for fabrication of functional materials containing CNTs. In this work, we prepared polysvinyl benzoate derivative having chloromethyl groups on its side chains and attempted to achieve chemical bond formation of the side chains with multi-walled carbon nanotubes (MWCNTs) by UV light irradiation.

The polymer was synthesized by esterification of polyvinyl alcohol with p-(chloromethyl)benzoyl chloride. Degree of the esterification was estimated by means of ultraviolet absorption spectroscopy. The polymer and MWCNTs were mixed in 1-methyl-2-pyrrolidone and irradiated with UV light (250-385nm) from a xenon light source at room temperature for 24 hours. Polymer films were made by solution casting, and X-ray photoelectron spectra (XPS) and Raman spectra of them were recorded. The XPS were recorded using the equipment installed in the Laboratory of XPS analysis, Hokkaido University. Similar UV irradiation and characterization using MWCNTs treated with hydroxylammonium chloride to enhance their dispersion in solvent were also carried out in the same manner. To observe the temperature change of the samples induced with infrared light (IR), the samples were irradiated with IR from a xenon light source for 5 min. Their temperature changes during and after the irradiation were observed by using a thermal imaging camera.

From the result of elemental analysis based on XPS, it was found that the content of Cl in the samples decreased after the UV irradiation. Also, on the basis of the Raman spectra, surface deformation of MWCNTs was observed after the UV irradiation. The similar spectral features were also observed also in the case of MWCNTs treated with hydroxylammonium chloride. These results support the radical formation from polymer side chains and the chemical bond formation between the radicals and MWCNTs. While polymer film fabricated without MWCNTs showed only small temperature change during IR irradiation, temperature of the film containing MWCNTs significantly rose with IR irradiation (Fig. 1). This result indicates that the polymer-MWCNT films fabricated in the present way can be used as photothermal conversion materials.

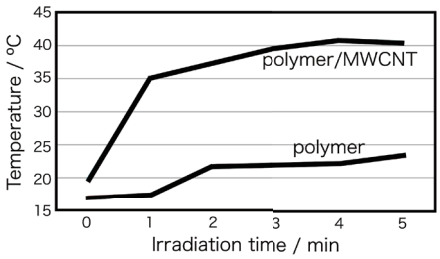

Fig.1 Temperature change induced by IR irradiation.

This work was supported by Nanotechnology Platform Program of the MEXT, Japan, and JSPS KAKENHI.

Corresponding Author: T. Takada
Tel: +81-123-27-6056, Fax: +81-123-27-6056, E-mail: t-takada@photon.chitose.ac.jp

Single-Step Extraction of Semiconducting Single-Wall Carbon Nanotubes by Aqueous-Two Phase (ATP) System

○Tomohiko Komuro,[1] Haruka Omachi,[1] Jun Hirotani,[2] Ryo Kitaura,[1] Yutaka Ohno,[2,3] and Hisanori Shinohara[1]*

[1] Department of Chemistry & Institute for Advanced Research, Nagoya University, Nagoya 464-8602, Japan. [2] Graduate School of Engineering, Nagoya University, Nagoya, 464-8603, Japan, [3] Institute of Materials and Systems for sustainability, Nagoya University, Nagoya, 464-8603, Japan

Semiconducting single-wall carbon nanotubes (s-SWCNTs) are promising materials for electronic devices [1]. However, because the conventional as-grown carbon nanotubes contain ca. 30 % metallic (m-) SWCNTs, separation is required to obtain high purity s-SWCNTs. In 2013, Zheng and co-workers first demonstrated spontaneous partition of s- and m-SWCNTs by using aqueous two-phase (ATP) system [2]. The method, however, requires a multi-step extraction to attain high purity s-SWCNTs. In addition, there has been no study reported on thin film transistor (TFT) fabrication using ATP-extracted s-SWCNTs.

In this work, a rapid and single-step ATP extraction of highly enriched s-SWCNTs is demonstrated. The extraction with the combination of polyethylene glycol and polysaccharide yielded >95% purity of s-SWCNTs from arc-discharge samples (Figure 1). After extensive screenings, we were able to fabricate the s-SWCNTs thin films so-extracted. Figure 2 shows the AFM image of such s-SWCNTs film, which exhibits a uniform and thin film composed of isolated CNTs. The electronic measurement of so-fabricated TFT will also be reported in the presentation.

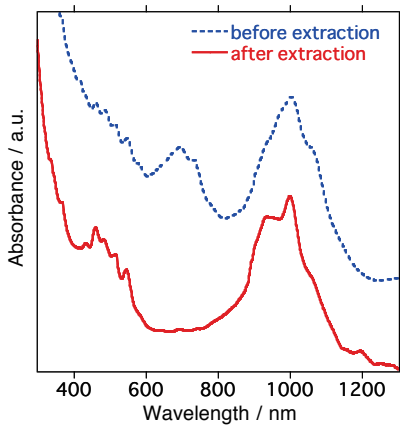

Figure 1. Optical absorption spectra of SWCNT dispersions

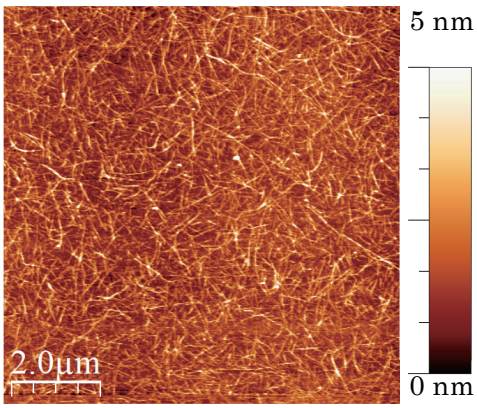

Figure 2. AFM image of extracted s-SWCNT film

[1] D. Park *et al., Appl. Phys. Lett.,* **82**, 2145 (2003) [2] M. Zheng *et al.*, *J. Am. Chem. Soc.*, **135**, 6822 (2013)

Corresponding Author: Hisanori Shinohara
Tel: +81-52-789-2482, Fax: +81-52-747-6442, E-mail: noris@nagoya-u.jp

Formation of cross-linked polymer network around single-walled carbon nanotubes

Yusuke Tsutsumi[1], ○Tsuyohiko Fujigaya[1,2,3], and Naotoshi Nakashima[1,2]

[1] *Department of Applied Chemistry, Graduate School of Engineering, Kyushu University, 744 Motooka, Fukuoka 819-0395, Japan*
[2] *WPI-I2CNER, Kyushu University 744 Motooka, Nishi-ku, Fukuoka 819-0395, Japan*
[3] *PRESTO, JST, 4-1-8 Honcho, Kawaguchi, Saitama, 332-0012, Japan*

Synthesis of a cross-linked polymer on single-walled carbon nanotubes (SWNTs) is a promising method for functionalization of the SWNTs due to their high coating stability together with their intactness to the SWNTs. We here reveal a requirement for vinyl monomers to form such cross-linked polymers on the SWNTs, which is highly important to generalize this method as well as to develop many polymer-SWNT hybrids with a unique structure and functions.

Poly(ethylene glycol) methacrylate (PEG-MA) (average molecular weight (Mn) = 526), *N*, *N*-dimethylacrylamide (DMAAm), methyl methacrylate (MMA), vinyl acetate (VA), methyl acrylate (MA), acrylamide (AAm) and 2-hydroxyethyl methacrylate (HEMA) were chosen as the vinyl monomers. *N*, *N'*-methylenebisacrylamide (BIS) was used as a cross-linker monomer. The SWNTs were individually solubilized in a 0.2 wt% sodium dodecyl sulfate (SDS) aqueous solution, to which a specific monomer and ammonium persulfate (APS) as an initiator were added, then heated at 70 ºC. After heating for 7 h, the obtained solution was then filtered (1st filtration) using a membrane filter (molecular weight cut-off = 10,000) to remove any excess amounts of SDS and unreacted monomers, then the precipitate generated after the redispersion in water was removed by a 2nd filtration using cotton as a filter to provide an aqueous solution of the polymer-SWNT hybrids[1, 2].

Fig. 1 shows the absorption spectra (b-g) and photographs (i-o) of the aqueous dispersions of the polymer-SWNT hybrids. As shown in Figs. 1i-1n, the SWNT/poly(PEG-MA) (SWNT/PPEG), SWNT/poly(DMAAm) (SWNT/PDMAAm), SWNT/poly(MMA) (SWNT/PMMA), SWNT/poly(VA) (SWNT/PVA) and SWNT/poly(MA) (SWNT/PMA) provided transparent black-colored solutions, while a light black color was observed for the SWNT/Poly(AAm) (SWNT/PAAm). In contrast, an aggregate was formed during the preparation of the SWNT/Poly(HEMA) (SWNT/PHEMA) (Fig. 1o). The origin of such differences will be discussed [3].

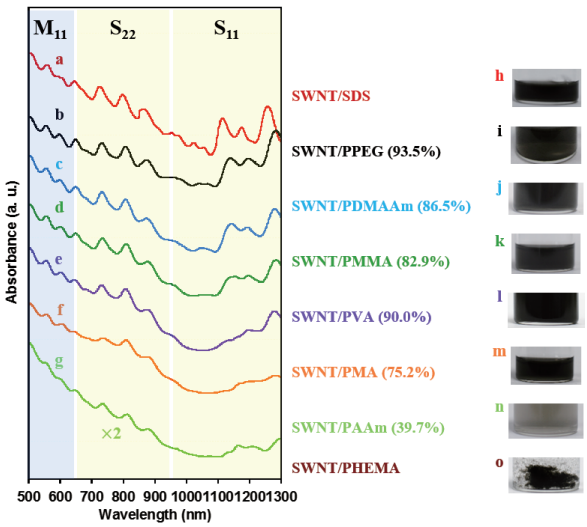

Fig.1 (a) Absorption spectrum and (h) photograph of SWNTs solubilized in SDS aqueous solution. (b-g) Absorption spectra and (i-n) photographs of the polymer-SWNT hybrids in an aqueous solution. Yields of the polymer-SWNT hybrids are also shown in parenthesis. (o) Photograph of SWNT/PHEMA in an aqueous solution before the 2nd filtration.

[1] T. Fujigaya et al. *RSC Adv.*, 2014, 4, 6318.
[2] T. Fujigaya et al. *Nanoscale* 2015, 7, 19534.
[3] T. Fujigaya et al. *Chem. Lett.*, in press.

Corresponding Author: Tsuyohiko Fujigaya
E-mail: fujigaya-tcm@mail.cstm.kyushu-u.ac.jp
Tel & Fax: +81-92-802-2842

Disulfide bond formation of thiols using single-wall carbon nanotubes

○Atsushi Hirano [1], Momoyo Wada [1], Takeshi Tanaka [1], Hiromichi Kataura [1]

[1] *Nanomaterials Research Institute, National Institute of Advanced Industrial Science and Technology (AIST), Ibaraki 305-8565, Japan*

Carbon nanotubes are known to be oxidized by O_2/H_2O redox couple in aqueous solutions. Such oxidation reaction is reversible and can be reduced by reductants. Recently, thiols, e.g. cysteine and dithiothreitol (Fig.1), are reported to have ability to reduce the oxidized carbon nanotubes [1,2]. However, the mechanism of the reduction remains unclear. In this study, we demonstrated that two thiol groups form a disulfide bond through the reduction reaction. The disulfide bond formation was also found to occur on the matrices immobilizing carbon nanotubes in a liquid chromatography system.

Suspension of carbon nanotubes, which were synthesized by the HiPco process, containing cysteine was subjected to ultrasonication. Supernatant of the suspension was collected after ultracentrifugation. Fig.2A shows absorption spectra of cysteine in the supernatants in presence and absence of the carbon nanotubes. A spectral shoulder was observed around 250 nm in the presence of the carbon nanotubes, which is correspond to disulfide bond. Similar results were also obtained for other thiols such as dithiothreitol (data not shown). Fig.2B shows absorption spectra of carbon nanotubes dispersed in 1% SDS at different concentrations of cysteine. The spectral intensities in S_{11} bands were found to be restored by the addition of cysteine. It was thus concluded that thiols reduce the carbon nanotubes and then form disulfide bonds. The reaction was also available on matrices immobilizing the carbon nanotube in a liquid chromatography system (data not shown). This system is reusable and will be useful as a chemical reactor for thiols.

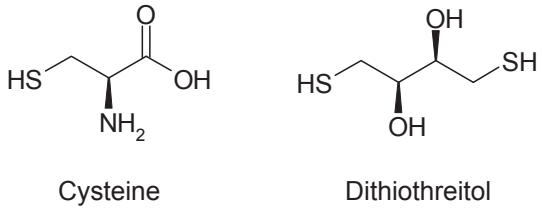

Fig.1 Chemical structure of cysteine and dithiothreitol

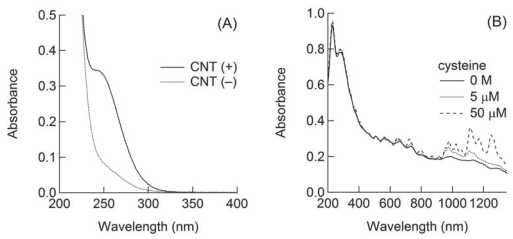

Fig.2 (A) Absorption spectra of cysteine subjected to ultrasonication in the presence and absence of the carbon nanotubes. (B) Absorption spectra of the carbon nanotubes at different cysteine concentrations.

[1] N. V. Kurnosov; V. S. Leontiev; A. S. Linnik; V. A. Karachevtsev. Chem. Phys. Lett. **623**, 51 (2015).
[2] S. Sen; F. Sen; A. A. Boghossian; J. Q. Zhang; M. S. Strano. J. Phys. Chem. C **117**, 593 (2013).

Corresponding Author: A. Hirano
Tel: +81-29-849-1064, Fax: +81-29-861-2786
E-mail: hirano-a@aist.go.jp

Thermoelectric characterizations of carbon nanotube/curable resin

○Wenxin Huang[1], Tsuyohiko Fujigaya[1,2,3], and Naotoshi Nakashima[1,2]

[1] *Department of Applied Chemistry, Graduate School of Engineering, Kyushu University, 744 Motooka, Fukuoka 819-0395, Japan*
[2] *WPI-I[2]CNER, Kyushu University 744 Motooka, Nishi-ku, Fukuoka 819-0395, Japan*
[3]*PRESTO, JST, 4-1-8 Honcho, Kawaguchi, Saitama, 332-0012, Japan*

Polymer composites containing carbon nanotubes (CNT/polymer) are a promising thermoelectric (TE) material, due to their high electrical conductivity of the CNTs together with the low thermal conductivity of the polymers. Previously, we reported that the single-walled carbon nanotubes (SWNTs) can be homogeneously embedded in the photo-curable resin matrix (R712, Kayarad, Nihon Kayaku) and the thermal conductivity of SWNTs has severely suppressed [1], which suggests that the composite (SWNT/R712) is a potential TE material. In this work, we first optimized the preparation condition such as mixing technique to improve the electrical conductivity. Then we fabricated the composite films (CNT/R712) with different CNT loading amount using three types of CNTs and evaluated their TE properties.

SWNTs (HiPco, Unidym) were added to R712 and mixed by tube homogenizer (Tube drive VT-1, BioLabs), bead mill homogenizer (Tube drive VT-1, BioLabs) and tip homogenizer (Polytron, KINEMATICA), respectively, for 30 min (4000 rpm). The obtained pastes were further mixed after adding 1 wt % of photo-initiator (IRGACURE819) and then degassed for 10 min by conditioning mixer (THINKY) at 2200 rpm. The pastes poured into the molds (50 μm in depth) were exposed to UV light (high pressure Hg lamp, SEN, LIGHTS CORP.) for 4 min to initiate the curing reaction to afford HiPco/R712 films. SWNTs (eDIPS, Meijo) and multi-walled carbon nanotubes (MWNTs, Nikkiso) were used as CNTs in the same fashion to prepare eDIPS/R712 and MWNT/R712 films by tube homogenizer.

Figure 1 shows HiPco/R712 films fabricated by 3 different homogenizers and we found that the film prepared by the tube homogenizer (Figure 1a.) demonstrates the best dispersibility, as clearly indicated by its color. Indeed, surface resistivity measurements revealed this film showed a lower resistance value (4.46×10^4 Ω/sq.) than the films prepared by bead mill homogenizer (Figure 1b. $>10^7$ Ω/sq.) and tip homogenizer (Figure 1c. $>10^7$ Ω/sq.). Tube homogenizer dispersion was applied to prepare HiPco/R712, eDIPS/R712 and MWNT/R712 films and their TE properties (Table 1.) were measured. We found eDIPS/R712 film illustrates the highest ZT value due to the high electrical conductivity and Seebeck coefficient. Since CNT/R712 was viscous solution before curing reaction, we can expect the printable fabrication of integrated TE device with this material.

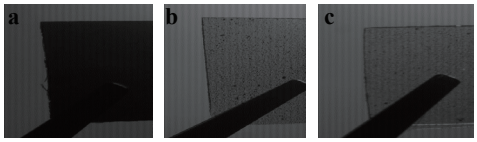

Figure 1. Photos of films prepared by tube homogenizer (a), bead mill homogenizer (b) and tip homogenizer (c), contained 0.1 wt% of HiPco SWNTs.

Table 1. The TE properties of CNT/R712 films (0.5 wt%) prepared by the tube homogenizer

	HiPco/R712	eDIPS/R712	MWNT/R712
Electrical conductivity (S m^{-1})	2.459	4.902	1.683
Seebeck coefficient (μV K^{-1})	30.10	52.57	25.90
Thermal conductivity (W m^{-1} K^{-1}, through plane)	0.247	0.300	0.277
ZT	**2.699×10^{-6}**	**13.64×10^{-6}**	**1.236×10^{-6}**

[1] T. Fujigaya, T. Fukumaru, and N. Nakashima, *Synth. Met.,* **2009**, *159,* 827-830. Tel & Fax: +81-92-802-2842
Corresponding Author: Tsuyohiko Fujigaya E-mail: fujigaya-tcm@mail.cstm.kyushu-u.ac.jp

Environmentally Stable Carrier Doping into Carbon Nanotube Films by Extraordinary Molecular Lewis Acid

○Kazuma Funahashi[1], Naoki Tanaka[2], Yoshiaki Shoji[2], Ko Nakayama[3], Kaito Kanahashi[1], Hiroyuki Shirae[1], Suguru Noda[4], Takanori Fukushima[2] and Taishi Takenobu[1,3,5]

[1]Department of Advanced Science and Engineering, [3]Department of Applied Physics, [4]Department of Applied Chemistry, Waseda University, Shinjuku, Tokyo 169-8555, Japan
[2]Chemical Resources Laboratory, Tokyo Institute of Technology, 4259 Nagatsuta, Midori-ku, Yokohama 226-8503, Japan
[5] Kagami Memorial Laboratory, Waseda University, Shinjuku, Tokyo 169-0051, Japan

Carbon nanotube thin films (CNT-TFs) are one of the most promising materials as an alternative for commonly-used indium tin oxide (ITO) transparent electrodes because they are much flexible than ITO and high performance (sheet resistance (R_S) of 50-100Ω/sq at 85-90% transmittance) is realized by the chemical doping. However, in most previous reports, doped CNTs are not stable to air, including the hole doping by nitric acid, which is the most common doping method. In the nitric acid doping, it is reported that the 240-hours storing of doped samples in air results in 30% increase of R_S [1] and, thus, air-stable carrier dopants are strongly required for practical application. Therefore, in this work, we focus on the combination of the super Lewis acid, diarylborinium ion (Mes_2B^+; Mes (mesityl) = 2, 4, 6-trimethylphenyl) and thermally-stable counter anion, tetrakis (pentafluorophenyl) borate ($[(C_6F_5)_4B]^-$) (Fig.1) [2] as the novel air-stable dopants.

We used CNTs grown by enhanced direct injection pyrolytic synthesis method (eDIPS-CNT). These CNT thin films were immersed into the saturated *o*-dichlorobenzene solution of dopant, Mes_2B^+ $[(C_6F_5)_4B]^-$. As a reference, the nitric acid doping was also conducted. Before and after the above doping processes, we characterized these films by Vis-NIR absorption spectroscopy and four-probe resistance measurement. As a result, we confirmed the carrier doping into CNT films by both absorption and conductivity measurements, resulting in R_S reduction of -35% and one-month stability (Fig.2). Importantly, this R_S reduction is comparable to that of nitric acid and the stability is much superior.

In summary, we succeeded in air-stable carrier doping to CNT-TFs by the novel dopants, Mes_2B^+ and $[(C_6F_5)_4B]^-$, which promotes the use of CNT-TFs as future transparent electrodes.

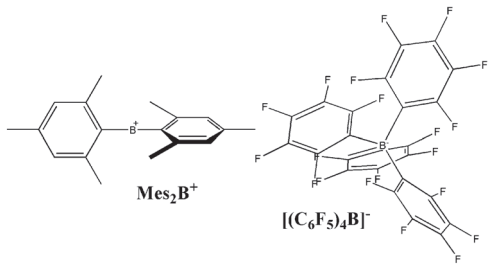

Fig. 1 Novel dopant; cation, Mes_2B^+ and counter anion, $[(C_6F_5)_4B]^-$

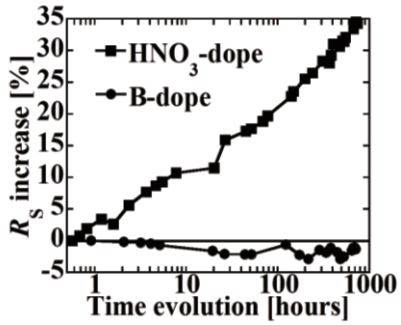

Fig. 2 Time evolution of *R*s increase in CNTs doped by nitric acid and novel dopant

[1] R. Jackson *et al*., *Adv. Funct. Mater*. **18**, 2548–54, 2008 [2] Y. Shoji *et al*., *Nat. Chem*. **6,** 498-503, 2014
Corresponding Author: T. Takenobu Tel & Fax: +81-3-5286-2981, Email: takenobu@waseda.jp

Effect of catalyst support on growth lifetime of carbon nanotube forest

○Takashi Tsuji, Shunsuke Sakurai, Maho Yamada, Don N. Futaba, Kenji Hata

CNT-Application Research Center, National Institute of Advanced Industrial Science and Technology (AIST), Tsukuba, 305-8565, Japan

Chemical vapor deposition (CVD) of vertically aligned carbon nanotube forest is one of the most powerful methods for a mass production of single-walled carbon nanotubes (SWNTs). To achieve a high efficiency in the above method, aluminum oxide (Al_2O_3) is frequently used as a key material for catalyst support. The important role of Al_2O_3 has been reported as the immobilization of iron particles to maintain small and homogeneously-sized catalyst particles during the CVD process. Magnesium oxide (MgO) is also known as the catalyst support for the growth of SWNT forest [1], though a SWNT forest higher than 100 μm has not been obtained yet. Amama et al. showed that subsurface diffusion of Fe catalyst on MgO support is much higher than that on Al_2O_3 support, and predicted a short lifetime of the catalyst on MgO support than catalyst on Al_2O_3 support [2].

In this study, we analyzed the growth curves (temporal changes in height) of CNT forest synthesized on Fe/MgO and Fe/Al_2O_3 catalyst systems. In our experimental conditions, the termination of CNT forest growth was always observed within 2 min on MgO support, though a long catalyst lifetime (>10 min) was confirmed on Al_2O_3 support. As a result, the height of CNT forest on MgO support was not higher than 200 μm. AFM observation shows the disappearance of Fe catalyst particles from the surface of MgO support within 5 minutes of annealing in the growth ambient without carbon feedstock, while the size and number density of Fe catalyst on Al_2O_3 support remain even after 10 minutes. These results indicate that a short growth lifetime of CNT forest on MgO is due to strong subsurface diffusion of Fe particles into support layer.

[1] C. Pint *et al*. J. Nanosci. Nanotech. **8**, 6158 (2008).
[2] P. B. Amama *et al*. Carbon **50**, 2396 (2012).

Corresponding Author: S. Sakurai
Tel: +81-29-861-4654, Fax: +81-29-861-4851,
E-mail: shunsuke-sakurai@aist.go.jp

Comparison between Reduced and Intentionally Oxidized Metal Catalysts for Growth of Single-Walled Carbon Nanotubes

○Yang Qian[1], Rong Xiang[1], Hua An[1], Taiki Inoue[1], Shohei Chiashi[1], Shigeo Maruyama[1, 2]

[1] *Department of Mechanical Engineering, The University of Tokyo, Tokyo 113-8656, Japan*
[2] *Energy NanoEngineering Laboratory, National Institute of Advanced Industrial Science and Technology (AIST), Tsukuba 305-8564, Japan*

Many efforts and progresses have been made in the past decades towards controlled production of single-walled carbon nanotubes (SWNTs). However, as the pearl of the crown, direct growth of SWNTs with defined structures and properties has been the bottleneck for decades [1]. This is strongly associated with the insufficient understanding of the catalytic formation process of SWNTs and thereby absents control over the product.

One important ingredient for efficient growth of SWNTs is the oxygen atmosphere. Besides the ethanol in alcohol catalytic chemical vapor deposition (ACCVD) [2], the water or oxygen gas in the super-growth also shows the important role of oxygen in the synthesis of SWNTs [3, 4]. However, the detailed mechanism how oxygen affects the catalysts or carbon deposition is still not yet fully clarified. In addition, some un-disclosed factors like chamber impurities and room moisture are often related with nanotube growth [5]. Therefore, a careful investigation on the catalytic behavior of oxide particles may also help to understand the effects of un-intentional catalyst oxidation that possibly exists sometimes, and hopefully the robustness of CVD process could be improved hereafter.

In this presentation, we perform a detailed comparative study on the catalytic behavior of metallic and oxidized particles in CVD synthesis of SWNTs. Intentionally oxidized Co particles are found also capable of growing SWNTs but the yield is significantly decreased. Meanwhile the SWNTs grown from oxidized particles show a smaller and narrower diameter distribution. X-ray photoelectron spectroscopy and in-plane transmission electron microscopy studies reveal that Co particles, though in CoO form before growth, are quickly reduced into metallic form by ethanol through an in-situ reduction process. However, this reduction process is strongly size-dependent and smaller particles are preferably reduced to grow SWNTs, resulting in the absence of larger-diameter SWNTs in the product. Accordingly, nucleation density decreases significantly and SWNT morphology changes from vertically aligned arrays to thin random networks. Our strategy has been further applied to Ni and the results are similar. Our findings are insightful for controlling the diameter and morphology of the produced SWNTs, as well as for improving the reproducibility and robustness of CVD process.

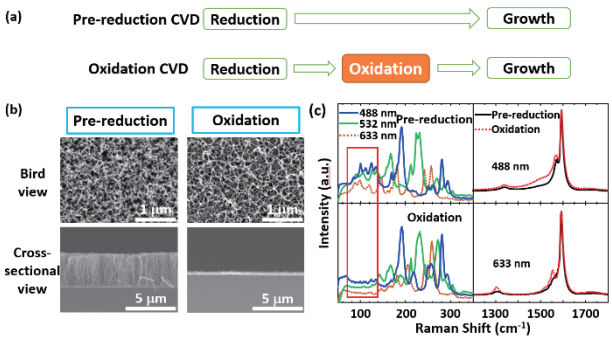

Fig.1 (a) Experimental flow of pre-reduction and oxidation CVD processes. (b) SEM images of the as-grown SWNTs from two CVD processes. (c) Raman spectra of the as-grown SWNTs from two CVD processes.

[1] T. Ebbesen *et al*. Nature **382**, 54 (1996). [2] S. Maruyama *et al*. Chem. Phys. Lett. **360**, 229 (2002). [3] K. Hata *et al*. Science, **306**, 1362 (2004). [4] G. Zhang *et al*. Proc. Natl. Acad. Sci. U. S. A. **102**, 16141 (2005). [5] C. Oliver *et al*. ACS Nano, **7**, 3565 (2013). Corresponding Author: S. Maruyama, Tel: +81-3-5841-6421, Fax: +81-3-5800-6983, E-mail: maruyama@photon.t.u-tokyo.ac.jp

3P-20

Controlled synthesis of single-walled carbon nanotubes with sputtered W-based catalyst

Hua An[1], Rong Xiang[1], Hiroki Takezaki[1], Shinnosuke Ohyama[1], Yang Qian[1],

Taiki Inoue[1], Shohei Chiashi[1], Shigeo Maruyama[1,2]

1. Department of Mechanical Engineering, the University of Tokyo, 7-3-1 Hongo, Bunkyo, Tokyo, 113-8656, Japan
2. Energy NanoEngineering Laboratory, National Institute of Advanced Industrial Science and Technology (AIST), 1-2-1 Namiki, Tsukuba, 305-8564, Japan

The application of single-walled carbon nanotubes (SWNTs) in nanodevices is limited by the impurities and mixed chiralities of SWNTs assemblies. Great efforts have been made in the purification and separation of SWNT mixtures. However, direct synthesis of SWNTs with single chirality is more challenging but attracts considerable attention among researchers. CoW clusters were recently reported to grow a single chirality, (12, 6) with over 90% abundance via high-temperature (1030° C) reduction and growth [1]. By further control of the catalyst structure and growth conditions, a zigzag SWNT (16, 0), with near 80%, was obtained [2].

In this report, we show that a sputtered CoW catalyst can selectively grow (12, 6) SWNTs by low pressure chemical vapor deposition at low temperature [3]. Statistical Raman mapping analysis and optical absorption spectrum of the as-grown SWNTs reveal that the abundance of (12, 6) is over 50%. Parametric study of this CoW bimetallic catalyst system demonstrates that the reduction temperature before growth is critical for the intermediate catalyst structure and the selectivity. Moreover, the morphology and structure of catalyst is investigated by electron diffraction, which discloses the complicated structure changes before and after growth. Further study is needed to optimize conditions to obtain better chirality control of SWNTs.

[1] F. Yang et al., Nature. **510**, 522(2014).
[2] F. Yang et al., J. Am. Chem. Soc. **137**, 8688 (2015).
[3] S. Maruyama et al., Chem. Phys. Lett. **360**, 229 (2002).

Corresponding Author: Shigeo Maruyama
Tel: +81-3-5841-6421, Fax: +81-3-5800-6983
E-mail: maruyama@photon.t.u-tokyo.ac.jp

Molecular dynamics simulation of single-walled carbon nanotubes grown from binary catalyst

○Yukai Takagi[1], Ryo Yoshikawa[1], Shohei Chiashi[1] and Shigeo Maruyama[1,2]

[1]*Department of Mechanical Engineering, The University of Tokyo, Tokyo 113-8656, Japan*
[2] *National Institute of Advanced Industrial Science and Technology (AIST), Tsukuba 305-8564, Japan*

Atomic scale simulation is important for analyzing the growth mechanism of single-walled carbon nanotubes (SWNTs). In molecular dynamics (MD) simulations, it has been observed that high quality SWNTs are grown from monometallic catalysts such as Co and Fe [1]. Some experiments have indicated the possibility that, by using binary (W-Co) catalysts, chirality of SWNTs can be controlled to a certain extent [2]. Therefore, simulations of SWNT growth from binary catalyst are desired for analyzing the function of binary alloy catalysts.

For expressing the interaction between W, Co and C, we newly made Tersoff-type potentials based on density functional theory calculation and genetic algorithm [3]. Then, we performed classical MD simulations by preparing a metal cluster with 60-104 atoms in a periodic cell ($10\times10\times10$ nm^3 , 1350-1500K) and supplying carbon atoms to the cell with keeping maximum 3 carbons in the cell. The catalyst contained 50-55 % Co and 45-50% W. We set up two types of initial position that W and Co atoms were alternately arranged and that W and Co were placed separately in two segments.

In simulations, the W-Co catalysts were solid and the structure of catalysts depended on the initial condition to some extent. It was observed that C atoms which bonded to W atoms did not connect another C atoms, and C atoms which formed cap structure were bonded to not W but Co. The Cap formation occurred fairly faster and SWNTs were grown more rapidly on W-Co catalyst than on monometallic catalysts [1]. It is suggested that Co has a main function of growing SWNTs and that W stabilizes the structure of catalysts and accelerates the lift-off of cap structure.

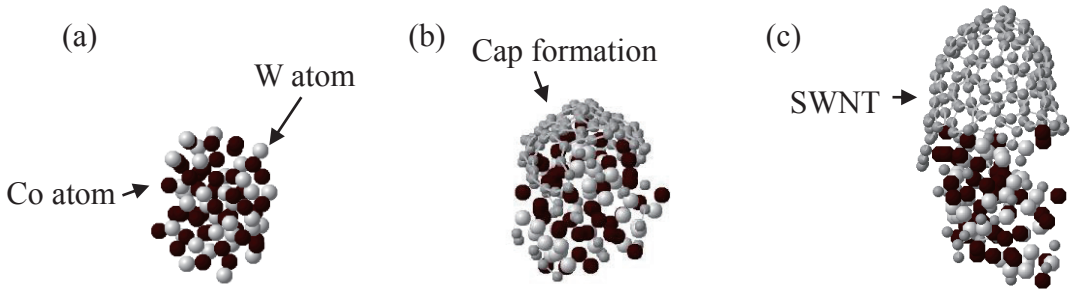

Fig. 1 Snap shots of SWNT growth in MD simulations. (a) W-Co catalyst ($W_{42}Co_{36}$) after anneal process, (b) Cap formation and (c) SWNT growth.

[1] K. Hisama et al., to be submitted.
[2] F. Yang et al. *Nature*, **510** (2014) 522.
[3] T. Kumagai et al. Modelling Simul. Mater. Sci. Eng. **14** (2006) S29.

Corresponding Author: Shigeo Maruyama Tel: +81-3-5841-6421, Fax: +81-3-5800-6983,
E-mail: maruyama@photon.t.u-tokyo.ac.jp

Quantifying the purity of semiconducting/metallic fractions in ELF separation of SWCNTs

○Yuki Kuwahara[1,3], Fusako Sasaki[1], Fumiyuki Nihey[2], Hiroyuki Endoh[2], Shinichi Yorozu[2], Takeshi Saito[1,3*]

[1] *Technology Research Association for Single Wall Carbon Nanotubes, Tsukuba 305-8565, Japan*

[2] *Smart Energy Research Laboratories, NEC Corporation, Tsukuba 305-8501, Japan*

[3] *National Institute of Advanced Industrial Science and Technology, Tsukuba 305-8565, Japan*

The purity characterization of semiconducting/metallic single-wall carbon nanotubes (SWCNTs) is important not only for the development of separation processes, but also for the investigation of semiconductor devices. Because it is well known that the purification of semiconducting SWCNTs considerably improves the performance of their semiconductor devices, further highly purified semiconducting SWCNTs are demanded for their integrations and practical uses [1]. Spectroscopic characterization methods such as optical absorption and resonance Raman are commonly used for their purity evaluation. However, when the purity becomes high, it is difficult to quantify it precisely. In this work, we report an evaluation method for the purity of the metallic/semiconducting SWCNTs separated by the electric-field-induced layer formation (ELF) method [2] based on the analysis results of optical absorption spectra.

In ELF separation, we can fractionate the pristine SWCNTs with the semiconductor purity of ca. 66% into semiconductor- and metal-enriched fractions without any apparent changes in the diameter distribution. In this situation, when we subtract the normalized spectrum of metal-enriched fraction from that of the pristine appropriately, only the contribution of the semiconducting SWCNTs in the pristine should be obtained. Figure 1 shows a typical analysis result of absorption spectra of separated SWCNTs. Here, the spectrum shape of calculated semiconducting SWCNTs was surely obtained from the normalized spectra of pristine and metal-enriched fraction. By using the calculated spectra of metallic and semiconducting SWCNTs, we quantified the metallic/semiconducting ratio/purity of separated SWCNTs. Detailed analysis method will be shown in the presentation.

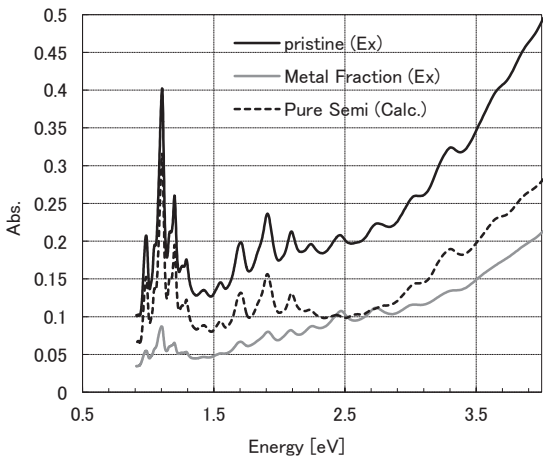

Fig. 1 Absorption spectra of pristine (black line), metal-enriched fraction (gray line) and calculated semiconducting SWCNTs (dash line).

Acknowledgment

This presentation is based on results obtained from a project subsidized by the New Energy and Industrial Technology Development Organization (NEDO).

References

[1] A. D. Franklin, Nature **498**, 443 (2013).

[2] K. Ihara *et al*., J. Phys. Chem. C **115**, 22827 (2011).

Corresponding Author: T. Saito

Tel: +81-29-861-4683, Fax: +81-29-861-4413, E-mail: takeshi-saito@aist.go.jp

STM/STS studies on Europium nanowires encapsulated in carbon nanotubes

○Terunobu Nakanishi[1], Ryo Kitaura[1], Shoji Yoshida[2],
Osamu Takeuchi[2], Hidemi Shigekawa[2] , Hisanori Shinohara[1]

[1] *Department of Chemistry and Institute for Advanced Research, Nagoya University, Nagoya, 464-8602, Japan*
[2] *Faculty of Pure and Applied Sciences, University of Tsukuba, Tsukuba, 305-8573, Japan*

The discovery of carbon nanotubes (CNTs) and their fascinating properties have ignited intense research interests on one-dimensional nanosystems. Although ultrathin atomic wires are one of the ideal one-dimensional systems, preparation of the ultrathin wires with diameters of 1~several nanometers has been difficult. Previously, we have reported the synthesis and characterization of ultrathin metal nanowires encapsulated in CNTs.[1][2] Here, we present the preparation and investigation of spatially-resolved electronic structure of Eu nanowires encapsulated in CNT (EuNW@CNT) by scanning tunneling microscopy/spectroscopy (STM/STS).

EuNW@CNT was synthesized by the direct nano-filling method[1] and deposited on Au(111) surface by the pulsed-jet deposition technique.[3] Figure 1 shows a STS spectrum of EuNW@CNT, where a new peak due to a localized density of states (DOS) of the encapsulated Eu nanowire can be seen. Figure 2 shows a d*I*/d*V* mapping observed at a bias voltage of -0.4 V, which corresponds to the voltage where the new DOS peak was observed. The bright region in the d*I*/d*V* map corresponds to the position where the encapsulated Eu nanowire locates. Spatially-resolved STS spectra reveal the position of Eu atoms in EuNW@CNT directly, which leads to a precise assignment of the STS peak and the interaction between Eu nanowires and CNTs.

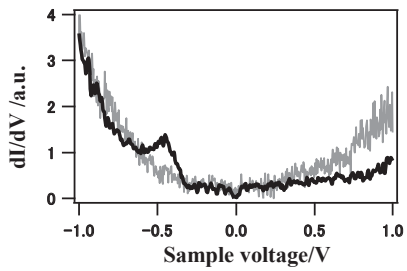

Fig.1 STS spectra of EuNW@CNT. Black curve is taken at Eu encapsulated point and gray curve is taken at empty area on the same CNT.

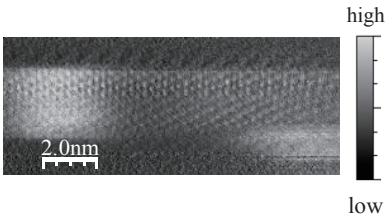

Fig.2 dI/dV mapping at -0.4 V. A bright spot on the left side of image is high localized density of state point where europium nanowire is encapsulated.

[1] R.Kitaura *et al*. Angew.Chem.Int.Ed. **48**, 8298, (2009).
[2] R.Nakanisihi *et al*. Phys. Rev. B**, 86** , 115445, (2012).
[3] N. Fukui *et al*. J. Nanosci. Nanotechnol. **7**, 4267 (2007).

Corresponding Author: H. Shinohara
Tel: +81-52-789-2477, Fax: +81-52-747-6442,
E-mail: r.kitaura@nagoya-u.jp and noris@nagoya-u.jp

Condensation reaction of 5,5"-dibromo-2,2':5'2"-terthiophene inside single-walled carbon nanotubes

○Makoto Sasaki[1], Takeshi Koyama[1], Hideo Kishida[1],
Yukihiro Yoshida[2], Gunzi Saito[2,3]

[1] *Department of Applied Physics, Nagoya University, Nagoya 464-8603, Japan*
[2] *Faculty of Agriculture, Meijo University, Nagoya 468-8502, Japan*
[3] *Toyota Physical and Chemical Research Institute, Nagakute 480-1192, Japan*

Single-walled carbon nanotubes (SWNTs) have a one-dimensional (1D) hollow cavity. Because of the confined space, SWNTs can be utilized as 1D chemical reactors, and various new 1D materials have been synthesized inside SWNTs [1, 2]. Recently, polymerization of oligothiophenes and electrochemical doping of the obtained polythiophenes inside SWNTs have been presented [3]. In the present study, we explore a new and facile synthetic route to doped conjugated polymers from single-species molecules by thermal polymerization under low temperatures.

5,5"-Dibromo-2,2':5'2"-terthiophene (Br_2-3T) was used as a precursor. Br_2-3T molecules were encapsulated in SWNTs by vapor phase reaction (10^{-5} torr at 160 °C for 24 h), and the molecules adsorbed outside SWNTs were removed by washing with toluene. The obtained composite materials are referred to as Br_2-3T/SWNT samples. Several pieces of Br_2-3T/SWNT samples were then thermally treated at 265 °C for 24 h for condensation reaction of the encapsulated molecules. These samples are referred to as Br_2-3T/SWNT(T) samples. We also prepared reference samples with terthiophene (3T) molecules as a precursor using a similar procedure.

The Raman spectrum for the Br_2-3T/SWNT sample is shown as a gray line in Figure 1. Two peaks are observed at 1455 and 1527 cm^{-1}, which are assigned to C=C symmetric and antisymmetric stretching modes of thiophene ring, respectively [4]. The peak positions are close to those of 3T [4], although slight shifts caused by interactions with SWNTs and/or bromine-termination are seen. It is suggested that the encapsulated molecules exist as Br_2-3T molecules. A black line in Figure 1 is the Raman spectrum for the Br_2-3T/SWNT(T) sample. The peaks of C=C symmetric and antisymmetric stretching modes show upshift to 1461 cm^{-1} and downshift to 1506 cm^{-1}, respectively. This result suggests that the number of thiophene rings increased to six [4]; namely, sexithiophene molecules were synthesized in SWNTs.

Optical absorption measurements support the condensation reaction of Br_2-3T. Comparison of the absorption spectra between the Br_2-3T/SWNT(T) and reference samples and energy dispersive x-ray spectroscopy suggest the Br-doping of the sexithiophenes.

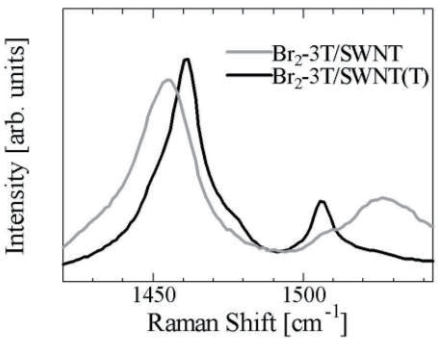

Fig. 1 Raman spectra for Br_2-3T/SWNT (gray line) and Br_2-3T/SWNT(T) (black line) samples.

[1] A. V. Talyzin *et al*. Nano Lett. **11**, 4352 (2011).
[2] Y. Nakanishi *et al*. Angew. Chem. Int. Ed. **54**, 10802 (2015).
[3] K. Miyaura *et al*. The 45th FNTG General Symposium, 1-12, (2013).
[4] Y. Furukawa *et al*. Synth. Met. **18**, 151 (1987).

Corresponding Author: T. Koyama
Tel: +81-52-789-4450, Fax: +81-52-789-4450
E-mail: koyama@nuap.nagoya-u.ac.jp

High-yield Filling of Hydroxylated Diamantane into Carbon Nanotubes

○Yusuke Nakanishi,[1] Haruka Omachi,[1] Natalie A. Fokina,[2] Ryo Kitaura,[1] Peter R. Schreiner,[2] Jeremy E. P. Dahl,[3] Robert M. K. Carlson,[3] and Hisanori Shinohara[1]

[1] *Department of Chemistry, Nagoya University, Nagoya 464-8602, Japan.*
[2]*Institute of Organic Chemistry, Justus-Liebig University, Heinrich-Buff-Ring 58, 35392 Giessen, Germany.*
[3]*Institute for Materials and Energy Science, Stanford University, Stanford, California 94305, United State.*

Carbon nanotubes (CNTs) are ideal molds for the synthesis of one-dimensional (1D) nanostructures. [1] As a part of our exploration for obtaining novel 1D nanomaterials by the CNT-templated annealing, we have worked on the syntheses of 1D nanodiamonds from diamantane, i.e., the molecule that can be superimposed on bulk diamond. [2] Although their fabrication has been achieved by the present research group, the yields were relatively low. One of the reasons lies on the severe inclusion of diamantane. In contrast to π-conjugated fullerenes, hydrogen-terminated diamantane is not easily taken up by CNTs. Preparation of highly filled CNTs must be accomplished to achieve high-yield production of 1D nanodiamonds, which allows for exploring for their potential applications.

Here we report new findings with regard to the selective introduction of diamantane skeleton into CNTs. 1,6-bis(hydroxymethyl)diamantane is inserted into CNTs with high yields under an optimized condition that inhibits the absorption of non-substituted diamantane (Fig. 1). Transmission electron microscopy revealed that the diol derivative forms a self-assembled structure within CNTs via a weak interaction. The presence of hydrogen bonding was inferred from infrared spectroscopy. This finding should be useful for the design and synthesis of the precursors for 1D nanodiamonds. Detailed discussion will be presented in the conference.

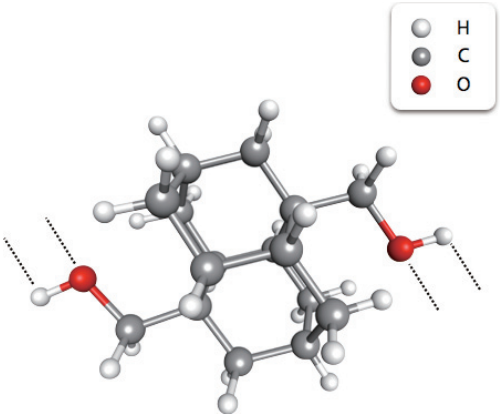

Fig. 1 Image of 1,6-bis(hydroxymethyl) diamantane.

[1] (a) R. Kitaura *et al*. ***Nano Lett.***, 8, 693 (2008); (b) Z. Wang *et al*. ***J. Am. Chem. Soc.***, 132, 13840 (2010); (c) H. E. Lim *et al*. ***ACS Nano***, 9, 5034 (2015). [2] (a) J. Zhang *et al*. ***Angew. Chem. Int. Ed.***, 52, 3805 (2013); (b) Y. Nakanishi *et al*. ***Angew. Chem. Int. Ed.***, 54, 10802 (2015).

Corresponding Author: H. Shinohara
Tel: +81-52-789-2482／Fax: +81-52-747-6442／E-mail: noris@nagoya-u.ac.jp

Vertically oriented Graphite layer formed on hot-implanted diamond (100) surface

○Masafumi Inaba[1], Wenxi Fei[1], Yu Hirano[1], Kazuma Suzuki[1], Hiroshi Kawarada[1]

[1] *Graduate School of Advanced Science and Engineering, Waseda University, Tokyo 169-8555, Japan*

Carbon nanomaterials, such as graphene and carbon nanotubes (CNTs), are formed on silicon carbide (SiC) by high temperature thermal annealing without any surface cap layer. Si atoms combine with oxygen from chamber residual and sublimate as silicon mono-oxide (SiO).[1] The remaining carbon atoms reform the nanocarbon materials. Also, for diamond surface, graphene layers parallel to the diamond (111) surface is formed by high temperature annealing.[2] In this study, we investigated the behavior of intercalated carbon atoms caused by implantation during the high temperature annealing on SiC and diamond using transmission electron microscopy (TEM).

Aluminum ions were implanted to both 4H-SiC (000-1) face (C-face) and the diamond substrate with (100) surface with the density of 10^{18} cm^{-3} for 1 μm thickness at the temperature of 500 ºC. The direction of the implantation was tilted by approximately 7 degrees to avoid channeling effect. The implantation condition was adjusted to form box profile of aluminum impurity. The implanted samples were annealed at the temperature of 1700 ºC in vacuum for 2 hours. The sample was observed by high resolution TEM.

Fig. 1 shows a TEM image of the surface graphite layers on SiC from the direction of [11-20]. Multilayered graphene sheets were lain on SiC. Fig. 2 shows a TEM image of the surface graphite layers from the direction of [110]. Vertically oriented carbon layer-like structure was observed with the thickness of ~10 nm. This corresponds to the graphite structure, and the interlayer distance was approximately 0.34 nm (graphite interlayer distance).

The formation mechanism of the vertically oriented graphite (VOG) we suspect is as follows. A part of the intercalating atoms caused by implantation moved to the surface and forms sp^2 layers. Generally, the diffusivity of atoms in diamond is extremely low, but it is possible for vacancies to enhance the diffusivity of atoms. The detail information will be reported on site.

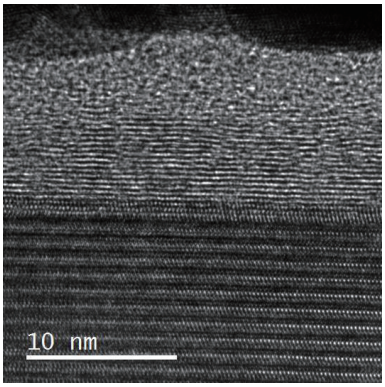

Fig. 1 Cross-sectional TEM image of graphene layers on SiC (000-1).

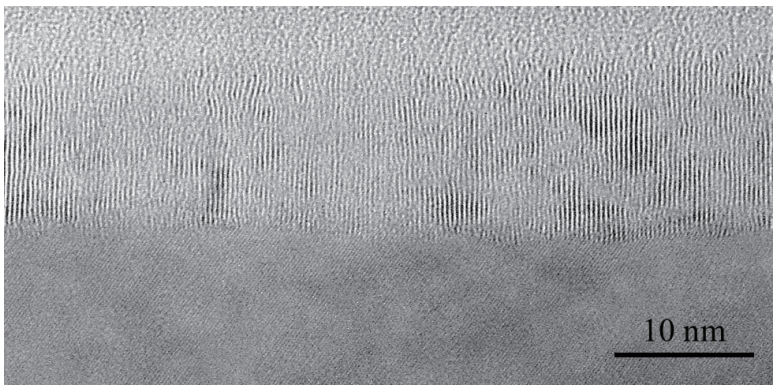

Fig. 2 Cross-sectional TEM image of vertically oriented graphite layers on diamond (100).

[1] M. Kusunoki, T. Suzuki, T. Hirayama, N. Shibata, and K. Kaneko, Appl. Phys. Lett. 77, 4 (2000).

[2] N. Tokuda, M. Fukui, T. Makino, D. Takeuchi, S. Yamsaki, and T. Inokuma, Jpn. J. Appl. Phys. 52, 11R (2013).

Corresponding Author: M. Inaba Tel&Fax: +81-3-5286-3391 E-mail: inaba-ma@ruri.waseda.jp

Synthesis Conditions of High-Quality and Large-Size Graphene by Alcohol CVD

○Kohei Tsushima[1], Masaki Sota[1], Xiao Chen[1], Rong Xiang[1], Taiki Inoue[1], Shohei Chiashi[1], Shigeo Maruyama[1, 2]

[1] *Department of Mechanical Engineering, The University of Tokyo, Tokyo 113-8656, Japan*
[2] *Energy NanoEngineering Lab., National Institute of Advanced Industrial Science and Technology (AIST), Ibaraki 305-8564, Japan*

Graphene has superior mechanical and electrical properties and is expected for application of innovative devices. Toward graphene industrialization, it is essential to obtain high-quality and large-size graphene. The chemical vapor deposition (CVD) is one of the most promising methods for producing such graphene. CVD growth of graphene on copper foils has been reported [1] and methane is often used as the carbon source. On the other hand, CVD growth of graphene using alcohol is recently reported [2]. In this study, we investigated synthesis conditions of graphene by alcohol CVD, and revealed the dependence of synthesis parameters on graphene growth rate.

A typical CVD procedure is as follows: 80-μm-thick copper foils were oxidized at 220 °C for 60 minutes in air. The pocket structure was formed by folding the copper foil [3]. The copper foil was put in CVD equipment, heated to 1075 °C with Ar buffer gas, and annealed at 1075 °C with Ar/H_2 buffer gas for 1 h. CVD was conducted by changing synthesis parameters with constant growth time of 2 h. The parameters include gas velocity, H_2 to ethanol partial pressure ratio, and ethanol partial pressure.

An optical image of the copper foil surface after CVD is shown in Fig. 1. It was oxidized in air for direct observation of graphene. Several isolated graphene which is considered as single-crystal is observed. The result shows the maximum growth rate is 1 mm/h, while it was ~0.2 mm/h in our previous study [2]. Figure 2 shows the dependence of ethanol partial pressure on growth rate at a constant gas velocity and partial pressure ratio. We found a positive correlation between ethanol partial pressure and growth rate. The effect of other parameters was also revealed. In conclusion, we succeeded in increasing graphene growth rate by adjusting synthesis conditions.

[1] X. Li, *et al*., Science **324**, 1312 (2009).
[2] X. Chen, *et al*., Carbon **94**, 810 (2015).
[3] X. Li, *et al*., J. Am. Chem. Soc. **133**, 2816 (2011).

Corresponding Author: S. Maruyama
Tel: +81-3-5841-6408, Fax: +81-3-5841-6408,
E-mail: maruyama@photon.t.u-tokyo.ac.jp

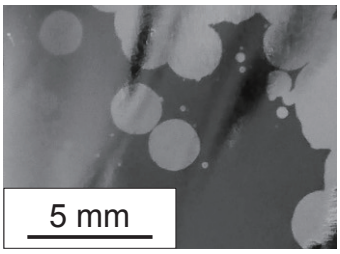

Fig. 1 Optical image of graphene on the copper foil.

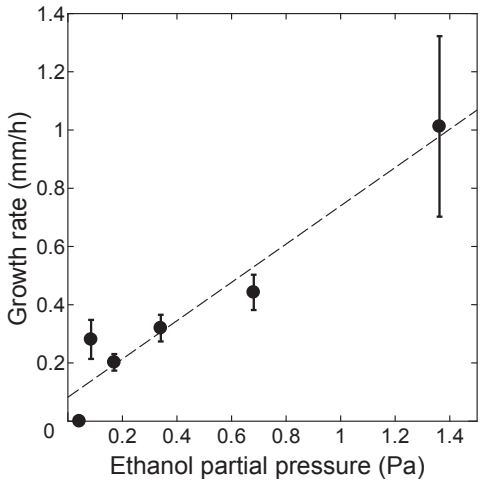

Fig. 2 The dependence of ethanol partial pressure on growth rate.

3P-28

Synthesis and Electronic Property of Fe Intercalated bilayer graphene

○Ryo Hoshino, Yutaro Hayashi, Nozomi Suzuki,
Tomoko Nagata, Nobuyuki Iwata, Hiroshi Yamamoto

College of Science &Technology, Nihon University, 7-24-1 Narashinodai, Funabashi-shi, Chiba 274-8501 japan

In order to realize superconductivity at room temperature, we fabricate metal intercalated bilayer graphene. The electron-exciton coupling is expected to generate high temperature superconductivity [1]. In this study, we report the synthesis of Fe intercalated bilayer graphene and its electric property.

The single-layered graphene sheet was grown on Cu foil by chemical vapor deposition (CVD) method, using CH_4, H_2 and Ar as process gases. After etching of Cu foil by $Fe(NO_3)_3$ aqueous solution, the single-layered graphene was transferred on SiO_2/Si substrate. On the single-layered graphene, additional single-layered graphene was transferred again to be bilayer graphene as shown in Fig. 1. Figure1 shows the Fe intercalation method. The Fe ions in $Fe(NO_3)_3$ aqueous solution during the Cu etching process was remained between bilayer graphene. From the results of SEM-EDX of Fe intercalated bilayer graphene, atomic % of the Fe was 12.40%. This result suggests that bilayer graphene was intercalated Fe by this intercalation method.

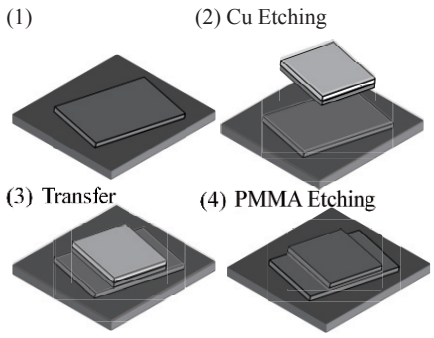

Figure-1. Fe intercalation method

[1] Akimitsu, Parity. MARUZEN. **05**, 6-12 (2008).

Corresponding Author: Nobuyuki Iwata
Tel: +81-47-469-5457
E-mail: iwata.nobuyuki@nihon-u.ac.jp

Enhancement of laser-induced water decomposition by 2D sheets studied by first-principles simulations

○Yoshiyuki Miyamoto[1], Hong Zhang[2], Xinlu Cheng[3], Angel Rubio[4]

[1] *Research Center for Computational Design of Advanced Functional Materials, AIST, Central 2, 1-1-1, Umezono, Tsukuba, 305-8568, Japan*
[2] *College of Physical Science and Technology, Sichuan University, Chengdu 610065, China*
[3] *Key Laboratory of High Energy Density Physics and Technology of Ministry of Education; Sichuan University, Chengdu, 610064, China*
[4] *Max Planck Institute for the Structure and Dynamics of Matter, Hamburg, Germany*

Photo-induced water decomposition with aid of photo-catalysis has become a hot topic since 1979 [1]. Photo-carrier generation and subsequent hole-transfer to water oxidation level and electron-transfer to reduction level protons are believed to play a main role [2]. Recently graphitic carbon nitride (gC_3N_4) sheets are found to assist water decomposition with UV and visible light [3,4] and usage of graphitic materials as photo-catalysis for water decomposition seems to be promising.

We here propose application of femtosecond laser, which has higher photon-flux than ordinary light thus can decompose water with higher yield. In this study, we have performed first-principles molecular dynamics for studying water decomposition under strong laser field with full-width of half maximum 10 fs and basic wavelength of 800 nm. In performing the simulation, we applied real-time propagation time-dependent density functional theory combined with Ehrenfest type molecular dynamics under presence of the laser field by using a code FPSEID [5] including optical field [6].

The threshold of laser-field intensity for decomposing an isolated water molecule was computed as 9 V/Å by using local density approximation and by using the generalized gradient approximation. On the other hand, this value is reduced less than 7 V/Å when water molecule is located above graphitic sheets, *i. e.* graphene, hexagonal boron nitride, and gC_3N_4. Fig. 1 shows snapshots of the results of water decomposition above a graphene sheet. We will discuss possible mechanisms of reducing threshold intensity and further applications.

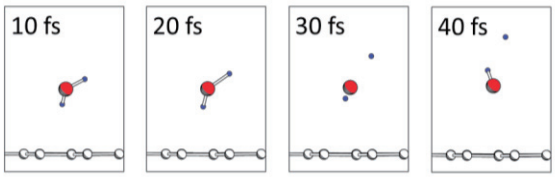

Fig.1 Snapshots of first-principles molecular dynamics of water decomposition above a graphene sheet

[1] T. Inoue, A. Fujishima, S. Konishi, and K. Honda, Nature, 277, **637** (1979).
[2] J. Wirth, R. Neumann, M.Antoniettib and P. Saalfrank, Phys. Chem. Chem. Phys. **16**, 15917 (2014).
[3] X. Wang *et al*, Nature Mat. **8**, 76 (2009).
[4] J. Liu *et al*, Science **347**,970 (2015).
[5] O. Sugino and Y. Miyamoto, Phys. Rev. B**59**, 2579 (1999).
[6] Y. Miyamoto and H. Zhang, Phys. Rev. B**77**, 165123 (2008).

Corresponding Author: Y. Miyamoto
Tel: +81-29-849-1498, Fax: +81-29-851-5426,
E-mail: yoshi-miyamoto@aist.go.jp

Solvothermal preparation of uranium oxide supported on reduced graphene oxide

○Li Ding, Pei Tang, Ding Ma, Yan Li

Key Laboratory for the Physics and Chemistry of Nanodevices, Beijing National Laboratory for Molecular Science, College of Chemistry and Molecular Engineering, State Key Laboratory of Rare Earth Materials Chemistry and Applications, Peking University, Beijing 100871, China

Uranium oxides have been used as good catalysts for different kinds of reactions owning to their special structural features and chemical properties [1]. The oxidation state of uranium is a crucial factor influencing its catalytic performance. Thus, the synthesis of pure phase uranium oxides with different oxidation states is very important for studying their catalytic properties [2]. Previously, uranium oxide at the nano size were synthesized in a mixture of oleic acid (OA) and, oleylamine (OAm) which surrounded the surface of particle and further hindered the application in catalysis [3][4]. In the present work, the uranium oxides loaded on the reduced graphene oxide (rGO) sheets were synthesized by solvothermal route as shown in Scheme 1. We found that the composition of the solvent is a key issue for controlling the phase of the products.The water present in the solvent was benefical for the formation of U_3O_8.And UO_2 was obtained favorablely in the solvent with ethylene glycol.

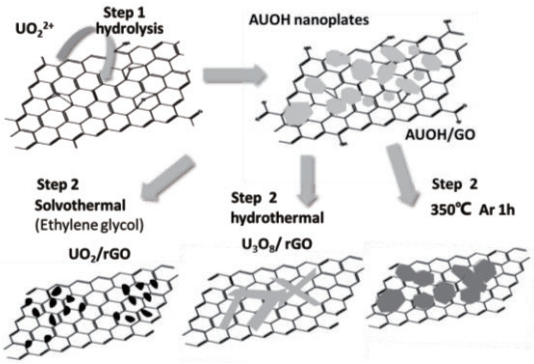

Schem 1. The formation of uranium oxide/rGO in a two step synthesis process. AUOH is ammonia uranium oxide hydrate.

[1] Taylor, S. H. *et al.*, Nature **1996,** *384* (6607), 341-343.
[2] Idriss, H. *et al.*, Journal of Catalysis **2004,** *224* (2), 358-369.
[3] Meyer, D. *et al.*, Nano Research **2013,** *7* (1), 119-131
[4] Cao, Y. C. *et al.*, Journal of the American Chemical Society **2006,** *128* (51), 16522-16523

Corresponding Author: Yan Li, Ding Ma
Tel: +86-10-62756773, Fax: +86-10-62751708; Tel：010-62758603, Fax：010-62758603;
E-mail:yanli@pku.edu.cn; dma@pku.edu.cn

Fabrication of planar heterojunction perovskite solar cells using graphene oxide as hole transport layer

○Shunjiro Fujii[1], Takeshi Tanaka[1], and Hiromichi Kataura[1]

[1]*Nanomaterials Research Institute, National Institute of Advanced Industrial Science and Technology (AIST), Ibaraki 305-8565, Japan*

Organometal halide perovskite solar cells are of special interest owing to solution-processable fabrications and their high power conversion efficiency (PCE). There are two main structures for the perovskite solar cells. One is a mesoporous structure [1] commonly using titanium dioxide as the electron transport scaffold layer. The other device structure is an inverted planar heterojunction (PHJ) [2], in which PEDOT:PSS is widely used as a hole transport material (HTM). Recently, carbon nanotube/graphene oxide (GO) layer has been demonstrated as efficient HTM of perovskite solar cells with mesoporous structure [3]. However, inverted PHJ perovskite solar cells using GO as HTM have not been investigated.

In this work, we fabricated inverted PHJ solar cells utilizing GO as HTM. The GO used in this study exhibited few-layered sheets with a typical thickness of below 2 nm (Figure 1). The device structure was Glass/ITO/GO/perovskite ($CH_3NH_3PbI_{3-x}Cl_x$)/Ag (Figure 2). Figure 3 shows the current density-voltage (J-V) curves for solar cells using PEDOT:PSS or GO as HTM. The PCEs extracted from the J-V curves were 5.1% and 4.0%, respectively. The detailed device characteristics will be discussed. This work was supported by KAKENHI Nos. 26790021, 25220602.

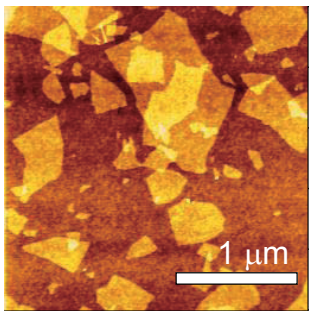

Figure 1 AFM image of GO spin-coated on SiO_2/Si.

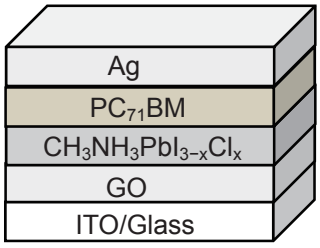

Figure 2 Schematic illustration of perovskite solar cell.

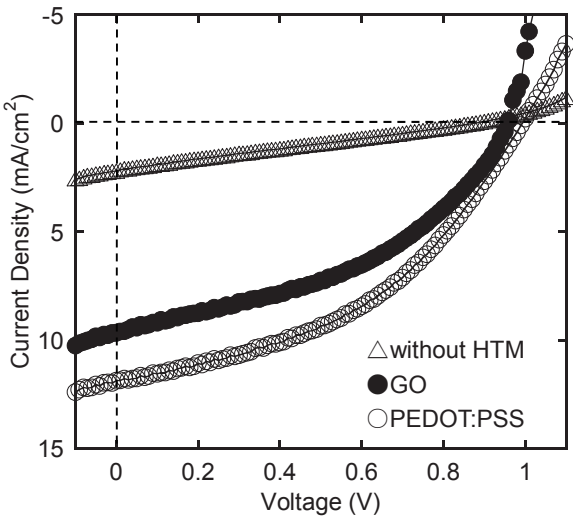

Figure 3 J-V characteristics under AM 1.5G (100 mW/cm^2).

[1] A. Kojima et al., J. Am. Chem. Soc. 131 (2009) 6050

[2] I. Jeon et al., Nano Lett. 15 (2015) 6665

[3] F. Wang et al., The 49th FNTG General symposium 2015, 3-8

Corresponding Author: Hiromichi Kataura
E-mail: h-kataura@aist.go.jp

3P-32

Investigation of Catalysis of Nitrogen-Doped Graphene for Oxygen Reduction Reaction

○Takeru Okada[1], Kumi. Y. Inoue[2], Tomokazu Matsue[2,3], Golap Kalita[4], Masaki Tanemura[4], Meyya Meyyappan[5], and Seiji Samukawa[1,3]

[1] *Institute of Fluid Science, Tohoku University, Sendai 980-8577, Japan*
[2] *Graduate School of Environmental Studies, Tohoku University*
[3] *WPI-AIMR, Tohoku University*
[4] *Department of Frontier Materials, Nagoya Institute of Technology*
[5] *NASA Ames Research Center*

Nitrogen-doped (N-doped) graphene promises to improve the application potential current graphene based devices. To this end, the bonding states between carbon and nitrogen atoms can be manipulated to tailor the properties of the doped graphene. For example, graphitic nitrogen is known to promote desired catalytic activities (oxygen reduction reaction, ORR) in graphene fuel-cell systems. While some studies have demonstrated the catalytic enhancement of N-doped graphene, they have also indicated that factors such as the location and the bonding state of the N-dopants may be determinants in graphene property design. According to previous report [1], graphitic N-dopants are better at enhancing graphene's catalytic activities, compared to their pyrrolic and pyridinic counterparts— illustrating the importance of the N-dopant bonding state. However, established nitrogen-doping methods lack selectivity in dopant chemical identity and in dopant location; both are key factors in graphene property design because the properties depend on the chemical identity and location of the dopant.

Recently we have reported a post-treatment method that selectively controls the location and bonding state for synthesizing N-doped graphene [2]. Our approach uses a charge neutral nitrogen beam with tunable beam energy to insert N-dopants into graphene. We utilize the beam energy to determine both the N-dopant locations and bonding state. We found bonding state of nitrogen depends on beam energy of neutral beam. The location and bonding state can be controlled in terms of the nitrogen doping of graphene. A low energy is suitable for the doping only at the edge. A CN single bond is dominantly formed under a moderate beam energy condition (7 eV), and a high energy NB forms a high doping concentration with defect formation.

Here we report investigation of electrochemical activity of graphitic nitrogen rich graphene. CVD grown graphene was transferred onto a rotating disk electrode. Then it was treated by neutral nitrogen beam under 7 eV condition. Electrochemical measurement was carried out in oxygen saturated 0.1 M KOH solution and N-doped graphene was used as the working electrode. ORR was considered to be detected around -0.2 V. Although quantitative analysis is still ongoing, the current density seems to be higher than that for pristine graphene. This implies catalytic effect and that the conductivity of graphene is enhanced by the insertion of nitrogen atom to hexagons in graphene. Detail will be discussed in the presentation.

[1] H. Wang *et al*. ACS Catalysis 2 781–94 (2012)
[2] T. Okada *et al*. Nanotechnology 26, 485602 (2015)

S.Samukawa and T. Okada
Tel: +81-22-217-5240/5318,
E-mail: samukawa@ifs.tohoku.ac.jp/okada@sammy.ifs.tohoku.ac.jp

3P-33

Nano-scale Characterization of Graphene by AFM-Raman Spectroscopy

○Yasushi Nakata[1], Yoshito Okuno[1], Sanpon Vantasin[2], Yoshito Tanaka[4], In-Sang Yang[3], Yukihiro Ozaki[2], and Nobuyuki Naka[1]

[1] Scientific and Semiconducting instruments R&D department Optical Analysis Team, HORIBA Ltd.
[2] School of Science and Technology, Kwansei Gakuin University, [3] Ewha Womans University, [4] The University of Tokyo

Graphene has attracted much attention for its promising variety of applications on nano-electronic device [1]. To evaluate the performance of the graphene devices, an investigation of their properties with nanometer spatial resolution is strongly demanded.

We have newly developed AFM-Raman system for side-illuminated Tip-Enhanced Raman Spectroscopy (TERS) as a powerful tool for nano-scale characterization. Fig.1 shows AFM and TERS image of special graphene, to which high current density of 3.0×10^{8} A/cm^{2} was applied, on silicon substrate. TERS image was constructed by plotting the peak intensity of Raman band appearing at 1530cm^{-1}, and it exactly corresponded to AFM image taken at same region. The spatial resolution in this image was estimated as 25 nm. Through detailed TERS image analysis, edge phonons [2], which are characteristic of graphene nanoribbons, were observed. We had peaks appearing at 1530 cm^{-1} and 1450 cm^{-1}, which are considered to be derived from armchair and zigzag structure. From the results, we assumed the high current density caused C-O bonding on the surface, which resulted in periodic defects or distortion of atomic arrangement. To best of our knowledge, this was the first time nano-spectroscopic studies of the graphene showing the characteristic of nanoribbons.

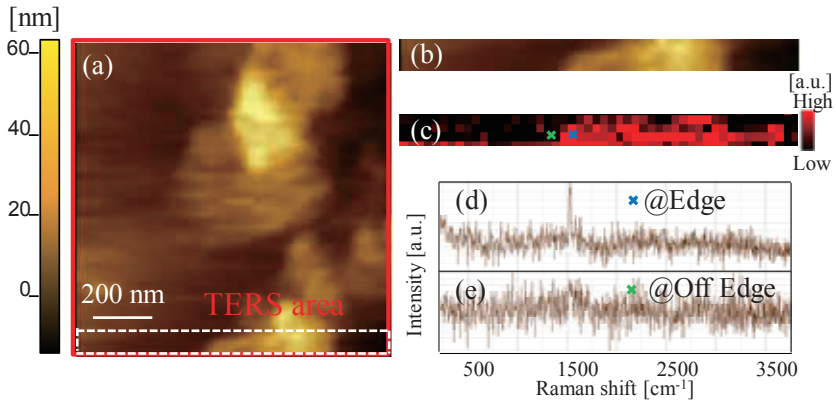

Fig.1 (a) AFM image of Graphene. (b) AFM image and (c) TERS image of Graphene in targeted area in (a). TERS spectra of (d) edge of graphene and (e) off graphene.

References
[1] K. S. Novoselov et. al., *Science*, **306**, 666 (2004)
[2] W. Ren et. al., *Phys. Rev. B*, **81**, 035412 (2010)

Corresponding Author: Y. Nakata
Tel: +81-75-325-5038, Fax: +81-75-315-9525,
E-mail: yasushi.nakata@horiba.com

Study on field emission sites of graphene emitter by field emission microscopy and field ion microscopy

○Noboru Yokoyama, Toru Hoshino, Kohji Iwata, Hitoshi Nakahara, Koji Asaka and Yahachi Saito

Department of Quantum Engineering, Nagoya University, Nagoya 464-8603, Japan

A time sequential series of field emission microscopy (FEM) patterns from a graphene emitter and the corresponding time trace of emission current under a constant voltage are shown in Fig. 1. The FEM patterns show a striped pattern (or "lip pattern") consisting of an array of streaked spots; the direction of striation is perpendicular to the graphene sheet, and each stripe is divided into two wings by a central dark band running parallel to the graphene sheet. With the elapse of time, the size of the lip pattern is extended with the increase of the number of striated spots, the emission current being concurrently increased even under the constant voltage.

Figs. 2 (a) and (b) show FEM patterns from a clean graphene emitter and Al-deposited one, respectively. Mean thickness of deposited Al was 5.9 nm. By the deposition of Al, a spotty pattern exhibiting 4-fold and 6-fold symmetries appeared. The contrast of the spotty pattern is reminiscent of the structure of an atomic cluster with a shape of cubo-octahedron (Fig. 2 (c)), which is a crystal form characteristic of face-centered cubic metals. The distance between neighboring atoms along the surface of Al is 0.286 nm when the lattice constant in the cluster is kept the same as that of bulk Al. Using this interatomic distance as a measure of the magnification of these FEM images, the spacing between adjacent streaked spots for clean graphene emitters is estimated to be in a range between 0.14 and 0.23 nm. The derived distances of 0.14 and 0.23 nm in the lip pattern are very close to the C-C bond length (0.144 nm) and the distance between the outermost carbon atoms at the zigzag edge (0.249 nm), respectively. In order to clarify the edge structure in atomic resolution, field ion microscopy of the graphene will be discussed.

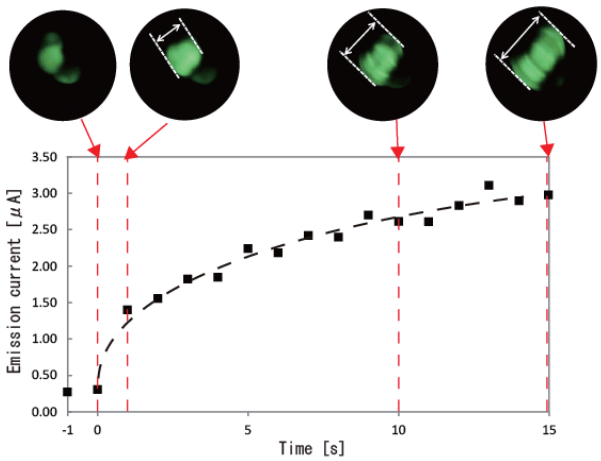

Fig.1 Change of FEM patterns and the corresponding time trace of emission current under constant voltage.

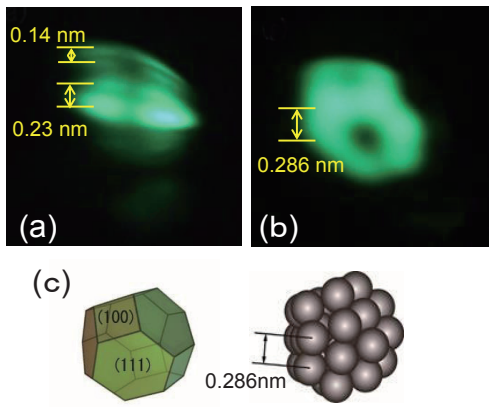

Fig.2 FEM pattern from (a) a clean graphene emitter, and (b) Al-deposited one. (c) Structure model of the Al cluster with the cubo-octahedral shape.

Corresponding Authors: N. Yokoyama, Y. Saito
Tel: +81-52-789-3714, Fax: +81-52-789-3703
E-mail: yokoyama@surf.nuqe.nagoya-u.ac.jp, ysaito@nagoya-u.jp

Dimensionality Dependence of Plasmon Resonance in Graphene Nanoribbons

°Takahiro Morimoto, Yoshiue Ikuta and Toshiya Okazaki
CNT-Application Research Center, National Institute of Advanced Industrial Science and Technology, Tsukuba 305-8565, Japan

The localized plasmon resonances are of particular interested because the observed phenomena drastically depend on various properties including geometry of nano-structures and excitation energy dispersions of carbon materials. Especially, the carbon nanotubes (CNTs) and graphene have been expected unique carrier density dependence originated from their linear energy dispersion and strongly confined structures [1,2]. Recently, we reported the plasmon resonance of clean CNT channels both single-walled [3] and multi-walled [4] CNTs. In these CNTs, the conventional carrier density dependence ($n_s^{1/2}$) never been observed by chemical doping measurements. In the case of graphene, the carrier density dependence of plasmon resonances is theoretically expected from $n_s^{1/4}$ (2D) to n_s^0 (1D) by decreasing confinement dimensions. Therefore, in this study, we will report the dimensionality dependence of plasmon resonance in graphene nano-ribbons fabricated from a single layer graphene.

Figure.1 shows the AFM image of the measured sample fabricated on the optical transparent SiO_2/Si substrate. The graphene nanoribbons were pattered as same length (750 nm) and different width (150 to 1000 nm) by the EB lithography. The optical and transport properties were measured with same sample on the same substrate. The carrier density of each nanoribbon was controlled by the gate voltage with conventional back gate configurations. The carrier density in each gate voltage was estimated from the Drude absorptions observed lower frequency regions. The Far-infrared (FIR) resonance signals were measured with polarized conditions as shown in Fig.1.

Figure.2 shows typical results of carrier density dependence of FIR resonance peak positions with different width samples. The wider width sample (2D) shows clear $n_s^{1/4}$ dependence as expected theoretical models. By decreasing width, however, the carrier density dependence is strongly suppressed as shown in Fig.2. In the narrow width sample, the carrier density dependence is lost and peak positions are almost constant.

We will discuss the details of the measurement and the analysis method. The comparison between measurement results and theoretical predictions are also shown in this presentation.

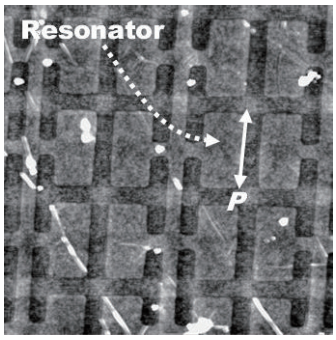

Fig.1 The AFM image of graphene nano-ribbons.

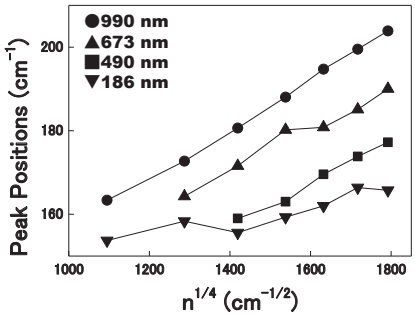

Fig.2 The carrier density dependence of FIR peak positions.

[1]T. Nakanishi and T. Ando. JPSJ, **78**, 114708, (2009). [2]S. Das Sarrma and E. H. Hwang. PRL, **102**, 206412, (2009). [3]T.Morimoto *et al.*, ACS Nano **8**, 9897 (2014). [4]T.Morimoto and T.Okazaki, APEX, **8**, 055101 (2015).

Corresponding Author: Takahiro. Morimoto
Tel: +81-29-861-3804, Fax: +81-29-861-6241,
E-mail: t-morimoto@aist.go.jp

3P-36

Wavelength dependence of surface roughness in photoreduction of graphene oxide

Maki Ueda[1], Yoshiki Yamamoto[2], Yuki Hirano[2], Kazuto Hatakeyama[3], Michio Koinuma[3], Yasumichi Matsumoto[3], Masahiro Hara[2], ○Hiroyuki Yokoi[4]

[1] Department of Materials Science and Engineering, Faculty of Engineering, Kumamoto University, Kumamoto, 860-8555, Japan
[2] Department of Physics, Graduate School of Science and Technology, Kumamoto University, Kumamoto, 860-8555, Japan
[3] Department of Applied Chemistry and Biochemistry, Graduate School of Science and Technology, Kumamoto University, Kumamoto, 860-8555, Japan
[4] Department of Materials Science and Engineering, Graduate School of Science and Technology, Kumamoto University, Kumamoto, 860-8555, Japan

Graphene oxide (GO) is graphene-like material which can be produced through oxidation of graphite. Carbon atoms in the basal plane or on the edges of GO are partially modified with functional groups containing oxygen. Several reduction processes have been investigated to restore its graphitic structure. However, it has been found very difficult to achieve it. For example, additional defects were induced and pores were formed eventually in GO sheets in a photoreduction process using ultra-high pressure mercury lamp[1].

In this study, we have conducted photoreduction of GO using monochromatic lights of 350, 450, 550 nm in wavelength. We analyzed the surface roughness of photoreduced GO sheets with an atomic force microscope (SPM-9700, Shimadzu Corp.). It has been found that the surface roughness becomes worse in 350 nm and does not change in 550 nm, but improves in 450 nm. There results might suggest that the functional group can be removed from GO selectively without destroying the graphitic network of GO by visible light with a shorter wavelength.

[1] M. Koinuma *et al*. J. Phys. Chem. C **116**, 19822 (2012).

Corresponding Author: H. Yokoi
Tel: +81-96-342-3727, Fax: +81-96-342-3710,
E-mail: yokoihr@kumamoto-u.ac.jp

3P-37

Raman intensity magnetic field dependence in graphene

○ Toshiya Shirakura[1], Riichiro Saito[1]

[1]*Department of Physics, Tohoku University, Sendai 980-8578, Japan*

In this work, we calculate magnetic field-dependence of Raman intensity of graphene in which the optical phonon and the inter Landau-level (LL) electronic transitions are coupled together. The physics of graphene in the presence of the magnetic field has been studied by the magneto Raman spectroscopy [1, 2, 3], in which the high quality of graphene samples are reflected by the long lifetime of the Dirac fermions and then the narrow spectral widths of the LL [4]. For evaluating the in-plane crystal size, the defects and the LL spectral width can be compared by using Raman spectroscopy in magnetic field [4, 5].

A previous theoretical work has calculated the Raman spectra of graphene under the magnetic field by using fitting parameter which corresponds to G-peaks from experiment of Raman spectra in their formula [6]. However, they did not consider the microscopic picture of interference of the peaks.

In this work, we directly calculate the G-band Raman spectra by considering electron-photon and electron-phonon interaction. In order to get the result, we consider time-dependent perturbation theory, and we adopt dipole approximation for electron-photon matrix element. Dipole approximation means that wave length of laser is sufficiently long compared with atomic bond length of graphene. In the case of electron-phonon interaction, only two phonon modes (iLO and iTO) contribute to the Raman intensity. By calculating Raman spectra in the LL quantized graphene, we will discuss the G-band magnetic field-dependence.

[1] M. O. Goerbig, *et al*., Phys. Rev. Lett. **103**, 087402 (2009).
[2] T. Ando, *et al*., J. Phys. Soc. Jpn. **76**, 024712 (2007).
[3] C. Faugeras, *et al*., Phys. Rev. Lett. **103**, 186803 (2009).
[4] J. Yan, *et al*., Phys. Rev. Lett. **105**, 227401 (2010).
[5] C. Faugeras, *et al*., Phys. Rev. Lett. **107**, 036807 (2011).
[6] C. Qiu, *et al*., Phys. Rev. B. **88**, 165407 (2013).

Corresponding Author: T. Shirakura,
E-mail: shirakura@flex.phys.tohoku.ac.jp

3P-38

Chemical vapor deposition growth of high-quality large-area hexagonal boron nitride monolayers and an application to passivation of black phosphorus

○Yuya Takabayashi, Sinha Sapna, Haruka Omachi, Hisanori Shinohara and Ryo Kitaura

Department of Chemistry, Nagoya University, Nagoya 464-8602, Japan

Hexagonal boron nitride (hBN) has attracted a great deal of attention not only as a substrate for high-quality atomic-layer devices but also as an ultrathin insulator for passivation and protection of reactive atomic layers. hBN possesses large bandgap (6 eV), high mechanical strength, high thermal stability and chemical inertness[1], and its monolayer form can be made and easily transferred onto desired substrates. These fascinating properties of hBN provide great potential in applications for ultrathin dielectric layers, tunneling barriers, and protective layers.

Monolayer hBN with uniform thickness, large grain size and high crystallinity is critical for these applications, and it is still a great challenge to prepare such hBN. Mechanical exfoliation provide high crystallinity hBN flakes, but in this case preparation of large-area monolayer hBN is extremely difficult. In contrast, the chemical vapor deposition (CVD), is a promising method to realize high-quality large-area hBN. We report here the CVD growth of hBN using a electropolished Cu foil as a substrate and application of the so-grown hBN to passivation of black phosphorus (BP).

Figure 1 shows a typical optical microscope image of monolayer hBN grains synthesized; the weak contrast region corresponds to hBN, whose lateral size is ~20 μm in edge length (Figure 1). Figure 2 shows a Raman spectrum that shows sharp Raman band assigned to the E_{2g} vibration mode. The full width at half-maximum (FWHM) value of the hBN peak is only 15 cm^{-1} and this sharpness of the FWHM suggests high crystalline hBN.

Furthermore, we have fabricated hBN/BP heterostructure by a dry transfer method we developed. Although BP rapidly degrades upon exposure to air [2], the hBN/BP heterostructure does not show any signs of degradation even after a week, which was confirmed by AFM observations (Figure 3). This result suggests that the present CVD-grown hBN is in a high-quality and good protection layers that easily applies to other 2D materials.

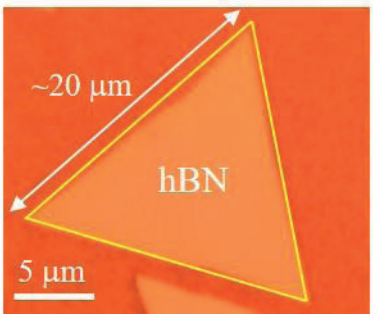

Fig.1 Optical images of hBN domains grown on Cu foil

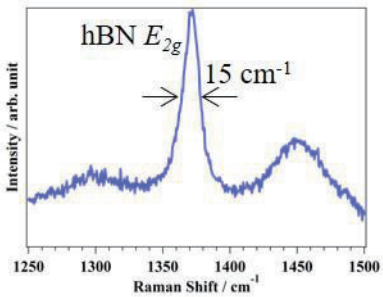

Fig.2 Raman spectra of the hBN transferred onto a SiO_2/Si substrate

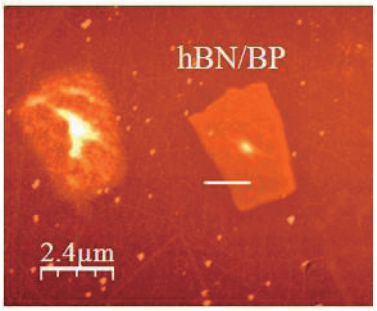

Fig.3 AFM image of hBN/BP heterostructure after a week

[1] L. Wang *et al. adv. Mater.* **26**, 1559(2013). [2] J. D. Wood *et al. Nano Lett.* **14**, 6964(2014).

Corresponding Author: R. Kitaura and H. Shinohara
E-mail: r.kitaura@nagoya-u.jp and noris@nagoya-u.jp

Insulator-to-Metal transition in polycrystalline MoS_2 films induced by electric double layer gating

○Takuya Osakabe[1], Jiang Pu[2], Yusuke Edagawa[1], Lain-Jong Li[3], Taishi Takenobu [1,2,4]

[1] *Department of Applied Physics, Waseda University, Shinjuku 169-8555, Japan*
[2] *Department of Advanced Science and Engineering, Waseda Univ.,Shinjuku 169-8555, Japan*
[3]*Physical Science and Engineering Division, KAUST, Thuwal 23955-6900, Saudi Arabia*
[4]*Kagami Memorial Laboratory, Waseda University, Shinjuku 169-8555, Japan*

Recently, transition metal dichalcogenide (TMDC) thin films have attracted attentions due to their unique optical and electrical properties. In particularly, electric double layer transistors (EDLTs) of single-crystal molybdenum dichalcogenide films (MoX_2, X = S, Se, Te) are very interesting because of the strong electric field and high density carrier accumulation, resulting in the electric field induced superconductivity and the peculiar role of strong spin orbit interactions [1,2]. However, until now, the electric field induced insulator-to-metal transition (IMT) in MoX_2 has only been observed in extremely tiny single-crystalline samples and, for future applications, it is very important to apply this technique into CVD-grown large-area samples. Although we observed the metallic behavior above 220 K in EDLTs of CVD-grown MoS_2 films previously [3], the metallicity at low temperature, which is the first important step for the electric field induced superconductivity, have not yet been clarified. Therefore, in this research, we tried to measure field effect induced transition in polycrystalline MoS_2 monolayer films at 2 K.

Figure 1 shows the device structure of EDLTs. As the gate dielectric, we selected the ion gel, which is mixture of ionic liquid (DEME-TFSI) and organic polymer (P(VDF-HFP)). Figure 2 shows the Temperature dependence of sheet resistance at various gate voltages and dashed line is the quantum resistance, which is the text-book border between insulator and metal. We successfully observed n-type transistor behavior and sheet resistance was less than the quantum resistance at gate voltage of 3.5V. Finally, by cooling the sample, we observed the solid evidence of IMT in polycrystalline films. Particularly, it remained metallic state at 2 K, which is the first mille stone for large-area electric field induced superconductors.

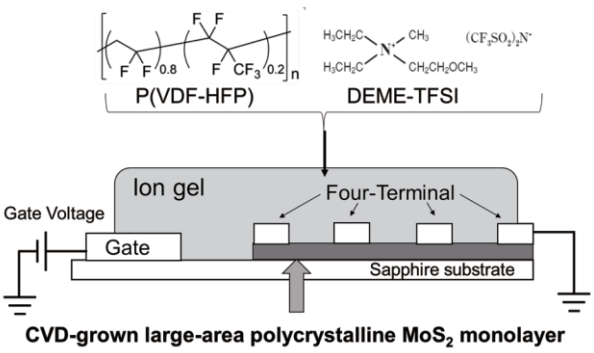

Fig.1. Device structure of large-area MoS_2 EDLTs

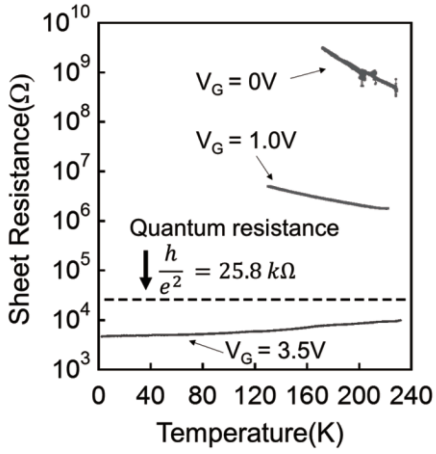

Fig.2. Temperature dependence of sheet resistance at various gate voltages

[1] J. T. Ye *et al., Science* 338, 1193 (2012). [2] Y. Saito *et al., Nature Phys* DOI: 10.1038/NPHYS3580 (2015).
[3] J. Pu, T. Takenobu *et al., Nano Lett.* 12, 4013 (2012).

Corresponding Author: Taishi Takenobu Tel&Fax:+81-3-5286-2981 E-mail: takenobu@waseda.jp

Position selective synthesis of monolayer and single crystal WS_2

○Tomoyuki Takahashi, Toshiaki Kato, Toshiro Kaneko

Department of Electronic Engineering, Tohoku University, Sendai 980-8579, Japan

Atomic scale two dimensional sheets attract intense attention due to their superior electrical, mechanical, and optical features [1, 2]. Layered transition metal dichalcogenide (TMD) is known as a true two-dimensional (2D) material with excellent semiconducting properties [3]. In spite of its potential, there are still remained lots of issues for the practical applications of TMD-based optoelectrical devices. In particular, the large area growth, defect free growth, and position selective growth are regarded as crucial issues in their production stage.

In this study, we have developed a novel synthesis method to realize the integrated synthesis of monolayer and single crystal tungsten disulfide (WS_2) array using Au dots as a nucleation promoter. Au dot arrays were fabricated with a conventional electron-beam lithography, vacuum evaporation, and lift-off process. WS_2 growth was carried out by atmospheric pressure thermal CVD with WO_3 as a source material.

Based on the systematic investigations, it is found that the nucleation of WS_2 with Au dots strongly relies on Au dots diameter and growth temperature. The crystallinity (single crystal or poly-crystal) of monolayer WS_2 is also found to be sensitive to the diameter of Au dots. The size distribution of WS_2 growing with Au dots was uniformed compared to that of without Au dots and the average size of monolayer WS_2 can be controlled by the growth temperature and Au dot distance. Through the adjustment of these growth conditions, we have succeeded in the synthesis of single crystal and monolayer WS_2 arrays in large scale with narrow size distributions (Fig. 1). This large-scaled and integrated synthesis of monolayer WS_2 array can contribute to the development of TMD-based high performance optoelectrical devices.

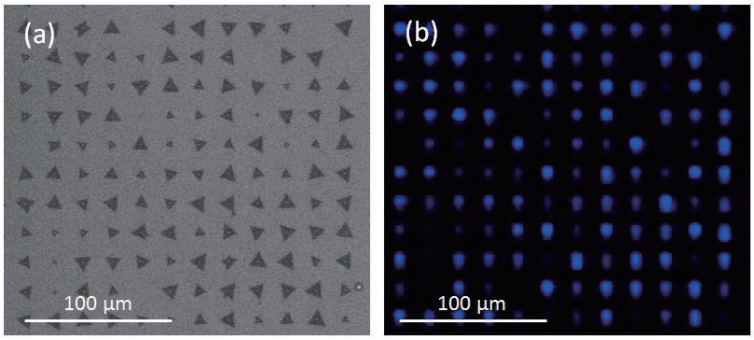

Fig. 1: (a) Scanning electron microscope image and (b) Photoluminescence intensity mapping image of large scale synthesis of monolayer and single crystal WS_2 array.

[1] T. Kato and R. Hatakeyama, ACS Nano **6**, (2012) 8508.
[2] T. Kato and R. Hatakeyama, Nature Nanotechnology **7**, (2012) 651.
[3] T. Kato and T. Kaneko, ACS Nano **8**, (2014) 12777.

Corresponding Author: T. Takahashi
Tel: +81-22-795-7046, Fax: +81-22-263-9225,
E-mail: takahashi13@ecei.tohoku.ac.jp

3P-41

Optical properties of monolayer-WSe_2/organic molecule heterostructure

○Shota Kimura[1], Daichi Kozawa[1], Keiichiro Matsuki[2], Shinichiro Mouri[3], Yuhei Miyauchi[3], Kazunari Matsuda[3], Lain-Jong Li[4] and Taishi Takenobu[1,2]

[1]Department of Applied Physics, [2]Department of Advanced Science and Engineering, Waseda University, Shinjuku Tokyo 169-8555, Japan
[3]Institute of Advanced Energy, Kyoto University, Gokasho, Uji, Kyoto 611-0011, Japan
[4] Physical Sciences and Engineering Division, KAUST, Thuwal 23955-6900, Saudi Arabia

Monolayers of transition metal dichalcogenides (TMDCs) are realized by the mechanical exfoliation method and, recently, unique interlayer phenomenon has been observed in their artificial hetero-bilayer, which is the combination of different types of TMDC monolayers [1, 2]. Although these new materials are interesting, clean and uniform interfaces between mechanically exfoliated monolayers are still difficult. To overcome these problems, we focused on organic molecules as a partner of TMDCs due to their no dangling bond and well-defined HOMO-LUMO gap, resulting in energetically-designed interface between organic crystal and TMDC monolayer. Here, we chose rubrene (5,6,11,12-tetraphenyltetracene, $C_{42}H_{28}$, Fig. 1) as organic molecules and fabricated rubrene/monolayer-WSe_2 heterostrucrure.

We prepared CVD-grown single crystals of WSe_2. Then, as shown in Fig. 2, we fabricated rubrene/monolayer-WSe_2 heterostrucrure by lamination of thin rubrene single crystals or vacuum vapor deposition of polycrystalline rubrene thin films. Very importantly, from the energy diagram of Fig. 1, we can expect the energetical coupling between rubrene and WSe_2 and, to confirm it, we measured PL spectra of rubrene. Finally, we observed the strong PL quenching on WSe_2 monolayers, indicating energy transfer from rubrene to WSe_2. Our results expand the possibility of new stacking combination, organic-inorganic hybrid heterostructure.

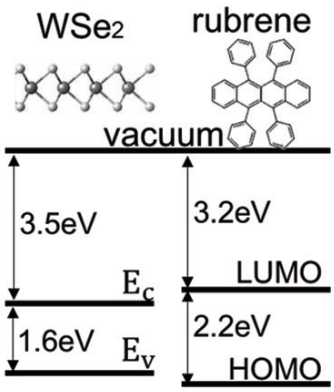

Fig.1 Energy diagram.

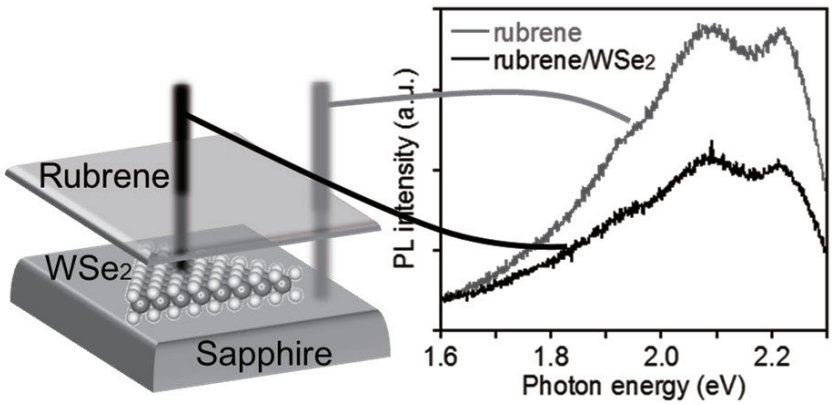

Fig.2 Schematic picture and PL of rubrene/1L-WSe_2 heterostructure.

[1] D. Kozawa *et al.*, arXiv: 1509.01875 [2] T. F. Heinz *et al.*, Nano Lett. 2015, 15(8):5033

Corresponding Author: Taishi Takenobu, Tel&Fax: +81-3-5286-2981, E-mail: takenobu@waseda.jp

Polarization-resolved photoluminescence mapping in monolayer transition metal dichalcogenides

○Yusuke Hasegawa[1], Feijiu Wang[1], Shun Aota[1], Shinichiro Mouri[1], Kazunari Matsuda[1] and Yuhei Miyauchi[1, 2]

[1]*Institute of Advanced Energy, Kyoto University, Uji, Kyoto 611-0011, Japan*
[2]*Japan Science and Technology Agency, PRESTO, 4-1-8 Honcho Kawaguchi, Saitama 332-0012, Japan*

Recently, 'valleytronics', which is expected as future optoelectronic technology relying on valley degree of freedom of electrons, has attracted much attention from the viewpoint of developing low energy consumption and high speed signal processing devices. One of the possible candidate materials is monolayer of transition metal dichalcogenides (1L-TMDs) such as MoS_2 and WSe_2 [1-3]. The intrinsic structural inversion asymmetry in these 1L-TMDs gives rise to coupling of electron (hole) spin and valley degrees of freedom. This characteristic enables valley-selective optical excitation in these materials using circular-polarized incident photons [1,2]. The 1L-TMDs have thus been intensively studied as promising materials for valleytronics [1,2]. However, correlations between observed valley polarization and local conditions in the 1L-TMDs such as local doping, strain, defects and edges have been unclear.

Here we study the spatial dependence of the polarized photoluminescence (PL) spectra in 1L-TMDs. We observed position- and polarization-resolved PL spectra of 1L-TMDs to visualize the position-dependent valley polarization degree as a function of in-plane coordinates.

Figure 1 shows the polarization-resolved PL intensity maps of 1L-MoS_2 at room temperature. Circular-polarized incident photons (1.96 eV) were set to be σ_+ helicity, and σ_+ and σ_- components of the PL signals were separately detected at the same time for each position on the sample. The PL intensity of the σ_+ emission (I_+) (averaged in the range of 1.82-1.88 eV, corresponding to exciton and trion PL) is higher than the σ_- emission (I_-), suggesting finite valley polarization in 1L-MoS_2 at room temperature [1,2] whereas low valley polarization on the multi-layer (ML) part. We will show the results for various 1L-TMDs and the spatial dependence of the observed valley polarization under variable temperature conditions. The correlations between the local conditions indicated by the PL spectra and the morphologies observed by optical and atomic force microscope will be also discussed.

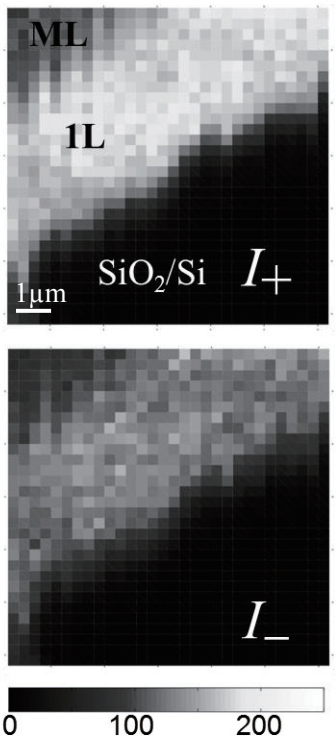

Fig.1 Polarization-resolved PL intensity maps of 1L-MoS_2 at room temperature for I_+ (top panel) and I_- (bottom panel) components. ML indicates the multi-layer part.

[1] K. F. Mak *et al*., *Nat. Nanotechnol.* **7**, 494 (2012).
[2] H. Zeng *et al*., *Nat. Nanotechnol.* **7**, 490 (2012).
[3] S. Mouri, Y. Miyauchi, K. Matsuda, *Nano Lett*. **13**, 5944 (2013).
Corresponding Author: Y. Miyauchi
Tel/Fax: +81-774-38-3465/+81-774-38-4567
E-mail: miyauchi@iae.kyoto-u.ac.jp

3P-43

Magnetism arising from pore edges of nanomesh on few-atomic layered hexagonal boron nitride

○K. Nagano, Y. Tagami, C. Ohata, G. Hashimoto[1], S. Katsumoto[1], K. Nomura, J. Haruyama

Faculty of Science and Engineering, Aoyama Gakuin University, 5-10-1 Fuchinobe, Sagamihara, Kanagawa252-5258, Japan
[1]Department of Applied Physics, The University of Tokyo, Tokyo 113-8656, Japan

Physics and applications of two-dimensional mono(few) atomic layers of various materials are attracting considerable attention (e.g., graphene, black phosphorene (BP), MoS_2 and h-BN). Among those, mono(few)-atomic layer of h-BN has been actively used for sufficient isolation between graphene and SiO_2/Si substrate. On the other hand, we have investigated magnetism arising from edges of graphene and BP.

In the case of graphene, flat band ferromagnetism arising from edges state of zigzag atomic-structure edges were theoretically well known. We experimentally observed it in hydrogen(H)-terminated graphene nanomesh (GNM), which has honeycomb like array of hexagonal nanopores with zigzag pore edges fabricated by non-lithographic method [1]. In contrast, the ferromagnetism disappeared in oxygen(O)-terminated GNM. For O-terminated few-layer BP nanomesh (BPNM) fabricated following the same method as that for GNM, we observed ferromagnetism approximately 10 – 100 times greater than those in H-terminated GNM, while it disappeared in H-terminated BPNM [2].

Here, we have fabricated few-layer h-BNNM using the same non-lithographic method applied to mechanically exfoliated h-BN. We find ferromagnetism in O-terminated BNNM. However, it is highly sensitive to annealing temperature after formation of nanomesh and also kinds of the foreign atoms for the pore edge termination. It is theoretically known that appearance of edge magnetism strongly depends on kinds of atoms at edge dangling bond (i.e., B or N) and its termination [3]. Various dependence (e.g., on annealing temperature, termination atoms) and theoretical discussion will be presented at poster.

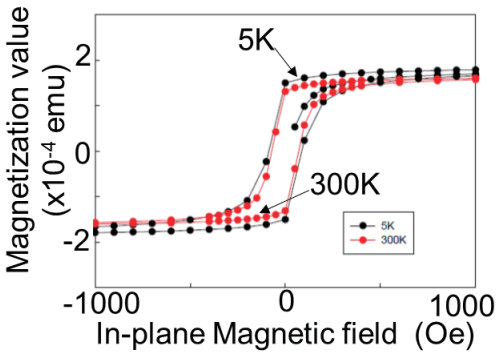

Fig. 1: Magnetization curve of oxidized few-layer h-BN nanomesh annealed at 500 ℃ under high vacuum right after the formation. It does not appear at annealing temperature (T_a) above 600℃ and the magnitude of saturation magnetization value decreases in the samples with T_a < 500℃.

[1] T. Hashimoto, J. Haruyama, S. Roche et al., *Appl. Phys. Lett.* **104**, 252410 and **105**, 183111 (2014)
[2] Y. Nakanishi, J. Haruyama, S. Roche et al., *Phys. Rev. Lett.* **In press**
[3] A. Du et al., *J. Am. Chem. Soc.* **131**, 17354 (2009)

Corresponding Author: J. Haruyama
Tel: +81-42-759-6256, E-mail: J-haru@ee.aoyama.ac.jp

Geometric and electronic structures of atomic layers of GaN

○Yanlin Gao, Susumu Okada

Graduate School of Pure and Applied Sciences, University of Tsukuba, Tsukuba, 305-8571, Japan

Two-dimensional (2D) materials with an atom thickness exhibit peculiar properties arising from the constituent elements and network topologies that allow them for being promising materials in the wide areas of the future nanotechnology. Following the discovery of graphene, h-BN and silicene have been synthesized by using various experimental techniques. GaN is a wide band gap semiconductor with excellent optical and electrical properties, which are applicable of optical and high frequency electronic devices because of their high carrier mobility and wide direct band gap. In the present work, we aim to explore the possibility of the 2D atomic network of GaN by analogy with h-BN as the other candidate of the III-V atomic layer materials, based on the density functional theory by combining with the effective screening medium method.

Our calculations show that GaN thin films with four or less atomic layers and (0001)/(000-1) surfaces prefer the layered structures consisting of planar GaN sheets rather than a Wurtzite crystal structure. For the monolayer of GaN, the GaN possesses hexagonal network with the optimum lattice constant of 3.2 Å (Fig. 1). The sheet is a semiconductor with indirect energy gap of 2.28 eV between K and G points for the valence band top and the conduction band bottom, respectively. By applying the compressive pressure along the lateral direction, the planar sheet undergoes a structural transition at a lattice constant of 2.8 Å, at which the GaN has a buckled structure as in the case of free standing silicene [Fig. 2(a)]. According to the buckled structure, GaN sheet is a metal with polarization normal to the atomic sheet. We further investigate the geometric and electronic structures of GaN sheet with structural buckling of which surfaces are fully hydrogenated. The calculations show that the fully hydrogenated GaN monolayer is a semiconductor with a direct band gap of 3.68 eV, and is endowed with a buckled structure with a height of 1.31 Å at the optimum lattice constant of 3.2 Å [Fig. 2(b)]. Interestingly, the out-of-plane polarization of hydrogenated GaN is opposite to that of the clean GaN under the compression. The fact indicates that the polarization tuning is possible by controlling the H coverage of the surfaces of GaN atomic layer.

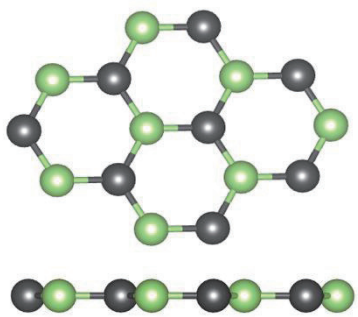

Fig. 1. The top and side views of planar 2D GaN sheet.

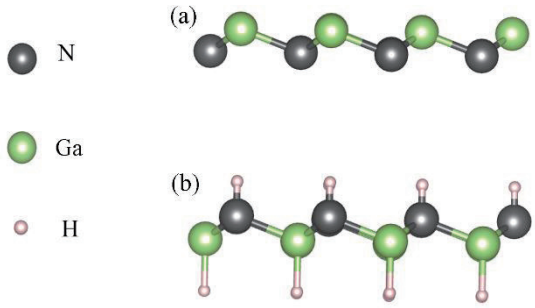

Fig. 2. Side views of (a) compressed and (b) hydrogenated 2D GaN layers.

Corresponding Author: Y. Gao
TEL: +81-29-853-5921, FAX: +81-29-853-5924
E-mail: ylgao@comas.frsc.tsukuba.ac.jp

Quantitative evaluation of size effect on macrophage uptake of carbon nanotubes by optical absorption measurement method

[O]Minfang Zhang[1]*, Naoko Tetsura[1], Kayo Ichiraku[1], Katsuhide Fujita[1], Sumio Iijima[1, 2], Masako Yudasaka[1, 2], Toshiya Okazaki[1]

[1]*National Institute of Advanced Science and Technology (AIST),*
[2]*Faculty of Science & Technology, Meijo University*

The safety assessment and toxicity evaluation of carbon nanotubes (CNTs) have been performed by using different types of CNTs with various surface properties, shapes, and sizes in vivo and in vitro. Although the results have shown that the long and short CNTs have different biodistribution and toxicity after intravenous or tracheal administration into mice, the size-effect of CNTs on cellular uptake and toxicity is still ongoing problem and the data reported previously often conflict. This is mainly due to the lack of a unified and standard approach to quantify CNTs within cells, which would be highly desirable. In this study, we have developed a method to quantify the amount of CNTs inside the cells by using the characteristics of CNT of optical absorption in near infrared region. Our purpose is to clarify the influence of CNTs sizes to the cellular uptake quantity and cytotoxicity *in vitro*.

For investigation of the size-effect, 7-types of CNTs (single- or multi-walled CNTs) with similar surface properties but different dynamic sizes measured by dynamic light scattering methods were exposed to macrophage of RAW 264.7. All types of CNTs were dispersed homogenously in 10 mg/mL of BSA aqueous solution by ultrasonic homogenizer for 5 h. The quantity of CNTs in cell lysate after incubation for 4-48 h was estimated from the absorbance of cell lysate at 750 nm. The results showed that the uptake of CNTs by macrophage is greatly dependent on the dynamic sizes of CNT-particles in dispersions, doses and incubation time. Especially, the cellular uptake quantities increased with the increase of sizes of CNTs. More CNTs taken up by cells, more cytotoxicity was found from the investigation of cell viability and ROS generation. The method proposed in this study is significantly important for the safety assessment and nanomedicine application of CNTs.

Corresponding Author: M. Zhang
E-mail: m-zhang@aist.go.jp

3P-46

Nitrogen-doped carbon preparation from organic frameworks with molecularly-ordered structures

Tomohiro Shiraki[1,2], Gayoung Kim[1], Naotoshi Nakashima[1,2]

[1] *Department of Applied Chemistry, Graduate School of Engineering, Kyushu University, Fukuoka 819-0395, Japan*
[2] *WPI-I2CNER, Kyushu University, 744 Motooka, Fukuoka 819-0395, Japan*

Hetero atom doping in carbon materials is a promising method to create new functions for future applications. In particular, nitrogen-doped carbons are attracting great attentions due to emergence of electrocatalytic activities on an oxygen reduction reaction (ORR), which is important to develop higher performance and low cost fuel cells without using rare metals such as platinum.[1]

In this study, we have newly fabricated nitrogen-doped carbons through carbonization using organic materials with molecularly-ordered structures, which are covalent organic frameworks (COFs)[2] constructed by crystalline molecular networks composed of covalently-linked organic molecules (Fig. 1). One of interesting features of COFs is facile geometrical design based on the molecular structures and combination of the building blocks, which allows a wide variety of architectural constructions, such as pore shapes and molecular arrangement. Recently, we have succeeded in room temperature synthesis of COF1 (Fig. 1), resulting in the formation of a highly crystalline structure compared to reported one.[3] Carbonization of COF1 at 700 °C under a nitrogen atmosphere provided a nitrogen-doped graphitic structure, which was confirmed by Raman and X-ray photoelectron spectroscopies.

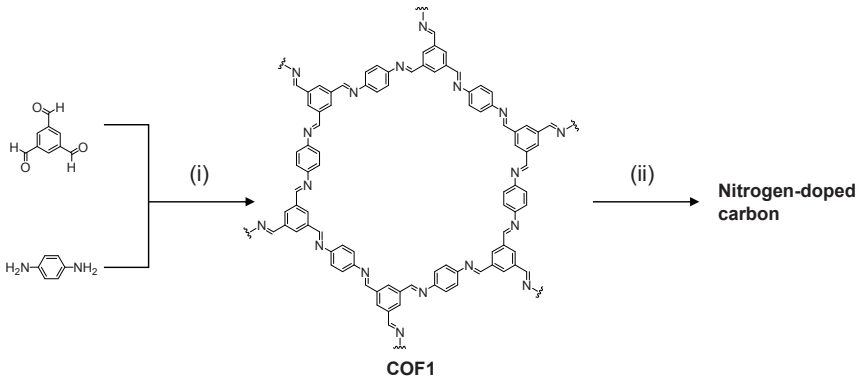

Fig.1 Schematic route for nitogen-doped carbon synthesis through carbonization of COF1: (i) room temperature synthesis, (ii) carbonization.

[1] L. Dai, Y. Xue, L. Qu, H.-J. Choi, J.-B. Baek, Chem. Rev. **115**, 4823 (2015)
[2] J. W. Colson, W. R. Dichtel, Nat. Chem. **5**, 453 (2013)
[3] T. Shiraki, G. Kim, N. Nakashima, Chem. Lett. **44**, 1488 (2015)

Corresponding Author: T. Shiraki
Tel: +81-92-802-2841, Fax: +81-92-802-2840,
E-mail: shiraki.tomohiro.992@m.kyushu-u.ac.jp

3P-47

Development of Multi-stage Ion Trap Ion Mobility System for Separation of Charged Particles with Long-range Manipulation.

○Hironobu Matsubayashi, Yasuhiro Hiroshiba, Ryota Jinnouchi,
Wataru Ohkawa, and Toshiki Sugai,

Department of Chemistry, Toho University, Miyama 2-2-1 Funabashi, 274-8510, Japan

Ion mobility spectrometry (IMS) have revealed varieties of novel information on nano materials. Novel Structures of metallofullerenes have been revealed by IMS[1]. Furthermore our newly developed ion trap ion mobility measurement system can hold the charged particles for more than 2 hours realizing observations on long term structural changes[2]. However those measurements mainly performed on a single particle and the structural resolution is limited because the system utilizes only two trap units and the transfer length is restricted to 3 mm. To break these limits to introduce new functions such as separation, here we present the development of multi-stage system.

Figure 1 shows the schematic view of the system, which consists of an electrospray ionization source for salt solution, and 10 separated quadrupole ion trap units. To each units, radio frequency field and DC bias were applied to confine and manipulate the particles. The movements of the particles were observed by the semiconductor laser eradiation.

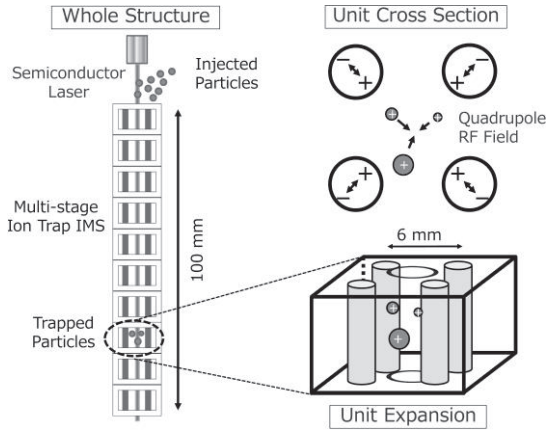

Fig. 1 Schematic View of Multi-stage Ion Trap Ion Mobility System.

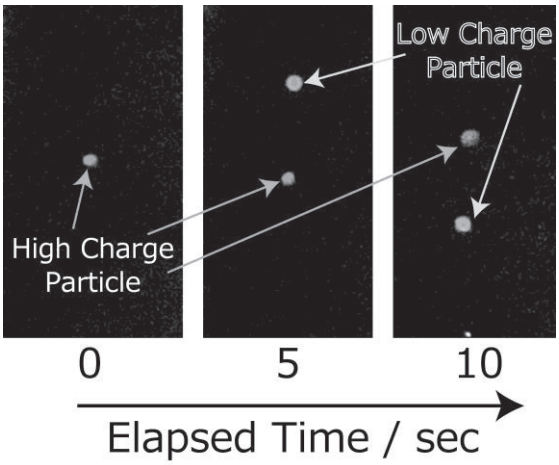

Fig. 2 Particle Separation

Figure 2 shows the observed separation of two particles. The high charge particle (r=280 nm and q=+40e) stayed in one unit while the low charge particle (r=350 nm and q=+10e) passed through. Both of them were transferred from the injection point to the trap point achieving the movement of 80 mm, which is 30 times longer than that realized in the previous system.

[1] T. Sugai *et al.*, *J. Am. Chem. Soc.* ***123***, 6427 (2001).
[2] T. Sugai *et al.*, 42nd *Fullerene-nanotube-graphene conference.* 3-13

TEL: +81-47-472-4406, E-mail: sugai@chem.sci.toho-u.ac.jp

Observation of Nano Particles by Ion Trap Ion Mobility.

○Ryota Jinnouchi, Yasuhiro Hiroshiba, Hironobu Matsubayashi,
Wataru Ohkawa, Takuma Ito, and Toshiki Sugai,

Department of Chemistry, Toho University, Miyama 2-2-1 Funabashi, 274-8510, Japan

Ion mobility spectrometry (IMS) have revealed varieties of novel information on nano materials. For example, novel structures of metallofullerenes have been revealed by IMS[1]. Furthermore our ion trap ion mobility measurement system can hold the charged particles for more than 2 hours realizing observations on long term structural changes[2]. However the detected particles have been limited to μm sized ones because of the trap efficiency and detection sensitivity. Here we present the observation of particles with a radii of 50 nm by the newly developed ion trap ion mobility system.

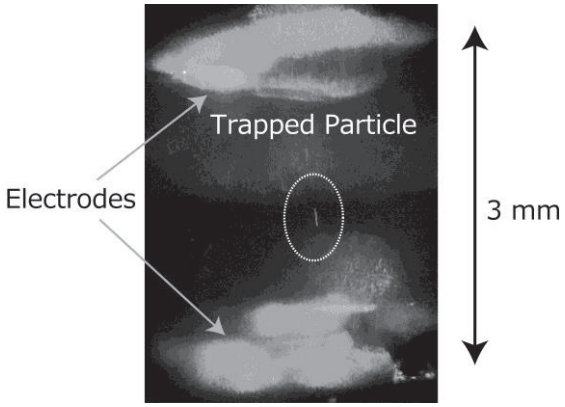

Fig. 1 Observed charged particles with a radius of 50 nm and a charge of +4000e.

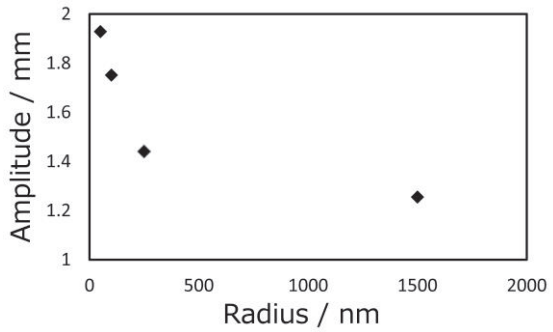

Fig. 2 Amplitude Dependence on Particle Radii

Figure 1 shows the trapped and detected nano polystyrene particle with a radius of 50±5 nm and a charge of +4000e. Since the up and down continuous motion was applied to the particle to measure its mobility, its image was observed to be a trace and the amplitude of the trace is proportional to its mobility. Figure 2 shows the amplitude dependence on the particle size. Apparently, the amplitude rapidly increases as the size decreases up to nm level. The amplitude has been observed to be quite steady for μm level particles [3] so that the results show that the collision processes of nano particles with nitrogen and oxygen molecules in air are quite different those of micro particles. We are going to study various nano materials with this system.

[1] T. Sugai *et al.*, *J. Am. Chem. Soc.* ***123***, 6427 (2001).
[2] T. Sugai *et al.*, 42nd *Fulluerene-nanotue-graphene conference.* 3-13
[3] Y. Hiroshiba *et al.,* 50th *Fulluerene-nanotue-graphene conference.*

TEL: +81-47-472-4406, E-mail: sugai@chem.sci.toho-u.ac.jp

発表索引
Author Index

Author Index

2016 年 2 月 19 日発行

第 50 回フラーレン・ナノチューブ・グラフェン総合シンポジウム
講演要旨集

≪フラーレン・ナノチューブ・グラフェン学会≫
〒113-8656 東京都文京区本郷 7-3-1
東京大学大学院工学系研究科　機械工学専攻
丸山研究室内
Phone/Fax：03-3830-4848
E-mail：fntg@photon.t.u-tokyo.ac.jp
URL：http://fullerene-jp.org
印刷　/　製本　（株）創志企画

JEOL
Solutions for Innovation

GRAND ARM

Atomic Resolution electron Microscope

JEM-ARM300F

JEM-ARM300Fは、JEM-ARM200Fで培った高安定化技術を基に開発された装置です。
冷陰極電界放出電子銃を標準搭載し、STEMおよびTEMに球面収差補正装置が
搭載可能な最高加速電圧300 kVの世界最高峰の超高分解能電子顕微鏡です。

300 kV STEM Imaging（GaN[211]）
暗視野像　Ga-Ga 原子カラム

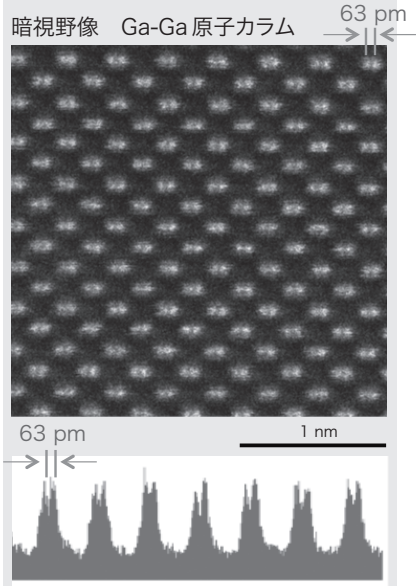

80 kV TEM Imaging（グラフェン）

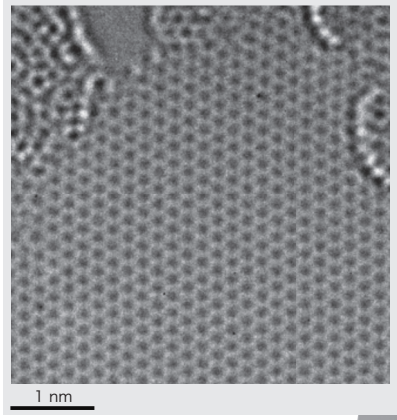

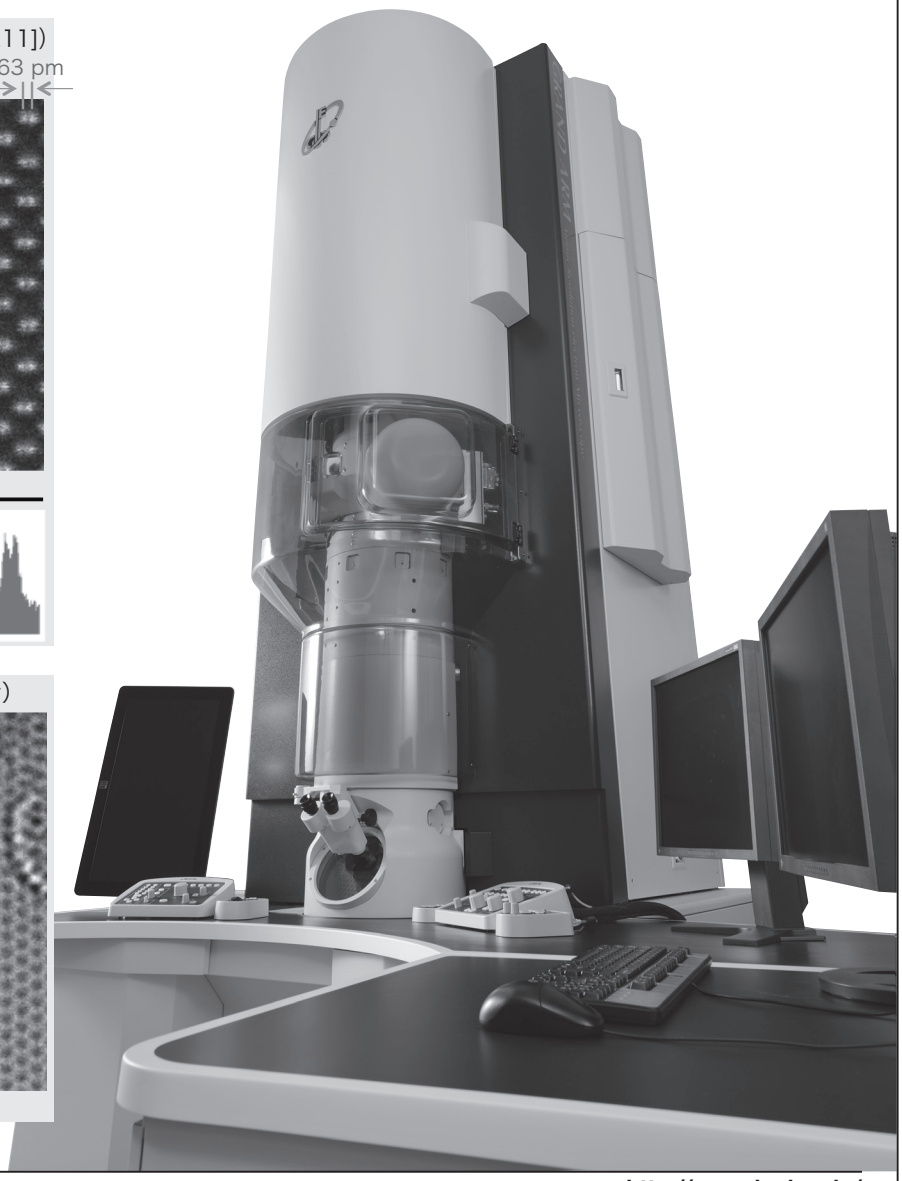

日本電子株式会社　本社・昭島製作所　東京都昭島市武蔵野3-1-2　TEL(042)543-1111　http://www.jeol.co.jp/
営業企画室　東京都千代田区大手町2-1-1　TEL(03)6262-3560　｜　西日本ソリューションセンター　大阪市淀川区西中島5-14-5　TEL(06)6305-0121
■東　京　電子光学機器営業グループ　TEL(03)6262-3581　｜　分析機器営業グループ　TEL(03)6262-3582　｜　産業機器営業部　TEL(03)6262-3570
半導体機器営業部　TEL(042)528-3491　｜　医用機器営業グループ　TEL(03)6262-3583
■札　幌　TEL(011)726-9680　｜　■仙　台　TEL(022)222-3324　｜　■筑　波　TEL(029)856-3220　｜　■横　浜　TEL(045)474-2181　｜　■名古屋　TEL(052)581-1406
■大　阪　TEL(06)6304-3941　｜　■広　島　TEL(082)221-2500　｜　■高　松　TEL(087)821-0053　｜　■福　岡　TEL(092)411-2381

誘導体化フラーレン用HPLCカラム

COSMOSIL® Buckyprep-D

COSMOSIL

● 誘導体化フラーレン用HPLCカラム

● トルエン移動相中で誘導体化フラーレンが分離可能

■C60インデン付加体の分析例

C60インデンは誘導体化フラーレンの一種であり、有機薄膜太陽電池のn型半導体材料として注目されている化合物です。コスモシール Buckyprep-Dを用いることにより高い分離性能が得られます。

COSMOSIL Application Data

Column:
Column size: 4.6mmI.D.-250mm
Mobile phase: Toluene
Flow rate: 1.0 ml/min
Temperature: 30°C
Detection: UV 325nm

Sample: C_{60} [Indene]$_2$ (1.0mg/ml)
Inj.Vol.: 1.0µl

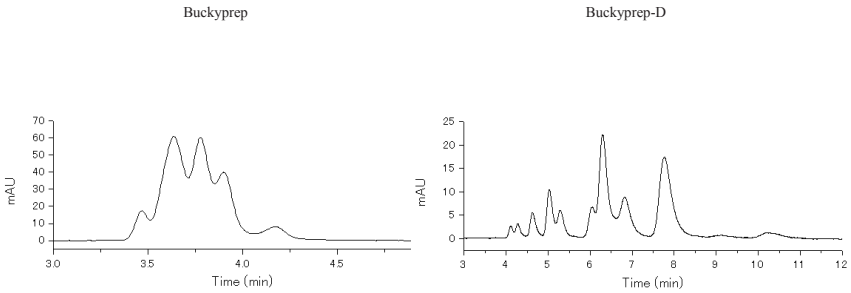

Data courtesy of Yusuke Tajima, Dr. Sci.
Organic Optoelectronics Laboratory, RIKEN (Institute of Physics and Chemistry)

NACALAI TESQUE, INC

■Buckyprepシリーズの用途

フラーレン分離のスタンダードカラム → COSMOSIL Buckyprep
誘導体化フラーレンの分離 → COSMOSIL Buckyprep-D
金属内包フラーレンの分離 → COSMOSIL Buckyprep-M

・誘導体化フラーレン (Buckyprep-D)

COSMOSIL Application Data

Column: Buckyprep-D
Column size: 4.6mmI.D.-50mm
Mobile phase: Toluene
Flow rate: 1.0 ml/min
Temperature: 30°C
Detection: UV325nm

Sample:
1; C_{60} (0.125mg/ml)
2; C_{70} (0.250mg/ml)
3; [*6,6*]-Phenyl-C_{61} Butyric Acid Methyl Ester [PCBM] (0.125mg/ml)
4; [*6,6*]-Phenyl-C_{71} Butyric Acid Methyl Ester [[70]PCBM] (0.375mg/ml)

Inj.Vol. 1.0µl

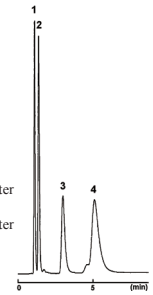

NACALAI TESQUE, INC

・金属内包フラーレン (Buckyprep-M)

COSMOSIL Application Data

Column: Buckyprep-M
Column size: 4.6mmI.D.-250mm
Mobile phase: Toluene
Flow rate: 1.0 ml/min
Temperature: 30°C
Detection: UV312nm

Sample:
$Sc_2@C_{76}(I)$
$Sc_2@C_{78}$
$Sc_2@C_{80}(I)$
C_{86}

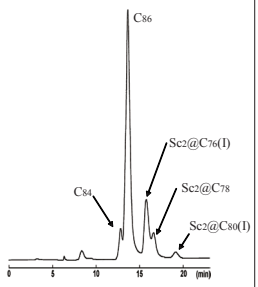

Sample courtesy of Prof. H.Shinohara,
Department of chemistry, Nagoya University

NACALAI TESQUE, INC

詳しい情報はWeb siteをご覧ください。

ナカライテスク株式会社
〒604-0855 京都市中京区二条通烏丸西入東玉屋町498

価格・納期のご照会 フリーダイヤル 0120-489-552
製品に関するご照会 TEL : 075-211-2746 FAX : 075-211-2710
Web site :http://www.nacalai.co.jp

書籍のご案内

◈定価は本体価格＋税です。

カーボンナノチューブ・グラフェンハンドブック

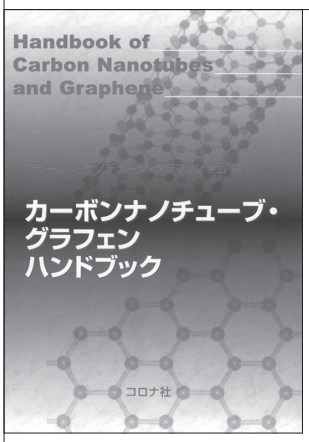

フラーレン・ナノチューブ・グラフェン学会 編
B5判／368頁
本体10,000円

本ハンドブックでは，カーボンナノチューブの基本的事項を解説しながら，エレクトロニクスへの応用，近赤外発光と吸収によるナノチューブの評価と光通信への応用の可能性を概観。最近嘱目のグラフェンやナノリスクについても触れた。

カーボンナノチューブの基礎

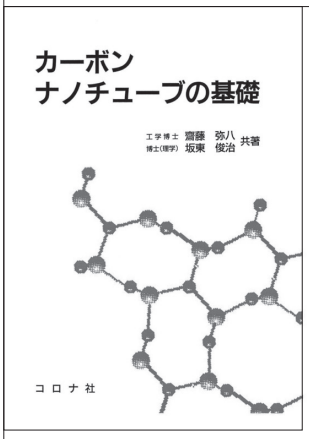

齋藤弥八・坂東俊治 共著
A5判／220頁
本体2,800円

カーボンナノチューブはC_{60}フラーレンに次ぐ新しい炭素材料であり，エレクトロニクスやエネルギー分野への応用が注目されている。本書は，ナノチューブとその関連物質の作製法，構造，物性および応用を平易に述べた入門書である。

カーボンナノチューブの材料科学入門

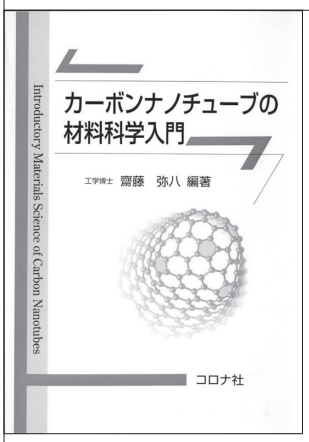

齋藤弥八 編著
坂東俊治・中山喜萬・春山純志・久保佳実 共著
A5判／250頁
本体3,400円

材料科学に新分野を創出し，エレクトロニクスからエネルギー分野まで広範囲な応用が期待されるナノテクノロジー材料の典型物質「カーボンナノチューブ」について，その製法から物性，実用の可能性までを解説した。

関連書籍のご案内

詳説 半導体物性

David K. Ferry 著／落合勇一・関根智幸・青木伸之 共訳／A5判／2016年2月刊

小さなものをつくるための ナノ/サブミクロン評価法

―μmからnm寸法のものをつくるための材料,物性,形状,機能の評価法―

肥後矢吉 編著／A5判／208頁／本体3,000円

（エコトピア科学シリーズ 2）

環境調和型社会のための ナノ材料科学

名古屋大学エコトピア科学研究所 編／A5判／186頁／本体2,600円

ワイドギャップ半導体パワーデバイス

山本秀和 著／A5判／230頁／本体3,500円

科学技術と共に歩む

株式会社 コロナ社

〒112-0011 東京都文京区千石4-46-10 振替00140-8-14844
TEL (03)3941-3131（代），-3132，-3133（営業部直通）
http://www.coronasha.co.jp FAX (03)3941-3137
E-mail eigyo@coronasha.co.jp

溶液中の物質のナノレベル微細化・分散

BRANSON 超音波ホモジナイザー

昨今のナノ・テクノロジーの発展及び粉体関連技術の発展により、より微細な粒子に対する分散処理の要望が増えてまいりました。
超音波ホモジナイザーを使用し、均質な乳化分散処理を行い、安定させることにより製品の機能は向上します。一次粒子の凝集力にも拠りますが概ね 100nm 程度までの分散力があります。
ブランソン社の超音波ホモジナイザーは、コンバーター部での超音波振動変換効率が 98%以上ある為、ホーン先端部の振幅の安定性が高く、強力なキャビテーションが得られ、高効率で、再現性の高い破砕・分散処理が可能です。
ブランソン社では卓上型実験用 20kHz 機・40kHz 機、及び 1,100W～3,300W の高出力機で大量処理も可能なシステムも用意しております。

超音波ホモジナイザー（20kHz）
BRANSON　SONIFIER シリーズ

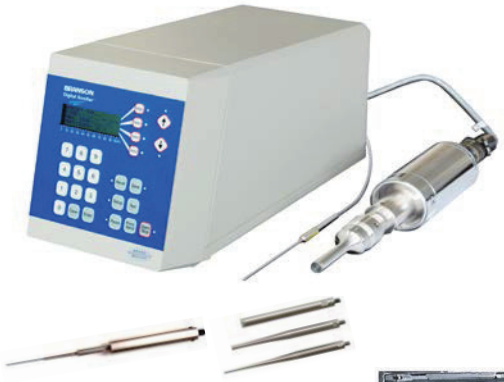

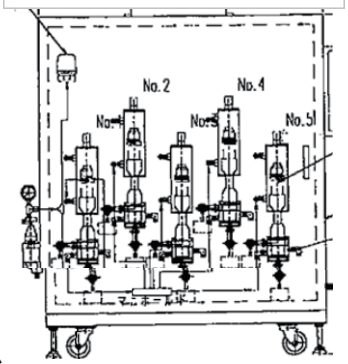

大量処理システム

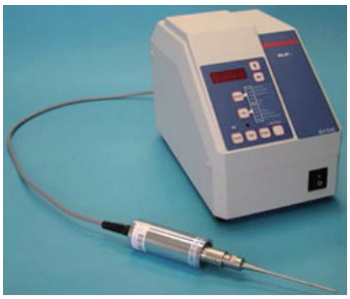

微量用・超音波ホモジナイザー
BRANSON　SLPe　（40kHz）

主なアプリケーション

分散

カーボンナノチューブ　有機・無機顔料　感光体　記録材料　磁性粉　シリカ　アルミナ　セラミック　ポリマー　ラテックス　製紙　ファンデーション　光触媒　触媒　半導体　電子基盤　液晶　セメント　ワクチン　体外診断薬　歯磨き粉　貴金属　金属　宝石　タイヤ　発酵菌類　その他

乳化

エマルジョン製剤　農薬　トナー　ラテックス　界面活性剤　クリーム　乳液　クリーム　等

株式会社 セントラル科学貿易
本社：111-0052 東京都台東区柳橋 1-8-1
Tel 03-5820-1500 Fax 03-5820-1515
URL http://www.cscjp.co.jp/
大阪支店：Tel 06-6325-3171 Fax 06-6325-5180
福岡営業所：Tel 092-482-4000 Fax 092-482-3797
札幌出張所：Tel 011-764-3611 Fax 011-764-3612

AIXTRON

アイクストロン社
カーボンナノチューブ&グラフェン成長用CVD装置 Black Magic

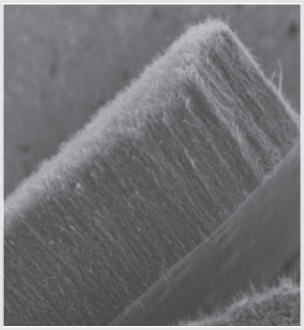

Dense CNT

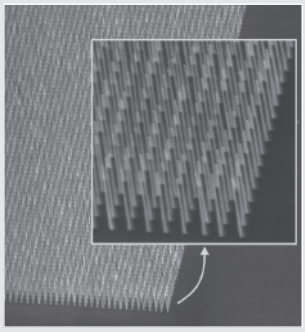

Horizontal SWCNT

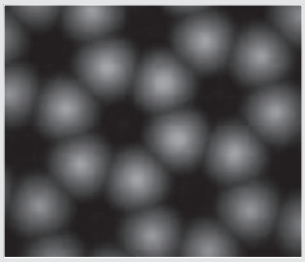

Graphene

- 装置導入後、スピーディに希望のCNTやグラフェンを成長可能
- オリジナルレシピ付き「Thermal CVDとPlasma CVDの2モードに対応」
  (シングルCNT用、ダブルCNT用、マルチCNT用、グラフェン用、横方向CNT用、低圧力プロセス用、高速成長CNT用など)
- あらゆる基板サイズに対応 (研究用2"、4"、6"モデルから量産用最大300mmモデルまで)
- プラズマによる簡単なクリーニングと高メンテナンス性
- 世界中の大学・研究所・企業へ多数納入実績あり

アイクストロン株式会社 www.aixtron.com
〒140-0001 東京都品川区北品川1-8-11 Daiwa品川Northビル 9F
E-mail: JAPANINFO@aixtron.com
Tel: 03-5781-0931 Fax: 03-5781-0940

販売代理店： **丸文株式会社** www.marubun.co.jp
〒103-8577 東京都中央区日本橋大伝馬町8番1号
E-mail: kagaku@marubun.co.jp
Tel: 03-3639-1336 Fax: 03-3662-1349

MITSUWA FRONTECH

Sincere Spirit

フラーレン・ナノチューブ・グラフェンの評価装置を紹介致します！

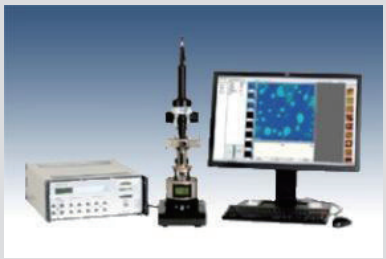

高分解能小型試料用AFM
Mutimode 8 AFM

・複雑なパラメーターを入力しなくても測定出来るSCAN ASSIST HR搭載

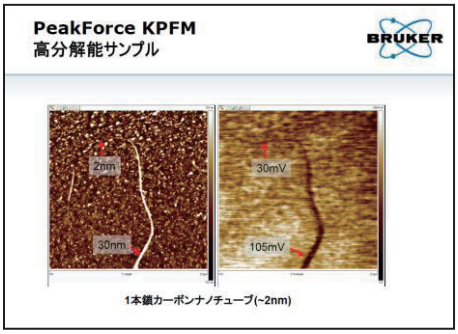

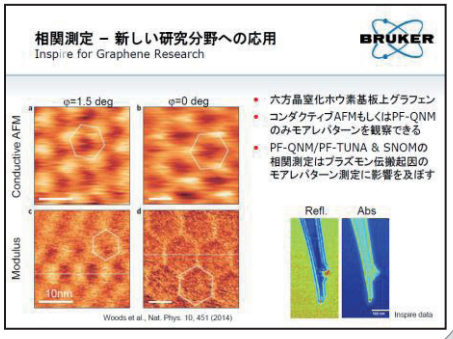

A4サイズコンパクトFT-IR
ALPHA

・A4サイズの小型タイプ
- ・グローブボックスに入る大きさ！
- ・本体寸法：W22cm × D30cm × H25cm
- ・本体重量：7kg

・震動に強い光学計
- ・Bruker Optics独自のRockSolid干渉計搭載
- ・強固な干渉計に震動に強い堅牢構造なので、持ち運んでも光軸がブレにくい

・様々なモジュール（透過測定・ダイヤモンドATR等）が特別な工具なく簡単に交換出来ます

パルスNMR方式粒子界面評価装置
Acorn Area

最適な分散状態を簡易的に測定致します

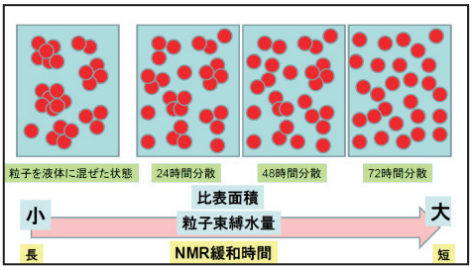

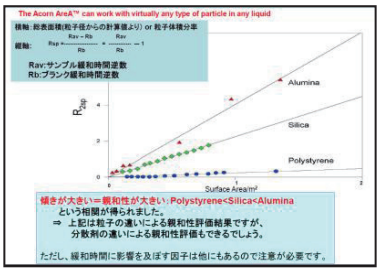

株式会社三ツワフロンテック

首都圏営業課　〒103-0004　東京都中央区東日本橋2-8-5
東日本橋グリーンビルアネックス8F
TEL：03-5823-2323　FAX：03-3863-5188

本　　社　〒530-0041　大阪市北区天神橋3-6-24
TEL.06（6351）9631　FAX.06（6351）9632

宇部支店　〒755-0053 山口県宇部市西中町4-28
千葉営業所　〒260-0834　千葉市中央区今井1-19-12（MKビル）
神奈川営業所　〒252-0804　神奈川県藤沢市湘南台1-7-4（綴ビル）
つくば営業所　〒305-0817　茨城県つくば市研究学園5-12-10
滋賀営業所　〒520-3032　滋賀県栗東市苅原278（メゾンドケイズ）
岡山営業所　〒710-0826 岡山県倉敷市老松町3-8-7(ビバリーガーデン老松)
広島営業所　〒733-0821 広島市西区庚午北2-17-4（船本ビル）
周南営業所　〒744-0002 山口県下松市東海岸通り1-11

nanom フロンティアカーボンのフラーレン製品

銘　柄		分子構造	純度(HPLC面積%、代表値) 内容他	最低数量 (g)
nanom purple フラーレンC60	ST	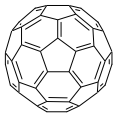	99	10
	TL		99.5	2
	SU		99.5/昇華精製品	2
	SUH		99.9/昇華精製品	1
	SC		99.9/昇華精製/単結晶品	1
nanom orange フラーレンC70	ST	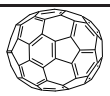	97	1
	SU		98/昇華精製品	0.5
nanom mix 混合フラーレン	ST	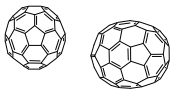	C60,C70,その他高次 フラーレンの混合物 ※微粒化品(ST-F)もあります	50
nanom spectra [60]PCBM (phenyl C61-butyric acid methyl ester)	E100	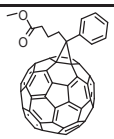	99	1
	E100H		99.5	1
	E102		99.9	0.5
nanom spectra [70]PCBM (phenyl C71-butyric acid methyl ester)	E110	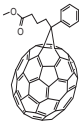 主成分	99/異性体トータル ※位置異性体の混合物	0.5
	E112		99.5/異性体トータル ※位置異性体の混合物	0.5
nanom spectra　Q100 [60]インデン付加体		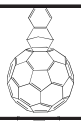	99	0.5
nanom spectra　Q400 [60]インデン2付加体		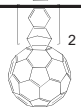	99/異性体トータル ※位置異性体の混合物	1
nanom spectra　D100 水酸化フラーレン		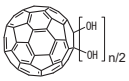 (n = ca.10)	$C_{60}OH_n$　n=10を主成分とする混合物	1
nanom spectra　A100 水素化フラーレン		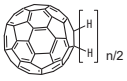 (n = ca. 30)	$C_{60}H_n$　n=30を主成分とする混合物	1

※銘柄、取扱数量等は予告無く変更する場合がございます。 ※試験研究用途向けです。

当社製品は、下記から購入いただけます。直接お問い合わせください。

・関東化学株式会社　試薬事業本部
〒103-0022 東京都中央区日本橋室町2-2-1　TEL:03-6214-1090　FAX:03-3241-1047
http://www.kanto.co.jp　E-mail:reag-info@gms.kanto.co.jp

・中山商事株式会社　筑波営業所　(担当　落合敬宝)
〒300-2651茨城県つくば市鬼ケ窪1139-1　TEL:029-847-7355　FAX:029-847-1923
E-mail:nst15@nakayama-co.jp

＜本資料に関するお問い合わせ先＞
フロンティアカーボン株式会社【担当:梶原】
〒100-8086　東京都千代田区丸の内2-6-1丸の内パークビルディング24階
TEL:03-3210-2620　FAX:03-3210-4606　http://www.f-carbon.com
※弊社へのお問い合わせはHPよりお願いいたします。

Frontier Carbon Corporation